MECHANISMS OF METHYLMERCURY-INDUCED ASTROCYTE TOXICITY: A COMPARATIVE STUDY BETWEEN CEREBELLAR AND CORTICAL ASTROCYTES

By

Rosa Julia Jaiman-Cruz

A DISSERTATION

Submitted to
Michigan State University
in partial fulfillment of the requirements
for the degree of

Neuroscience – Environmental Toxicology – Doctor of Philosophy

2017

ABSTRACT

MECHANISMS OF METHYLMERCURY-INDUCED ASTROCYTE TOXICITY: A COMPARATIVE STUDY BETWEEN CEREBELLAR AND CORTICAL ASTROCYTES

By

Rosa Julia Jaiman-Cruz

Methylmercury (MeHg) can affect both the peripheral and central nervous system; however, granule cells in the cerebellum are preferential targets of MeHg neurotoxicity. The loss of granule cell after MeHg exposure is believed to be the result of unregulated elevations in intracellular calcium concentrations ($[Ca^{2+}]_i$) that lead to glutamate excitotoxicity. Astrocytes are the main cell type responsible for buffering the excess extracellular glutamate levels, preventing the excitotoxicity of neurons. However, MeHg can also affect astrocytes and increase their $[Ca^{2+}]_i$. MeHg-induced cytotoxicity in astrocytes has been studied in the forebrain cortex. However, effects on cerebellar astrocytes are less studied. Because regional differences can occur in astrocytes between the two areas, in this dissertation we compared MeHg toxicity on cerebellar and cortical astrocytes, and aimed to understand different toxicological effects of MeHg on these astrocytes, such as, the increase in extracellular glutamate levels and cytotoxicity. After an acute exposure to MeHg, there was a regional, but not a typological difference in astrocyte viability, in where cerebellar astrocytes were more susceptible to MeHg than cortical astrocytes. One difference between cortical and cerebellar astrocytes that might contribute to the cerebellar astrocytes susceptibility to MeHg was the contribution of calcium (Ca^{2+}) to cell death. It was found that intracellular Ca^{2+} plays a role in MeHg-induced cortical astrocyte death. However, both intracellular and extracellular Ca^{2+} contribute to cerebellar astrocyte death. Another factor that contributes to the regional susceptibility of cerebellar astrocytes to MeHg was the Ca^{2+}-dependent vesicular release of glutamate. These releases

occurred in cerebellar astrocytes and not in cortical astrocytes, and were not due to the smooth endoplasmic reticulum (SER), but to the interaction of MeHg with the mitochondria, L-type and N-type voltage-gated Ca^{2+} channels (VGCCs). However, there were no differences in the contribution of these intracellular storages and Ca^{2+} channels to the reduction of viability. MeHg can also affect the excitatory amino acid transporters (EAATs), inducing an upregulation and dysfunction of these proteins. By studying the effect of MeHg on astrocytes, we found that the Ca^{2+}-dependent vesicular release of glutamate from cerebellar astrocytes and the dysfunction of the EAATs contribute to cerebellar astrocyte susceptibility. The noticeable effects of MeHg exposure in glutamate levels observed on cerebellar astrocytes might contribute to the preferential sensitivity of the granule cells to MeHg by further increasing neuronal excitotoxicity.

To Dad, Mom, Julissa, Melissa, and Cesar
I am the product of their love and sacrifice. I will always love you.
This is for all of you.

ACKNOWLEDGEMENTS

I would like to thank my mentor, Dr. William Atchison, for believing in my potential as a scientist, giving me the opportunity to participate in the Bridge to Neuroscience Program, and accepting me to be part of his lab. Thank you for your patient and support. I also want to thank my guidance committee members: Dr. Caryl Sortwell, Dr. Colleen Hegg, and Dr. Brian Gulbransen, for generously offering their time, and for their invaluable advice and careful consideration of my experiments. I honestly appreciate it. To Drs. James Galligan and Robert Roth of the Neuroscience program and Institute for Integrative Toxicology, respectively, for providing me the opportunity to achieve my goal of becoming a neurotoxicologist.

I would also like to extend my sincere gratitude to Dr. Ravindra Hajela and Dawn Autio, for teaching me the techniques needed for my experiments. Thanks to my "lab sisters": Noge, Monica, and Jordan. You have become more than just great colleagues. You are my friends. Thank you all for your kindness and help all these years. To Jessica Ortiz, Paige McKeon, Yolimar Colon, and Nicole Rivera, undergraduate students I have had the honor of mentoring, for their help collecting the data analyzed in this dissertation.

To my father, for teaching me the value of hard work and providing me with words of wisdom and inspiration. No matter how tired you were, you were always there for us. To my mother, for being a devoted mother to her daughters. You gave up many great things in life in order to raise us. Because of you, I learned to always do my best and give my all in every situation. There are no words that can truly express my appreciation to the both of you.

To Julissa Jaiman, for being a role model and an example a sister could ever ask for. You are the bravest and strongest woman I ever knew. To Melissa Jaiman, for being with me through

every phase of my life. You are more than my sister. You are my best friend. To my soulmate, Cesar Lugo, for being my rock, my happiness, and my motivation. There have been complex and immense challenges throughout this journey. You have always stayed by my side and given me the strengths to address and face them with an overcoming faith in God. I love you with all my heart and always will.

Finally, I am forever grateful to God. He is the Alpha and Omega, the Beginning and the End. This work would not have been possible without Him.

TABLE OF CONTENTS

LIST OF TABLES

LIST OF FIGURES

KEY TO ABBREVIATIONS

ALS - Amyotrophic lateral sclerosis

AMPA - α-amino-3-hydroxy-5-methyl-4-isoxazolepropionic acid

ANOVA - Analysis of variance

ATP - Adenosine 5'-triphosphate

ATPase - Adenylpyrophosphatase

BAPTA-AM - 1,2-Bis(2-aminophenoxy)ethane-N,N,N′,N′-tetraacetic acid tetrakis(acetoxymethyl ester)

Ca^{2+} - Calcium

$[Ca^{2+}]_i$ - Intracellular calcium concentration

$CaCl_2$ - Calcium chloride

Calcein-AM - calcein acetoxymethyl ester

CCCP - Carbonyl cyanide m-chlorophenyl hydrazone

CHO - Chinese hamster ovary cells

CNS - Central nervous system

CO_2 - Carbon dioxide

DAPI - 4',6-diamidino-2-phenylindole

DIV - Day *in vitro*

DMEM - Dulbecco's modified eagle medium

DMSO - Dimethyl sulfoxide

DNase I - Deoxyribonuclease I

EAA - Excitatory amino acid

EAAC1 - Excitatory amino acid carrier 1

EAATs - Excitatory amino acid transporters

EGTA - Ethylene glycol-bis(2-aminoethylether)-N,N,N',N'-tetraacetic acid

EthD-1 - Ethidium homodimer-1 EthD

FBS - Fetal bovine serum

g - Force of gravity

GABA - Gamma-aminobutyric acid

GFP - Green fluorescent protein

GFAP - Glial fibrillary acidic protein

GLAST - Glutamate aspartate transporter

GLT1 - Glutamate transporter 1

GSH - Glutathione

GVIA - ω - Conotoxin GVIA

h – hours

HBS - HEPES-buffered saline

HEPES - 4-(2-hydroxyethyl)-1-piperazineethanesulfonic acid

Hg – Mercury

HgS - Mercury sulfide

HVA - High voltage-activated

K^+ - Potassium

KCl - Potassium chloride

KH_2PO_4 - Monopotassium phosphate

LDH - Lactate dehydrogenase

LVA - Low voltage-activated

μm - Micrometer

μL - Microliter

μM - Micromolar

M - Molar

MeHg - Methylmercury

$MgSO_4$ - Magnesium sulfate

min - Minute

mL - Milliliter

mm - Milimeter

mM – Millimolar

mPTP - Mitochondrial transition pore

MTT - Methylthiazolyldiphenyl-tetrazolium bromide

NaCl - Sodium chloride

Na^+ - Sodium

Na_2HPO_4 - Disodium phosphate

ng - Nanogram

NGS - Normal goat serum

nm - Nanometer

nM – Nanomolar

NMDA - N-methyl-D-aspartate

Nrf_2 - Nuclear factor erythroid 2-related factor 2

O^2 - Oxygen

O-2A - Oligodendrocyte type 2 astrocyte

PBS - Phosphate-buffered saline

ROI - Regions of interest

ROS - Reactive oxygen species

SLC1A3 - Solute carrier family 1 member 3

SEM - Standard error of the mean

SER - Smooth endoplasmic reticulum

SNAP-23 - Synaptosome-associated protein of 23 kDa

VGCCs - Voltage-gated calcium channels

VGLUTs - Vesicular glutamate transporters

CHAPTER ONE: INTRODUCTION

A. Methylmercury

Methylmercury (MeHg) is an organometallic cation composed of mercury (Hg). Hg is a persistent substance that comes from natural and human sources. For example, Hg can be dispersed into the air through the weathering of rocks containing Hg. Also, Hg can be released into the environment through human activities, such as the incineration and burning of fossil fuel (Hansson, 1988). Hg can be present in the environment in metallic forms and various inorganic and organic complexes. Once in the environment, transformations between different forms of Hg can occur. Sulfate-reducing bacteria, mainly from muddy deposits in water bodies, take up Hg sulfide (HgS) and through metabolic process convert it to MeHg (Hamdy & Noyes, 1975; Jensen & Jernelöv, 1969; Jernelov, 1969). These bacteria use sulfur rather than oxygen as a part of their respiration system and it is believed that the uptake of the Hg complex HgS occurs via passive diffusion (Benoit, Gilmour, Mason, & Heyes, 1999). Once the bacteria have taken up the HgS complex, they use a detoxification enzyme to change the sulfur (S) element of the complex to a methyl group, forming MeHg (Hamdy & Noyes, 1975). After the methylation process, the bacteria transport the MeHg back into the aquatic environment, where it is taken up by other microorganisms. The microorganisms are consumed by fish, and the smaller fish are consumed by larger fish; in this way, MeHg bioaccumulates up the food chain. This is shown in Figure 1.1. Such bioaccumulation can result in very high concentrations of MeHg in large predatory fish species, such as tuna, swordfish, and shark (Table 1.1). This becomes a threat to populations that consume this nourishment (Atwell, Hobson, & Welch, 1998; Clarkson, 1995).

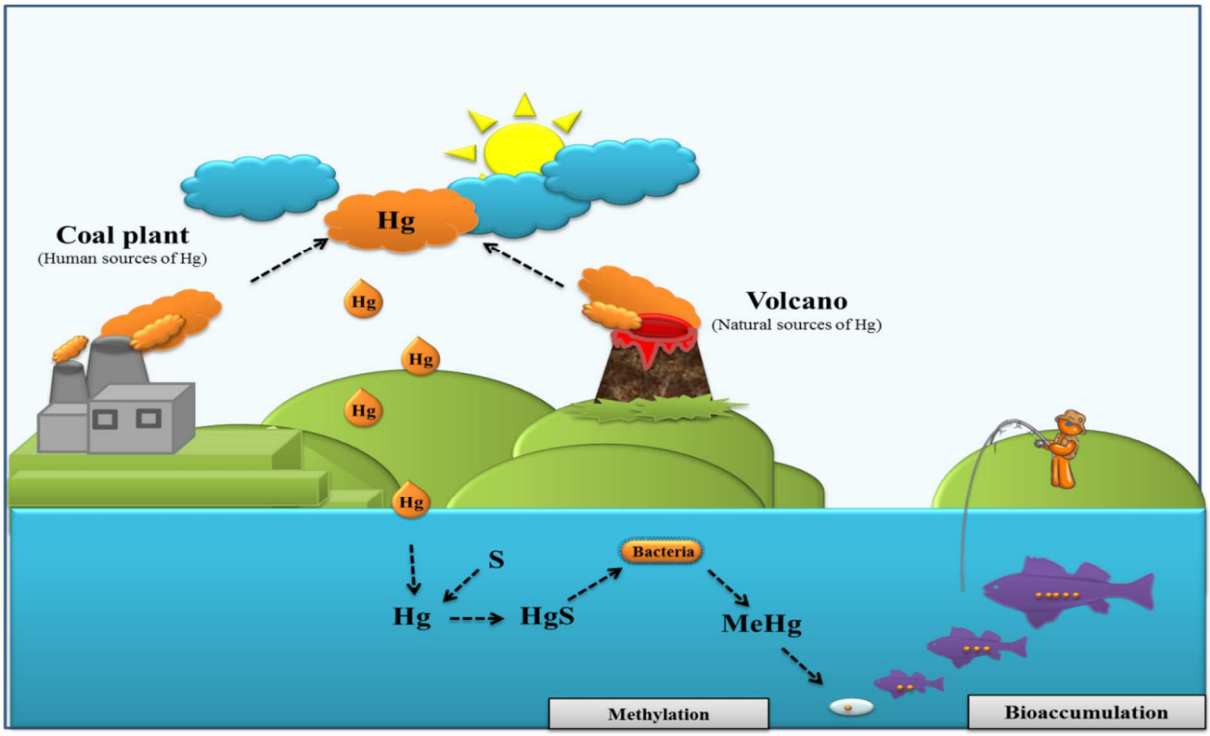

Figure 1.1. Sources, methylation, and bioaccumulation of Hg. Hg is a persistent substance that can be released into the environment through natural and human sources. Once in the environment, Hg is converted into MeHg by the action of bacteria. After the methylation process, the bacteria transport the MeHg back into the aquatic environment, where it is taken up by other microorganisms. The microorganisms are consumed by fish and the smaller fish are consumed by larger fish. In this way, MeHg bioaccumulates up the food chain. This becomes a threat to populations that consume this nourishment.
For interpretation of the reference to color in this and all other figures, the reader is referred to the electronic version of this dissertation.

Species	Hg concentration mean (PPM)
Shrimp	0.009 ppm
Salmon	0.022 ppm
Tuna (Canned, Light)	0.126 ppm
Tuna (Fresh, Frozen)	0.386 – 0.689 ppm
Shark	0.979 ppm
Swordfish	0.995 ppm
Tilefish	1.123 ppm

Table 1.1. Example of Hg concentration in several aquatic species. Hg concentration is presented in parts per million (PPM). The table presents the species from lowest to highest level of Hg. Table modified from https://www.fda.gov/food/foodborneillnesscontaminants/metals/ucm115644.htm

A.1. Methylmercury absorption and excretion

MeHg can bioaccumulate readily in living systems due to its binding properties. Once inside the organism, MeHg binds to thiol groups, forming a covalent bond that is strong, but reversible (Sugiura, Tamai, & Tanaka, 1978). Because of its reversible binding characteristic, MeHg can change through thiol proteins and move easily throughout the body. Approximately 95% of MeHg taken orally is absorbed by the gastrointestinal tract (Aberg et al., 1969). It can also be absorbed through the skin and lungs (Council, 2000).

Once absorbed, MeHg enters the blood circulation. More than 90% of the MeHg that is found in the bloodstream is transported into red blood cells (Kershaw, Dhahir, & Clarkson, 1980), due to its complex with cysteine residues in the hemoglobin (Doi, 1991). The L-system amino acid carrier, mistaking the MeHg-cysteine complex for L-methionine, carries the MeHg through the tightly packed endothelial cells of the blood-brain barrier (Kerper, Ballatori, & Clarkson, 1992). Inside the endothelial cells, glutathione (GSH) binds to MeHg and forms a MeHg-GSH complex that is transported into the brain by the GSH carrier. In other words, MeHg enters into the endothelial cells on the blood side as MeHg-cysteine and comes out into the extracellular fluid of the brain as MeHg-GSH (Kerper, Mokrzan, Clarkson, & Ballatori, 1996). This is demonstrated in Figure 1.2. Approximately 10% of the MeHg that is found in the brain is demethylated to inorganic Hg (Council, 2000; Dunn & Clarkson, 1980; Elinder, Gerhardsson, & Oberdoerster, 1988). MeHg can be transported into the fetus and the fetal brain (Kajiwara, Yasutake, Adachi, & Hirayama, 1996; Koos & Longo, 1976).

The daily excretion of MeHg is about 1% of the human body burden (Clarkson, Friberg, Nordberg, & Sager, 2012), where 90% of MeHg is excreted in feces as Hg and the rest 10% is excreted in the urine as Hg (Council, 2000; Miettinen, 1973). The MeHg-GSH complex is

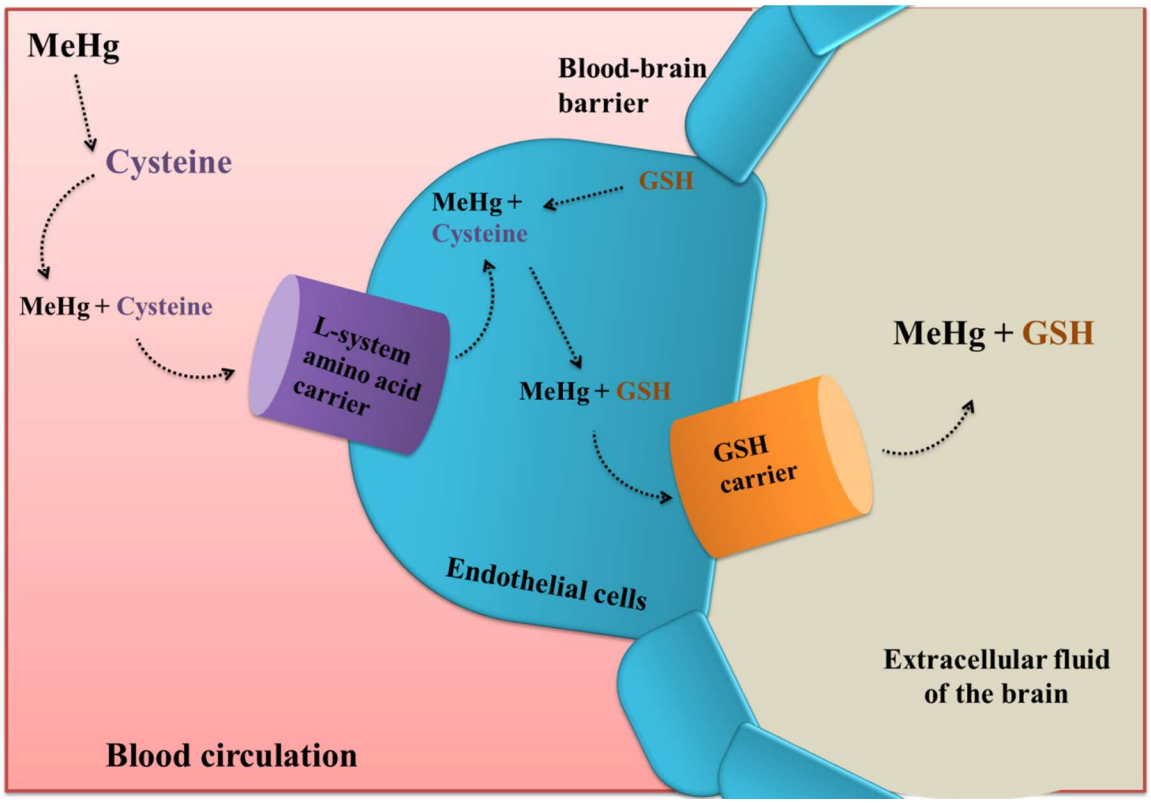

Figure 1.2. MeHg crosses the blood-brain barrier. Once absorbed, MeHg enters the blood circulation, and then it forms a complex with cysteine residues in the hemoglobin. The L-system amino acid carrier transports the MeHg through the tightly packed endothelial cells of the blood-brain barrier. Inside the endothelial cells, glutathione (GSH) binds to MeHg and forms a MeHg-GSH complex that is transported into the brain by the GSH carrier. In other words, MeHg enters the endothelial cells on the blood side as MeHg-cysteine and comes out into the extracellular fluid of the brain as MeHg-GSH.

involved in excretion (Kromidas, Trombetta, & Jamall, 1990). Lactation increases clearance of MeHg from blood (Skerfving, 1988). In the whole body, the half-life elimination is approximately 70-80 days (Aberg et al., 1969; Kershaw et al., 1980; Miettinen, 1973), but it varies depending on the species, doses, sex, and animal strain (Nielsen, 1992).

A.2. Episodes of methylmercury toxicity

There were two main episodes of MeHg toxicity. One of these episodes happened in Minamata, Japan in the 1950s by a chemical plant operated by the Chisso Corporation. This plant was producing acetaldehyde and used Hg as a catalyst in its production. They discharged the Hg into Minamata Bay, contaminating its fish, which then experienced elevated levels of Hg ranging from 5.61 to 35.7 ppm. Humans and animals who consumed these contaminated fish (and shellfish) subsequently experienced Hg poisoning. High levels of Hg (up to 705 ppm) were detected in the hair of these individuals. Approximately 1,043 of 2,252 patients died due to MeHg poisoning attributed to waste effluent from Chisso Corporation (Harada, 1995).

Another main episode of MeHg toxicity happened in Iraq in the early 1970's. This event started when people ate homemade bread prepared from grain treated with a MeHg-containing fungicide. Approximately 459 of 6,530 people affected died because of MeHg poisoning. MeHg poisoning in Iraq was more acute and with higher exposure concentrations than those experienced in Minamata Bay, though the clinical signs and symptoms of poisoning were similar (Bakir, 1973). Common signs and symptoms of MeHg include ataxia, dysarthria, visual disturbance, sensory changes, weakness, hyperreflexia, involuntary movements, and muscle and joint pain (Amin-Zaki et al., 1979; Harada, 1978). However, these symptoms often occurred following a latency period. In Iraq, victims started to present signs of poisoning weeks or

	Minamata, Japan	Iraq
Source	A chemical plant discharged Hg into Minamata Bay, contaminating its fish	People ate homemade bread prepared from grain treated with a MeHg-containing fungicide
Year	1950's	Early 1970's
People affected	Approx. 2,252 people affected	Approx. 6,530 people affected
Deaths	Approx. 1,043 deaths	Approx. 459 deaths
Type of poisoning	Chronic	Acute*

* MeHg poisoning in Iraq was more acute and with higher exposure concentrations than those experienced in Minamata Bay, though the clinical signs and symptoms of poisoning were similar (Bakir, 1973).

Table 1.2. Comparison between the two main episodes of MeHg toxicity: Japan and Iraq. There were two main episodes of MeHg toxicity. One of these episodes happened in Minamata, Japan in the 1950s by a chemical plant operated by Chisso Corporation. They discharged the Hg into Minamata Bay, contaminating its fish. Humans and animals who consumed these contaminated fish subsequently experienced Hg poisoning. Approximately 1,043 of 2,252 patients died. Another main episode of MeHg toxicity happened in Iraq in the early 1970's. This event started when people ate homemade bread prepared from grain treated with a MeHg-containing fungicide. Approximately 459 of 6,530 people affected died.

months after the exposure ended (Bakir, 1973; Weiss, Clarkson, & Simon, 2002). Likewise, in Minamata, low chronic doses of MeHg from contaminated fish did not produce observable behavioral effects for periods of time measured in years (Harada, 1995; Weiss et al., 2002). (Table 1.2). It was thought that the latency period in the acute poisoning was due to the slow production and accumulation of inorganic Hg, a toxic metabolite (Vahter et al., 1994). However other studies have demonstrated the opposite (Magos et al., 1985). Therefore, the mechanism that explains the latency period after an acute exposure is still unknown. For chronic MeHg exposure, a possible mechanism that explains the latency period emerged. It was proposed that MeHg can produce an initial cell loss and that with the aging process, more cells are reduced until those remains are too few to sustain a normal function (Weiss et al., 2002; Weiss & Simon, 1975).

Other episodes of MeHg contamination took place in Seychelles and Faroe Islands. The Seychelles Islands are a group of 115 islands that are located in the Indian Ocean. These islands have high fish consumption; therefore, they are greatly exposed to MeHg contamination. Surprisingly, studies have indicated that there is no consistent pattern of adverse associations between prenatal MeHg and the development of children (Davidson et al., 1994) and adolescents (Davidson et al., 2011).

In contrast, studies about inhabitants of the Faroe Islands, a group of 18 islands that are located in the North Atlantic Ocean, have shown neurotoxicity effect due to prenatal and postnatal exposure to MeHg (Grandjean, Weihe, Debes, Choi, & Budtz-Jørgensen, 2014; Myers & Davidson, 1998). This group of islands is exposed to MeHg through the consumption of whale meat and fish, especially cod. Because cod had approximately 95% lower MeHg concentrations than whale meat, it is believed that the neurotoxicity that the people of Faroe Island suffered was

due to the consumption of whale meat (Booth & Zeller, 2005). As a matter of comparison, it is possible that the high consumption of whale in the Faroe Island, explains the difference in toxicity between those islands and the Seychelles Islands (Booth & Zeller, 2005; Myers & Davidson, 1998). However, the genetic variances between the two populations could also play a role.

In a study done in the United States (U.S.), in where the hair of children and women of childbearing age was obtained to assess mercury levels, it was found that Hg levels in hair were associated with age and fish consumption frequency (McDowell et al., 2004). Similarly, Mahaffey and colleagues (2009) found that the Hg concentrations in the blood of adult women in the U.S. were associated with fish consumption. Other studies in which the authors described the levels of Hg in the blood of children and women of childbearing age in the U.S. found that approximately 8% of women had concentrations higher than the concentration recommended by the U.S. Environmental Protection Agency (Schober et al., 2003). The findings of these studies demonstrate that the contamination of MeHg through food consumption is also happening in the U.S.

Hg contamination can also occur through artisanal and small-scale gold mining (ASGM) in where Hg is used to extract gold (Nakazawa et al., 2016). In ASGM, Hg is mixed with gold-containing materials, forming an Hg-gold amalgam, which is then heated, vaporizing the Hg to obtain the gold that remains (Gunson & Veiga, 2004). At present, ASGM constitutes the main source of Hg released into the environment. It is estimated that 1,600 metric tons of Hg are released every year due to ASGM. This releasing of Hg comprises about 37% of global atmospheric emissions, becoming the largest emitters of this metal (UNEP 2013). In 2016, it was one of the major pollution problems in the world. Approximately 10–15 million miners,

including 4.5 million women and 1 million children, are involved in the production of 500 to 800 metric tons of gold per year. An estimated 100 million people from more than 70 countries depend, directly or indirectly, on ASGM for their living (Bender, Lymberidi-Settimo, & Groth III, 2014; Veiga et al., 2004). Accordingly, ASGM activities have resulted in major occupational Hg exposure, with the evidenced intoxication of miners reported around the world (Veiga et al., 2004).

B. Cerebellum

The cerebellum is well known for motor coordination and learning. Studies have suggested that the cerebellum may also play a role in cognitive functions, including working memory (Schmahmann & Sherman, 1997). The cerebellum has a three-layer structure, in where different neurons and glial cells are arranged: molecular layer, Purkinje cell layer, and internal granular layer (Figure 1.3). The molecular layer contains the dendritic trees of the Purkinje cells, the parallel fibers, and the fibers of Bergmann glia. The Purkinje cell layer has the somata of the Purkinje cell and Bergmann glia. The internal granular layer has the somata of the granular cells. The cerebellum has two main types of afferent inputs: climbing fibers and mossy fibers (Hashimoto & Hibi, 2012).

In the internal granule layer, mossy fibers synapse with the dendrites of granule cells that are in contact with the axons of Golgi cells. This structure is called the cerebellar glomeruli. In the cerebellar glomeruli, mossy fibers release glutamate producing excitation in granule cells, and Golgi cells release GABA producing a recurrent inhibition in the same cells (Hashimoto & Hibi, 2012). The $GABA_A$ receptor activation on granule cells contributes to an inhibition that

fine-tune the excitability of these cells to optimize information sent from mossy fibers to granule cells (Mapelli, Solinas, & D'Angelo, 2014).

Granule cells send this information to Purkinje cells through its parallel fibers, specialized axons that ascend to the molecular layer. At the molecular layer, parallel fibers synapse with the dendritic spines of Purkinje cells and produce excitation by releasing glutamate. Purkinje cells also receive information from climbing fibers, the other type of afferent inputs into the cerebellum. Climbing fibers, which originate from the inferior olive nuclei, form an excitatory synapse with Purkinje cell dendrites in the molecular layer. The information from mossy—parallel fiber connection and the climbing fibers is combined by the Purkinje cell. Climbing fibers can moderate the effectiveness of the mossy—parallel fiber connection with Purkinje cells, thus regulating the motor function of the cerebellum (Hashimoto & Hibi, 2012; Purves et al., 2001).

Bergmann glial cell, a highly diversified astrocyte, can facilitate several functions that optimize information processing in the cerebellum. In the developing brain, Bergmann glial cells are important for the migration and correct layering of granule cells in the cerebellum. In the developed brain, this astrocyte has several important roles, such as plasticity (Balakrishnan & Bellamy, 2009; Balakrishnan, Dobson, Jackson, & Bellamy, 2014), extracellular ion homeostasis (Wang et al., 2012), metabolic function and neuroprotection (Jakoby et al., 2012; Poblete-Naredo et al., 2011), and synapse structure and function (Iino et al., 2001; Saab et al., 2012). The deletion of the AMPA receptors of Bergmann glial cells has resulted in physiological and structural changes that were accompanied by behavioral impairments in fine motor coordination (Saab et al., 2012). Because Bergmann glial cells contribute to information processing, it is

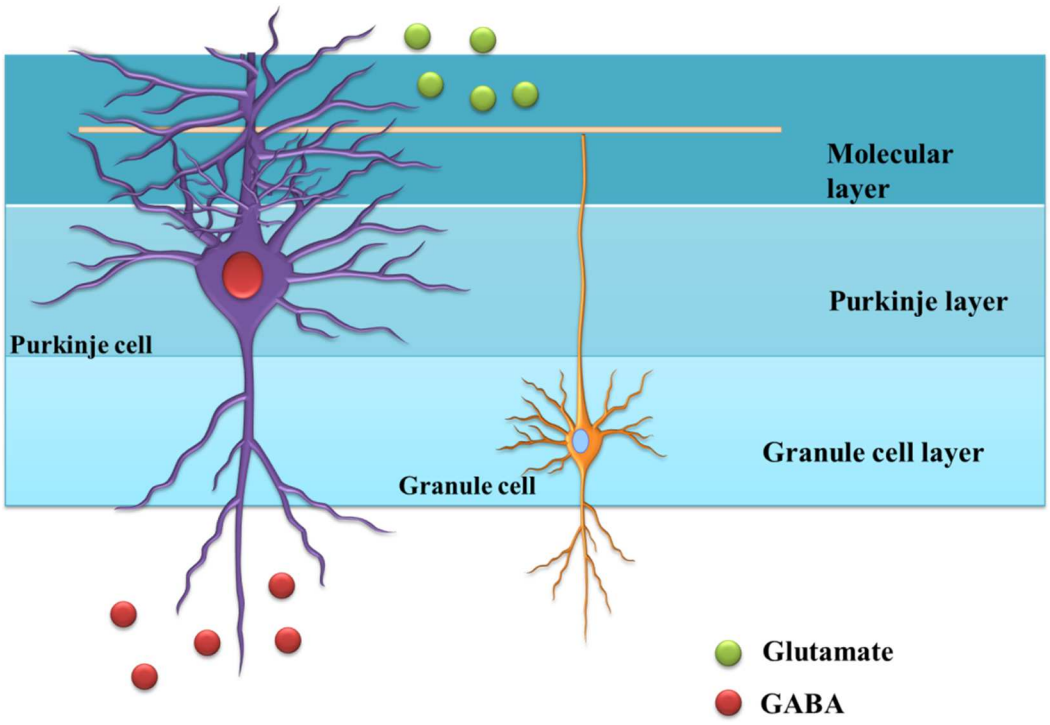

Figure 1.3. Location and function of the main cerebellar neurons. There are two main neurons that play important roles in the cerebellar circuit: cerebellar granule cells and Purkinje cells. The granule cell is located on the granule cell layer. The cell body of the Purkinje cells is located on the Purkinje cell layer. The molecular layer contains the dendritic trees of the Purkinje cells and parallel fibers. Purkinje cells are activated by the parallel fibers of the granule cells and provide inhibition to the deep nuclei. Granule cells have a very important role in the cerebellum since they are the only glutamatergic neurons in the cerebellar cortex. Image modified from Motifolio Anatomy Drawing Toolkit available from http://www.motifolio.com/anatomy.html.

hypothesized that these glial cells are involved in the fine-tuning activity of the cerebellum (De Zeeuw & Hoogland, 2015).

C. Mechanisms of methylmercury-induced neurotoxicity

MeHg neurotoxicity can occur after acute or chronic exposure. The developing nervous system is particularly sensitive to MeHg, but the adult nervous system can also be affected (as described above in the Minamata and Iraq cohorts). Pathological examination of patients with MeHg poisoning shows that lesions typically happen in the occipital lobes near the calcarine fissure, and the cerebellum (Atchison, 2005; Takeuchi, Morikawa, Matsumoto, & Shiraishi, 1962). The occipital lobe is essential for vision. The effect of MeHg on the occipital lobe of monkeys produced blurred vision and permanent adverse effects on spatial vision (Rice & Gilbert, 1982). Experiments performed in rats demonstrated that MeHg exposure produced similar effects on the cerebellum; however, damage to cerebral cortical neurons was not observed (Chang & Hartmann, 1972).

In the cerebellum, MeHg accumulates mainly in the Purkinje cells, Bergmann glial cells, and other astrocytes and glial cells of white matter, not in granule cells (Leyshon-Sørland, Jasani, & Morgan, 1994). However, the granule cells are more susceptible to MeHg than the other cells (Edwards, Marty, & Atchison, 2005; Leyshon-Sørland, Jasani, & Morgan, 1994). MeHg can produce loss of the granule cells in the cerebellum (Choi, Lapham, Amin-Zaki, & Saleem, 1978; Eto & Takeuchi, 1978; Takeuchi et al., 1962).

Exposure to this toxicant during development leads to impaired synaptogenesis and impaired migration of granule cells, causing a disorganized cerebellar architecture (Choi et al., 1978). MeHg-induced impairment of granule cells migration has been demonstrated *in vitro*

(Sass, Haselow, & Silbergeld, 2001) and in organotypic slice cultures (Kunimoto & Suzuki, 1997; Mancini, Autio, & Atchison, 2009). Organotypic cultures of rat cerebellar slice cultures exposed to acute and/or high levels of MeHg showed an inhibited migration of the external granule cells towards the internal granular layer in a dose-dependent manner (Kunimoto & Suzuki, 1997). Another experiment performed on organotypic cultures, but with chronic low-levels of MeHg, showed an impaired development of the cerebellar cortex that may occur due to delayed synaptogenesis and maturation of granule cells in the internal granule layer (Mancini et al., 2009). Bradford and colleagues (2016) found that during development or early stages of migration, granule cells exposed acutely to MeHg had an increase in $[Ca^{2+}_i]$. Because $[Ca^{2+}_i]$ is crucial for granule cell migration (Komuro & Kumada, 2005), it is possible that MeHg-induced imbalance of $[Ca^{2+}_i]$ produces the impairment of granule cell migration.

The granule cells have a very important role in the cerebellum since they are the only glutamatergic neurons in the cerebellar cortex. Loss of these neurons in mice that possess the weaver mutation produces ataxia, mild locomotor hyperactivity, and occasionally, tonic-clonic seizures (Sotelo, 1975). These symptoms are similar to those seen in MeHg poisoning.

It is hypothesized that multiple mechanisms contribute to MeHg-induced neurotoxicity and that these mechanisms might be additive or synergistic (Atchison & Hare, 1994). Among the mechanisms most frequently emphasized, calcium (Ca^{2+}) dysregulation and glutamate excitotoxicity are discussed here.

C.1. Methylmercury-induced calcium dysregulation

Ca^{2+} is an important regulator of many neuronal processes, such as signal transduction pathways, gene transcription (West et al., 2001), growth cone elongation (Mattson & Kater,

1987), and neurotransmitter and gliotransmitter release (Mothet et al., 2005; Rubin, 1970). The concentration of extracellular Ca^{2+} is 10,000 higher than intracellular Ca^{2+}concentration ($[Ca^{2+}]_i$), making the entry of Ca^{2+} a highly regulated process. In fact, the cell can use different Ca^{2+} entry pathways, such as plasma membrane receptors and voltage-dependent ion channels.

Cytosolic Ca^{2+} can also be elevated by the release of Ca^{2+} from intracellular stores, like the smooth endoplasmic reticulum (SER) (Berridge & Taylor, 1988). Once inside the cell, Ca^{2+} is buffered by the mitochondria (Rizzuto, Brini, Murgia, & Pozzan, 1993; Rizzuto, De Stefani, Raffaello, & Mammucari, 2012) (for review see: Clapham, 1995). This is demonstrated in Figure 1.4. Due to the special importance of Ca^{2+} for neuronal functions, its dysregulation can eventually lead to neuronal pathologies (Wojda, Salinska, & Kuznicki, 2008; Zündorf & Reiser, 2011).

Marty and colleagues (1997) found that MeHg produced two distinctive phases of $[Ca^{2+}]_i$ elevations. The first phase involves the release of Ca^{2+} from intracellular storages (Bearrs, Limke, & Atchison, 2001; Limke, Otero-Montañez, & Atchison, 2003), and the second phase consists of extracellular Ca^{2+} fluxes into the cell (Marty & Atchison, 1997). These changes in $[Ca^{2+}]_i$ caused by MeHg exposure can produce granule cell death (Gassó et al., 2001; Marty & Atchison, 1998).

In addition to granule cells, neuroblastoma cells (Hare, McGinnis, & Atchison, 1993; Hare & Atchison, 1995a, 1995b; Petroni, Tsai, Mondal, & George, 2013), mouse thymocytes (Oyama, Carpenter, Ueno, Hayashi, & Tomiyoshi, 1995) human lymphocytes and monocytes (Shenker et al., 1992; Shenker et al., 1993; Tan, Tang, Castoldi, Manzo, & Costa, 1993), and rat forebrain synaptosomes (Denny, Hare, & Atchison, 1993; Komulainen & Bondy, 1987;

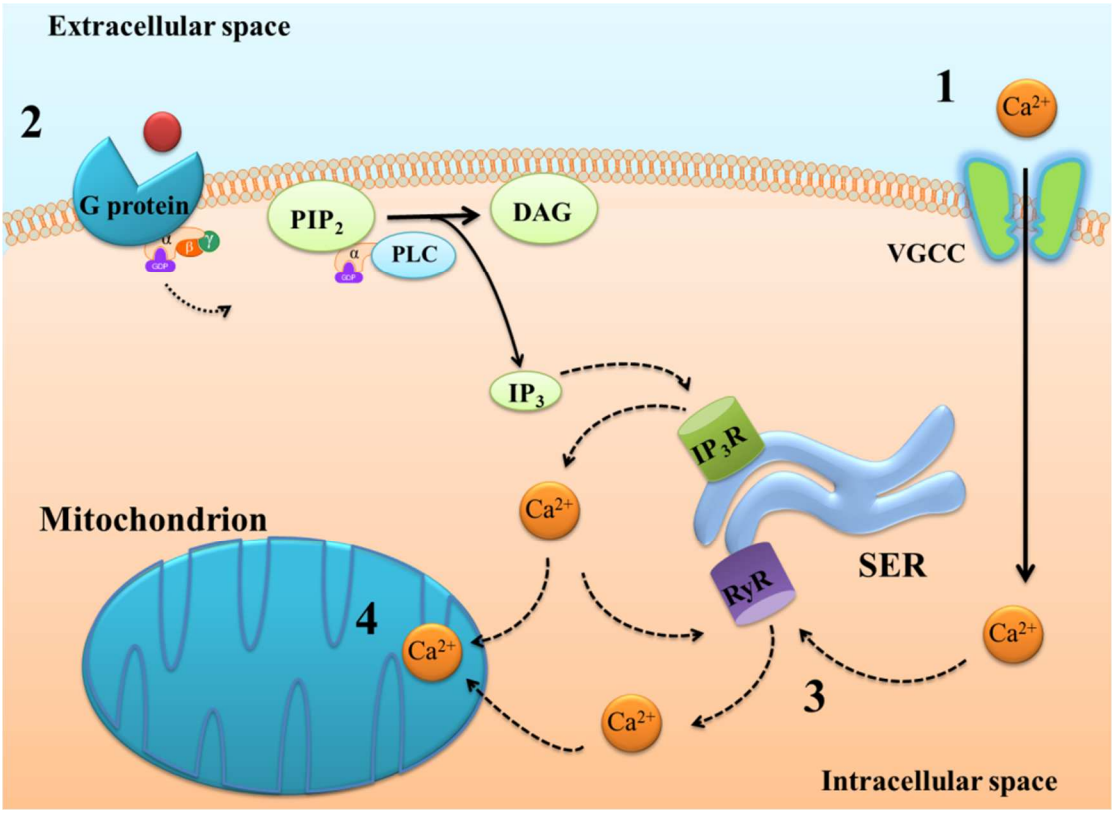

Figure 1.4. Intracellular calcium homeostasis. 1. VGCCs facilitate Ca^{2+} influx as a result of a depolarization of the plasma membrane. 2. The activation of the G-protein receptor triggers the phospholipase enzyme. This enzyme forms the IP_3 that binds to the IP_3 receptor on the SER. The IP_3 receptor works as a Ca^{2+} channel, thus it releases Ca^{2+} from the SER into the cytoplasm. 3. The increase in cytoplasmic Ca^{2+} concentration triggers Ca^{2+} release from the ryanodine receptors by CICR. 4. Mitochondria buffer cytosolic Ca^{2+}. Image modified from Motifolio Anatomy Drawing Toolkit available from http://www.motifolio.com/anatomy.html.

Levesque, Hare, & Atchison, 1992) have shown an increase in $[Ca^{2+}]_i$ and a decrease in viability produced by MeHg exposure. MeHg can produce dysregulation of Ca^{2+} through its effects on the SER, mitochondria, and Ca^{2+} channels. A representation of the $[Ca^{2+}]_i$ changes after MeHg exposure is shown in Figure 1.5.

The SER is an organelle located in the cells of eukaryotic organisms, which can regulate cytosolic Ca^{2+} levels. Once the G-protein receptor on the surface of the cell gets activated, it triggers the phospholipase enzyme. This enzyme forms the inositol trisphosphate (IP_3) that diffuses into the endoplasmic reticulum and binds to the IP_3 receptor. The IP_3 receptor works as a Ca^{2+} channel, thus it releases Ca^{2+} from the SER into the cytoplasm. The increase in cytoplasmic Ca^{2+} concentration triggers Ca^{2+} release from the ryanodine receptors by a phenomenon known as Ca^{2+}-induced Ca^{2+} release (CICR) (Berridge & Taylor, 1988) (for review see: Clapham, 1995).

The SER makes a relatively small contribution to the intracellular Ca^{2+} change that happens in rat granule cells after MeHg exposure. However, this release of Ca^{2+} plays an important factor in MeHg-induced cell death (Limke, Bearss, et al., 2004). The release of Ca^{2+} from the SER produced by MeHg comes primarily from IP_3 receptors, with a minimal contribution of Ca^{2+} from the ryanodine receptors. MeHg can also interact with muscarinic M3 receptors, a G-protein coupled receptors, and increase $[Ca^{+2}]_i$ by IP_3 pathway (Limke, Bearss, & Atchison, 2004). In NG108-15 cells, MeHg interacts directly with the receptor to cause Ca^{2+} release (Hare & Atchison, 1995a). The elevated $[Ca^{+2}]_i$ levels in the cells caused by MeHg trigger CICR from the ryanodine-sensitive store of the SER (Atchison, 2005; Limke, Heidemann, & Atchison, 2004).

Other G-protein coupled receptors affected by MeHg toxicity are the bradykinin

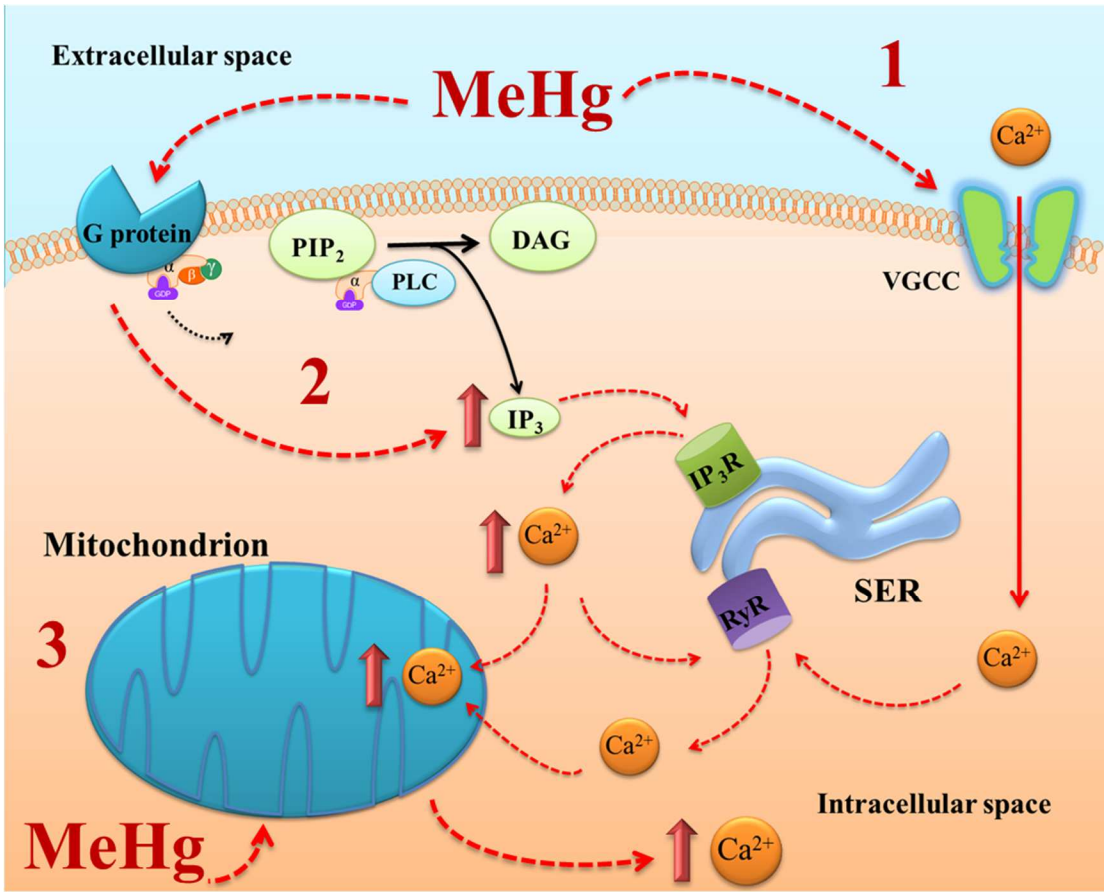

Figure 1.5. MeHg-induced dysregulation of $[Ca^{2+}]_i$ homeostasis. 1. MeHg affects the VGCCs, increasing the influx of Ca^{2+}. It is hypothesized that MeHg might use Ca^{2+} channels to move through the plasma membrane. 2. MeHg also increases IP_3 production, which triggers a release of Ca^{2+} through the IP_3 receptors. This elevation of $[Ca^{2+}]_i$ produces CICR through the ryanodine receptors. The mitochondria buffer the Ca^{2+} released from the SER. 3. The excess of Ca^{2+} buffered into the mitochondria, combined with direct effects of MeHg on the mitochondria, leads to the opening of the mPTP and the release of Ca^{2+} into the cytosol of the cell. Image modified from Motifolio Anatomy Drawing Toolkit available from http://www.motifolio.com/anatomy.html.

receptors, which are located on the surface of the cell. There are two subtypes of bradykinin receptors: B1 and B2 (Hall, 1992, 1997). The activation of these receptors produces an increase of internal $[Ca^{2+}]_i$ in neurons (Thayer, Perney, & Miller, 1988) and astrocytes, and can produce glutamate release from astrocytes (Gimpl, Walz, Ohlemeyer, & Kettenmann, 1992; Jeftinija, Jeftinija, & Stefanovic, 1997; Parpura et al., 1994). The continuous presence of a bradykinin receptor agonist can rapidly desensitize this ligand-receptor-G protein (Blaukat, Micke, Kalatskaya, Faussner, & Müller-Esterl, 2003).

Previous experiments on NG108-15 cells have shown that pretreatment with bradykinin reduced significantly the increase in $[Ca^{+2}]_i$ induced by MeHg. This suggests that bradykinin and MeHg seem to release a common pool of intracellular Ca^{2+} from the cell. It can also suggest an interaction of MeHg with the bradykinin receptors (Hare & Atchison, 1995a).

The other organelle that contributes to the increase in $[Ca^{+2}]_i$ after MeHg exposure is the mitochondria. Normally, this organelle buffers cytosolic Ca^{2+}. The Ca^{2+} of the cytosol is taken up into the matrix by the mitochondrial Ca^{2+} uniporter that is located on the inner mitochondrial membrane. The increase in intramitochondrial Ca^{2+} concentration produces adenosine 5'-triphosphate (ATP) synthesis. The release of this Ca^{2+} back into the cytosol of the cell can occur via a sodium-Ca^{2+} exchange protein (Gunter & Gunter, 1994). The efflux of Ca^{2+} can also be produced by the reversal of the uniporter and by the transient opening of the mitochondrial permeability transition pore (mPTP) (Bernardi, 2013; Bernardi & von Stockum, 2012). The release of Ca^{2+} from the mitochondria can produce neurotransmitter release (Rizzuto, 2003; Yang, He, Russell, & Lu, 2003).

MeHg can produce a mitochondrial dysfunction by causing a reduction in Ca^{2+} uptake and increasing its release (Levesque and Atchison, 1991). There are two possible mechanisms

for MeHg-induced mitochondrial dysfunction (Roos, Seeger, Puntel, & Vargas Barbosa, 2012). The first mechanism involves a direct interaction of MeHg with mitochondrial proteins. For example, MeHg interacts with the respiratory proteins in the mitochondria, inhibiting protein synthesis and interfering with the electron transport chain (Verity, Brown, & Cheung, 1975). The second mechanism involves an indirect interaction of MeHg, in where MeHg-induced increase in $[Ca^{+2}]_i$ produces excessive uptake of Ca^{2+} into the mitochondria, leading to an inhibition of the mitochondrial function. The increased levels of Ca^{2+} inside the mitochondria produce an inhibition of the electron transport chain and the mitochondrial ATPase. It also dissipates the mitochondrial proton gradient, which leads to a loss of ATP synthesis and an opening of the mPTP (Gunter & Gunter, 1994; Simpson & Russell, 1998). The opening of the mPTP, due to an acute exposure of MeHg, produces an increase in $[Ca^{+2}]_i$ in granule cells (Limke & Atchison, 2002). The inhibition of the opening of the mPTP protects the neuron from MeHg-induced cytotoxicity (Limke & Atchison, 2002; Qu et al., 2013). In contrast to the small contribution of the SER, the mitochondria contribute to a large portion of the intracellular Ca^{2+} detected in cerebellar granule cells after MeHg exposure. It also contributes to granule cell death (Limke & Atchison, 2002).

Lastly, MeHg produces dysregulation of Ca^{2+} through Ca^{2+} channels. Voltage-gated Ca^{2+} channels (VGCCs) are ionotropic channels that serve as an entry route for extracellular Ca^{2+}. They facilitate Ca^{2+} influx as a result of a depolarization of the plasma membrane of cells, such as muscle cells, neurons, and glial cells. The influx of Ca^{2+} through Ca^{2+} channels can produce various effects, such as contraction of muscles, propagation of electrical signals, control of gene transcription, and release of neurotransmitters and hormones. These channels are divided into two classes based on the degree of depolarization needed for their activation: high voltage-

activated (HVA) and low voltage-activated (LVA). The HVA VGCCs include the L-, N-, P/Q-, and R-type channels (Cav1.2, 2.2, 2.1, and 2.3, respectively). The LVA VGCC includes only T-type channels. HVA channels are multimeric proteins formed by α1, β, α2δ, and sometimes γ subunits. The α1 constitutes the pore-forming subunit and confers the ion selectivity and pharmacological properties of the channels. The other subunits, β, α2δ, and γ, are accessory subunits that modulate the voltage-dependence of activation and inactivation kinetics of the channel (for review see: Kochegarov, 2003; Yamakage & Namiki, 2002).

The L-type and the N-type VGCCs are of particular importance to the work presented in this dissertation. The "L" in L-type VGCCs stands for long-lasting current (for review see: Catterall, Perez-Reyes, Snutch, & Striessnig, 2005). L-type Ca^{2+} channels are activated by voltage commands positive to -10 mV. These channels can be blocked by dihydropyridines (DHPs) (Fox, Nowycky, & Tsien, 1987), such as nimodipine, an antagonist used in this dissertation.

In neurons, L-type channels are mainly present in the soma and dendrites; however, they are not present in the axons (Ahlijanian, Westenbroek, & Catterall, 1990; Westenbroek, Ahlijanian, & Catterall, 1990). L-type Ca^{2+} channel-mediated Ca^{2+} entry in the somatodendritic compartment might be important for initiating intracellular regulatory events that may play a role during neuronal differentiation. Due to its location in the cell, these channels may also play a role in postsynaptic integration during basal synaptic transmission and after synaptic plasticity (Bi & Poo, 1998; Magee & Johnston, 1997; Yuste & Denk, 1995).

N-type VGCCs are termed “N” because they were first identified in neurons (for review see: Catterall, Perez-Reyes, Snutch, & Striessnig, 2005). N-type Ca^{2+} channels are activated after depolarizations greater than -30 mV (Fox, Nowycky, & Tsien, 1987). These channels are

irreversibly antagonized by a snail toxin isolated from the Conus geographus snail called ω-conotoxin GVIA (GVIA) (Kerr & Yoshikami, 1984; Olivera, McIntosh, Curz, Luque, & Gray, 1984). The GVIA-sensitive component makes the majority of the HVA current in chick dorsal root ganglion neurons (Aosaki & Kasai, 1989; Kasai, Aosaki, & Fukuda, 1987), rat sympathetic neurons and PC12 cells (Plummer, Logothetis, & Hess, 1989). The N-type Ca^{2+} channels are located in the active zone of the nerve terminal. Due to this location, they play an important role in exocytosis (Bezprozvanny, Scheller, & Tsien, 1995; Dunlap, Luebke, & Turner, 1995; R. J. Miller, 1990; Stanley, 1997; Wu, Westenbroek, Borst, Catterall, & Sakmann, 1999). Previous studies demonstrated that N-type Ca^{2+} channels play a prominent role in synaptic vesicle recycling and glutamate release in developmental stage (Iwasaki & Takahashi, 1998; Pravettoni et al., 2000; Scholz & Miller, 1995; Verderio, Coco, Fumagalli, & Matteoli, 1995).

The pathology of VGCCs in the cerebellum is largely characterized by ataxia. This happens in the stargazer mice that possess a recessive mutation on chromosome 15, which silences the expression of the VGCCs subunit γ2 (Letts et al., 1998; Sharp et al., 2001). Chemicals like MeHg can also affect the function of Ca^{2+} channels (Leonhardt, Pekel, Platt, Haas, & Büsselberg, 1995; Marty & Atchison, 1998; Sirois & Atchison, 2000) and produce symptoms, such as ataxia (Charbonneau et al., 1974; Harada, 1995; Hunter, Bomford, & Russell, 1940).

MeHg exposure affects the function of HVA VGCCs. The proteins of the cell membrane are the first to come in contact with exogenous compounds; therefore, it is not surprising that MeHg affects the function of Ca^{2+} channels. Studies in murine neuromuscular junctions (Atchison, 1986; Atchison, 1987), in NG108-15 cells (Hare & Atchison, 1995b) and in cerebellar granule cells (Marty & Atchison, 1997; Sirois & Atchison, 2000) propose that MeHg might use

Ca^{2+} channels to move through the plasma membrane. It is hypothesized that the influx of MeHg through Ca^{2+} channels contributes to the MeHg-induced rise in intracellular Ca^{2+} (Hare, McGinnis, & Atchison, 1993; M. F. Hare & Atchison, 1995b; Marty & Atchison, 1997). In cerebellar granule cells, MeHg induces entry of Ca^{2+} through L, N, and/or P/Q-type VGCCs and produces cell death (Marty & Atchison, 1997). MeHg can also affect other cell types, such as synaptosomes (Atchison, Joshi, & Thornburg, 1986), and PC12 cells, where it blocks the L-type and N-type Ca^{2+} channels (Shafer & Atchison, 1991). The increase in intracellular Ca^{2+} by MeHg on the VGCCs may participate in altered patterns of spontaneous and nerve-evoked release of neurotransmitters (Atchison, 1986).

C.2. Methylmercury-induced release of glutamate neurotransmitter

As previously stated, MeHg can induce glutamate release through the increase of $[Ca^{2+}]_i$; this increase is produced by intracellular Ca^{2+} stores and membrane Ca^{2+} channels. MeHg can also produce an increase in Ca^{2+} concentration and glutamate release by its effect on glutamate receptors, such as α-amino-3-hydroxy-5-methyl-4-isoxazolepropionic acid (AMPA) and N-methyl-D-aspartate (NMDA) receptors. MeHg sensitizes AMPA receptors in mice, causing an entry of Ca^{2+} through the cell membrane (Johnson et al., 2011). Studies in which an NMDA receptor antagonist was used, show protection of primary motor neurons (Ramanathan and Atchison, 2011), cortical neurons (Xu et al., 2013) and SH-SY5Y cells (Petroni et al., 2011) from MeHg-induced Ca^{2+} dysregulation and cytotoxicity.

Excitation of cells can be inhibited by the interaction of the agonist gamma-aminobutyric acid (GABA) on the GABA receptor. However, MeHg blocks $GABA_A$ receptors in neurons. The block of inhibitory postsynaptic currents in neurons after MeHg exposure occurs earlier in

granule cells than in neighboring Purkinje cells (Yuan & Atchison, 2003). It was hypothesized that the differential sensitivity to MeHg exposure was due to the differential expression of $GABA_A$ receptor phenotypes in granule and Purkinje cells (Herden, Pardo, Hajela, Yuan, & Atchison, 2008). Granule cells are the only neurons in the cerebellum that express the α6 subunit-containing $GABA_A$ receptor (Luddens, Pritchett, Kohler, Killisch, & Keinanen, 1990; Varecka, Wu, Rotter, & Frostholm, 1994), which plays a crucial role in regulating granule cell excitability by controlling a tonic inhibitory conductance (Brickley, Cull-Candy, & Farrant, 1996). A whole-cell recording study performed on cerebellar granule cells (α_6-containing) and cerebral cortical neurons (α_6-deficient) found that GABA current in granule cells was more sensitive to the effects of MeHg than were in cortical cells. However, the author also found that the expression of the α_6 subunit alone does not produce the sensitivity observed in cerebellar granule cells. Therefore, other factors may be involved in the blocking of $GABA_A$ receptors in granule cells (Herden et al., 2008).

Yuan and Atchison (1997) found that the $GABA_A$ receptor antagonist, bicuculline, inhibits the initial increase in excitatory transmission produced by MeHg. For this reason, it is hypothesized that MeHg unmasks an excitatory effect by decreasing tonic $GABA_A$ receptor function to mediate inhibitory neurotransmission, thereby causing an increase in glutamate release from granule cells (Atchison, 2005; Arakawa, Nakahiro, & Narahashi, 1991). The released glutamate can increase $[Ca^{2+}]_i$ by interacting with metabotropic glutamate receptors of the nerve terminal or by depolarizing the cell membrane (Atchison, 2005). The presence of glutamate in the extracellular environment for long period of time can trigger excitotoxicity (Olney, 1978; Olney, Price, Samson, & Labruyere, 1986). Because in the absence of glutamate neurons are unaffected by the exposure to Hg (Brookes, 1992), it is possible that MeHg-induced

release of glutamate might be the main factor that causes MeHg-induced neuronal death.

D. Astrocytes

The term “astrocyte” was based on the morphology of the cell since its multiple processes make it look like a star. It is estimated that astrocytes compromise 20-25% of the total volume of the brain. In fact, in some brain regions, this cell might be even up to 50% (Hansson, 1988; Tower, 1988). These glial cells are the most numerous and diverse neuroglial cells in the central nervous system (CNS) (Hansson, 1988), and can be characterized by using an astrocyte marker called glial fibrillary acidic protein (GFAP).

D.1. Heterogeneity of astrocytes

Astrocytes from different parts of the CNS can react differently to the same stimulus (Blomstrand, Åberg, Eriksson, Hansson, & Rönnbäck, 1999; Cavalcante, Garcia-Abreu, Moura, Silva, & Barradas, 1996; Han, Koh, Lee, & Seong, 2004) due to their diverse biochemical characteristics. Like neurons, several types of astrocytic populations can coexist within a given brain region (Matyash & Kettenmann, 2010). Based on the morphology and distribution of astrocytes in the CNS, they have been traditionally classified as protoplasmic and fibrous astrocytes (Miller & Raff, 1984).

Protoplasmic astrocytes are particularly found in gray matter. They have a more complex morphology than fibrous astrocytes. Protoplasmic astrocytes are characterized by having spherical to oval nuclei and highly branched processes that occupy a large volume of their size. Fibrous astrocytes are found in white matter and have a predominantly star-like morphology

(Montgomery, 1994). These astrocytes are characterized by having oval nuclei and many filaments with little to moderate branching (for review see: Reichenbach & Wolburg, 2005).

Another classification of astrocytes, based on morphologic and immunohistochemical methods, was proposed by Raff and colleagues, in which astrocytes were divided into type 1 and type 2 astrocytes. Type 1 astrocytes are found in both developing grey and white matter. Type 1 astrocytes express GFAP but do not express A2B5 protein. Type 2 astrocytes are more neuron-like and are primarily found in white matter (Raff, Abney, Cohen, Lindsay, & Noble, 1983). These cells contact the neurons at the nodes of Ranvier (Raff et al., 1983; M. C. Raff, 1986). Type 2 astrocytes possess the A2B5 protein, which can be used in immunostaining techniques to differentiate between types 1 and type 2 astrocytes (Raff, Williams, & Miller, 1984). Representative micrographs of type 1 and type 2 astrocytes are shown in Figure 1.6. The morphological characteristics and regional origins of type 1 and type 2 astrocytes suggest that these two types of astrocytes could correspond to protoplasmic and fibrous astrocytes, respectively (Raff, Abney, & Miller, 1984; Raff, Williams, et al., 1984). A comparison between type 1 and type 2 astrocytes are shown in Table 1.3.

There have been several theories about the regional differences between astrocytes. Astrocyte heterogeneity might be due to: 1. phenotypic plasticity in the differentiated astrocytes, 2. separate astrocyte lineages, or 3. a combination of both. The plasticity theory presupposes that the heterogeneity in astrocytes is a consequence of extrinsic determinants, in which environmental cues (input) are obtained by the cell and expressed as phenotypic changes (output). In this theory, astrocytes are in an interdependent relationship with neurons, in which the astrocyte phenotype is designed or modified by the neurons that are near to them to facilitate

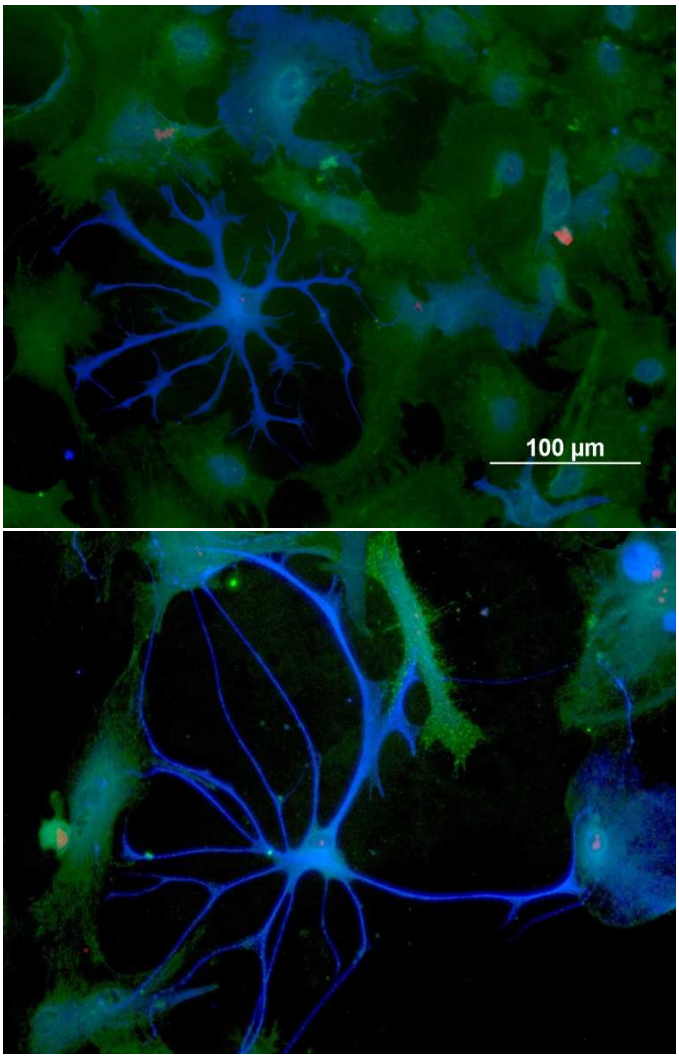

Figure 1.6. Representative micrographs of type 1 and type 2 astrocytes. Immunocytochemical images of type 1 and type 2 cortical astrocyte culture after a cytotoxicity assay using EthD-1 (20X). Type 1 astrocytes are stained only with GFAP (blue), type 2 astrocytes are stained with GFAP (blue) and A2B5 (green), and dead astrocytes have the nucleus stained with ethidium homodimer (red).

	Type 1 astrocytes	Type 2 astrocytes
Location	**Grey and white matter**	**White matter**
Protein expression	**Express GFAP but do not express A2B5 protein**	**Express GFAP and A2B5 protein**
Morphology	**Fibroblast-like morphology**	**Neuron-like morphology**
Progenitor cell	**GRP cell**	**O-2A cell**
Function	**Modulate neuronal function in the synaptic cleft**	**Modulate neuronal function in the neuronal axons**

Table 1.3. Comparison between type 1 and type 2 astrocytes. Type 1 astrocytes have a fibroblast-like morphology and are found in both developing grey matter and white matter. These astrocytes come from the glial-restricted precursor cell. Type 1 astrocytes express GFAP but do not express A2B5 protein. Type 2 astrocytes have a neuron-like morphology and are primarily found in white matter. These cells contact the neurons at the nodes of Ranvier. Type 2 astrocytes come from oligodendrocyte- type 2 astrocyte (O-2A) progenitor cells.

information processing (Hewett, 2009). The reason for the heterogeneity in astrocytes can also be a combination of these two theories.

The astrocyte lineage theory suggests that astrocytes in different regions of the CNS might originate from distinct progenitors (Bayraktar et al., 2015; Hewett, 2009). In early stages, the stem cells are present in both ventricular zone and subventricular zone. However, at later stages, stem cells are present in the adult brain and can be found in the ependymal layer lining the ventricular system (Johansson et al., 2015). Fibroblast growth factor (FGF)-dependent neuroepithelial stem cells are a class of stem cells that can generate neurons, astrocytes, and oligodendrocytes (Rao, 1999; Kalyani, Hobson, & Rao, 1997; Ray et al., 1993). FGF-dependent neuroepithelial stem cells generate neuron-restricted precursor cells that generate neurons (Mayer-Proschel et al., 1997). FGF-dependent neuroepithelial stem cells can also generate glial-restricted precursor cells that generate both astrocyte precursor cells and O-2A precursor cells (Rao, Noble, Mayer-Pröschel, 1998). The astrocyte precursor cells then differentiate into type 1 astrocytes (Mi, & Barres, 1999; Rao, 1999). The O-2A precursor cells generate oligodendrocytes and type 2 astrocytes (Raff, Miller, & Noble 1983). This is summarized in Figure 1.7.

Studies have demonstrated that astrocytes are more complex than previously thought. For instance, a study showed that astrocytes can be divided into nine different classes based on three complementary astrocyte labeling methods: GFAP–GFP-expressing mice and GFAP and S100β immunostaining. These nine classes were: radial cells, Bergmann glia, protoplasmic astrocytes or type 1 astrocytes, fibrous astrocytes or type 2 astrocytes, velate glia, marginal glia, perivascular glia, and ependymal glia (Emsley & Macklis, 2006). Due to the extensive literature available

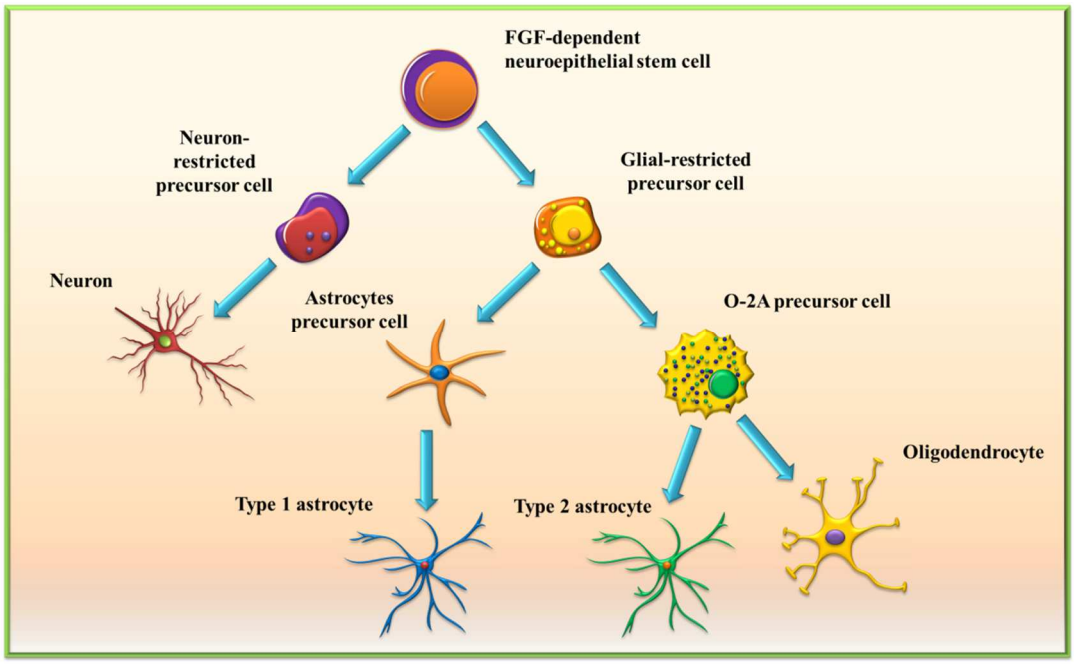

Figure 1.7. Possible astrocyte lineage. FGF-dependent neuroepithelial stem cells generate neuron-restricted precursor cells that generate neurons. FGF-dependent neuroepithelial stem cells can also generate glial-restricted precursor cells that generate both O-2A precursor cells and astrocyte precursor cells. The O-2A precursor cells generate oligodendrocytes and type 2 astrocytes. The astrocyte precursor cells then differentiate into type 1 astrocytes. Image modified from Motifolio Anatomy Drawing Toolkit available from http://www.motifolio.com/anatomy.html.

regarding traditional classifications of astrocytes, the present work focuses on type 1 and type 2 astrocytes.

D.2. Function of astrocytes

Astrocytes once referred to as a merely supportive cell type, are now recognized as glial cells with many important and diverse functions. Astrocytes perform functions, such as providing neurons with metabolic support, controlling extracellular potassium (K^+) homeostasis, buffering of glutamate excess, supplying glutamine to maintain glutamatergic neurotransmission, and many others.

1. Astrocytes provide neuronal metabolic support. Astrocytes can make contact with blood vessels, where they take up glucose from the blood, converting it to lactate. Then, astrocytes provide lactate to neurons as an energy substrate. Fascinatingly, this glial cell is the only cell type in the brain that can synthesize glycogen, and thus can work as an energy reservoir (for review see: Tsacopoulos & Magistretti, 1996). This is shown in Figure 1.8.

2. Astrocytes control extracellular K^+ homeostasis. After neuronal depolarization, there is an increase in positive charge that causes K^+ to move out of the cell. This release of K^+ from cells can modulate neuronal activity. Astrocytes remove excess K^+ from extracellular space, maintaining levels stable at their resting value (for review see: Walz, 2000). This is demonstrated in Figure 1.9.

3. Astrocytes buffer excess extracellular glutamate. Glutamate is the major excitatory

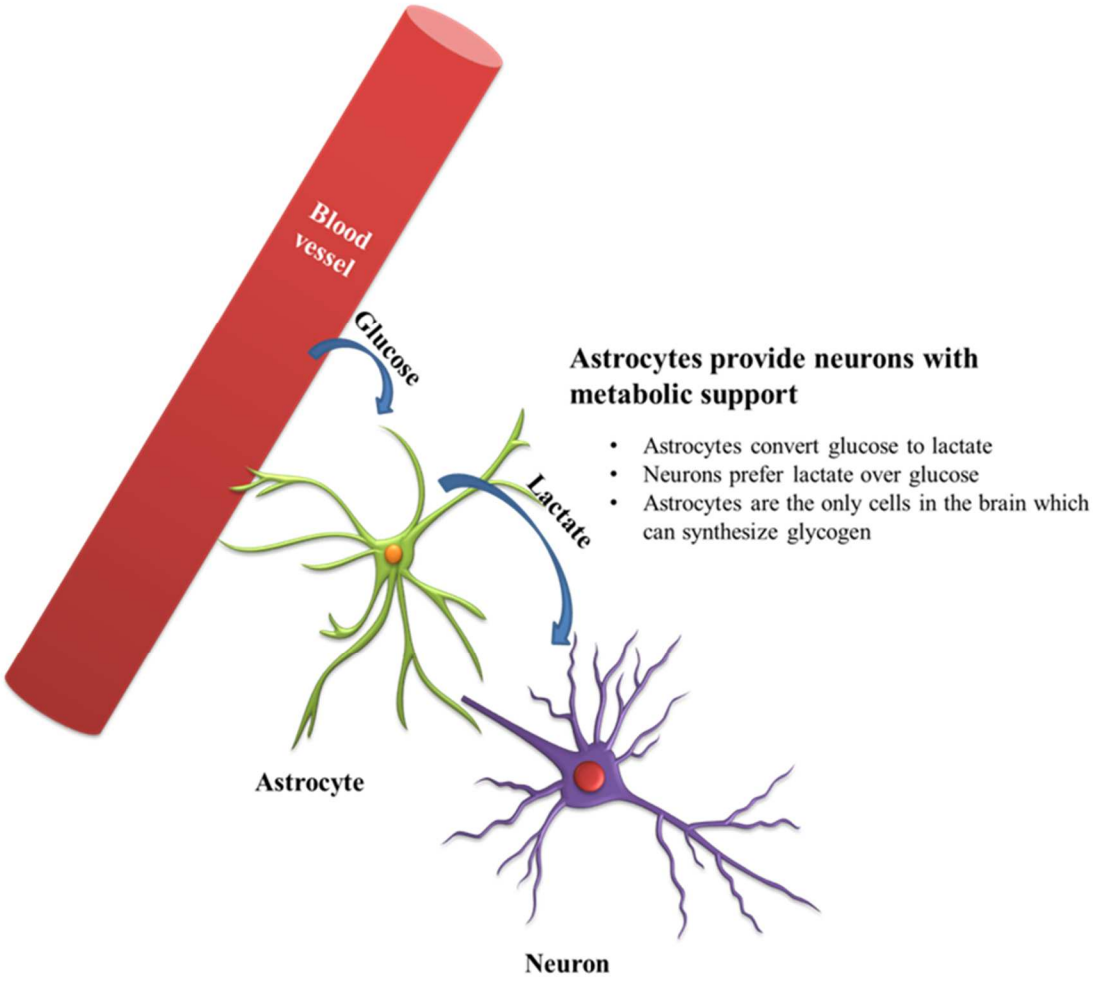

Figure 1.8. Astrocytes provide neuronal metabolic support. Astrocytes can make contact with blood vessels, where they take up glucose from the blood and convert it to lactate. Then, astrocytes provide lactate to neurons as an energy substrate. Fascinatingly, this glial cell is the only cell type in the brain that can synthesize glycogen, and thus can work as an energy reservoir. Image modified from Motifolio Anatomy Drawing Toolkit available from http://www.motifolio.com/anatomy.html.

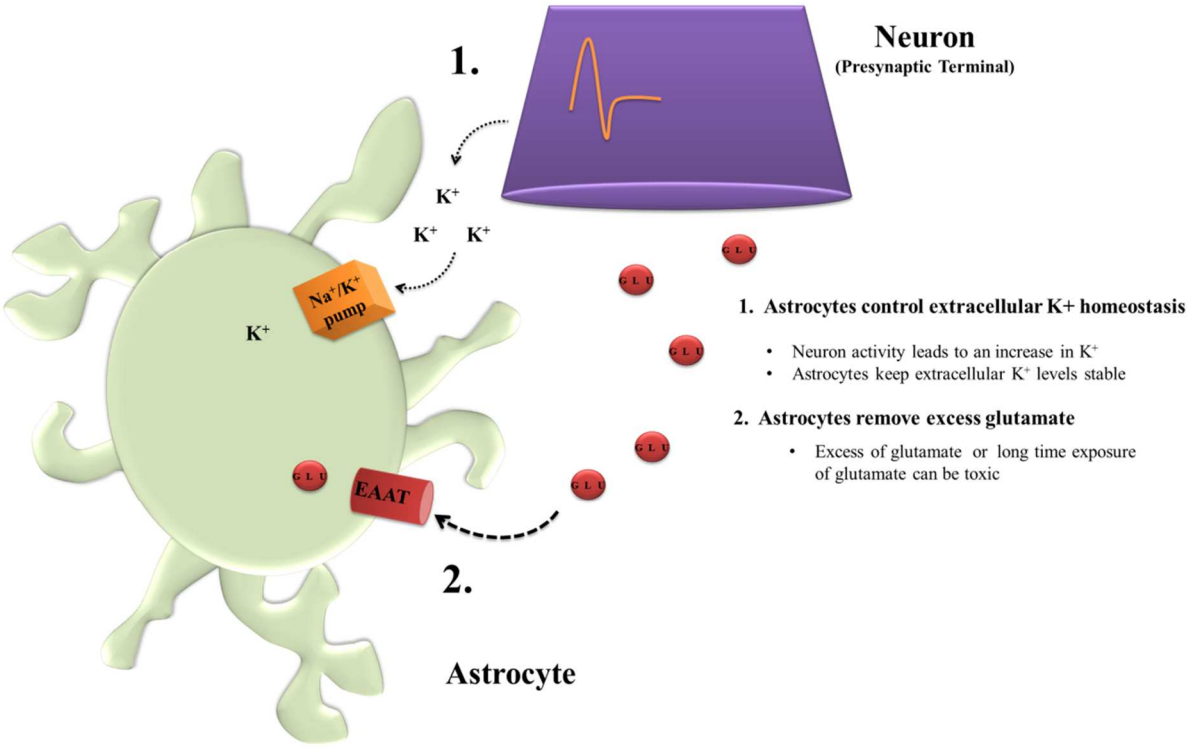

Figure 1.9. Astrocytes maintain an extracellular balance. 1. Astrocytes control extracellular K^+ homeostasis. After neuronal depolarization, there is an increase in positive charge that causes K^+ to move out of the cell. This release of K^+ from cells can modulate neuronal activity. Astrocytes remove excess K^+ from extracellular space through the Na+/K+ pump, maintaining levels stable at their resting value. 2. Astrocytes buffer excess extracellular glutamate. Glutamate is the major excitatory neurotransmitter. If this neurotransmitter is present in the extracellular environment for periods of time, it can trigger excitotoxicity and produce cell death. Astrocytes can remove 80% of the glutamate released; and therefore, prevent glutamate excitotoxicity.

neurotransmitter. If this neurotransmitter is present in the extracellular environment for periods of time, it can trigger excitotoxicity and produce cell death (Olney, 1978; Olney, Price, Samson, & Labruyere, 1986). Astrocytes can remove 80% of the glutamate released, and therefore prevent glutamate excitotoxicity (Danbolt, 2001; Rothstein et al., 1996). Astrocytes buffer glutamate through excitatory amino acid transporters (EAATs). There are five subtypes of glutamate transporters from the glutamate transporter family that are known as EAAT1–5. In animals, EAAT1–3 proteins are known as glutamate aspartate transporter (GLAST), glutamate transporter 1 (GLT1), and excitatory amino acid carrier 1 (EAAC1), respectively (Arriza, Eliasof, Kavanaugh, & Amara, 1997; Arriza et al., 1994; Fairman, Vandenberg, Arriza, Kavanaugh, & Amara, 1995; Pines et al., 1992). EAAT2 or GLT-1 is the most abundant subtype of glutamate transporter in the CNS, and hence it plays an important role in the regulation of glutamate neurotransmission (Furuta, Rothstein, & Martin, 1997; Lehre & Danbolt, 1998). This is demonstrated in Figure 1.9.

4. Astrocytes supply glutamine. Astrocytes supply glutamine to neurons in order to maintain glutamatergic neurotransmission. There are two ways in which astrocytes provide glutamine: by the enzymatic convention of glutamate into glutamine or by the synthesis of glutamine. After the extracellular glutamate is transported inside the astrocytes through EAAT, it is converted to glutamine by the astrocytic-specific glutamine synthetase. Glutamine is later released by the astrocytic system N transporters. Glutamine does not activate the glutamate receptor; therefore, it can be transported to the extracellular space without causing toxic effects. The system S transporters located on neurons take the glutamine inside the cytosol, where it is

converted to glutamate by glutaminase (for review see: Bak, Schousboe, & Waagepetersen, 2006). About 85% of the glutamate cycles in the glutamate-glutamine cycle; however, 15% is oxidized during the process. As a result, another way for glutamine synthesis emerges from this process. Astrocytes can also provide glutamine through the De novo synthesis of glutamate. This synthesis is performed by an enzyme called "pyruvate carboxylase" that is located in astrocytes (Patel, 1974; Waagepetersen, Qu, Schousboe, & Sonnewald, 2001), rather than in neurons (Shank, Bennett, Freytag, & Campbell, 1985). Through this process, a new molecule of glutamate is formed inside the astrocytic cytosol. Glutamate is then transformed into glutamine via glutamine synthesized and released into the extracellular space (Martinez-Hernandez, Bell, & Norenberg, 1977; Norenberg & Martinez-Hernandez, 1979). This is shown in Figure 1.10.

D.3. Calcium in astrocytes

Astrocytes can undergo $[Ca^{2+}]_i$ changes either spontaneously or in response to synaptic activity. Astrocytic Ca^{2+} can propagate to neighboring astrocytes over a long distance via Ca^{2+} waves. Astrocytes from different brain regions can exhibit distinct features of Ca^{2+} activity (Takata & Hirase, 2008). For example, intercellular Ca^{2+} waves can propagate differently from white to grey matter in astrocytes (Schipke et al., 2001). Many researchers have used Ca^{2+} sensitive dyes, such as fura 2 to investigate the effect of ligands on astrocytes Ca^{2+} levels. They have demonstrated that astrocytes have a wide variety of receptors that are linked to Ca^{2+} regulations (Charles, Merrill, Dirksen, & Sandersont, 1991; Cornell-Bell, Finkbeiner, Cooper, & Smith, 1990; Salm & McCarthy, 1990). It was also found that the increase in intracellular Ca^{2+} in

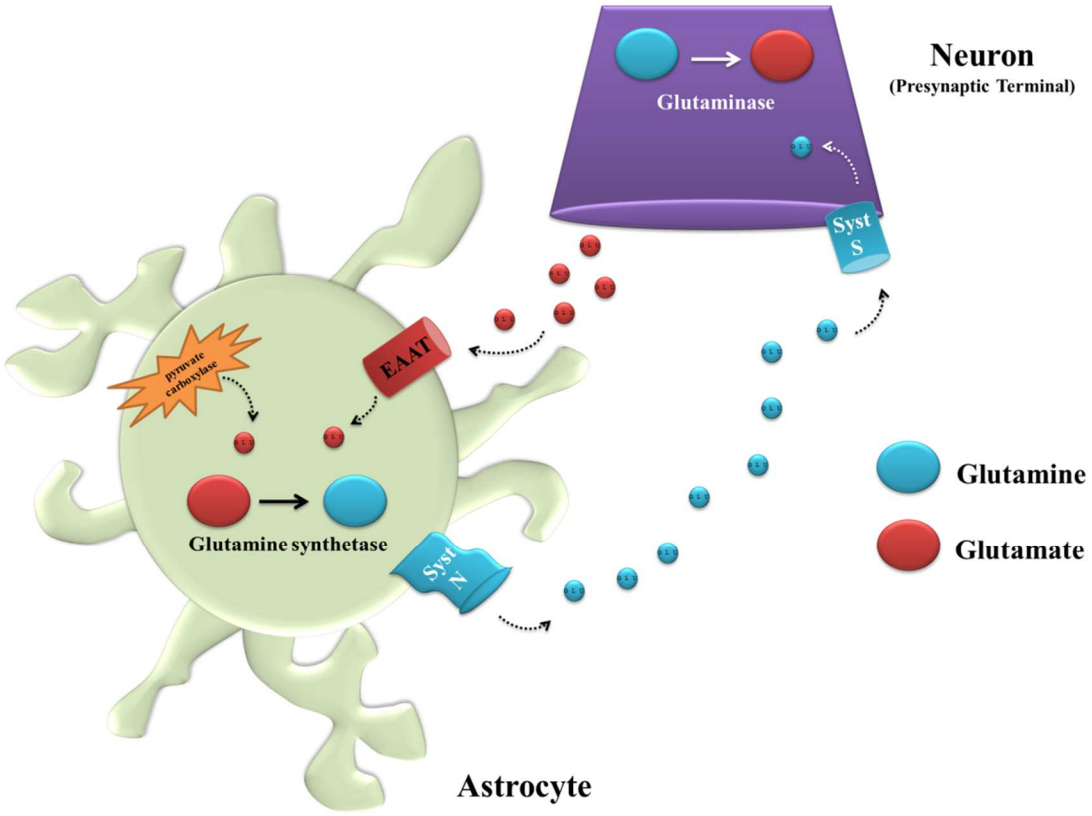

Figure 1.10. Astrocytes supply glutamine. After the extracellular glutamate is transported inside the astrocytes through EAAT, it is converted to glutamine by the astrocytic-specific glutamine synthetase. Glutamine is later released by the astrocytic system N transporters. The system S transporters located on neurons take the glutamine inside the cytosol, where it is converted to glutamate by glutaminase. About 15% of the glutamate is oxidized during this process. As a result, another way for glutamine synthesis emerges from this process. Astrocytes can also provide glutamine through the De novo synthesis of glutamate. This synthesis is performed by an enzyme called "pyruvate carboxylase" that is located in astrocytes. Glutamate is then transformed into glutamine via glutamine synthesized and released into the extracellular space.

astrocytes can result from the release of Ca^{2+} from intracellular storages and from the influx of Ca^{2+} through Ca^{2+} channels (for review see: Finkbeiner, 1993).

Astrocytes can release Ca^{2+} from intracellular stores and increase their $[Ca^{2+}]_i$ after the activation of ionotropic and metabotropic glutamate receptors. NMDA receptor can be found in cortical, spinal and cerebellar astrocytes, and when activated can induce a focal Ca^{2+} elevation (Schipke et al., 2001; Verkhratsky & Kirchhoff, 2007). In cerebellar astrocytes, AMPA receptors have been shown to be highly permeable to Ca^{2+} (Burnashev et al., 1992). Glutamate can stimulate the metabotropic glutamate receptor in astrocytes. The activation of the metabotropic glutamate receptor leads to Ca^{2+} release from internal stores (Cornell-Bell et al., 1990).

Another kind of receptors that when activated induces an increase in $[Ca^{2+}]_i$ are the bradykinin receptors. Astrocytes possess bradykinin receptors, especially the bradykinin receptor 2 (Gimpl et al., 1992). It has been reported that astrocyte cultures from cortex, cerebellum, and spinal cord respond to bradykinin (Cholewinski, Hanley, & Wilkin, 1988; Cholewinski & Wilkin, 1988). The activation of bradykinin receptors in astrocytes leads to an increase in Ca^{2+} concentration and glutamate release (Parpura et al., 1994).

Astrocytes can also increase their $[Ca^{2+}]_i$ through the influx of Ca^{2+} through Ca^{2+} channels (for review see: Finkbeiner, 1993). The expression of VGCCs in astrocytes is of particular importance due to the relevant role of internal Ca^{2+} as a second messenger. Stimuli that depolarize astrocytes can be sufficient to induce Ca^{2+} influx through Ca^{2+} channels. Increased extracellular K^+ concentrations from neuronal depolarization can induce Ca^{2+} influx through VGCCs on astrocytes (Duffy & MacVicar, 1996; Latour, Gee, Robitaille, & Lacaille, 2001).

In 1984, MacVicar showed for the first time that astrocytes in primary cultures express functional VGCCs (MacVicar, 1984). These findings were later confirmed by pharmacological

and physiological research that reported L-type and T-type Ca^{2+} currents in cultured astrocytes (Barres, Chun, & Corey, 1989; De Pina-Benabou, Srinivas, Spray, & Scemes, 2001; B. MacVicar & Tse, 1988). Today we know that astrocytes possess several functional VGCCs. Studies have reported the presence of N-type, L-type, R-type, and T-type VGCCs on astrocytes (D'Ascenzo et al., 2004; Latour, Hamid, Beedle, Zamponi, & Macvicar, 2003).

L-type Ca^{2+} channels appear to be the major type of Ca^{2+} channels found in cultured cortical astrocytes (Barres et al., 1989; Corvalan, Cole, de Vellis, & Hagiwara, 1990; MacVicar & Tse, 1988). The density of L-type Ca^{2+} channels in cortical astrocytes is enough to affect membrane electrophysiological proprieties and increase internal Ca^{2+} concentration (MacVicar, 1984; Macvicar, Hochman, Delay, & Weiss, 1991).

D.4. Astrocytes release glutamate

Astrocytes are located in close proximity to pre and postsynaptic neurons. This proximity of astrocytes to neurons allows them to be exposed to neurotransmitters. Astrocytes possess neurotransmitter receptors that can be activated by the binding of the neurotransmitters. The activation of the astrocytes neurotransmitter receptors produces a release of gliotransmitter and factors. This release of gliotransmitter can then affect both pre- and postsynaptic neurons. Some examples of gliotransmitters and factors released from astrocytes are d-serine, ATP, GABA, glutamate, and others (for review see: Araque et al., 2014). Studies demonstrated that astrocytes from the hippocampal dentate gyrus can release glutamate and activate neuronal NMDA receptors (Jourdain et al., 2007). Other studies show that astrocytes exposed to bradykinin result in a release of glutamate (Parpura et al., 1994). In this research, we focus on the glutamate release from astrocytes.

Contrary to neurons, astrocytes can release glutamate through different mechanisms. So far, six different mechanisms have been studied: reversal of uptake by glutamate transporters (Szatkowski, Barbour, & Attwell, 1990), cell swelling (Kimelberg, Goderie, Higman, Pang, & Waniewski, 1990), glutamate exchange via the cysteine-glutamate antiporter (Warr, Takahashi, & Attwell, 1999), release through ionotropic purinergic receptors (Duan et al., 2003), functional unpaired hemichannels (Ye, Wyeth, Baltan-Tekkok, & Ransom, 2003), and Ca^{2+}-dependent exocytosis (Parpura et al., 1994).

In 1994, Parpura discovered that astrocytes can release glutamate through Ca^{2+}-dependent mechanisms and that this release can modulate neuronal activities. The study shows that bradykinin can increase intracellular Ca^{2+} elevations in cultured astrocytes, resulting in the release of glutamate. The release of glutamate by astrocytes activates the NMDA receptor of surrounding neurons, producing a further increase in intracellular Ca^{2+}. Thus, an increase in $[Ca^{2+}]_i$ in astrocytes can be sufficient to cause glutamate release (Parpura et al., 1994). These findings have been supported by other studies. For instance, it was found that by buffering cytoplasmic Ca^{2+} with 1,2-Bis(2-aminophenoxy)ethane-N,N,N′,N′-tetraacetic acid tetrakis(acetoxymethyl ester) (BAPTA-AM) or depleting internal Ca^{2+} stores with thapsigargin, the release of glutamate from astrocytes is reduced (Araque, Sanzgiri, Parpura, & Haydon, 1998; Bezzi et al., 1998).

It has been suggested that exocytosis is the primary mechanism by which astrocytes release glutamate after an intracellular Ca^{2+} increase. Astrocytes have the secretory proteins necessary for gliotransmitter vesicular exocytosis, which includes the core SNARE complex: synaptobrevin 2, syntaxin 1 and synaptosome-associated protein of 23 kDa (SNAP-23) (Araque, Li, Doyle, & Haydon, 2000; Crippa et al., 2006; Hepp et al., 1999; Jeftinija et al., 1997;

Maienschein, Marxen, Volknandt, & Zimmermann, 1999; Montana, Ni, Hua, & Parpura, 2004; Parpura, Fang, Basarsky, Jahn, & Haydon, 1995; Pasti, Zonta, Pozzan, Vicini, & Carmignoto, 2001), and a Ca^{2+} sensor synaptotagmin 4 (Crippa et al., 2006; Zhang et al., 2004). The proteins necessary to transport glutamate into vesicles have also been discovered in astrocytes. One of these proteins is the vesicular glutamate transporter (VGLUT). The existence of vesicular proteins in astrocytes suggests that astrocytes release glutamate via a vesicular pathway (Malarkey & Parpura, 2008).

Previous studies have used Rose Bengal, a polyhalogenated fluorescein derivative, to inhibit the vesicular release of glutamate. Rose Bengal is a potent membrane-permeant inhibitor (K(i) = 19 nM) of glutamate uptake into isolated synaptic vesicles (Ogita et al., 2001). This inhibitor does not affect H^+-pump adenylpyrophosphatase (ATPase), but it reduces the proton gradient necessary for glutamate uptake into the vesicular lumen. The reduction of the proton gradient through VGLUTs decreases the intravascular proton concentration created by the vacuolar-type H^+-ATPase. Therefore, by the inhibition of VGLUTs and their proton gradient activity, Rose Bengal would lead to vesicular acidification. Studies have shown that the release of glutamate produced by bradykinin can be significantly reduced by the preincubation with Rose Bengal (Montana et al., 2004).

The increase in glutamate can produce more release of glutamate from this glial cell. Studies have demonstrated that local extracellular glutamate concentration can induce vesicular exocytosis in astrocytes, incrementing the amount of extracellular glutamate (Xu et al., 2007). The glutamate homeostasis in the brain is later balanced by its uptake. Higher extracellular glutamate levels or malfunctions of astrocytic glutamate transporters can lead to neuronal excitotoxicity (Schousboe & Waagepetersen, 2005). However, studies have demonstrated that

astrocytes can also be affected by glutamate excitotoxicity and that their vulnerability to this cell death mechanism varies from one region to another (David, Yamada, Bagwe, & Goldberg, 1996; Matute, Alberdi, Ibarretxe, & Sánchez-Gómez, 2002; Prieto & Alonso, 1999). The glutamate-induced gliotoxicity is mediated predominantly by a depletion of cytoplasmic GSH that resulted from the loss of glutamate inside the cell. This action leads to oxidative death (Chen, Liao, & Kuo, 2000).

E. Methylmercury-induced toxicity in astrocytes

In the absence of glutamate, neurons are unaffected by the exposure to Hg. This suggests that neuronal dysfunction comes after the effect of MeHg on astrocytes (Neville Brookes, 1992). MeHg preferentially accumulates in Bergmann glial cells, and other astrocytes and glial cells of white matter (Leyshon-Sørland, Jasani, & Morgan, 1994; Oyake, Tanaka, Kubo, & Chichibu, 1966). This toxicant produces a reactive gliosis of Bergmann glia in the molecular layer and astrocytes of the internal granule layer (Roda et al., 2008). MeHg is transported inside the astrocytes by the L-system transporter (Aschner, Eberle, Goderie, & Kimelberg, 1990). The mechanisms of MeHg efflux from astrocytes are controversial. Fujiyama proposed that MeHg conjugation with GSH is the major pathway of MeHg efflux (Fujiyama, Hirayama, & Yasutake, 1994). However, Aschner suggested that MeHg conjugates with L-cysteine and efflux from astrocytes through L-system transporter (Aschner, Eberle, & Kimelberg, 1991). Several mechanisms of MeHg toxicity in astrocytes have been studied, such as increase in reactive oxygen species (ROS), astrocyte swelling, decrease in glutamate uptake, amino acid release, and intracellular Ca^{2+} increase (see: Shanker, Syversen, & Aschner, 2003; Marty, Lundback, Autio, & Atchison, 2006).

Studies demonstrate that MeHg produces ROS (Ali, LeBel, & Bondy, 1991; Ganther et al., 1972). One way for MeHg to induce ROS in astrocytes is through the demethylation of MeHg. Studies using primary astrocyte models show that the conversion of MeHg into inorganic Hg increases with oxidative stress (Shapiro & Chan, 2008). Another way for MeHg to induce ROS in astrocytes is through the inhibition of cysteine uptake. Cysteine is a precursor of GSH (Kranich, Dringen, Sandberg, & Hamprecht, 1998); therefore, by inhibiting cysteine uptake, there is a reduction of the GSH levels in astrocytes. GSH plays a key role as an antioxidant in mammalian cells (Dringen, Pfeiffer, & Hamprecht, 1999; Jain, Mårtensson, Stole, Auld, & Meister, 1991; Kaur, Aschner, & Syversen, 2006). It has been shown that toxicity of MeHg can be increased by decreasing intracellular GSH levels (Aschner, Mullaney, Wagoner, Lash, & Kimelberg, 1994), or reduced by increasing intracellular GSH levels (Mullaney, Fehm, Vitarella, Wagoner, & Aschner, 1994; Park, Lim, Chung, & Kim, 1995). Different mechanisms of GSH protection have been elucidated, among which are the conjugation of GSH with MeHg, the buffering of MeHg by GSH, and GSH acting as an antioxidant. The depletion of GSH in astrocytes increases MeHg accumulation and enhances MeHg-induced oxidative stress. The excessive ROS is associated with the activation of cytosolic phospholipases A2; this activation produces astrocyte swelling (for review see: Shanker et al., 2003).

Another important protein that is disrupted by MeHg exposure is the nuclear factor erythroid 2-related factor 2 (Nrf2). NrF2 is a key factor when determining the protective antioxidant response against environmental toxicants. MeHg decreases Nrf2 activity, producing astrocyte death (Wang, Jiang, Yin, Aschner, & Cai, 2009).

Another way in which MeHg affects astrocytes is through the decrease in glutamate uptake. MeHg produces a concentration- and time-dependent decrease in glutamate uptake in

astrocytes (Aschner et al., 1990; N Brookes & Kristt, 1989; Qu, Syversen, Aschner, & Sonnewald, 2003). Previous studies have shown that MeHg inhibits the transportation of d-aspartate, a glutamate analog, in cultured astrocytes (Aschner et al., 1994; Aschner, Rising, & Mullaney, 1996). In a study performed on Chinese hamster ovary cells (CHO) transfected with the glutamate transporter subtypes GLAST or GLT-1, MeHg increased GLT-1 mRNA expression, but had no effect on GLAST. However, as GLT-1 protein levels decreased, GLAST protein levels increased (Mutkus, Aschner, Syversen, & Aschner, 2005). Conversely, another study performed on primary astrocytes from rats found a downregulation of both GLAST and GLT-1 in mRNA and protein levels at 10 μM MeHg (Liu et al., 2016). Due to the lack of research and the discrepancy in results, more research needs to be performed to determine the effect of MeHg on GLAST and GLT-1. However, all the results suggest an increase in extracellular glutamate due to MeHg effect on EAATs.

MeHg can also increase extracellular glutamate levels by producing glutamate release from astrocytes. Aschner and colleagues (1993) showed that 10 μM MeHg produced an efflux of glutamate and aspartate from astrocytes. The authors examined whether blockage of conductive ion fluxes, which has been implicated in astrocytic swelling, could reverse the MeHg-induced efflux of these amino acids. They concluded that the mechanisms associated with excitatory amino acid (EAA) efflux after MeHg treatment and the mechanisms associated with EAA after swelling differed. Therefore, this proves that other mechanisms by which glutamate efflux astrocytes are yet to be elucidated.

Other studies have also shown changes in extracellular EAA levels following MeHg treatment. However, it is important to highlight that these studies were focused on either the inability of astrocytes to uptake glutamate or the efflux of glutamate due to astrocytic swelling

(Aschner et al., 1993; Qu et al., 2003). In the present study, we examine the effect of MeHg on Ca^{2+}-induced vesicular release of glutamate in astrocytes.

Lastly, another way in which MeHg affects astrocytes is through the increase in $[Ca^{2+}]_i$. MeHg produces Ca^{2+} entry into the cytosol and Ca^{2+} release from intracellular storages in type 2 cerebellar astrocytes, inducing a triphasic response. The intracellular stores participate in all the three phases of the triphasic response. However, the extracellular Ca^{2+} influx contributes to the first and third phase of type 2 cerebellar astrocyte response. Marty and colleagues (2006) studied the contribution of various intracellular Ca^{2+} pools to the MeHg response. To evaluate the role of the SER in Ca^{2+} release during MeHg exposure, they used thapsigargin, an inhibitor of the sarco/endoplasmic reticulum Ca^{2+} ATPase. Surprisingly, astrocytes treated with thapsigargin and MeHg exhibited a higher increase in $[Ca^{2+}]_i$ compared with astrocytes exposed to MeHg only. Therefore, exclusion of the SER Ca^{2+} pool increased the MeHg-induced Ca^{2+} increase, suggesting that the SER pool does not contribute to the MeHg-induced increase in $[Ca^{2+}]_i$. To evaluate the contribution of the mitochondria in the increase of $[Ca^{2+}]_i$, they used carbonyl cyanide m-chlorophenyl hydrazone (CCCP) to cause Ca^{2+} release and inhibition of the mitochondrial Ca^{2+} accumulation. They found that the mitochondria contribute to early changes in $[Ca^{2+}]_i$. Therefore, the mitochondria, but not the SER contributed to the $[Ca^{2+}]_i$ elevations. However, with the use of CCCP, they were unable to alleviate the entire increase in $[Ca^{2+}]_i$, suggesting that other cell components may also play a role in intracellular Ca^{2+} dysregulation.

Changes in $[Ca^{2+}]_i$ occurs faster in astrocytes than in granule cells; in where at 0.5, 1 and 2 μM MeHg astrocytes showed a $[Ca^{2+}]_i$ increases at 7.2, 3.2 and 2.2 min (Marty, Lundback, Autio, & Atchison, 2006), and granule cells showed a $[Ca^{2+}]_i$ increases at 10, 7 and 5 min, respectively (Marty & Atchison, 1997). This data could support the hypothesis which states that neurotoxicity

mediated by MeHg occurs secondary to effects on glial cell functions (Aschner, Yao, Allen, & Tan, 2000). In this dissertation, we considered the previous data and aimed to determine whether changes in $[Ca^{2+}]_i$ are sufficient to alter astrocytes cell function and induce cell death.

F. Differences between cortical and cerebellar astrocytes toxicity to methylmercury

Differences between cortical and cerebellar astrocytes after MeHg treatment have been studied (Adachi & Kunimoto, 2005; Gassó et al., 2001; Morken, Sonnewald, Aschner, & Syversen, 2005; Mundy & Freudenrich, 2000). Research demonstrates differences in the MTT activity and the ROS levels in cortical and cerebellar astrocytes (Kaur, Aschner, & Syversen, 2007; Morken et al., 2005).

Morken and colleagues (2005) showed a difference between cortical and cerebellar astrocytes, in where, at low MeHg concentrations with a prorogated exposure time of 24 h, there was a decrease in the MTT activity in cortical astrocytes. A decrease in MTT activity was not observed in cerebellar astrocytes. This suggests a susceptibility of the cortical astrocyte mitochondria to the toxic effects of MeHg. However, another study that used ^{13}C nuclear magnetic resonance spectroscopy found that the percentage of [U-^{13}C] glutamate used for energy production was decreased after 4 h of 25 μM and 50 μM MeHg exposures in cerebellar astrocytes (Qu et al., 2003). These results indicate a selective mitochondrial vulnerability due to the inhibitory effect of MeHg on these astrocytes. The mitochondria are shown to be affected in both cerebellar and cortical astrocytes after MeHg treatment; therefore, these studies do not provide enough evidence for the differential susceptibility between cortical and cerebellar astrocytes.

Another study that tried to understand differential susceptibility between cortical and cerebellar astrocytes demonstrated that cerebellar astrocyte cultures were more vulnerable to ROS than cortical astrocyte cultures after MeHg treatment, and that MeHg produces higher levels of ROS in cerebellar astrocytes than in cortical astrocytes. It was hypothesized that the higher amount of GSH in cortical astrocytes after exposure to MeHg could be the reason why these astrocytes are less susceptible to MeHg toxicity. However, cerebellar neurons are more susceptible to MeHg toxicity than cortical neurons and there are no differences in their levels of GSH. For this reason, differential levels of GSH in cortical and cerebellar astrocytes do not provide an explanation for the differential susceptibility to MeHg toxicity in astrocytes (Kaur, Aschner, & Syversen, 2007). Thus, better explanations for the differences in susceptibility between astrocytes after MeHg treatment are needed.

G. Methylmercury-induced astrocyte death

It has been shown that MeHg can cause necrotic cell death (Miura, Imura, & Clarkson, 1987; Nakada & Imura, 1983). However, other studies have attributed cell death to the activation of apoptotic pathways, at least at lower MeHg concentrations (Kunimoto, 1994; Nagashima et al., 1995). In a recent study focused on the mechanisms of MeHg toxicity in primary astrocytes and neurons of rats, the authors argued that there was a glutamate mechanism that mediated cytoskeletal disruption and induced apoptosis in neurons, and a glutamate-independent mechanism that mediated cytoskeletal disruption and induced necrosis in astrocytes (Pierozan et al., 2016). Therefore, most of the studies indicate that MeHg induces astrocyte death by necrosis.

H. Hypothesis and aims

MeHg affects the nervous system, especially the granule cells in the cerebellum (Hunter & Russell, 1954). The reason for the sensitivity of the granule cells to MeHg is believed to be the result of unregulated elevations in $[Ca^{2+}]_i$ (Atchison, 2005; Limke, Bearss, & Atchison, 2004). The increase of $[Ca^{+2}]_i$ produces an increase in glutamate release which results in excitotoxicity (Atchison, 2005). This is shown in Figure 1.11. Astrocytes can buffer excess glutamate from the extracellular space, protecting the neurons from excitotoxicity (Anderson & Swanson, 2000). It has been hypothesized that neurotoxicity by MeHg occurs secondary to effects on glial cell functions (Aschner, Yao, Allen, & Tan, 2000). Therefore, understanding the effect of MeHg on astrocytes will help us understand the sensibility of granule cells to MeHg.

MeHg-induced cytotoxicity in astrocytes has been studied extensively in the cortical layer (Aschner, Conklin, Yao, Allen, & Tan, 1998; Aschner, Rising, & Mullaney, 1996; Aschner, Vitarella, Allen, Conklin, & Cowan, 1998). However, effects on cerebellar astrocytes are less studied. Because regional differences can occur in astrocytes between the two areas, there is a critical need to understand the effect of MeHg on cerebellar astrocytes. The goal of this dissertation is to compare MeHg toxicity on cerebellar and cortical astrocytes, and to understand the contribution of astrocytes during MeHg-induced neuronal toxicity. We hypothesize that an acute MeHg exposure will induce different toxicological effects on cerebellar and cortical astrocytes, such as cytotoxicity and increase in extracellular glutamate levels. A representation of this hypothesis is shown in Figure 1.12.

The effects caused by an acute MeHg exposure on astrocytes were assessed by three studies. The first study, presented in Chapter 2, was designed to examine whether there are

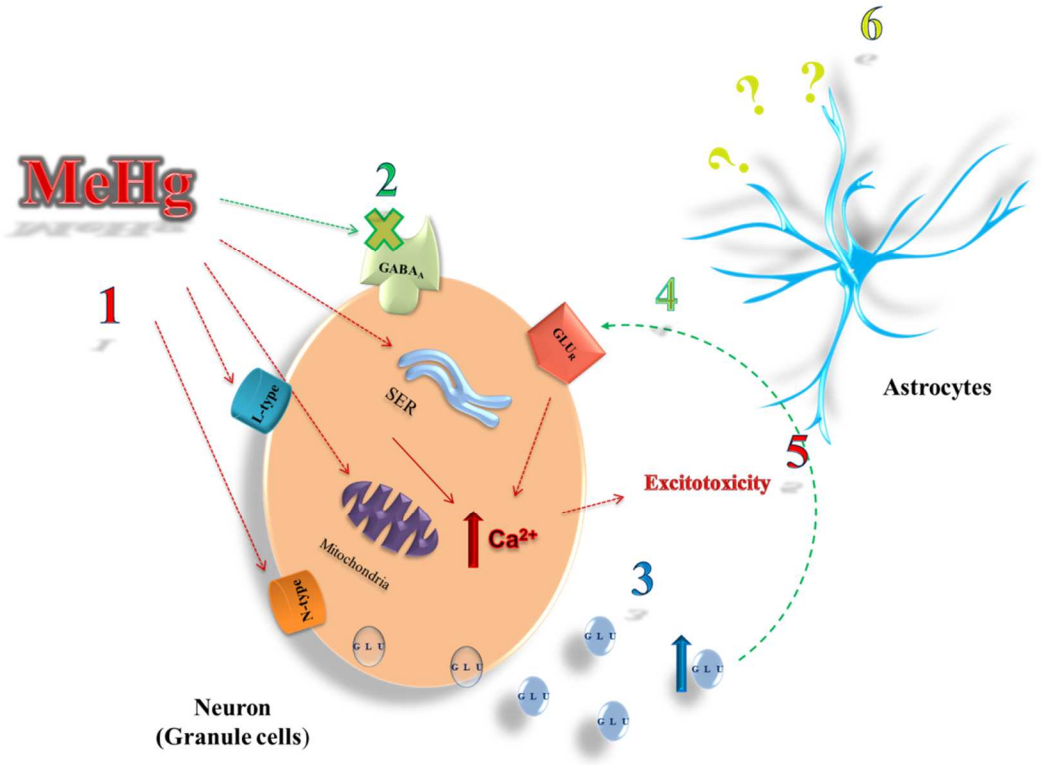

Figure 1.11. Mechanisms of MeHg-induced toxicity in granule cells. 1. MeHg increases the internal $[Ca^{+2}]_i$ by interacting with the mitochondria, the SER, and VGCCs, such as L-type and N-type Ca^{+2} channels. 2. MeHg blocks $GABA_A$ receptors, which can decrease the function of the channel to mediate inhibitory neurotransmission. 3. The increase in $[Ca^{+2}]_i$ and the inhibition of the inhibitory function produce a high vesicular release of glutamate. 4. Glutamate interacts with the glutamate receptors, increasing $[Ca^{2+}]_i$. 5. Eventually, granule cells die by the excitotoxicity of glutamate. 6. Astrocytes are the main cells in charge of buffering glutamate and protecting granule cells from excitotoxicity. What happened to astrocytes? Are they not preventing excitotoxicity? Image modified from Motifolio Anatomy Drawing Toolkit available from http://www.motifolio.com/anatomy.html.

typological or/and regional differences in the viability of cortical and cerebellar astrocytes after an acute exposure to MeHg, and to understand factors that can contribute to such differences. The second study, presented in Chapter 3, was designed to examine whether an acute exposure to MeHg can produce changes in extracellular glutamate levels in cortical and cerebellar astrocytes, and to understand the possible mechanisms that can contribute to such changes. Finally, the role of cerebellar astrocytic organelles and membrane proteins in the release of glutamate and the decrease in viability after an acute exposure to MeHg is investigated in Chapter 4. Together these studies propose a mechanism for MeHg toxicity in astrocytes that can contribute to the susceptibility that cerebellar neurons have to MeHg.

I. Primary astrocyte cell cultures as a model to study methylmercury toxicity

Over the past decades, it has been discovered that astrocytes have a more important role in the CNS activities than previously thought. The majority of our current knowledge about astrocytes has been obtained from studies performed on primary cultures of astrocytes. Such cultures have been a vital tool for understanding the function of astrocytes in physiological and pathological conditions. By using *in vitro* techniques, we are able to obtain more information regarding the mechanisms of MeHg in astrocytes. This information is difficult to obtain by using *in vivo* models. Therefore, the experiments in this dissertation were performed on primary mice cortical and cerebellar astrocyte cultures to allow for detailed study of the actions of MeHg in those cells. Both cortical and cerebellar astrocytes were used in order to compare the astrocytes from the region of the brain where neurons are more susceptible to MeHg (cerebellum) with the astrocytes from the region of the brain where neurons are less susceptible to MeHg (forebrain).

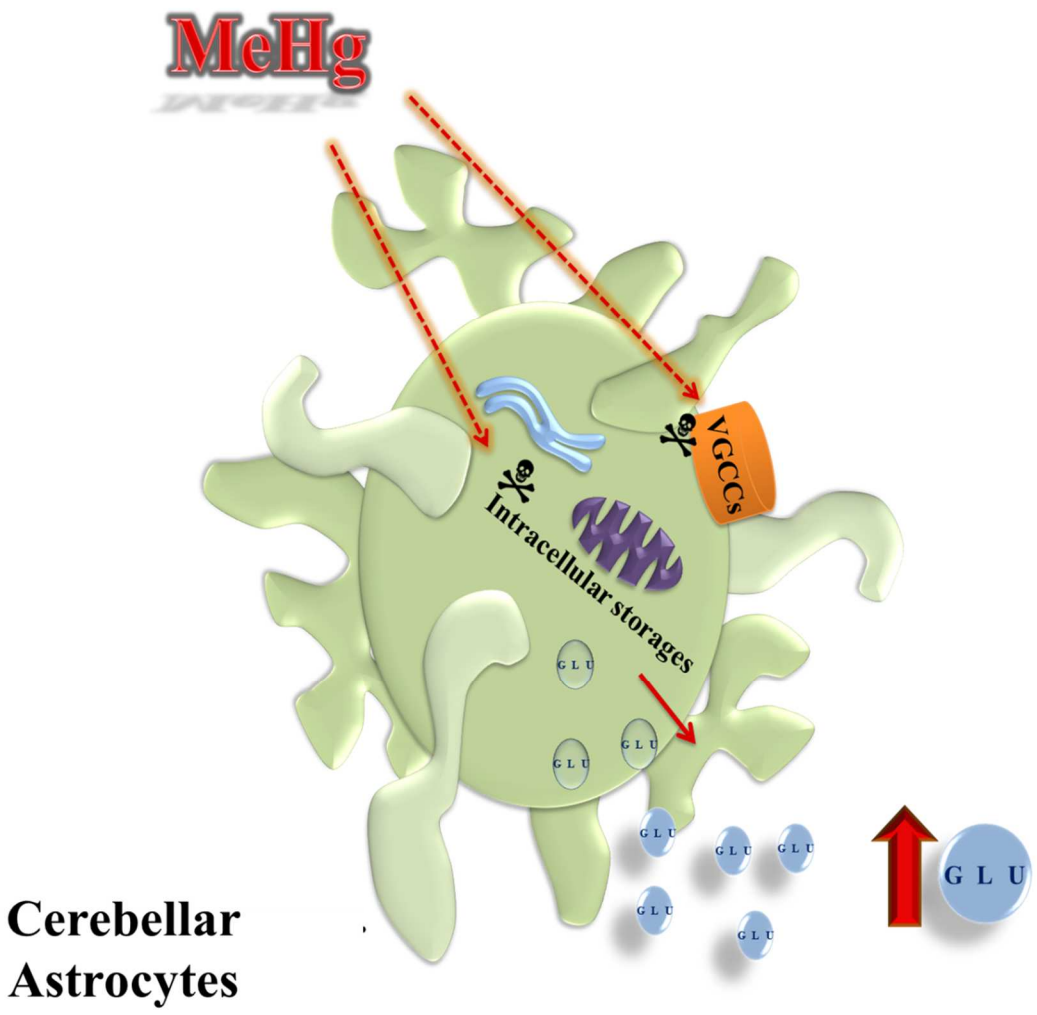

Figure 1.12. Hypothesized MeHg toxicity in astrocytes. We hypothesize that an acute MeHg exposure will induce different toxicological effects on cerebellar and cortical astrocytes, such as cytotoxicity and increase in extracellular glutamate levels. We also hypothesize that MeHg will interact with intracellular storages and VGCCs in cerebellar astrocytes.

By comparing astrocytes from these two different brain regions, we might be able to elucidate possible mechanisms of MeHg toxicity.

Astrocytes were isolated from neonatal mice of both sexes of approximately 7-8 days old. This age goes parallel with previous studies performed on primary cultures of cerebellar granule cells (Fonfría, Vilaró, Babot, Rodríguez-Farré, & Sunol, 2005; Kaur, Aschner, & Syversen, 2006; Limke et al., 2004; Limke, Otero-Montañez, & Atchison, 2003). After isolation, the astrocytes continued to grow and mature in cultures. In the experiments performed for this dissertation, all astrocytes were used at day *in vitro* (DIV) 13-15 to allow for maturation of cells. At these DIV, astrocytes possess L-type and N-type VGCCs (Latour, Hamid, Beedle, Zamponi, & Macvicar, 2003), glutamate receptors (Biber et al., 1999), bradykinin receptors (Gimpl, Walz, Ohlemeyer, & Kettenmann, 1992), and glutamate transporters (Kondo et al., 1995). Therefore, astrocytes express many membrane proteins that are present in functional mature astrocytes.

Due to the important role that astrocytes in the CNS play in preventing excitotoxicity, primary cultures of astrocytes are a suitable model for the study of MeHg neurotoxicity.

J. Techniques

J.1. Viability/Cytotoxicity Assay

Viability/Cytotoxicity Assay (Molecular Probes Inc., OR, USA) is used to identify the astrocytes that are dead or alive. By using the Viability/Cytotoxicity Assay, the membrane of the healthy cells are stained in the color green with acetoxymethyl ester (calcein-AM) and the nucleus of dead cells are stained in the color red with ethidium homodimer-1 (EthD-1). Live cells are known to possess an omnipresent intracellular esterase activity. Calcein-AM, which is membrane permeable and non-fluorescent, crosses the membrane of the live cells and generates

an intense green fluorescence due to an enzymatic hydrolysis by the intracellular esterase activity. EthD-1 enters dead cells through its damaged membrane and binds to nucleic acids in both DNA and RNA, producing a bright red fluorescence. EthD-1 is highly positive; therefore, it will not cross cell membranes to stain living cells (for review see: Fritzsche & Mandenius, 2010). In our dissertation, we focused on the total amount of astrocytes and the amount of astrocytes that contained EthD-1 to obtain the percentage of viable cells.

$$\text{Percentage of live astrocytes} = \left(\frac{(Total\ amount\ of\ astrocytes - Amount\ of\ dead\ astrocytes\ )}{Total\ amount\ of\ astrocytes}\right) \times 100$$

Astrocytes can buffer dyes, such as ethidium bromide (EtBr), through connexin and pannexin hemichannels (for review see: Sáez et al., 2010; Giaume et al., 2013). However, other studies demonstrated that the influx of EtBr is mainly through connexins, rather than through pannexins (Retamal et al., 2007). In our studies, we used EthD-1, which has a different chemical structure and a higher sensitivity than EtBr. Unlike EtBr, EthD-1 does not seem permeable to hemichannels. Previous studies, aimed at investigating the effect of intrinsic and extrinsic factors on astrocytes, have used EtBr to study the hemichannel function and EthD-1 to study cellular viability in the same project (Abudara et al., 2015; Ramachandran et al., 2007). Several other studies have used EthD-1 to access astrocyte viability (Yu et al., 2002; Gabryel et al., 2002; Vaughan et al., 1995).

To the best of our knowledge, there are no studies that demonstrate that MeHg produces an uptake of EtBr by affecting the activity of hemichannels in astrocytes. Because there are no studies that demonstrate either an uptake of EthD-1 through hemichannels or an effect of MeHg on the activity of astrocytic hemichannels, in this dissertation we consider the astrocytes that contain EthD-1 as astrocytes that are dead.

J.2. Immunocytochemistry

Immunocytochemistry (ICC) is the detection of antigens in a cell by means of specific antibodies. The advantage of ICC over other protein detection methods is the capacity to verify the presence of an antigen with its location in a cell and to distinguish between cells in a tissue or cells in a cell culture dish. This technique is important for the study of cell function in normal and pathological tissues. ICC also provides a semiquantitative approach that allows us to estimate the levels of protein expression in a determinate cell (for review see: Ramos-Vara, 2011; de Matos, 2010).

J.3. Glutamate assay

Glutamate assay is a colorimetric assay that quantitates the amount of glutamate by measuring the chromogenic reaction product at a characteristic wavelength. The concentration of glutamate is determined by an enzymatic activity, which results in a colorimetric (450 nm) product relative to the glutamate present. This enzymatic activity is based on the synthesis of α-ketoglutarate from glutamate by glutamate dehydrogenase. This assay is fast and very sensitive. It provides detection of the glutamate in a variety of samples, including cell culture supernatants. We used the commercially available kit from Sigma-Aldrich Co. (St. Louis, MO).

CHAPTER TWO:

DIFFERENTIAL REGIONAL SUSCEPTIBILITY OF CEREBELLAR AND CORTICAL ASTROCYTES TO METHYLMERCURY-INDUCED CYTOTOXICITY: POTENTIAL ROLE OF INTRA- AND EXTRACELLULAR CALCIUM

A. Abstract

The objective of the present study was to examine whether there were typological or/and regional differences in the viability of cortical and cerebellar astrocytes after an acute exposure to MeHg, and to understand if intracellular and extracellular Ca^{2+} can contribute to such differences. Primary astrocyte cultures from the cerebellum and cortical forebrain layer were obtained from 7 to 8 day old C57BL/6 mice. At 13-15 DIV, cells were exposed for 3 h to 0, 1, 2, or 5 μM MeHg. In order to distinguish between type 1 and type 2 astrocytes, cells were stained with the antibodies A2B5 and GFAP. Cytotoxicity was measured immediately after the 3 h of exposure or 24 h after exposure using ethidium homodimer-1 (EthD-1) and acetoxymethyl ester (calcein-AM). To determine if astrocyte death was due to an increase in intracellular Ca^{2+}, the chelator BAPTA-AM (10 μM) was added. To test whether extracellular Ca^{2+} contributed to cytotoxicity, the cell-impermeant chelator ethylene glycol-bis(2-aminoethylether)-N,N,N',N'-tetraacetic acid (EGTA) (0.02 mM) was used in a Ca^{2+}-free buffer. Although there were no significant differences in viability between types of astrocytes from the same brain region, there were differences in viability when comparing the same type of astrocytes from cortex and cerebellum. Cortical astrocytes treated with BAPTA-AM + 5 μM MeHg had an increase in normalized viability of approximately 75% in comparison with cortical astrocytes that were treated with 5 μM MeHg. In cerebellar astrocytes, BAPTA-AM + MeHg significantly reduced the incidence of MeHg-induced cell death to approximately 54% and 50% at both 2 μM and 5 μM MeHg respectively, compared to the MeHg group that did not receive BAPTA-AM. EGTA did not protect cortical astrocytes from MeHg-induced cytotoxicity. However, it significantly reduced the incidence of MeHg-induced cell death to 68% and 89% at 2 μM and 5 μM MeHg, respectively in cerebellar astrocytes. Thus, while both cortical and cerebellar astrocytes undergo

MeHg-induced cytotoxicity, the sensitivity of this glial cell in the two regions differs, as does the relative contribution of intracellular and extracellular Ca^{2+} to cytotoxicity. It is possible that this susceptibility of cerebellar astrocytes to MeHg contributes to the susceptibility of granule cells to this metal in the cerebellum.

B. Introduction

MeHg contamination remains a global health concern. This potent neurotoxicant is mainly contained in fish, which becomes a threat to populations with high consumption of this nourishment (Li, Feng, & Qiu, 2010). MeHg can affect both the peripheral and central nervous system; however, the granule cells in the cerebellum are preferential targets of MeHg neurotoxicity (Hunter & Russell, 1954). The granule cells have an important role in cerebellar function because they are the only glutamate-releasing neurons in the cerebellar cortex. Dysfunction of the granule cells has been associated with ataxia (Ohgoh, Yamazaki, Ogura, Nishizawa, & Tanaka, 2000; Zhong et al., 2005) and cognitive deficit (Ogura et al., 2002). The precise cellular mechanism for the loss of granule cell viability after MeHg exposure is unknown, though it is believed to be the result of unregulated elevations in $[Ca^{2+}]_i$ (Atchison, 2005; Limke, Heidemann, & Atchison, 2004).

MeHg can produce two distinctive phases of $[Ca^{2+}]_i$ elevation in granule cells. The first phase involves the release of Ca^{2+} from intracellular storages (Bearrs, Limke, & Atchison, 2001; Limke, Otero-Montañez, & Atchison, 2003) and the second phase consists of extracellular Ca^{2+} fluxes into the cell (Marty & Atchison, 1997). These changes in $[Ca^{2+}]_i$, caused by MeHg exposure can produce granule cell death (Gassó et al., 2001; Marty & Atchison, 1998).

In addition to the granule cells, other cell types have shown an increase in $[Ca^{2+}]_i$ and a decrease in viability produced by MeHg exposure, including neuroblastoma cells (Hare, McGinnis, & Atchison, 1993; Hare & Atchison, 1995a, 1995b; Petroni, Tsai, Mondal, & George, 2013), mouse thymocytes (Oyama, Carpenter, Ueno, Hayashi, & Tomiyoshi, 1995), human lymphocytes and monocytes (Shenker et al., 1992; Shenker et al., 1993; Tan, Tang, Castoldi,

Manzo, & Costa, 1993), and rat forebrain synaptosomes (Denny, Hare, & Atchison, 1993; Komulainen & Bondy, 1987; Levesque, Hare, & Atchison, 1992).

The increase in $[Ca^{+2}]_i$ has been associated with an increase in glutamate release (Bal Price, Moneer, & Brown, 2002; Bollmann, Sakmann, & Borst, 2000), which can produce excitotoxicity (Mark et al., 2001; Olney, 1994). MeHg can also block $GABA_A$ receptors in granule cells. The effect of MeHg on $GABA_A$ receptors suggests a decrease in the function of the channel to mediate inhibitory neurotransmission, thereby causing an increase in glutamate release (Atchison, 2005; Herden, Pardo, Hajela, Yuan, & Atchison, 2008; Yuan & Atchison, 2003).

Astrocytes are an important type of glial cells that can buffer excess glutamate from the extracellular space, protecting the neurons from excitotoxicity (Anderson & Swanson, 2000). It has been shown that astrocytes from different parts of the nervous system can react differently to the same stimulus (Blomstrand, Åberg, Eriksson, Hansson, & Rönnbäck, 1999; Cavalcante, Garcia-Abreu, Moura, Silva, & Barradas, 1996; Han, Koh, Lee, & Seong, 2004). Like neurons, several types of astrocytic populations can coexist within a given brain region. Classically, by using immunohistochemical methods and morphological criteria, astrocytes have been classified into protoplasmic and fibrous types. Fibrous astrocytes are characterized by having many glial filaments, as opposed to protoplasmic astrocytes that have fewer glial filaments. Another classification of astrocytes, based on morphologic and immunohistochemical methods, was proposed by Raff and colleagues, in which astrocytes were divided into type 1 and type 2 astrocytes. Type 1 astrocytes are fibroblast-like, while type 2 astrocytes are more neuron-like and come from O-2A progenitor cells. Type 1 astrocytes are found in both developing grey and white matter, while type 2 astrocytes are primarily found in white matter (Raff, Abney, Cohen,

Lindsay, & Noble, 1983). The morphological characteristics and regional origins of type 1 and type 2 astrocytes suggest that these two types of astrocytes could correspond to protoplasmic and fibrous astrocytes, respectively (Miller & Raff, 1984).

Astrocytes can also be targeted by MeHg. Aschner and colleagues (2000) have hypothesized that neurotoxicity by MeHg occurs secondary to effects on glial cell functions, such as disruption of glutamate uptake (Albrecht, Talbot, Kimelberg, & Aschner, 1993), increases in Na^+ uptake via the Na^+/H^+ antiporter, astrocytic swelling, and alterations in spatial K^+ buffering (Aschner, Conklin, Yao, Allen, & Tan, 1998; Aschner, Vitarella, Allen, Conklin, & Cowan, 1998).

MeHg-induced cytotoxicity in astrocytes has been studied extensively in the cortical layer. However, effects of MeHg on cerebellar astrocytes are less studied. The present study was designed to examine whether there are typological or/and regional differences in the viability of cortical and cerebellar astrocytes after an acute exposure to MeHg, and to understand factors that can contribute to such differences. First, we examined the differences in toxicity after an immediate and delayed exposure to MeHg in cortical and cerebellar astrocytes. Then, we studied the typological differences between type 1 and type 2 astrocytes from the cortex and cerebellum. To understand some factors that can contribute to regional differences, we sought to determine whether MeHg-induced changes in $[Ca^{2+}]_i$ can produce differences in viability in cortical and cerebellar astrocytes. To determine if astrocyte death was caused by an increase in intracellular Ca^{2+}, the chelator BAPTA-AM was used. In order to determine if astrocyte death was caused by the extracellular Ca^{2+} that entered the cell, the cell-impermeant chelator EGTA was used.

C. Materials and methods

C.1. Materials and experimental solutions

High glucose Dulbecco's modified Eagle's medium (DMEM), heat inactivated horse serum, fetal bovine serum (FBS), antibiotic-antimycotic, and Trypan Blue Stain (0.4%) were obtained from Gibco (Grand Island, NY). The following items were purchased from Sigma-Aldrich Co. (St. Louis, MO): 4-(2-hydroxyethyl)-1-piperazineethanesulfonic acid (HEPES), deoxyribonuclease I (DNase I), trypsin, glutamine, poly-D-lysine, BAPTA-AM, and EGTA. Methylmercuric chloride was purchased from ICN Biomedicals Inc. (Aurora, OH).

Experimental solutions were prepared by diluting stock solutions and using HEPES-buffered saline solution (HBS), which contained (mM) 150 NaCl, 5.4 KCl, 1.8 $CaCl_2$, 0.8 MgSO4, 20 D-glucose, and 20 HEPES (free acid) (pH 7.3). The EGTA-containing buffer had the same constituents as HBS minus $CaCl_2$ and plus 0.02 mM EGTA (final $[Ca^{2+}]$ = 60 nM) (Marty & Atchison, 1997). BAPTA-AM was prepared as a 20 mM stock solution in dimethyl sulfoxide (DMSO).

C.2. Preparation of primary cerebral cortical and cerebellar astrocyte cultures

Primary cultures of cortical and cerebellar astrocytes were obtained from 7-8 days old C57BL/6 mice by using a modification of the method described by Inglefield et al (Inglefield, Mundy, & Shafer, 2001). Briefly, following removal of the brain and separation of the cerebral cortical layer and cerebellum, cells were digested for 4 min at 37°C with trypsin 0.025% (w/v) in a buffer that contained: 5.0 mM KCl, 0.20 mM KH_2PO_4, 137.0 mM NaCl, 0.17 mM Na_2HPO_4, 5.0 mM D-glucose, 59.0 mM sucrose, and 0.1 mg/ml antibiotics, pH 7.3. Cerebral cortex and cerebellum were kept separate to avoid cross-contamination. Trypsin was inactivated by the

addition of .016% (w/v) DNase I diluted in the above-described buffer for 4 min at 37°C. Then, cell media containing warmed DMEM supplemented with 10% (w/v) horse serum, 10 mM HEPES, 2 mM glutamine, and 0.1 mg/ml antibiotics was added to this mixture. Cells were centrifuged at 500 X g for 5 min. The resulting pellet was resuspended in DMEM-containing DNase I and recentrifuged at 500 g X for 5 min. Then, cells were resuspended one last time in DMEM and recentrifuged at 500 X g for 5 min. All animal procedures were in adherence with NIH guidelines and approved by MSU Institutional Animal Use and Care Committee.

C.3. Purification of astrocytes

Cortical and cerebellar cell cultures were purified individually by using Anti-GLAST (ACSA-1) MicroBead Kit (Miltenyi Biotec Inc., San Diego CA). Briefly, cells were incubated for 10 min in 20 µM of Anti-GLAST (ACSA-1)-Biotin. Then, cells were washed with 2 ml of ice-cold phosphate-buffered saline ((PBS); containing 137 mM NaCl, 2.7 mM KCl, 1.4 mM NaH_2PO_4, and 4.3 mM Na_2HPO_4, pH 7.4) containing 0.5% FBS (and centrifuged at 300 X g for 10 min. The resulting pellet was dissociated and incubated for 15 min with 20 µL of Anti-Biotin MicroBeads. After the incubation period, cells were washed with 2 ml of PBS containing 0.5% FBS and centrifuged at 300 X g for 10 min. The final pellet was dissociated and passed through a 70 µm nylon mesh (Miltenyi Biotec Inc., San Diego CA). Astrocyte culture was loaded onto an MS column (Miltenyi Biotec Inc., San Diego CA), which was placed in the magnetic field of a MACS Separator (Miltenyi Biotec Inc., San Diego CA). The column was rinsed by using 0.5% FBS in PBS. Isolated GLAST positive cells were retained in the column and removed by using cell media.

C.4. Cell plating

Cells were plated at a density of 1×10^5 cells/dish onto 35-mm Petri dishes coated with poly-D-lysine and maintained in a 37°C incubator with 95% O_2 and 5% CO_2. TC20 Automated Cell Counter (Bio-Rad Laboratories Inc., Hercules, CA) was used to obtain an equal density of live cells in all the cell cultures. Cell media was replaced every other day. No antibiotic was added after the third replacement of cell media because it could alter the function of Ca^{2+} channels (Atchison, Adgate, & Beaman, 1988; Redman & Silinsky, 1994).

C.5. Methylmercury treatment

Methylmercuric chloride was dissolved in deionized water to a final concentration of 10 mM to serve as a stock solution. Working solutions were diluted on the same day in HBS. At 13-15 DIV, astrocytes were exposed for 3 h to 0, 1, 2, or 5 μM MeHg. This extended growing time *in vitro* was needed for the astrocytes to express their distinctive characteristics. Anti-GFAP antibody and fluorophores DAPI were used to access the purity of the astrocytes in cell culture (purity: ≥99%). Cells were analyzed immediately after the 3 h of exposure or 21 h after the 3 h of exposure, which is referred in this chapter as 24 h after exposure or "delayed". To test the effect of BAPTA-AM with MeHg, cells were incubated for 65 min with 10 μM of BAPTA-AM and co-treated with BAPTA-AM and MeHg for 3 h. The pre-incubation time and concentration of BAPTA-AM were used because they have previously demonstrated to attenuate the decrease in granule cell viability produced by MeHg (Marty & Atchison, 1998). To test the effect of EGTA with MeHg, the cells were co-treated for 3 h with EGTA in a Ca^{2+}-free HBS. In both cases, cytotoxicity was performed 24 h after the co-treatment.

C.6. Cytotoxicity

For the cytotoxicity assay, cells were removed from the conditioned medium and rinsed twice with HBS. The Viability/Cytotoxicity Assay (Molecular Probes Inc., OR, USA) was used to identify the astrocytes that were dead or alive. Astrocytes were incubated with 0.3 μM calcein-AM and 0.075 μM EthD-1 for 20 min at room temperature. The cells with calcein-AM, which labels healthy cells in green, and EthD-1, which labels the nucleus of dead cells in red, were rinsed twice with HBS. To determine the cytotoxicity of MeHg in type 1 and 2 astrocytes, only EthD-1 was used.

C.7. Immunocytochemistry

Astrocytes were fixed in cold 4.0% (v/v) p-formaldehyde in PBS for 15 min. Slides were rinsed in PBS three times and then treated for 30 min with 0.1% (v/v) Triton-X in PBS containing 5% (v/v) normal goat serum (NGS). To determine if there was a difference in cytotoxicity between type 1 and type 2 astrocytes, several antibodies were used. First, after three rinses in PBS, a marker for astrocytes called rabbit Anti-GFAP (Millipore Corporation, Temecula, CA) was used at a concentration of 1:1000. Then, after 24 h, the slides were rinsed in PBS and labeled with an antibody cocktail containing mouse anti-neuron surface antigen (A2B5) Alexa Fluor 488 conjugated monoclonal antibody at a concentration of 1:40 (Millipore Corporation, Temecula, CA), and a secondary antibody Alexa Fluor 405 goat anti-rabbit (Invitrogen Corporation, Carlsbad, CA) at a concentration of 1:200. To determine the percentage of astrocytes present in the cell cultures, cells were labeled overnight with GFAP at a concentration of 1:1000. After 24 h, the slides were rinsed in PBS and labeled with secondary antibody Alexa Fluor 405 goat anti-rabbit (Invitrogen Corporation, Carlsbad, CA) at a

concentration of 1:200. Then, cells were mounted on glass slides by using a mounting medium with DAPI (Vectashield Hard Set, Vector, Burlingame, CA).

C.8. Data acquisition and analysis

The photos were merged by using the results of the cytotoxicity assay and the immunocytochemistry. All the astrocytes were stained with GFAP color blue. Only type 2 astrocytes were stained with A2B5 the color green. Astrocytes that contained the EthD-1 the color red were counted as dead cells. Cells were examined by using the Nikon Eclipse Ti with NIS-Elements BR software (Nikon Instruments Inc., Melville, NY, USA). All images were obtained with 20X oil immersion objectives by using the same acquisition configuration, including exposure time and neutral density filters. To determine the effect of MeHg on the astrocytes, a one-way analysis of variance (ANOVA) was used. To compare between groups, a two-way ANOVA followed by Tukey's procedure for post-hoc comparisons were used. $P < 0.05$ was considered to be statistically significant.

D. Results

D.1. Immediate and delayed acute methylmercury treatment

Viability was measured either immediately after the 3 h of MeHg treatment (immediate) or 21 h after the 3 h of MeHg treatment (delayed). There were no differences from control values immediately after the 3 h of MeHg treatment in cortical astrocytes. However, after the cells were returned to the media for 21 h, there was a significant decrease in cortical astrocyte viability to approximately 66% of control for cells exposed to 5 μM MeHg. There was also a significant decrease in viability (47%) at 5 μM MeHg when immediate and delayed treatment were compared (Fig. 2.1.A). In cerebellar astrocytes, a significant decrease in viability to approximately 48% of control for cells exposed to an immediate treatment of 5 μM MeHg was obtained. The delayed MeHg treatment produced cytotoxicity in a concentration-dependent manner in cerebellar astrocytes with a significant reduction in viability to approximately 69% and 97% of control values at 2 μM and 5 μM MeHg, respectively. There was also a significant difference in viability (61%) at 2 μM MeHg and (48%) at 5 μM MeHg when immediate and delayed treatments in cerebellar astrocytes were compared (Fig. 2.1.B).

There was a significant difference in the decrease of viability (30%) at 5 μM MeHg when immediate treatment of cortical astrocytes and immediate treatment of cerebellar astrocytes were compared (Fig. 2.2), and a significant difference in the decrease of viability (52%) at 2 μM and (31%) 5 μM MeHg when delayed treatment of cortical astrocytes and delayed treatment of cerebellar astrocytes were compared (Fig. 2.3).

D.2. Typological and regional effects of an acute delayed methylmercury treatment

A

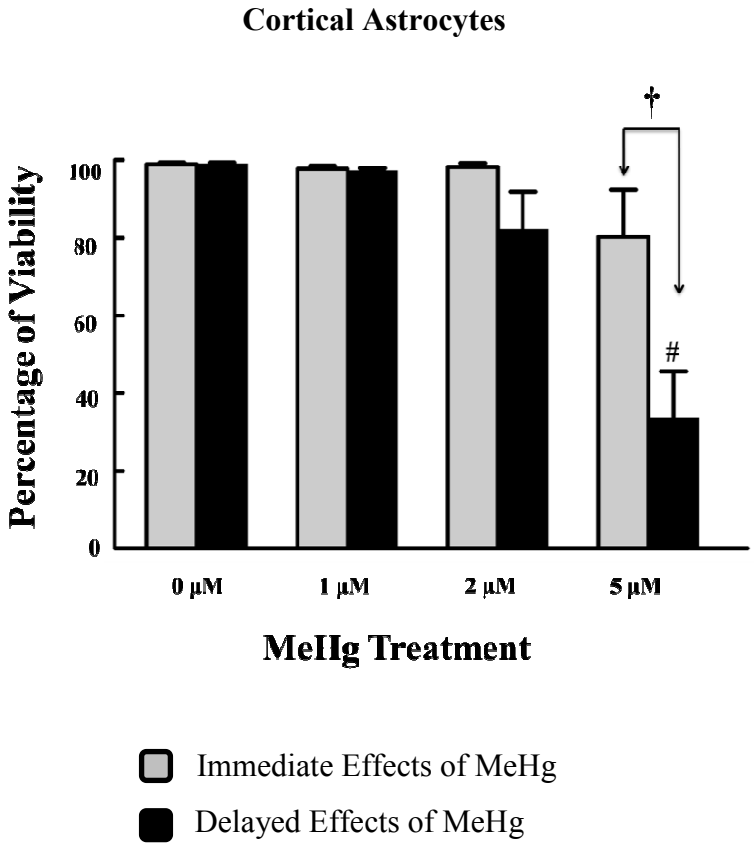

Figure 2.1. Immediate and Delayed MeHg treatments caused a significant change in viability in cerebellar astrocytes. Delayed MeHg treatment caused a more prominent effect than immediate MeHg treatment in both cerebellar and cortical astrocytes. (**A**).Comparison between immediate and delayed effects of MeHg in cortical astrocytes. (**B**). Comparison between immediate and delayed effects of MeHg in cerebellar astrocytes. Percentage of viability at 0 µM, 1 µM, 2 µM, and 5 µM MeHg ($n \geq 5$). Viability was measured either immediately after the 3 h of exposure (immediate), or 24 h after the exposure to MeHg (delayed) using EthD-1 and calcein-AM. Values are mean ± SEM. * denotes $p < 0.05$ compared with 0 µM of immediate MeHg exposure. # denotes $p < 0.05$ compared with 0 µM of delayed MeHg exposure. † denotes $p < 0.05$ between immediate and delayed MeHg exposures. One-way ANOVA was used to compare within groups. Two-way ANOVA was used to compare between groups. Tukey's post-hoc comparison was used.

Figure 2.1 (cont'd)

B

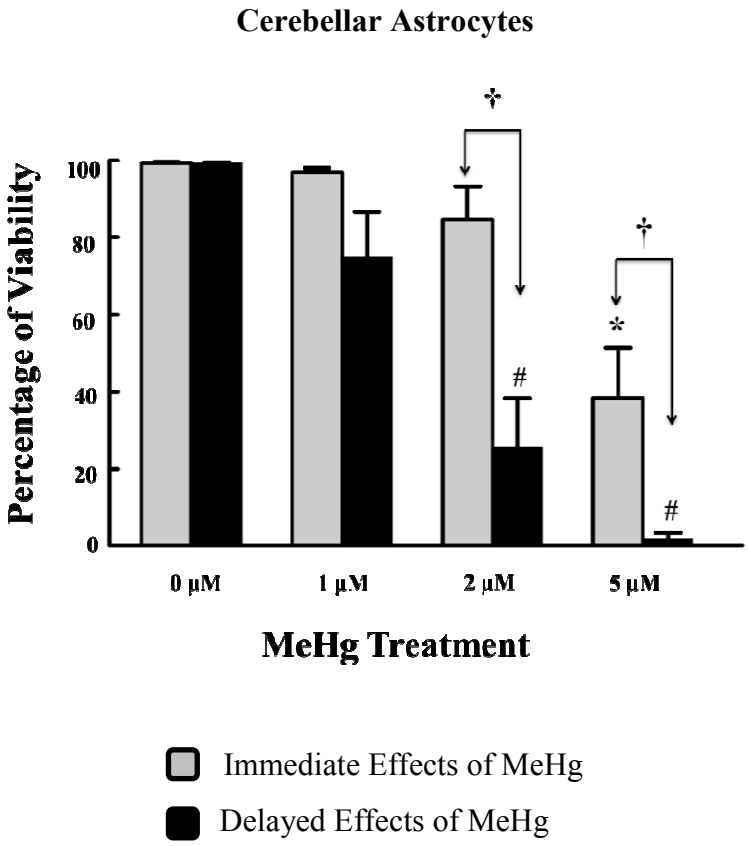

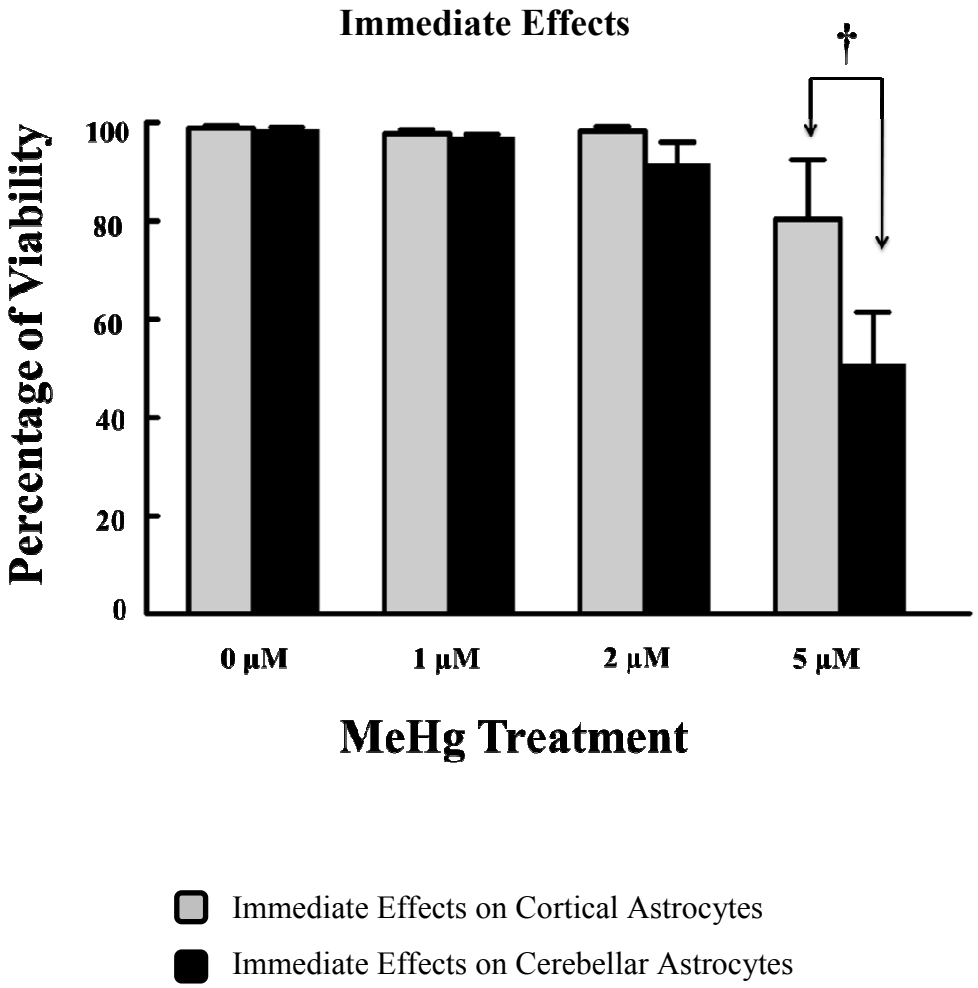

Figure 2.2. Immediately after MeHg exposure, cerebellar astrocytes had a higher change in viability than cortical astrocytes. Percentage of viability at 0 µM, 1 µM, 2 µM, and 5 µM MeHg (n=5). Viability was measured immediately after 3 h of exposure using EthD-1 and calcein-AM. Values represent mean ± SEM. † denotes $p < 0.05$ between immediate effects of MeHg on cortical and cerebellar astrocytes. Two-way ANOVA followed by Tukey's post-hoc comparison were used.

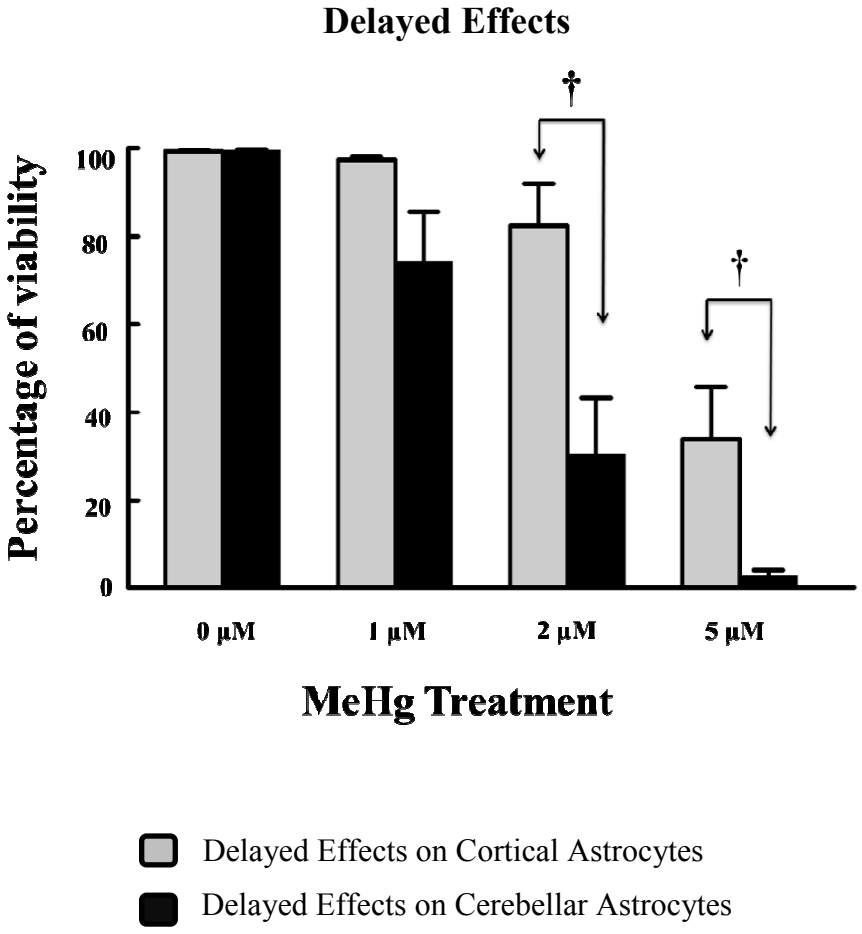

Figure 2.3. Cerebellar astrocytes were more susceptible to delayed MeHg exposure than cortical astrocytes and showed a concentration-dependent change in viability. Percentage of viability at 0 µM, 1 µM, 2 µM, and 5 µM MeHg (n=6) was plotted on the x-axis. Viability was measured 24 h after the exposure to MeHg using EthD-1. Values are mean ± SEM. † denotes $p < 0.05$ between delayed and immediate MeHg exposures. Two-way ANOVA was followed by Tukey's post-hoc comparisons.

These experiments were designed to examine whether there were typological or/and regional differences in astrocytes after an acute delayed treatment of MeHg. Cortical and cerebellar astrocytes were stained with the antibodies A2B5 and GFAP, and the fluorophore EthD-1. Type 1 astrocytes were stained only with antibody GFAP (blue). Type 2 astrocytes were stained with antibody A2B5 (green) and GFAP (blue), and the dead astrocytes showed a red fluorescence in their nuclei due to EthD-1. Figure 2.4 shows cortical astrocytes treated with 0 μM, or 5 μM MeHg and stained with A2B5, GFAP, and EthD-1.

The percentage of type 1 and type 2 astrocytes that was present in the cell culture at each MeHg treatment was monitored to assure that there were no changes, and that the possible difference in toxicity between the two types of astrocytes in the same brain region was independent of changes in the percentages of the types of astrocytes present in each cell culture treated with MeHg. There were no differences in the percentage of type 1 and type 2 cortical astrocytes present in the cell culture at each MeHg treatment (Fig. 2.5.A). There were no differences in the percentage of type 1 and type 2 cerebellar astrocytes present in the cell culture at each MeHg treatment (Fig. 2.5.B).

Both type 1 and type 2 cortical astrocytes had a significant decrease in viability to approximately 71% and 61%, respectively of control values for cells exposed to 5 μM MeHg. However, there were no differences between type 1 and type 2 cortical astrocytes at any MeHg treatment (Fig. 2.6.A). In the cerebellum, type 1 astrocytes had a significant decrease in viability to approximately 63% and 95% of control values at 2 μM and 5 μM MeHg, respectively. Type 2 cerebellar astrocytes had a significant decrease in viability to approximately 74% and 97% of control values at 2 μM and 5 μM MeHg, respectively. Likewise, there were no differences between type 1 and type 2 cerebellar astrocytes at any MeHg treatment (Fig. 2.6.B).

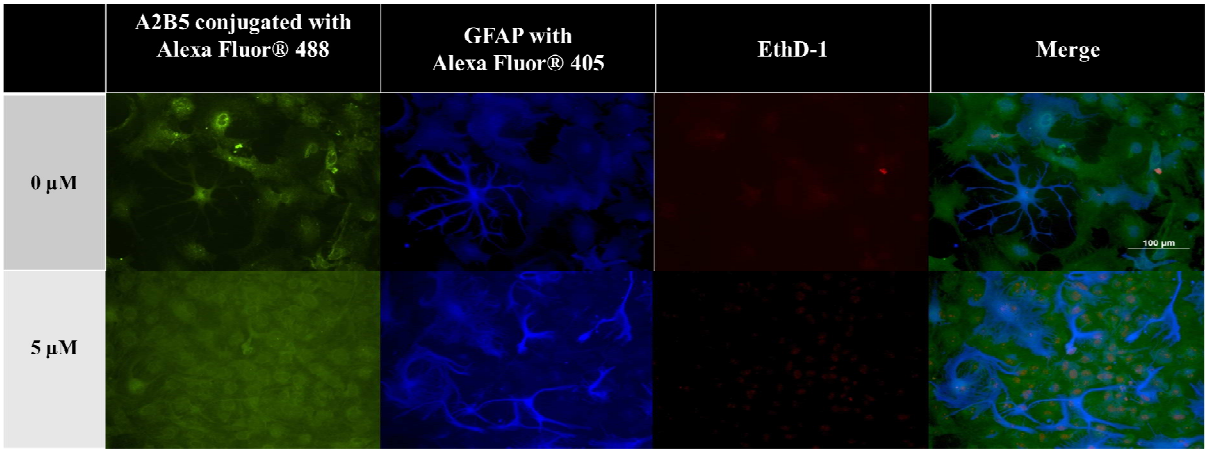

Figure 2.4. Fluorescence micrographs stained with A2B5, GFAP, and EthD-1. Type 1 astrocytes were stained only with GFAP (blue), type 2 astrocytes were stained with A2B5 (green) and GFAP (blue), and the dead astrocytes showed a red fluorescence in their nuclei due to EthD-1. Micrographs were merged to analyze the cytotoxicity present in type 1 and type 2 astrocytes from cerebellum and forebrain cortex (20x). The present micrographs demonstrate the staining in cortical astrocytes at 0 µM and 5 µM MeHg.

A

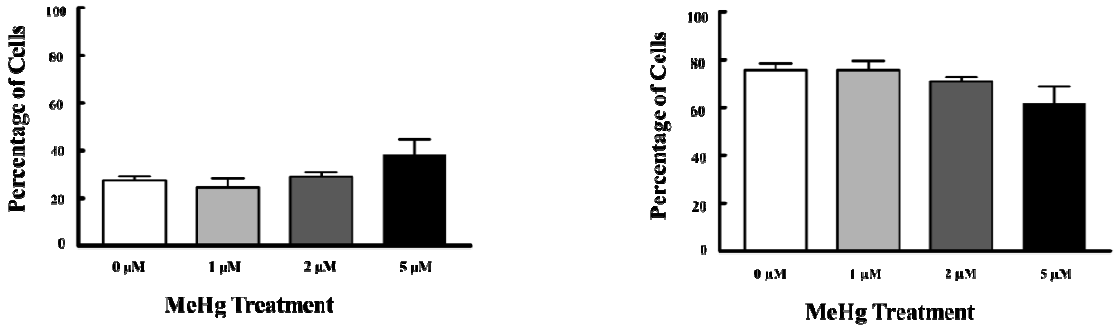

B

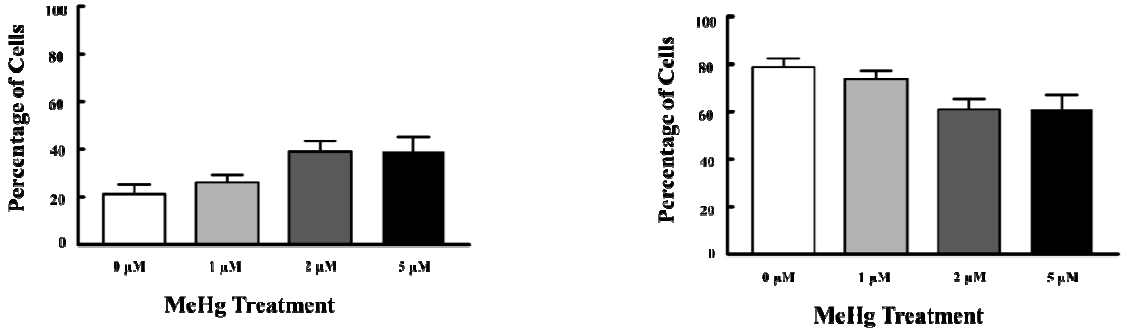

Figure 2.5. There were no differences in the percentage of type 1 and type 2 cortical and cerebellar astrocytes present in the cell culture at each MeHg treatment. (A). Percentage of type 1 (left) and type 2 (right) cortical astrocytes present in cell culture. (**B**). Percentage of type 1 (left) and type 2 (right) cerebellar astrocytes present in cell culture. Percentage at 0 µM, 1 µM, 2 µM, and 5 µM MeHg (n=6). A2B5 and GFAP antibodies were used to distinguish between type 1 and type 2 astrocytes. One-way ANOVA followed by Tukey's post-hoc comparison were used.

A \

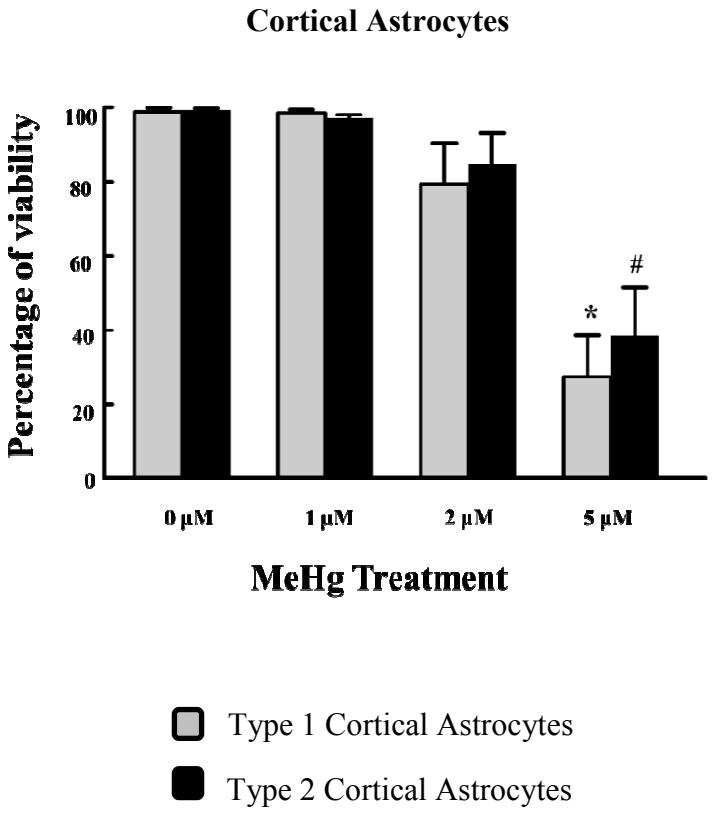

Figure 2.6. There was no significant difference between type 1 and type 2 astrocytes from the same brain region after delayed MeHg exposure. (A). Type 1 vs. type 2 cortical astrocytes. (**B**). Type 1 vs. type 2 cerebellar astrocytes. Percentage of viability at 0 µM, 1 µM, 2 µM, and 5 µM MeHg (n=6). A2B5 and GFAP were used to identify types of astrocytes. Viability was measured 24 h after the exposure to MeHg using EthD-1. Values represent mean ± SEM. * denotes $p < 0.05$ compared with 0 µM MeHg of type 1 astrocytes. # denotes $p < 0.05$ compared with 0 µM MeHg of type 2 astrocytes. There were no significant differences between type 1 and type 2 in cortical and cerebellar astrocytes. One-way ANOVA was used to compare within groups. Two-way ANOVA was used to compare between groups. Tukey's post-hoc comparison was used.

Figure 2.6 (cont'd)

B

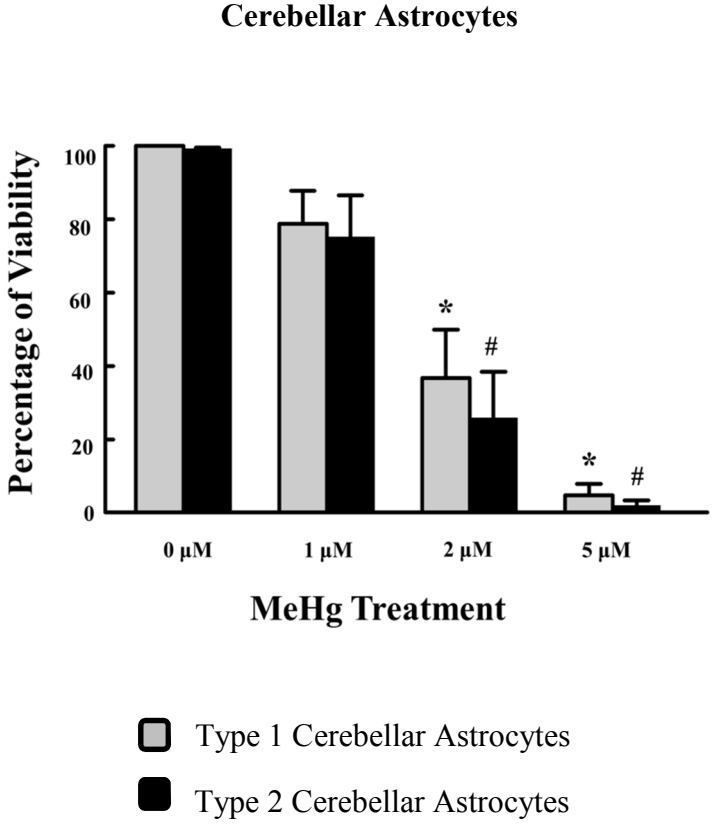

Although there were no significant differences between types of astrocytes from the same brain region, there were differences when comparing the same type of astrocytes from different parts of the brain. There was a significant difference in the decrease of viability (43%) at 2 μM MeHg when type 1 cortical astrocytes and type 1 cerebellar astrocytes were compared (Fig. 2.7.A). Also, there were significant differences in the decrease of viability (59%) at 2 μM and (37%) 5 μM MeHg, when type 2 cortical astrocytes and type 2 cerebellar astrocytes were compared (Fig. 2.7.B).

D.3. Extracellular and intracellular calcium contribution to cytotoxicity after an acute delayed methylmercury treatment

These experiments aimed to understand possible factors that can contribute to the differences between cortical and cerebellar astrocytes after an acute delayed MeHg treatment. To determine if astrocyte death was caused by an increase in intracellular Ca^{2+}, the chelator BAPTA-AM was used. Cells were pre-incubated with 10 μM BAPTA-AM for 65 min and co-incubated with MeHg. There were no decreases in viability in cortical astrocytes at any MeHg + BAPTA-AM concentrations when compared with 0 μM MeHg + BAPTA-AM (Fig. 2.8.A). However, cerebellar astrocytes showed a significant reduction in viability (47%) at 5 μM MeHg + BAPTA-AM when compared with 0 μM MeHg + BAPTA-AM (Fig. 2.8.B).

In order to determine if astrocyte death was caused by the extracellular Ca^{2+} that entered the cell, the cell-impermeant chelator EGTA was used. There were significant reductions in viability in cortical (45%) and cerebellar (8%) astrocytes when 0 μM MeHg + EGTA and 5 μM MeHg + EGTA were compared (Fig. 2.9.A-B).

A

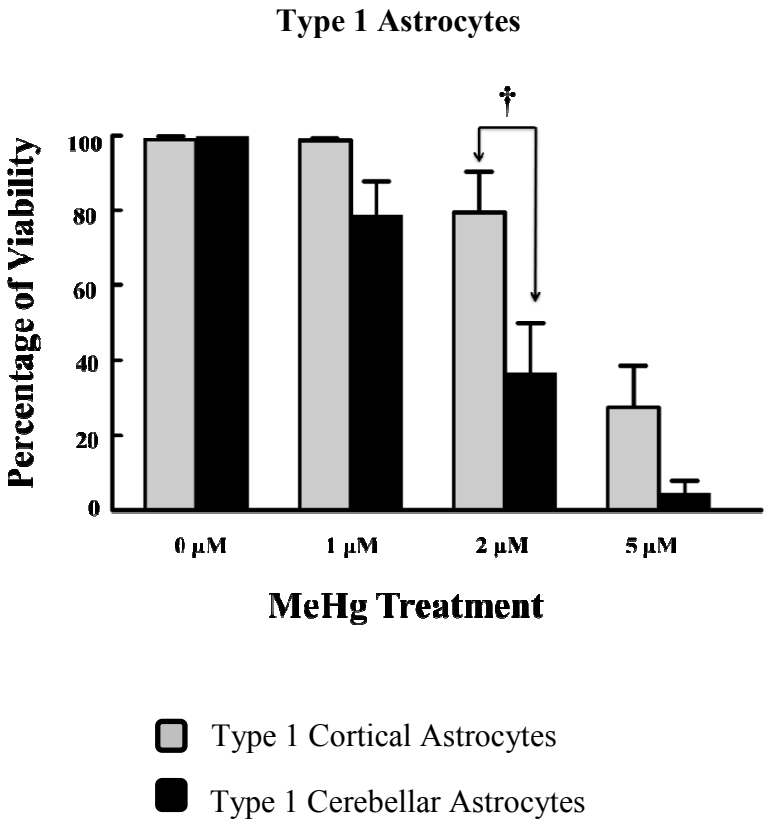

Figure 2.7. Type 1 and type 2 cerebellar astrocytes were more susceptible to delayed MeHg treatment that type 1 and type 2 cortical astrocytes. (A). Type 1 cortical vs. type 1 cerebellar astrocytes. **(B)**. Type 2 cortical astrocytes vs. type 2 cerebellar astrocytes. Percentage of viability at 0 µM, 1 µM, 2 µM, and 5 µM MeHg (n=6). A2B5 and GFAP were used to identify types of astrocytes and EthD-1 was used to identify dead astrocytes. Values are mean ± SEM. † denotes $p < 0.05$ between cortical and cerebellar astrocytes. Two-way ANOVA followed by Tukey's post-hoc comparison were used.

Figure 2.7 (cont'd)

B

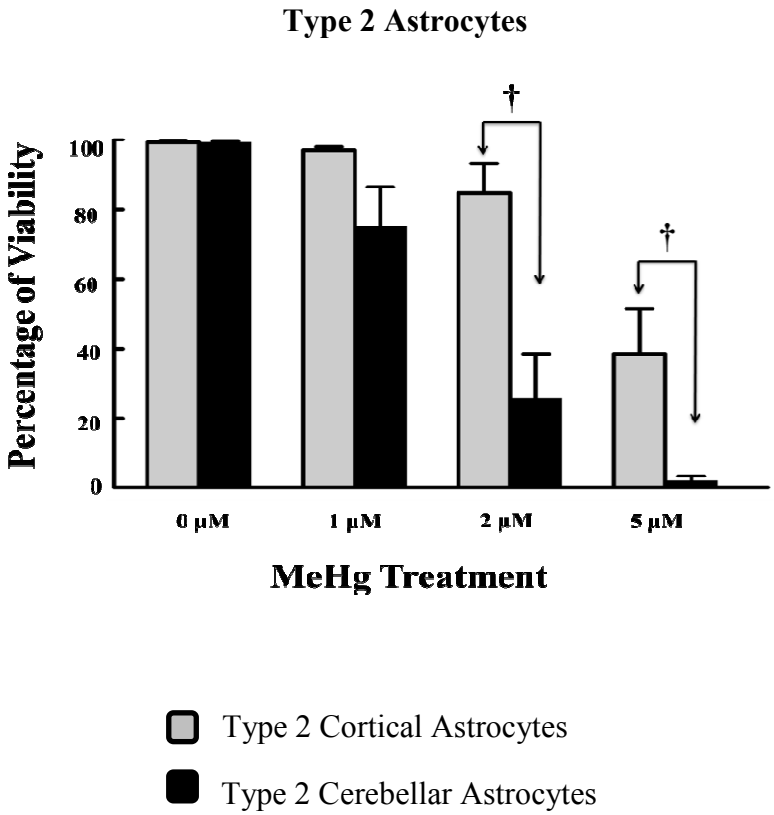

A

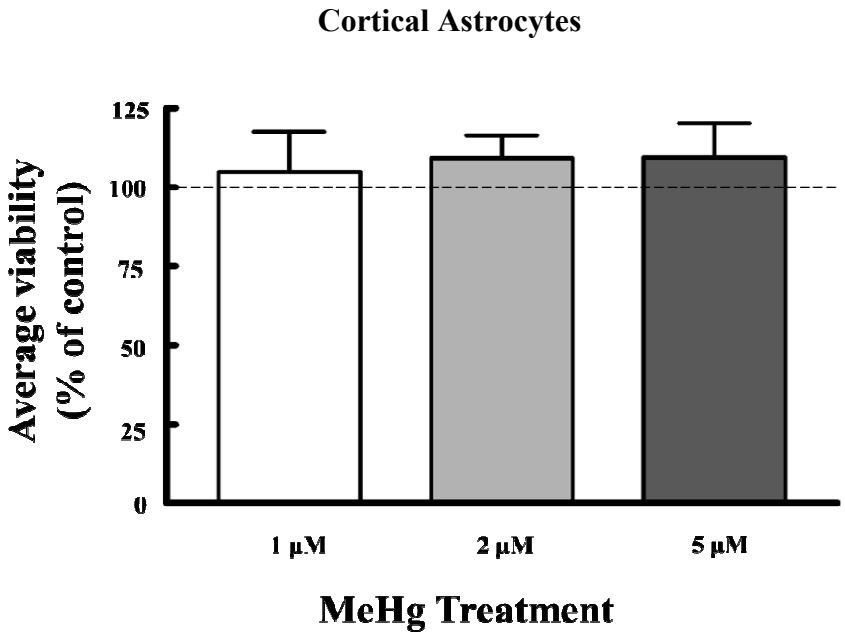

Figure 2.8. The treatment of BAPTA-AM + MeHg was able to prevent cortical astrocytes mortality and reduce cerebellar astrocytes mortality. (A). Effect of MeHg + BAPTA-AM on cortical astrocytes. **(B)**. Effect of MeHg + BAPTA-AM on cerebellar astrocytes. Average viability (% of control) at 0 µM, 1 µM, 2 µM, and 5 µM MeHg (n=6). Viability was measured 24 h after the exposure to MeHg using EthD-1 and calcein-AM. Results were normalized to MeHg-free cells treated with BAPTA-AM. Values are mean ± SEM. * denotes $p < 0.05$. One-way ANOVA followed by Tukey's post-hoc comparison were used.

Figure 2.8 (cont'd)

B

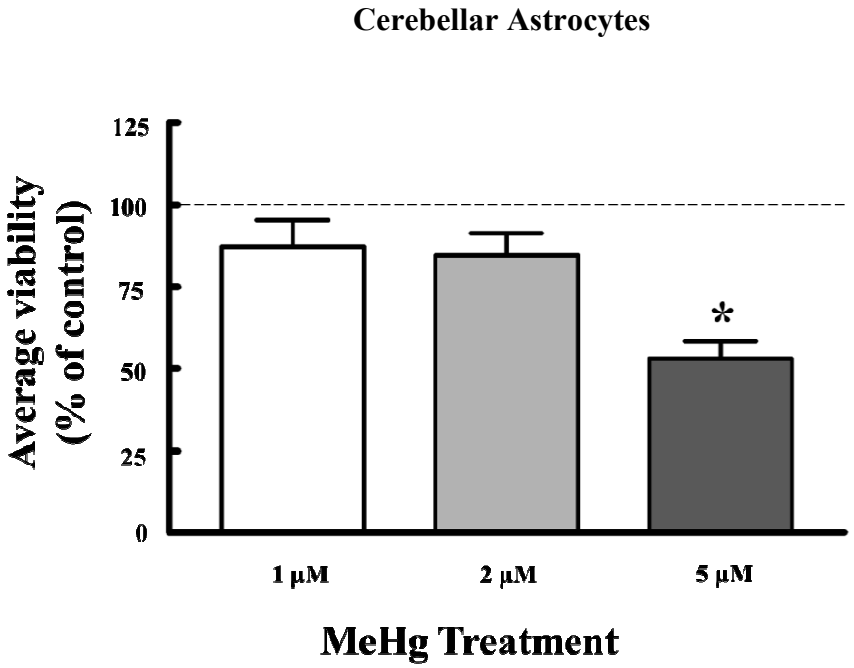

A

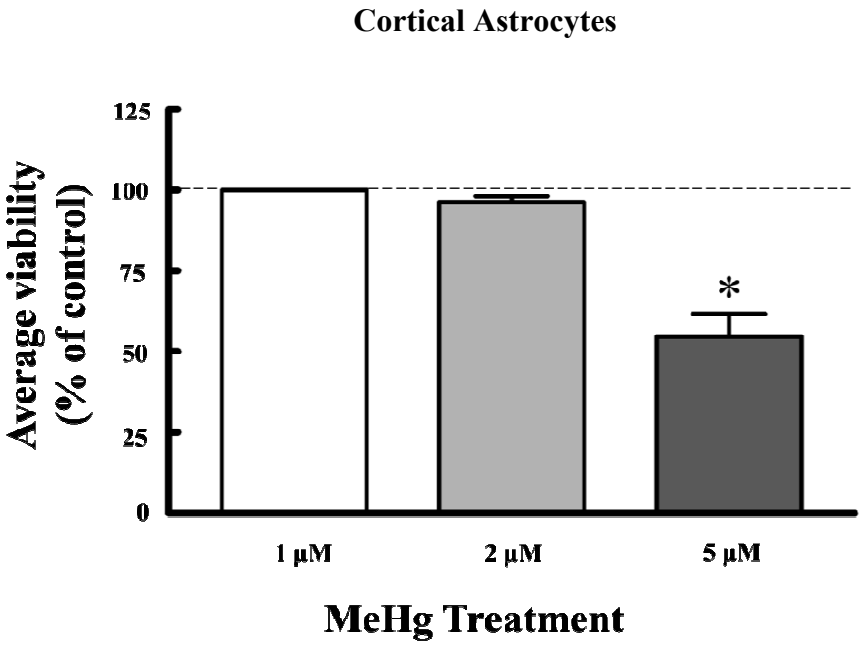

Figure 2.9. The treatment of EGTA + MeHg was able to reduce cerebellar astrocytes mortality. (A). Effect of MeHg + EGTA on cortical astrocytes. **(B)**. Effect of MeHg + EGTA on cerebellar astrocytes. Average viability (% of control) at 0 µM, 1 µM, 2 µM, and 5 µM MeHg (n=6). Viability was measured 24 h after the exposure to MeHg using EthD-1 and calcein-AM. Results were normalized to MeHg-free cells treated with EGTA. Values are mean ± SEM. * denotes $p < 0.05$. One-way ANOVA followed by Tukey's post-hoc comparison were used.

Figure 2.9 (cont'd)

B

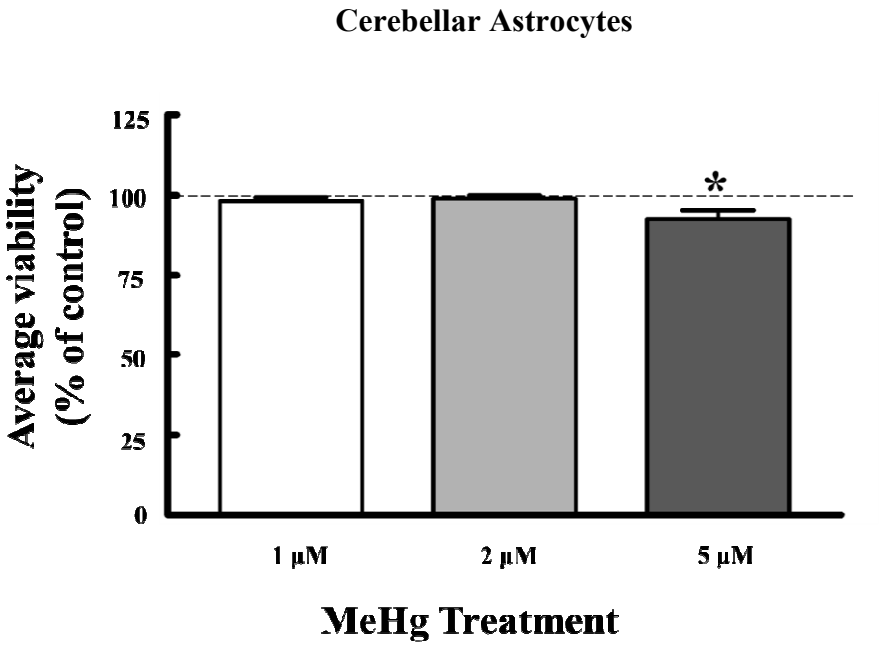

Cortical astrocytes treated with BAPTA-AM + 5 μM MeHg prevented the decrease in cell viability of approximately 75% in comparison with cortical astrocytes that were treated with 5 μM MeHg. The increase in viability in cortical astrocytes was more notable with the co-treatment of BAPTA-AM than with the co-treatment of EGTA, with a significant difference in normalized viability of 55% between both treatment groups at 5 μM MeHg (Fig. 2.10.A).

In the cerebellum, 2 μM and 5 μM MeHg + BAPTA-AM and MeHg + EGTA prevented the decrease in cell viability in comparison with 2 μM and 5 μM MeHg. The cerebellar astrocyte death decreased approximately 54% and 68% at 2 μM MeHg + BAPTA-AM and MeHg + EGTA respectively, when compared with 2 μM MeHg. The cerebellar astrocyte death also decreased approximately 50% and 89% at 5 μM MeHg + BAPTA-AM and MeHg + EGTA respectively, when compared with 5 μM MeHg. Although both co-treatment groups prevented the decrease in cell viability in cerebellar astrocytes, there was a higher reduction in cell death of approximately 39% in the MeHg + EGTA treatment group in comparison with the MeHg + BAPTA-AM treatment group at 5 μM MeHg (Fig. 2.10.B).

Therefore, the extracellular Ca^{2+} that entered the cell played a more crucial role in cerebellar astrocytes than cortical astrocytes, and the increase in intracellular Ca^{2+} from intracellular storage played a more important role in cortical astrocytes than cerebellar astrocytes at higher MeHg toxicity.

A

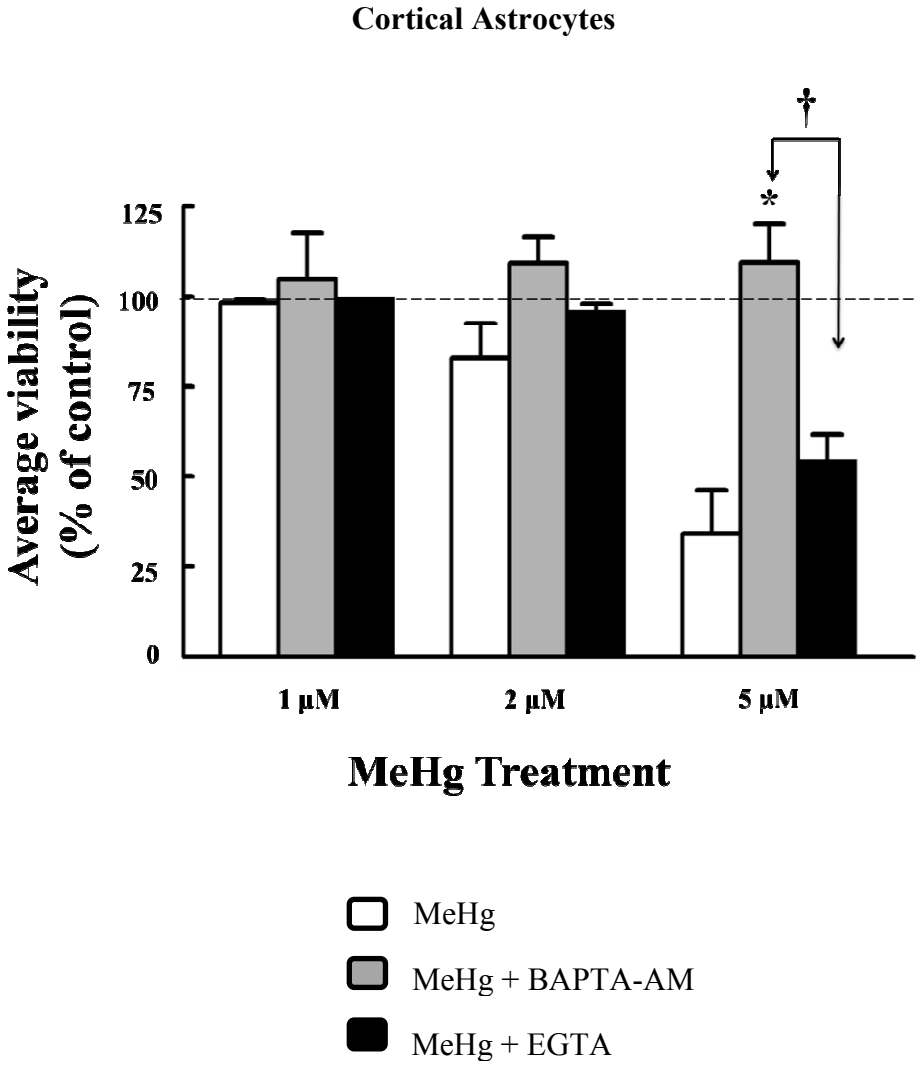

Figure 2.10. The contribution of intra- and extracellular Ca^{2+} to MeHg cytotoxicity differ in cortical and cerebellar astrocytes. (A). Effect of MeHg, MeHg + BAPTA-AM and MeHg + EGTA on cortical astrocytes. **(B)**. Effect of MeHg, MeHg + BAPTA-AM and MeHg + EGTA on cerebellar astrocytes. Average viability (% of control) at 0 µM, 1 µM, 2 µM, and 5 µM MeHg (n=6). Viability was measured 24 h after the exposure to MeHg. Results were normalized to 0 µM MeHg, 0 µM MeHg + BAPTA-AM or 0 µM MeHg + EGTA. Values are mean ± SEM. * denotes $p < 0.05$ compared with MeHg group. † denotes $p < 0.05$ between MeHg + BAPTA-AM and MeHg + EGTA. One-way ANOVA was used to compare within groups. Two-way ANOVA was used to compare between groups. Tukey's post-hoc comparison was used.

Figure 2.10 (cont'd)

B

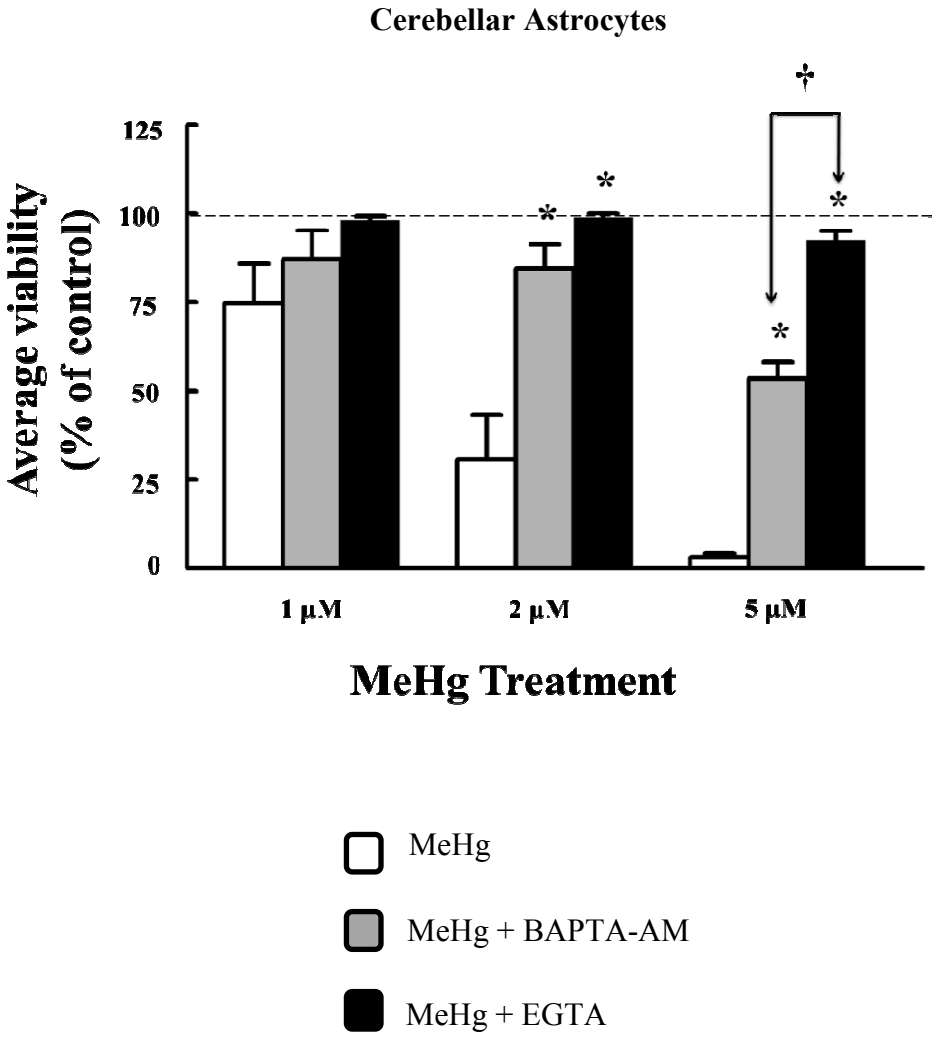

E. Discussion

The main purpose of this chapter was to examine whether there were typological or/and regional differences in the viability of type 1 and type 2 cortical and cerebellar astrocytes after an acute exposure to MeHg, and if so, to understand factors that can contribute to such differences. Previous studies have found some differences between cortical and cerebellar astrocytes after MeHg treatment with respect to changes in MTT-reduction, lactate dehydrogenase (LDH) leakage, and cellular content of glutathione (Morken, Sonnewald, Aschner, & Syversen, 2005). In the current study, we were focused on the effect of MeHg on viability, using probes that assess intracellular esterase activity and plasma membrane integrity. Also, we queried whether MeHg-induced changes in Ca^{2+} in astrocytes can contribute to differences in viability between cortical and cerebellar astrocytes.

The first experiment was designed to determine the immediate and delayed effects of MeHg on cortical and cerebellar astrocytes. Although both groups had the same time of MeHg exposure (3 h), it was demonstrated that there was a higher change in viability after a delayed treatment than an immediate treatment in cortical and cerebellar astrocytes. The same delayed effects happened in humans after acute and chronic MeHg exposures. In Iraq, for example, after an acute poisoning of MeHg caused by consumption of contaminated bread, victims started to present signs of poisoning weeks or months after the exposure ended (Bakir, 1973; Weiss, Clarkson, & Simon, 2002). Likewise, in Minamata, low chronic doses of MeHg from contaminated fish did not produce observable behavioral effects for periods of time measured in years (Harada, 1995; Weiss et al., 2002).

When we examined regional differences between cortical and cerebellar astrocytes, cerebellar astrocytes were more susceptible to MeHg than cortical astrocytes in both immediate

and delayed exposures. For the rest of the experiments, a delayed exposure was used because it mimics a more realistic human exposure.

Subsequently, we aimed to assess typological differences after an acute delayed MeHg exposure in cortical and cerebellar astrocytes. Studies have demonstrated that astrocytes are more complex than previously thought. For instance, a recent study showed that astrocytes can be divided into 9 different classes based on three complementary astrocyte labeling methods—GFAP–GFP-expressing mice and GFAP and S100β immunostaining (Emsley & Macklis, 2006). In the present study, we focused on the more traditional classification of astrocytes due to its extensive literature. Here, it was discovered that there were no differences in viability between type 1 and type 2 astrocytes in both the cortex and the cerebellum after MeHg exposure. Therefore, there was a regional, but not a typological difference in astrocyte viability after an acute MeHg treatment. In other words, type 1 and type 2 astrocytes are equally affected at the given MeHg concentrations; however, cerebellar astrocytes are more susceptible than cortical astrocytes. It is possible that this susceptibility of cerebellar astrocytes to MeHg contributes to the susceptibility of granule cells to this metal in the cerebellum.

Because it has been repeatedly proven that Ca^{2+} plays an important role in the mechanisms of MeHg toxicity (Atchison, 2005; M. F. Hare & Atchison, 1995a; Levesque et al., 1992; Limke & Atchison, 2002; Limke, Bearss, & Atchison, 2004; Limke, Heidemann, et al., 2004; Marty & Atchison, 1997, 1998), we aimed to determine whether MeHg-induced changes in $[Ca^{2+}]_i$ was related to regional differences that exist between cortical and cerebellar astrocytes.

BAPTA-AM, an intracellular Ca^{2+} chelator, was able to prevent cortical astrocytes mortality and reduce cerebellar astrocytes mortality in the presence of MeHg. This means that although both cortical and cerebellar astrocytes are affected by MeHg-induced increases in

internal Ca^{2+} concentration, the cortical astrocytes are more susceptible to these elevations. In a previous study, it was found that MTT activity was decreased in cortical astrocytes at lower MeHg concentrations, but this decrease was not observed in cerebellar astrocytes (Morken et al., 2005). This mitochondrial dysfunction in cortical astrocytes may produce less Ca^{2+} buffering, making the viability of cortical astrocytes more dependent on $[Ca^{2+}]_i$ changes than cerebellar astrocytes.

The findings of the present study are consistent with the findings of Marty and Atchison, who aimed to analyze changes in cerebellar granule cell viability after an elevation in $[Ca^{2+}]_i$ induced by MeHg. They found that MeHg produced a decrease in viability in granule cells that can be prevented by the use of the chelator BAPTA-AM (Marty & Atchison, 1998).

When EGTA was used, it was able to reduce, but not prevent cerebellar astrocyte mortality. However, the reduction in mortality was higher in cerebellar astrocytes than cortical astrocytes. The effect of MeHg on cells due to external Ca^{2+}-depended elevations in $[Ca^{2+}]_i$ have been previously observed by using EGTA. In synaptosomes, the increase in $[Ca^{2+}]_i$ was strictly dependent on extracellular Ca^{2+} (Denny & Atchison, 1994). Similarly, in NG108-15 cells, a component of the elevations in $[Ca^{2+}]_i$ was extracellular Ca^{2+}-dependent (M. Hare et al., 1993). Another study, in which VGCCs blockers (nifedipine and omega-conotoxin-MVIIC) were used, it was found that MeHg affected L-, N-, and/or Q-type Ca^{2+} channels, altering the Ca^{2+} homeostasis in cerebellar granule cells (Marty & Atchison, 1997). Although that study showed the possible pathway affected by MeHg that produced an influx of Ca^{2+}, no viability was performed. Gasso and colleagues (2001) used flunarizine to study the effect of MeHg on cell viability after Ca^{2+} influx through Ca^{2+} channels. They discovered that Hg could mediate cytotoxicity of granule cells through the influx of Ca^{2+} via Ca^{2+} channels. This chapter has

demonstrated that like granule cells, the viability of astrocytes was affected by the influx of Ca^{2+} produced by MeHg exposure.

In conclusion, there is a regional, but not a typological difference in the effect of MeHg on astrocytes. Astrocytes of the cerebellum are more susceptible to MeHg than astrocytes of the cortex. This susceptibility of cerebellar astrocytes may contribute to the susceptibility of granule cells in the cerebellum. In order to understand possible factors that can contribute to the differences between cortical and cerebellar astrocytes, extracellular and intracellular Ca^{2+} contribution to astrocyte viability after an acute delayed MeHg treatment were assessed. It was found that extracellular Ca^{2+} that entered the cell played a more important role in cerebellar astrocytes than cortical astrocytes and that the increase in intracellular Ca^{2+} from intracellular storage plays a more important role in cortical astrocytes mortality at higher MeHg toxicity than cerebellar astrocytes.

In the current study, we did not examine whether MeHg induced cell death by apoptotic or necrotic pathways in the astrocytes. It has been shown that MeHg can cause necrotic cell death (Miura, Imura, & Clarkson, 1987; Nakada & Imura, 1983). However, other studies have attributed cell death to the activation of apoptotic pathways, at least at lower MeHg concentrations (Kunimoto, 1994; Nagashima et al., 1995). In a recent study focused on the mechanisms of MeHg toxicity in primary astrocytes and neurons of rats, the authors argued that there was a glutamate mechanism that mediated cytoskeletal disruption and induced apoptosis in neurons, and a glutamate-independent mechanism that mediated cytoskeletal disruption and induced necrosis in astrocytes (Pierozan et al., 2016).

Another issue that needs to be addressed is the mechanisms by which changes in Ca^{2+} concentration due to MeHg exposure produce a decrease in viability. Data in the present study

did not clearly indicate the role of the mitochondria and the SER from astrocytes in intracellular Ca^{2+} concentration after an acute exposure to MeHg. Nor did the present study indicate the role of Ca^{2+} channels or other membrane proteins in Ca^{2+} influx; hence, these questions should be investigated further.

CHAPTER THREE:

METHYLMERCURY-INDUCED CALCIUM-DEPENDENT VESICULAR RELEASE OF GLUTAMATE FROM CEREBELLAR ASTROCYTES CONTRIBUTES TO THEIR PREFERENTIAL SUSCEPTIBILITY TO METHYLMERCURY WHEN COMPARED WITH CORTICAL ASTROCYTES

A. Abstract

This chapter has two main objectives. The first objective is to examine whether an acute exposure to MeHg can produce changes in extracellular glutamate levels and reduce viability in cerebellar and cortical astrocytes. The second objective is to understand if Ca^{2+}-dependent vesicular release of glutamate and MeHg-induced alteration on EAATs levels can contribute to such changes. Primary astrocyte cultures from the cerebellum and cortical forebrain layer were obtained from 7 to 8 day old C57BL/6 mice. At 13-15 DIV, cells were exposed for 3 h to 0 μM, 1 μM, 2 μM, or 5 μM MeHg. Extracellular glutamate levels and cytotoxicity were measured immediately after the 3 h of exposure or 24 h after exposure. To test whether extracellular Ca^{2+} contributed to the extracellular glutamate levels, the cell-impermeant chelator EGTA (0.02 mM) was used in a Ca^{2+}-free buffer. To determine if the changes in extracellular glutamate levels and the decrease in viability were due to a Ca^{2+}-dependent vesicular release of glutamate from astrocytes, Rose Bengal (0.5 μM) was used. There was a concentration-dependent increase in extracellular glutamate in cerebellar astrocytes and these increase occurred at all MeHg concentrations. No changes in extracellular glutamate levels were observed in cortical astrocytes. The increase in extracellular glutamate levels in cerebellar astrocytes was also observed immediately after MeHg treatment. The changes in extracellular glutamate levels were extracellular Ca^{2+}-dependent and were due to a Ca^{2+}-dependent vesicular release of glutamate. After the co-treatment with Rose Bengal, we found that cerebellar astrocytic death was significantly reduced (61%) at 2 μM MeHg and (67%) at 5 μM MeHg. However, a significant amount of cerebellar astrocytic death of approximately 30% was obtained at 5 μM MeHg + Rose Bengal. Therefore, by reducing the extracellular glutamate levels, the astrocytic death was decreased, but not eliminated. This indicates that although excitotoxicity in astrocytes may play a

role in MeHg induced toxicity, there are other factors that can also contribute to astrocyte death at higher MeHg concentrations. However, by reducing the extracellular glutamate levels, the differences in susceptibility between cerebellar and cortical astrocytes were eliminated; suggesting that the excitotoxicity of astrocytes plays an important factor in the susceptibility of cerebellar astrocytes. Despite the preferential susceptibility of the cerebellum to MeHg-induced excitotoxicity, the cerebellar astrocytes possess higher EAATs levels than cortical astrocytes when treated with MeHg. Thus, it is possible that MeHg causes a dysfunction in this cerebellar protein that inhibits their normal buffering. The noticeable effects of MeHg exposure in glutamate levels observed in cerebellar astrocytes might contribute to the preferential sensitivity of the granule cells to MeHg.

B. Introduction

Mercury (Hg) contamination is still a problem. Currently, Hg is been highly used globally to extract gold in artisanal and small-scale gold mining (Nakazawa et al., 2016). Hg can methylate and transform into MeHg (Jensen & Jernelöv, 1969), a potent neurotoxicant that can produce neurological disorders (Harada, 1995; Rustam & Hamdi, 1974). Some signs and symptoms of MeHg exposure include ataxia, dysarthria, visual disturbance, sensory changes, weakness, hyperreflexia, involuntary movements, and muscle and joint pain (Amin-Zaki et al., 1979; Harada, 1978).

MeHg can affect both the peripheral and central nervous system; however, cerebellar granule cells in the cerebellum are preferential targets of MeHg (Hunter & Russell, 1954). The reason for this heightened sensitivity of the granule cells to MeHg is not well understood, although it is believed to be the result of unregulated elevations of $[Ca^{2+}]_i$ (Atchison, 2005; Limke, Heidemann, & Atchison, 2004).

Previous studies have demonstrated that MeHg can interact with intracellular organelles (Limke & Atchison, 2002; Limke, Bearss, & Atchison, 2004) and Ca^{2+} channels (Marty & Atchison, 1997; Sirois & Atchison, 2000) in the granule cells, resulting in an increase of $[Ca^{+2}]_i$. The increase in $[Ca^{+2}]_i$ can produce an increase in glutamate release, which can produce excitotoxicity in high extracellular levels (Mark et al., 2001; Olney, 1994). MeHg can also block $GABA_A$ receptors in this neuron, which suggests a decrease in the function of the channel to mediate inhibitory neurotransmission, thereby causing an increase in glutamate release (Atchison, 2005; Herden, Pardo, Hajela, Yuan, & Atchison, 2008; Yuan & Atchison, 2003).

Astrocytes possess EAATs, especially EAAT1 and EAAT2, making these cells important for buffering excess glutamate and protecting the neurons from excitotoxicity. However, recent

experiments have demonstrated that astrocytes can also be affected by glutamate excitotoxicity, and that their vulnerability to this cell death mechanism varies from one region to another (David, Yamada, Bagwe, & Goldberg, 1996; Matute, Alberdi, Ibarretxe, & Sánchez-Gómez, 2002; Prieto & Alonso, 1999). Astrocytes can also regulate synaptic transmission by releasing gliotransmitters, such as glutamate. This glial cell can release glutamate through different mechanisms, including Ca^{2+}-dependent vesicular exocytosis (Parpura et al., 1994).

Astrocytes can also be affected by MeHg. It has been hypothesized that neurotoxicity by MeHg occurs secondary to effects on glial cell functions (Michael Aschner, Yao, Allen, & Tan, 2000). MeHg produces a region-dependent toxicity in astrocytes. This toxicant produces different mechanisms of Ca^{2+}-induced cytotoxicity in cerebellar and cortical astrocytes. In Chapter 2, we found that extracellular Ca^{2+} has a more important role in cerebellar astrocytes than in cortical astrocytes and that increased levels of intracellular Ca^{2+} have a more important role in cortical astrocytes than in cerebellar astrocytes during MeHg-induced cytotoxicity at higher concentrations.

The present study was designed to examine whether an acute exposure to MeHg in astrocytes can produce changes in glutamate levels and to understand the mechanisms that can contribute to such changes. Therefore, we examined the effect of MeHg on extracellular glutamate levels of cortical and cerebellar astrocytes, and whether changes can occur immediately after MeHg treatment. To understand some mechanisms that can contribute to changes in extracellular glutamate levels, we sought to determine whether MeHg can produce vesicular exocytosis of glutamate from astrocytes and if this exocytosis was dependent on extracellular Ca^{2+}. Then, we performed an immunocytochemistry and studied the effect of MeHg on the mean fluorescence intensity levels of EAAT1 and EAAT2 proteins. Our results indicated

that MeHg induces an increase in Ca^{2+}-dependent glutamate release in cerebellar astrocytes but not cortical astrocytes, which could contribute to the susceptibility of the cerebellum to MeHg.

C. Materials and methods

C.1. Materials and experimental solutions

FBS, heat inactivated horse serum, high glucose DMEM, antibiotic-antimycotic, and Trypan Blue Stain (0.4%) were obtained from Gibco (Grand Island, NY). The following items were purchased from Sigma-Aldrich Co. (St. Louis, MO): HEPES, trypsin, DNase I, glutamine, poly-D-lysine, Rose Bengal, and EGTA. Methylmercuric chloride was obtained from ICN Biomedicals Inc. (Aurora, OH).

Experimental solutions were prepared on the day of each experiment by diluting stock solutions and using HBS, which contained (mM) 150 NaCl, 5.4 KCl, 1.8 $CaCl_2$, 0.8 MgSO4, 20 D-glucose, and 20 HEPES (free acid) (pH 7.3). The EGTA-containing buffer had the same constituents as HBS minus $CaCl_2$ and plus 0.02 mM EGTA (final $[Ca^{2+}]$ = 60 nM) (Marty & Atchison, 1997). Rose Bengal was dissolved into distilled water as a 25 mM stock solution.

C.2. Preparation of primary cerebral cortical and cerebellar astrocyte cultures

Primary astrocyte cultures from cerebral cortex and cerebellum were obtained from 7-8 days old C57BL/6 mice by using a modification of the method described by Inglefield et al (Inglefield, Mundy, & Shafer, 2001). Briefly, after the brain dissection and separation of the cerebral cortical layer and cerebellum, cells were digested for 4 min at 37°C with trypsin 0.025% (w/v) in a buffer that contained: 5.0 mM KCl, 0.20 mM KH_2PO_4, 137.0 mM NaCl, 0.17 mM Na_2HPO_4, 5.0 mM D-glucose, 59.0 mM sucrose, and 0.1 mg/ml antibiotics, pH 7.3. Cerebral

cortex and cerebellum were maintained apart to avoid cross-contamination. Trypsin was inactivated by 0.016% (w/v) DNase I diluted in HBS for 4 min at 37°C. Then, cell media containing warmed DMEM supplemented with 10% (w/v) heat-inactivated horse serum, 10 mM HEPES, 2 mM glutamine, and 0.1 mg/ml antibiotics was added to the cell culture. Cells were centrifuged at 500 X g for 5 min and the resulting pellet was resuspended in DMEM-containing DNase I and recentrifuged at 500 g X for 5 min. Finally, cells were resuspended for last time in DMEM and recentrifuged at 500 X g for 5 min. Animal procedures were in adherence with NIH guidelines and accepted by MSU Institutional Animal Use and Care Committee.

C.3. Purification of astrocytes

Cortical and cerebellar cell cultures were purified separately by using Anti-GLAST (ACSA-1) MicroBead Kit (Miltenyi Biotec Inc., San Diego, CA). Briefly, cells were incubated in 20 μM of Anti-GLAST (ACSA-1)-Biotin for 10 min. Then, cells were washed with ice-cold (PBS; containing 137 mM NaCl, 2.7 mM KCl, 1.4 mM NaH_2PO_4, and 4.3 mM Na_2HPO_4, pH 7.4) containing 0.5% FBS and centrifuged for 10 min at 300 X g. The resulting pellet was dissociated and incubated with 20 μL of Anti-Biotin MicroBeads for 15 min. After the incubation, cells were washed with PBS containing 0.5% FBS and centrifuged for 10 min at 300 X G. The final pellet was dissociated with the PBS solution described above and passed through a 70 μm nylon mesh (Miltenyi Biotec Inc., San Diego, CA). Cortical and cerebellar cell cultures were loaded onto separate MS column (Miltenyi Biotec Inc., San Diego, CA), which was placed in the magnetic field of a MACS Separator (Miltenyi Biotec Inc., San Diego, CA). The column was rinsed with PBS containing 0.5% FBS. Isolated pure astrocytes were retained in the column and removed by using cell media.

C.4. Cell plating

Astrocytes were plated at a density of 1×10^5 cells/dish onto 35-mm Petri dishes coated with poly-D-lysine and maintained in a 37°C incubator with 95% O_2 and 5% CO_2. TC20 Automated Cell Counter (Bio-Rad Laboratories Inc., Hercules, CA) was used to obtain an equal density of astrocytes in all the cell dishes. Cell media was changed every other day. Non-antibiotic media was used after the third replacement of cell media because it could affect the function of Ca^{2+} channels (Atchison, Adgate, & Beaman, 1988; Redman & Silinsky, 1994).

C.5. Methylmercury treatment

Methylmercuric chloride was dissolved in distilled water to a final concentration of 10 mM to serve as a stock solution and diluted to working concentrations on the same day in HBS. At 13-15 DIV, astrocytes were treated for 3 h with 0 μM, 1 μM, 2 μM, or 5 μM MeHg. Because MeHg can bind to serum proteins, cells were treated using HBS (Fang & Fallin, 1976). Astrocytes were analyzed 21 h after the 3 h of exposure or immediately after the 3 h of MeHg exposure. To test the effect of EGTA with MeHg, the cells were co-treated for 3 h with EGTA in a Ca^{2+}-free HBS. To test the effect of Rose Bengal with MeHg, the cells were pre-incubated for 15 min, co-treated for 3 h with MeHg, and placed in the cell media. The concentration of Rose Bengal used was 0.5 μM. Experiments in our laboratory demonstrated that pre-incubation of Rose Bengal with this concentration was able to significantly reduce the vesicular release of glutamate from cortical and cerebellar astrocytes after a 1 min of 1 μM Bradykinin (data not shown). Also, a study done by Montana et al. found that this concentration abolished mechanically induced glutamate release from astrocytes after 55 sec of 90 nM bradykinin

(Montana, Ni, Hua, & Parpura, 2004). In both EGTA and Rose Bengal experiments cytotoxicity was performed 24 h after the 3 h co-treatment with MeHg.

C.6. Assessment of extracellular glutamate levels

Glutamate concentrations in the media were determined by enzymatic, colorimetric assay, using a commercially available kit purchased from Sigma-Aldrich Co. (St. Louis, MO). Briefly, 50 µl of media was collected from each cell culture dish after the treatment of MeHg and mixed with the reaction mix. Glutamate concentration was determined after 30 min of incubation at 37º C, by an enzymatic activity, which resulted in a colorimetric (450 nm) product proportional to the glutamate present. The absorbance was recorded using an Infinite m1000 Pro microplate reader (Tecan, San Jose, CA). To ensure equal amounts of glutamate in the media in all the experiments, the levels of glutamate in media were measured in each experiment. To avoid deterioration of astrocytes, no additional glutamate was added into the media (Ye & Sontheimer, 1998). Because in the immediate treatment cells were treated with MeHg using HBS, we measured the changes of extracellular glutamate in HBS.

C.7. Cytotoxicity

The Viability/Cytotoxicity Assay (Molecular Probes Inc., OR, USA) was used to identify the viability of astrocytes after treatments. Astrocytes were incubated with 0.3 µM calcein-AM and 0.075 µM EthD-1 at room temperature for 20 min. The cells that were labeled with calcein-AM represented the healthy cells, and the ones labeled with EthD-1 represented the dead cells.

C.8. Immunocytochemistry

Cerebellar and cortical astrocytes were fixed in cold 4.0% (v/v) p-formaldehyde in PBS for 15 min. Cells were treated for 30 min with 0.1% (v/v) Triton-X in PBS containing 5% (v/v) NGS after rinsed in PBS. To determine the fluorescence intensity levels of EAAT1, the EAAT1/GLAST-1/SLC1A3 antibody (Novus Biologicals, Littleton, CO) was used at a concentration of 1:200. After 24 h, the slides were rinsed in PBS and labeled with secondary antibody Alexa Fluor 647 rabbit anti-goat (Invitrogen Corporation, Carlsbad, CA) at a concentration of 1:200. To determine the fluorescence intensity levels of EAAT2, the mouse monoclonal anti-excitatory amino acid transporter 2 Antibody, clone G6 (Millipore Corporation, Temecula, CA) was used at a concentration of 1:5000. Then, after 24 h, the slides were rinsed in PBS and labeled with secondary antibody Alexa Fluor 568 goat anti-mouse (Invitrogen Corporation, Carlsbad, CA) at a concentration of 1:200. To determine the percentage of astrocytes in the cell cultures, an indicator for astrocytes called rabbit Anti-GFAP (Millipore Corporation, Temecula, CA) was used at a concentration of 1:1000. Then, after 24 h, astrocytes were rinsed in PBS and labeled with secondary antibody Alexa Fluor 405 goat anti-rabbit (Invitrogen Corporation, Carlsbad, CA) at a concentration of 1:200. Astrocytes were mounted on glass slides by using a mounting medium with DAPI (Vectashield Hard Set, Vector, Burlingame, CA). Cell cultures were ≥99% pure astrocytes.

C.9. Data acquisition and analysis

The total change in glutamate levels in the media was obtained by subtracting the amount of glutamate obtained in the cell culture from the amount of glutamate obtained in a parallel dish that contained only media. For the immunocytochemistry, negative controls consisted of cells

with primary antibody only, secondary antibody only, and cells without antibodies. To determine the mean fluorescence intensity levels of EAAT1 and EAAT2 present in astrocytes after MeHg treatment, regions of interest (ROI) were drawn around different astrocytes, and background intensity per pixel was obtained with similar ROI size in each picture. The mean intensity per pixel was computed as the mean of the subtraction of the intensity per pixel of each cell from the corresponding background intensity per pixel. Astrocytes were examined by using the Nikon Eclipse Ti with NIS-Elements BR software (Nikon Instruments Inc., Melville, NY, USA). All images were acquired with 20X oil immersion objectives by using the same acquisition configuration, including exposure time, and neutral density filters. To determine the effect of MeHg on the astrocytes, a one-way ANOVA was used. To compare between groups, a two-way ANOVA followed by Tukey's procedure for post-hoc comparisons were used. $P < 0.05$ was considered to be statistically significant.

D. Results

D.1. Effect of methylmercury on the glutamate levels of cerebellar and cortical astrocytes

The 0 ng/mL, on the y-axis, represents the normal amount of glutamate in the media. Below the 0 ng/mL, represents less amount of glutamate in the media than the normal amount of glutamate present in media. Above the 0 ng/mL, represents more amount of glutamate than the normal amount of glutamate present in media. There was a significant increase in the concentration of glutamate in the media of cerebellar astrocytes to approximately 2.03, 3.11 and 3.7 ng/mL from control value (0 μM) at 1 μM, 2 μM, and 5 μM MeHg, respectively (Fig. 3.1.A). There were no differences from control in cortical astrocytes after MeHg treatment (Fig. 3.1.B).

MeHg was able to significantly increase the concentration of extracellular glutamate immediately after the 3 h of MeHg treatment in cerebellar astrocytes. There was a significant increase to approximately 0.43 ng/mL from control value at 5 μM MeHg (Fig. 3.2.A). There were no differences from control immediately after the 3 h of MeHg treatment in cortical astrocytes (Fig. 3.2.B).

D.2. Contribution of extracellular calcium to glutamate changes after methylmercury treatment

In order to determine if the changes in extracellular glutamate were caused by the extracellular Ca^{2+} that entered the cell, the cell-impermeant chelator EGTA (0.02 mM) was used in Ca^{2+}-free HBS. There was a significant decrease in extracellular glutamate levels in cerebellar astrocytes (2.19 ng/ml) at 1 μM, (3.28 ng/ml) 2 μM and (3.67 ng/ml) 5 μM MeHg after the co-treatment with EGTA, when compared with the MeHg group (Fig. 3.3.A). Also, there was a significant decrease in extracellular glutamate levels in cortical astrocytes at (1.30 ng/ml) 0 μM,

A

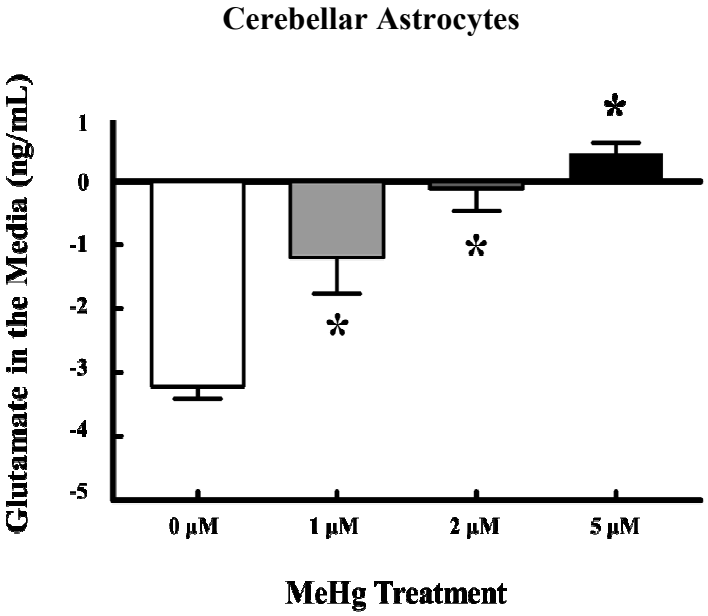

B

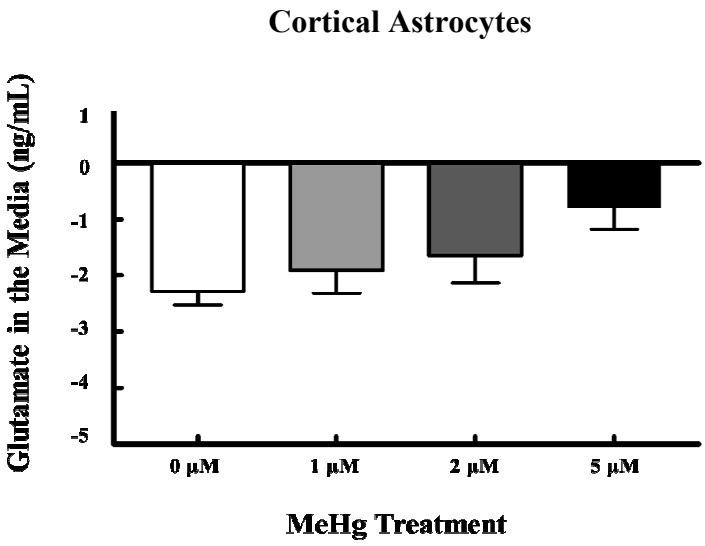

Figure 3.1. MeHg significantly increased the levels of extracellular glutamate in cerebellar astrocytes, but not in cortical astrocytes. (A). Effect of MeHg on cerebellar astrocytes. **(B)**. Effect of MeHg on cortical astrocytes. Glutamate in the Media (ng/mL) at 0 µM, 1 µM, 2 µM, and 5 µM MeHg (n=6). Values are mean ± SEM. * denotes $p < 0.05$. One-way ANOVA followed by Tukey's post-hoc comparison were used.

A

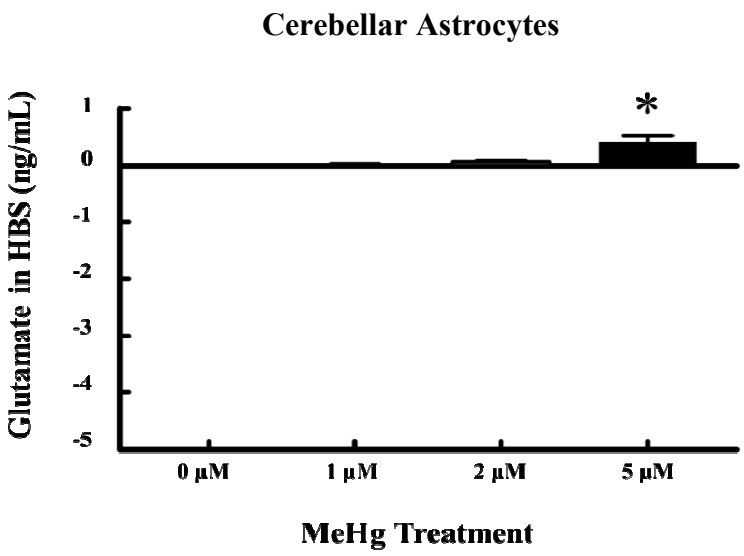

B

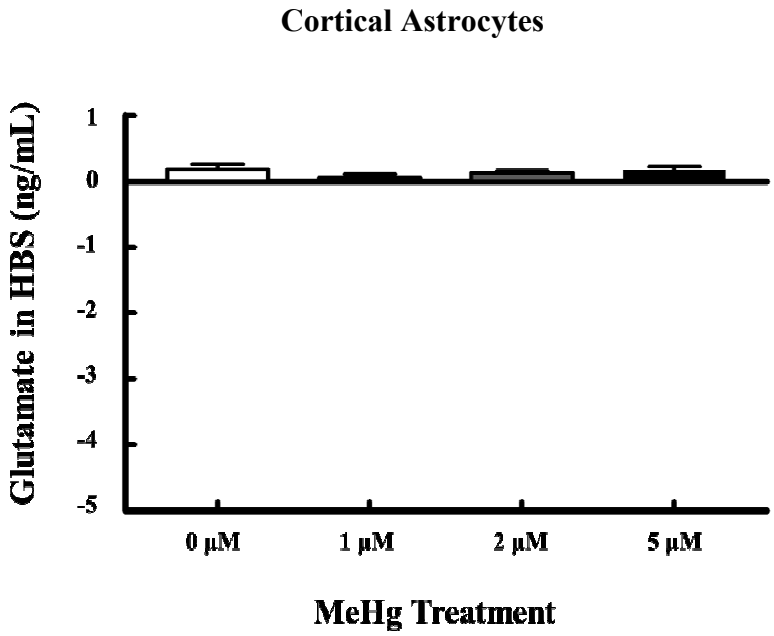

Figure 3.2. The increased levels of extracellular glutamate in cerebellar astrocytes occur immediately after MeHg exposure; no significant changes were observed in cortical astrocytes. (A). Effect of MeHg on cerebellar astrocytes. **(B)**. Effect of MeHg on cortical astrocytes. Glutamate in HBS (ng/mL) at 0 µM, 1 µM, 2 µM, and 5 µM MeHg (n=5). Values are mean ± SEM. * denotes $p < 0.05$. One-way ANOVA followed by Tukey's post-hoc comparison were used.

A

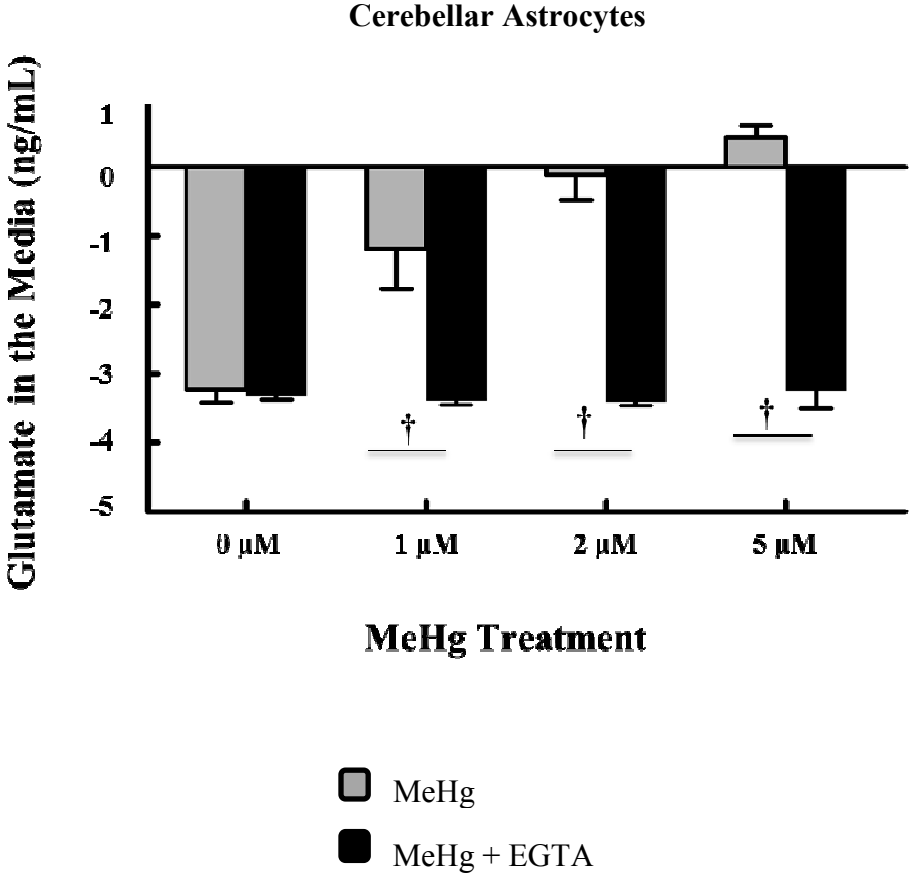

Figure 3.3. The increased levels of extracellular glutamate in cerebellar astrocytes induced by MeHg was dependent of extracellular Ca^{2+}; there was a Ca^{2+}-dependent change in the levels of extracellular glutamate in cortical astrocytes. (A). Effect of MeHg vs MeHg + EGTA on cerebellar astrocytes. **(B)**. Effect of MeHg vs MeHg + EGTA on cortical astrocytes. Glutamate in the Media (ng/mL) at 0 µM, 1 µM, 2 µM, and 5 µM MeHg ($n \geq 5$). Values represent mean ± SEM. * denotes $p < 0.05$ compared with 0 µM MeHg + EGTA. † denotes $p < 0.05$ between MeHg and MeHg + EGTA groups. One-way ANOVA was used to compare within groups. Two-way ANOVA was used to compare between groups. Tukey's post-hoc comparison was used.

Figure 3.3 (cont'd)

B

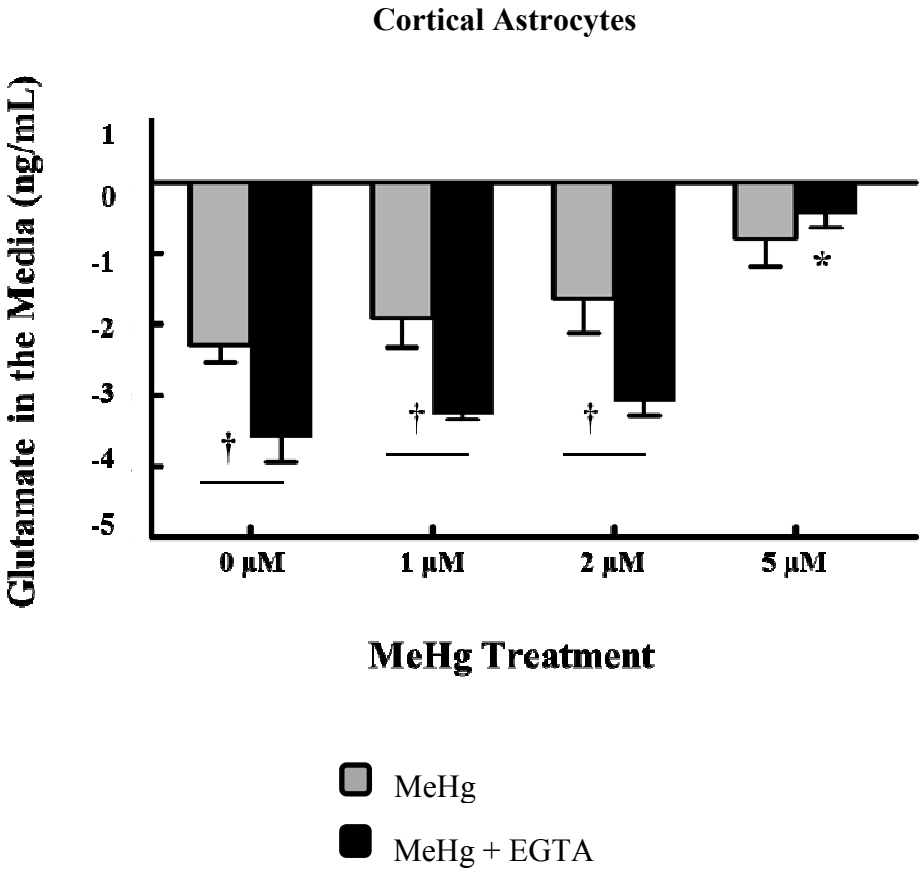

(1.35 ng/ml) 1 μM and (1.45 ng/ml) 2 μM MeHg after the co-treatment with EGTA, when compared with the MeHg group (Fig. 3.3.B).

D.3. Vesicular release of glutamate from astrocytes after methylmercury treatment

These experiments were designed to find out if MeHg can produce a vesicular release of glutamate from astrocytes. In order to determine if there was glutamate release from vesicles, Rose Bengal (0.5 μM) was used to inhibit the glutamate uptake into the vesicular lumen (Montana, Ni, Hua, & Parpura, 2004). There was a significant decrease in extracellular glutamate levels in cerebellar astrocytes (2.51 ng/ml) at 1 μM, (3.34 ng/ml) 2 μM and (3.20 ng/ml) 5 μM MeHg after the co-treatment with Rose Bengal, when compared with the MeHg group (Fig. 3.4.A). There were no significant differences between MeHg group and MeHg + Rose Bengal group in cortical astrocytes (Fig 3.4.B).

To determine if the increased levels of extracellular glutamate can produce cytotoxicity in astrocytes after MeHg treatment, EthD-1 and calcein-AM were used. MeHg produced cytotoxicity in a concentration-dependent manner in cerebellar astrocytes, with a significant reduction in viability to approximately 69% and 97% of control values at 2 μM and 5 μM MeHg, respectively. There was also a significant difference in viability to approximately 30% of control values at 5 μM MeHg + Rose Bengal. When MeHg group and MeHg + Rose Bengal group were compared, there was a significant difference in viability (61%) at 2 μM MeHg and (67%) at 5 μM MeHg (Fig. 3.5.A).

In cortical astrocytes, there was a significant decrease in viability to approximately 66% of control for cells exposed to 5 μM MeHg. There was also a significant difference in viability to approximately 26% of control values at 5 μM MeHg + Rose Bengal. When MeHg group and

A

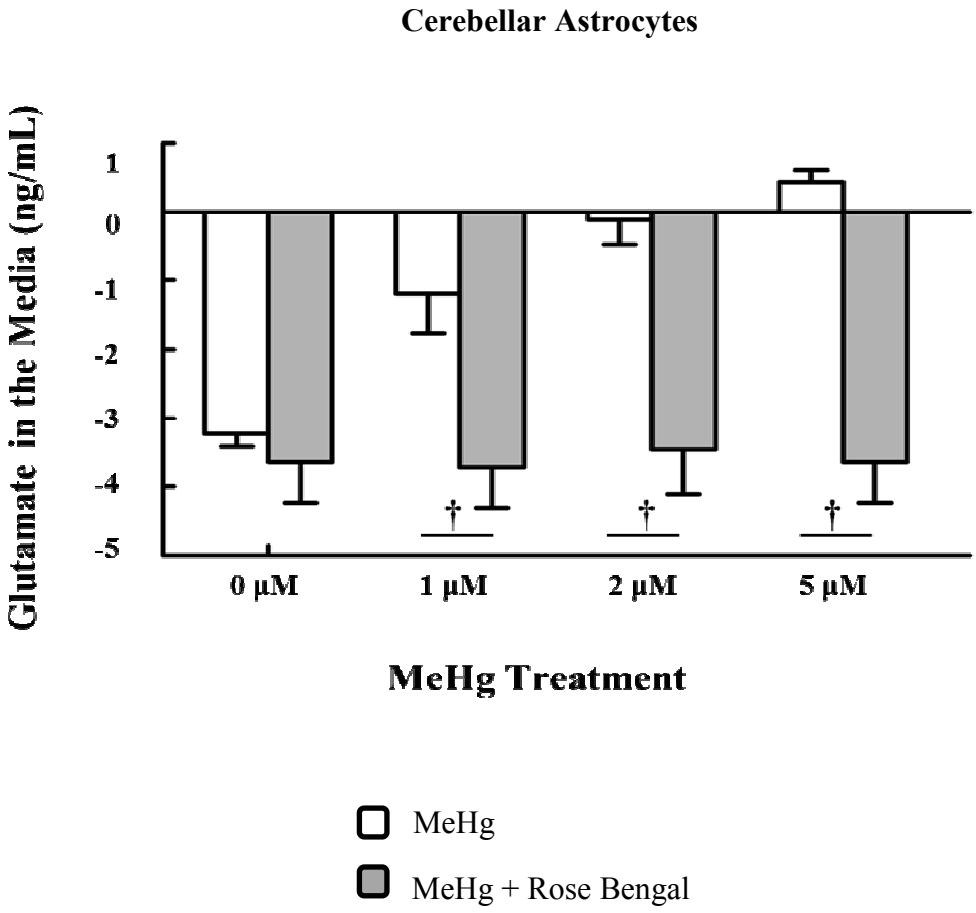

Figure 3.4. The increased levels of extracellular glutamate in cerebellar astrocytes induced by MeHg were due to a vesicular release of glutamate from astrocytes; no significant changes were observed in cortical astrocytes. (A). Effect of MeHg vs MeHg + Rose Bengal on cerebellar astrocytes. **(B)**. Effect of MeHg vs MeHg + Rose Bengal on cortical astrocytes. Glutamate in the Media (ng/mL) at 0 µM, 1 µM, 2 µM, and 5 µM MeHg ($n \geq 5$). Values represent mean ± SEM. † denotes $p < 0.05$ between MeHg and MeHg + Rose Bengal groups. Two-way ANOVA followed by Tukey's post-hoc comparison were used.

Figure 3.4 (cont'd)

B

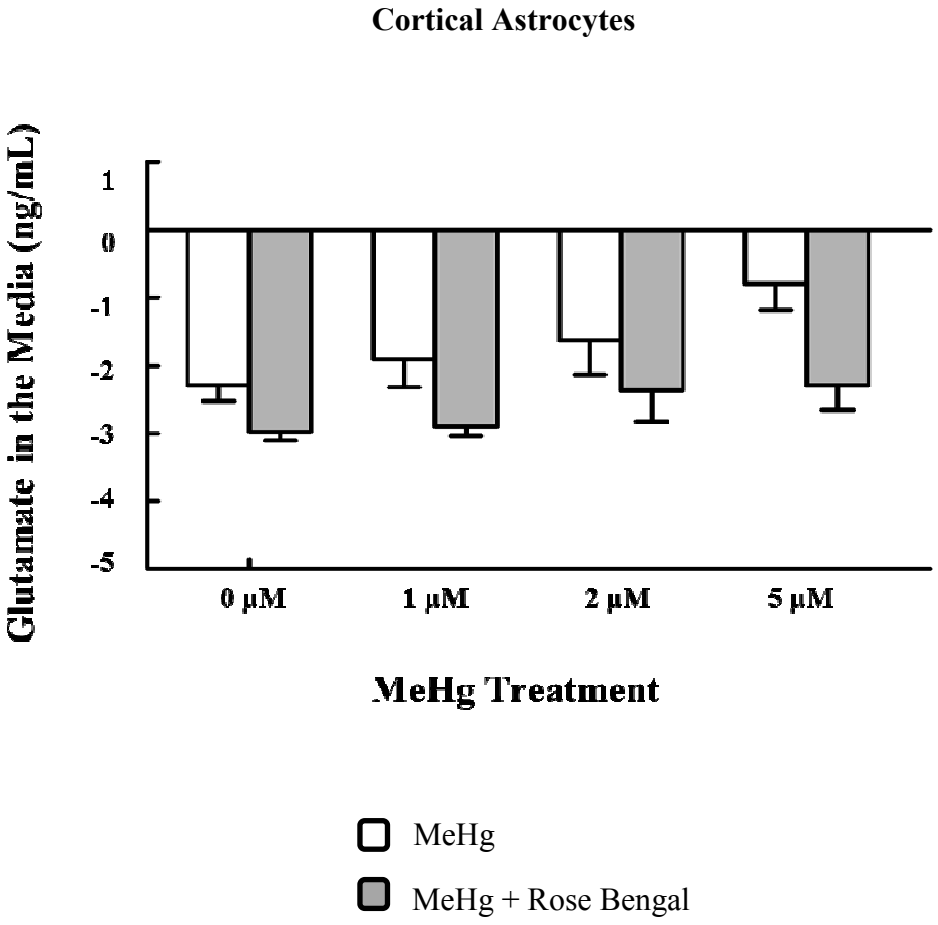

A

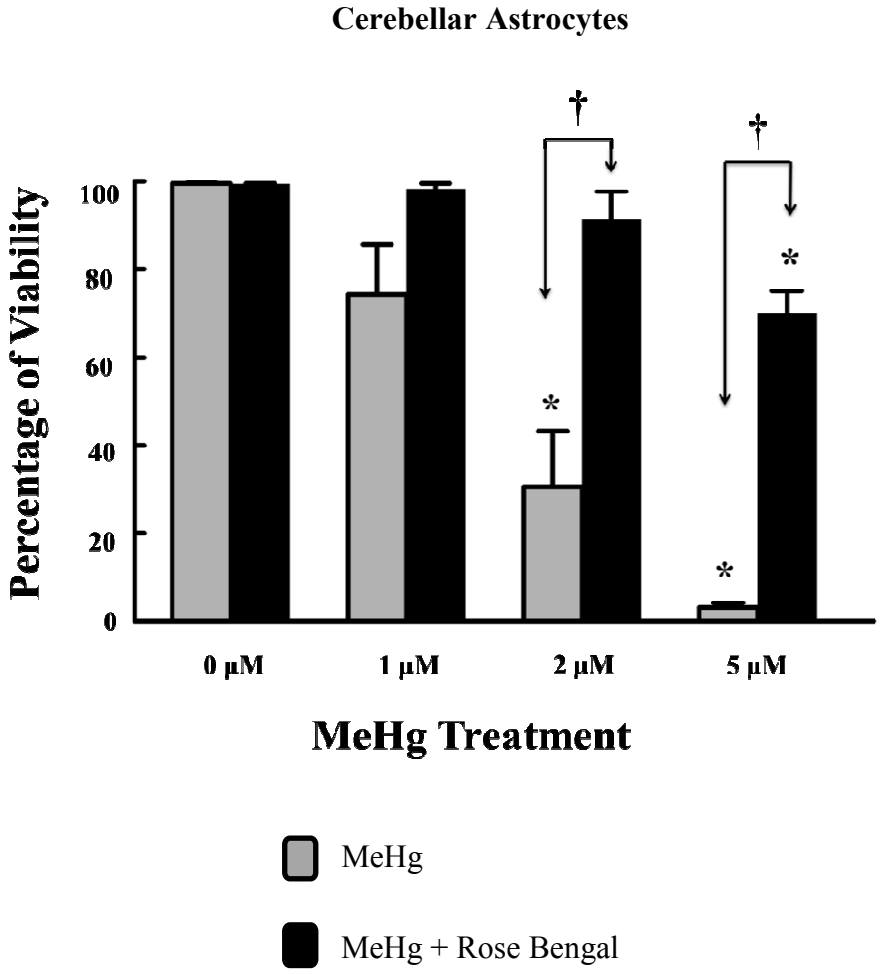

Figure 3.5. The inhibition of the vesicular release of glutamate from astrocytes reduces astrocyte death after MeHg treatment. (A). Effect of MeHg vs MeHg + Rose Bengal on cerebellar astrocytes. **(B)**. Effect of MeHg vs MeHg + Rose Bengal on cortical astrocytes. Viability was measured, using EthD-1 and calcein-AM. Values are mean ± SEM. * denotes $p < 0.05$ compared with 0 µM MeHg + Rose Bengal. † denotes $p < 0.05$ between MeHg and MeHg + Rose Bengal groups. One-way ANOVA was used to compare within groups. Two-way ANOVA was used to compare between groups. Tukey's post-hoc comparison was used.

Figure 3.5 (cont'd)

B

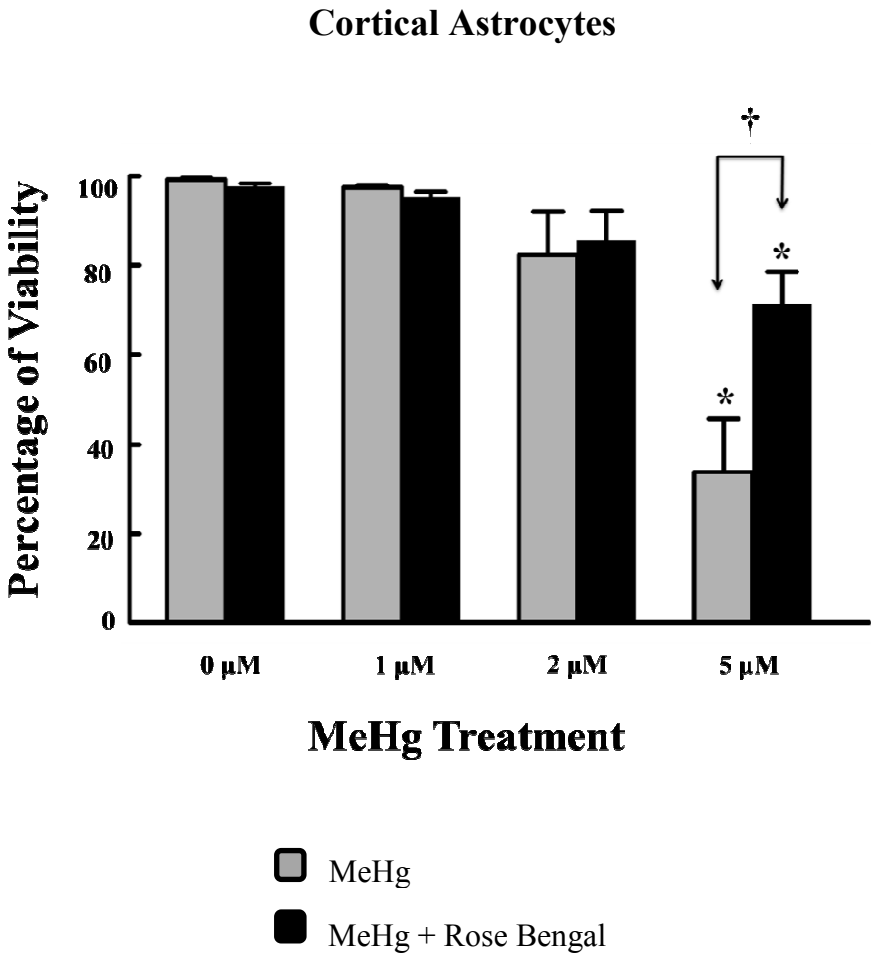

MeHg + Rose Bengal group were compared, there was a significant difference in viability (38%) at 5 μM MeHg (Fig. 3.5.B).

There were significant differences in the decrease of viability (52%) at 2 μM and (31%) 5 μM MeHg when cerebellar and cortical astrocytes were compared. However, these differences were eliminated after the co-treatment with Rose Bengal (Fig. 3.6.A-B).

D.4. Effect of methylmercury on the mean fluorescence intensity levels of EAAT1 and EAAT2 from cerebellar and cortical astrocytes

In order to determine the effect of MeHg on the EAAT1 and EAAT2 levels on cerebellar and cortical astrocytes, the mean fluorescence intensity of the astrocytes was obtained. There were no significant differences in the mean fluorescence intensity of the EAAT1 on cerebellar astrocytes.

In cortical astrocytes, there was a significant increase in the mean fluorescence intensity of the EAAT1 at 2 μM MeHg. However, when the cerebellar EAAT1 and cortical EAAT1 were compared, we observed higher mean fluorescence intensity in cerebellar astrocytes at the same MeHg concentration (Fig. 3.7).

When we studied the EAAT2, we found a significant increase in the mean fluorescence intensity at 2 μM MeHg in cerebellar astrocytes. No significant differences were observed neither in the mean fluorescence intensity of cortical astrocytes nor in the comparison between cerebellar EAAT2 with cortical EAAT2 (Fig. 3.8).

When the different EAATs from the same brain region were compared, we observed greater mean fluorescence intensity in cerebellar EAAT1 than cerebellar EAAT2 at 2 μM MeHg. No differences were found between the EAATs in cortical astrocytes (Fig. 3.9.A-B)

A

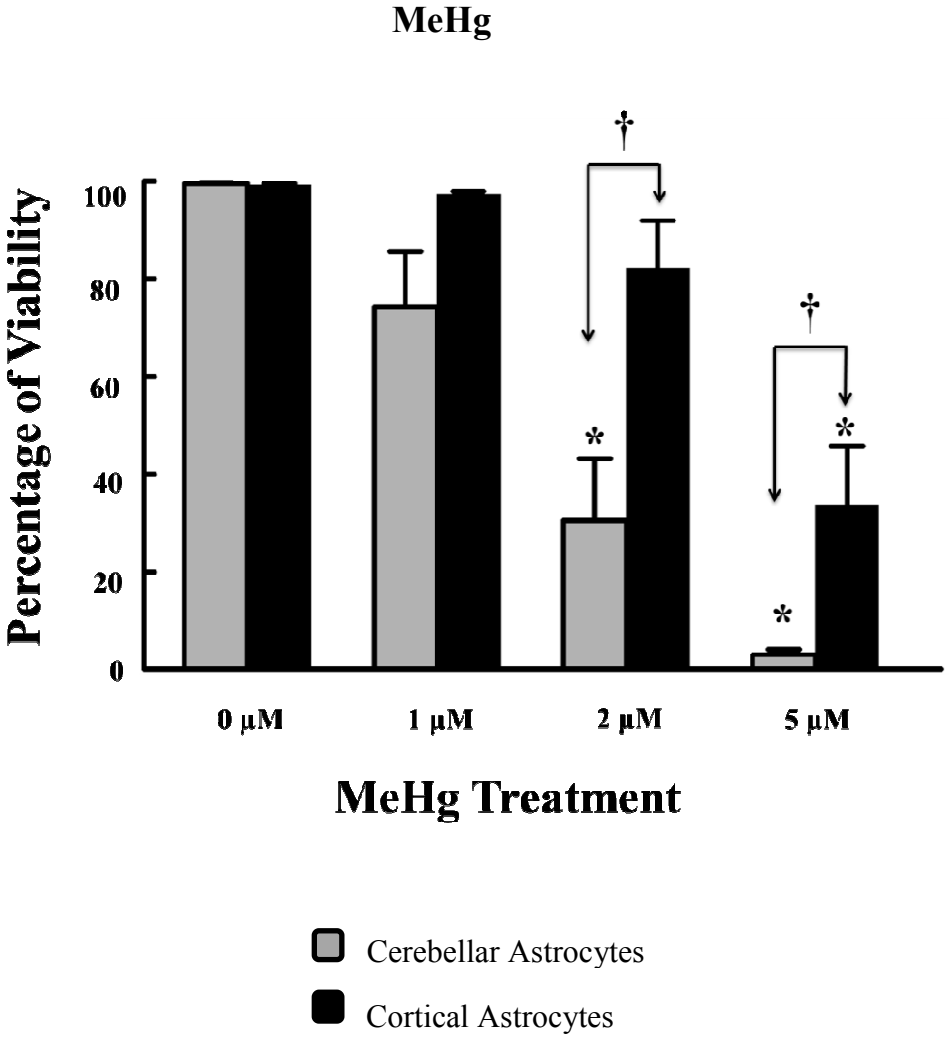

Figure 3.6. By inhibiting the vesicular release of glutamate after MeHg treatment, the differences in cytotoxicity between cerebellar and cortical astrocytes were eliminated. (A). Effect of MeHg on cerebellar and cortical astrocytes. **(B)**. Effect of MeHg + Rose Bengal on cerebellar and cortical astrocytes. Viability was measured using EthD-1 and calcein-AM. Values are mean ± SEM. * denotes $p < 0.05$ compared with 0 µM MeHg. † denotes $p < 0.05$ between cerebellar and cortical astrocytes. One-way ANOVA was used to compare within groups. Two-way ANOVA was used to compare between groups. Tukey's post-hoc comparison was used.

Figure 3.6 (cont'd)

B

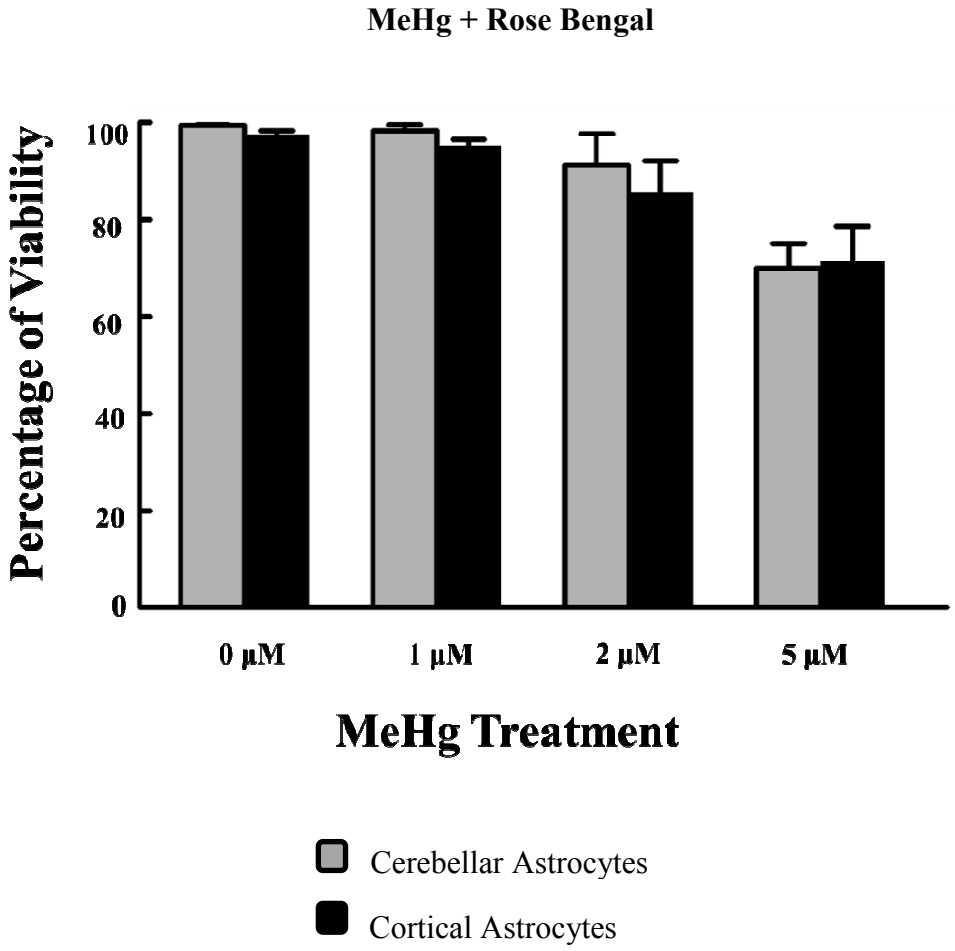

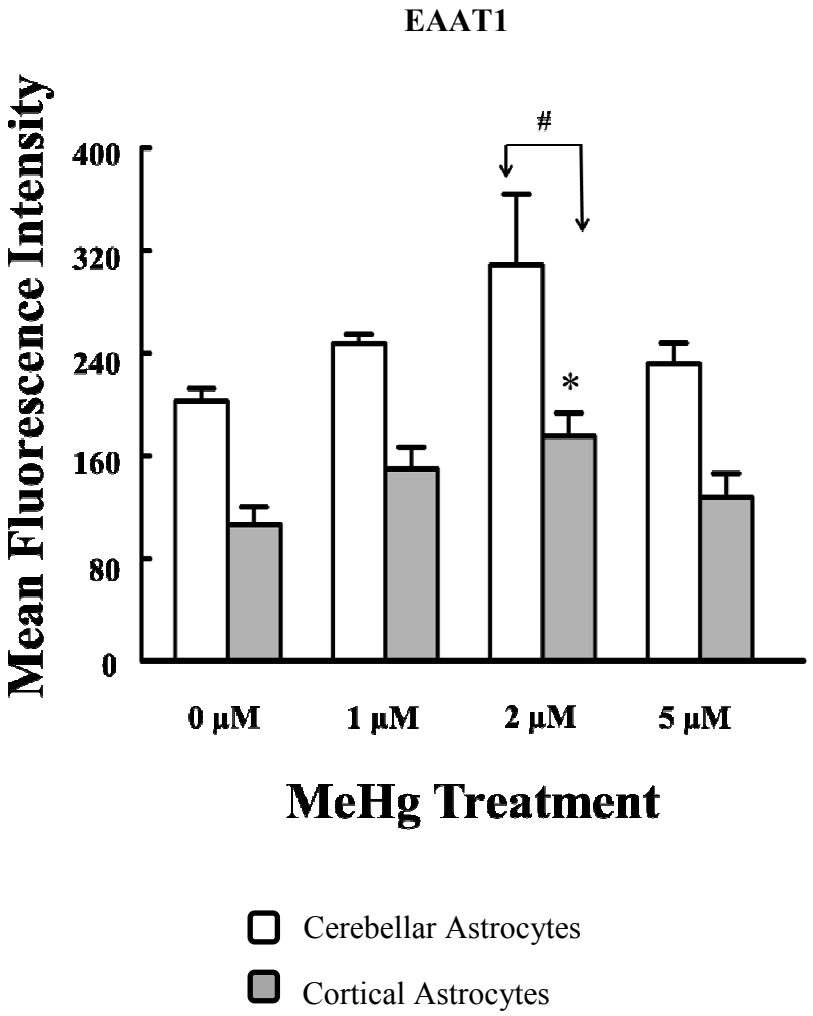

Figure 3.7. There was an increase in mean fluorescence intensity in EAAT1 from cortical astrocytes, however the mean fluorescence of EAAT1 was higher in cerebellar astrocytes. Mean fluorescence intensity at 0 µM, 1 µM, 2 µM, and 5 µM MeHg (n=5). Values represent mean ± SEM. * denotes $p < 0.05$ compared with control. # denotes $p < 0.05$ between cerebellar EAAT1 and cortical EAAT1 groups. One-way ANOVA was used to compare within groups. Two-way ANOVA was used to compare between groups. Tukey's post-hoc comparison was used.

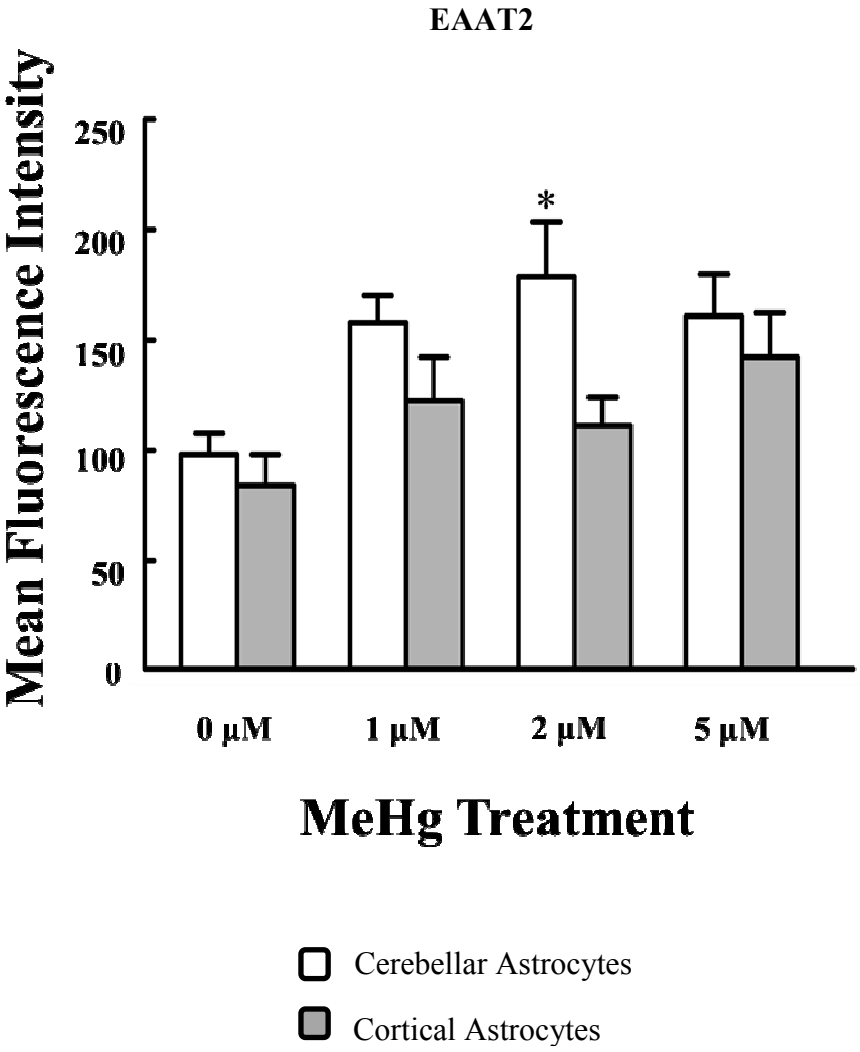

Figure 3.8. There was an increase in mean fluorescence intensity in EAAT2 in cerebellar astrocytes, no significant differences were observed between cerebellar and cortical EAAT2. Mean fluorescence intensity at 0 µM, 1 µM, 2 µM, and 5 µM MeHg (n=5). Values represent mean ± SEM. * denotes $p < 0.05$ compared with control. One-way ANOVA was used to compare within groups. Two-way ANOVA was used to compare between groups. Tukey's post-hoc comparison was used.

A

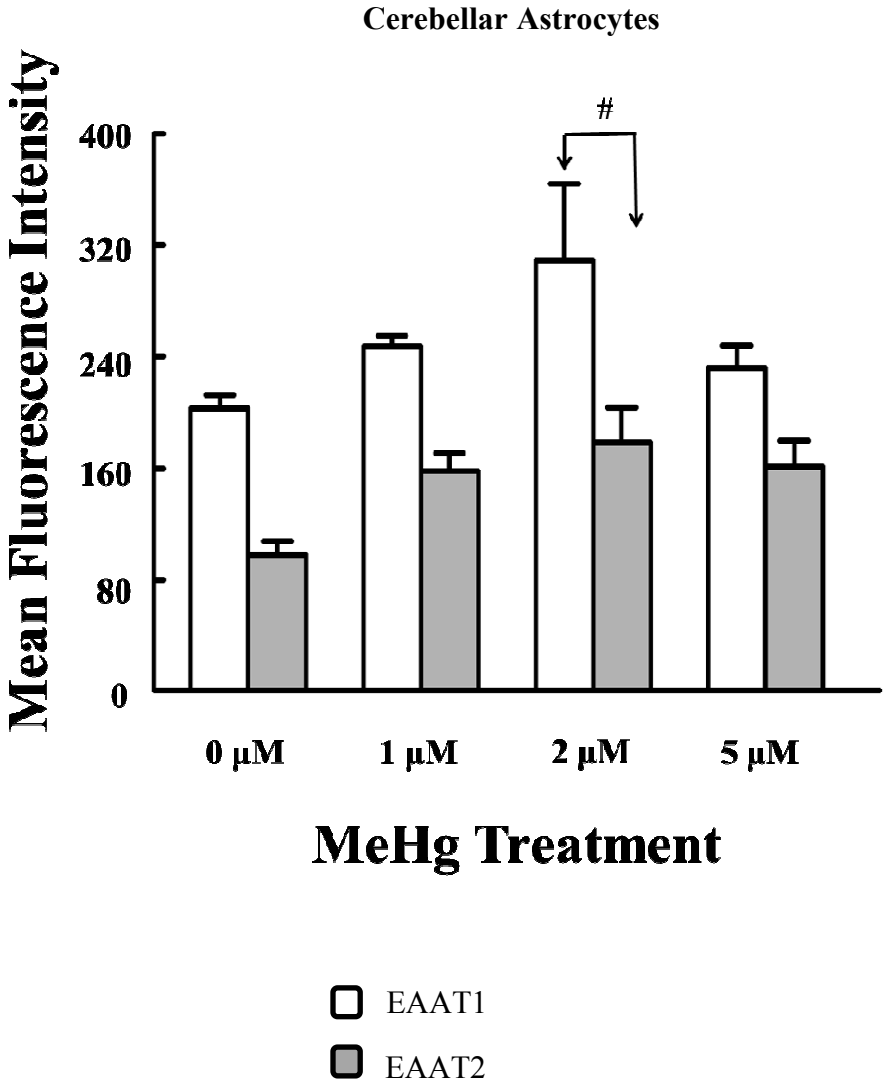

Figure 3.9. There was higher mean fluorescence intensity in EAAT1 when compared with EAAT2 in cerebellar astrocytes. (A). A comparison between EAAT1 and EAAT2 from cerebellar astrocytes. **(B)**. A comparison between EAAT1 and EAAT2 from cortical astrocytes. Mean fluorescence intensity at 0 µM, 1 µM, 2 µM, and 5 µM MeHg (n=5). Values represent mean ± SEM. # denotes $p < 0.05$ between cerebellar EAAT1 and EAAT2 groups. No differences between cortical EAAT1 and EAAT2 were observed. One-way ANOVA was used to compare within groups. Two-way ANOVA was used to compare between groups. Tukey's post-hoc comparison was used.

Figure 3.9 (cont'd)

B

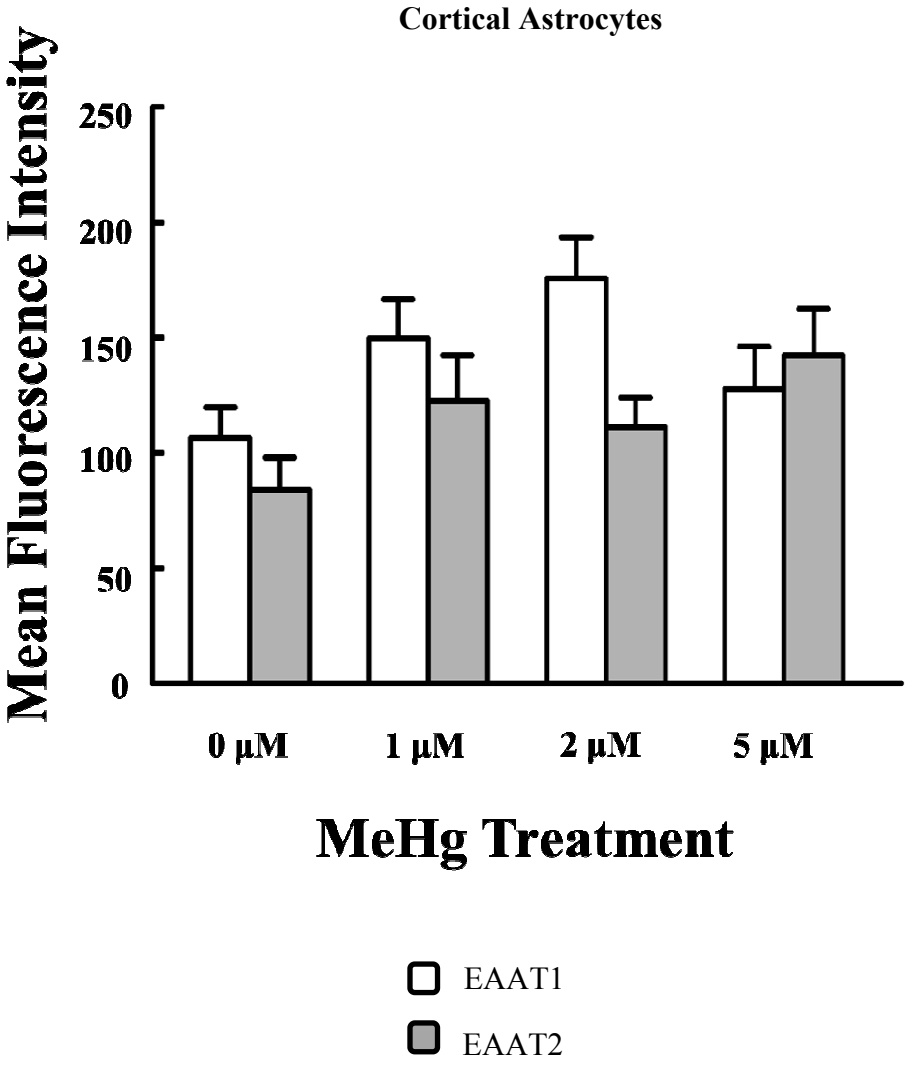

Representative micrographs of the significant increase in EAAT1 mean fluorescence intensity at 2 μM MeHg in cortical astrocytes are shown in Figure 3.10. Representative micrographs of the significant increase in EAAT2 mean fluorescence intensity at 2 μM MeHg in cerebellar astrocytes are shown in Figure 3.11.

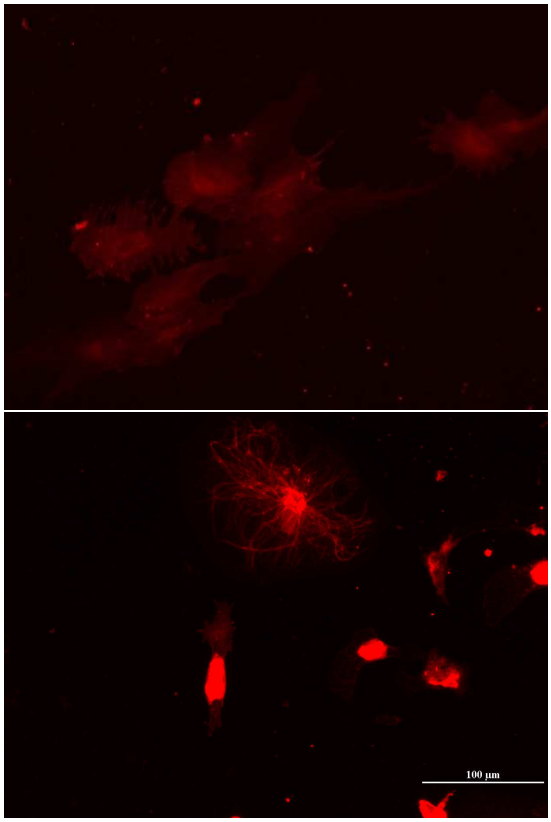

Figure 3.10. Representative micrographs of EAAT1 from cortical astrocytes. (A) Cortical astrocytes with 0 µM MeHg. **(B)** Cortical astrocytes with 2 µM MeHg. The EAAT1/GLAST-1/SLC1A3 antibody was used at a concentration of 1:200. The secondary antibody Alexa Fluor 647 rabbit anti-goat at a concentration of 1:200 was used. (20x).

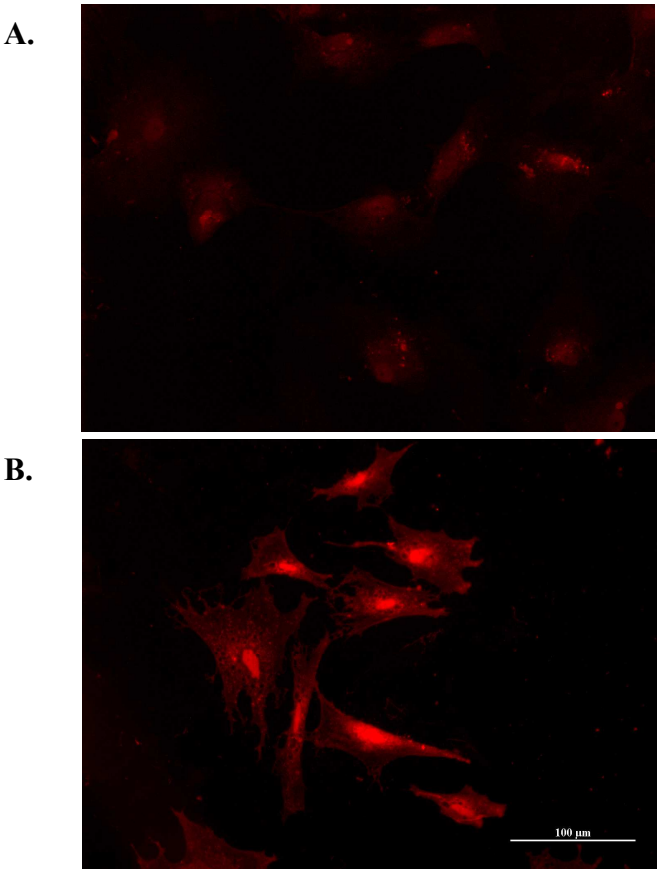

Figure 3.11. Representative micrographs of EAAT2 from cerebellar astrocytes. (A) Cerebellar astrocytes with 0 µM MeHg. **(B)** Cerebellar astrocytes with 2 µM MeHg. To determine the fluorescence intensity levels of EAAT2, the mouse monoclonal anti-excitatory amino acid transporter 2 Antibody, clone G6 was used at a concentration of 1:5000. Then, after 24 h, the secondary antibody Alexa Fluor 568 goat anti-mouse at a concentration of 1:200 was used. (20x).

E. Discussion

Granule cells in the cerebellum are particularly susceptible to MeHg toxicity. MeHg increases Ca^{2+} concentration in these cells, producing an increase in glutamate release, and eventually excitotoxicity. Astrocytes are the main cells responsible for the glutamate buffering and the prevention of excitotoxicity. The present study was designed to examine the extracellular glutamate levels in cerebellar and cortical astrocytes after an acute exposure to MeHg. Understating the effect of MeHg on extracellular glutamate levels in both cerebellar and cortical astrocytes will allow us to understand the susceptibility of the cerebellum to MeHg. Previous studies demonstrate the changes in extracellular EAA levels. However, these studies focused on the inability of astrocytes to uptake glutamate or the efflux of glutamate due to astrocytic swelling (M Aschner, Du, Gannon, & Kimelberg, 1993; Qu, Syversen, Aschner, & Sonnewald, 2003). In the present study, we performed parallel experiments, using cerebellar and cortical astrocytes, and aimed to understand the effect of MeHg on Ca^{2+}-induced vesicular release of glutamate in astrocytes. Evaluating the differences in glutamate release after MeHg exposure between cerebellar and cortical astrocytes allow us to understand the sensibility of cerebellar granule cells to MeHg toxicity.

By using microdialysis probe implanted in the frontal cortex of rats, Juarez and colleagues (2002) were able to detect significant elevations in extracellular glutamate at 10 μM and at 100 μM MeHg. The authors suggested that the elevations of extracellular glutamate were produced by an increase in glutamate release from neurons and an inhibition of glutamate uptake from astrocytes. Qu and colleagues (2003) performed *in vitro* studies, using primary cerebellar astrocyte cultures of mice and found a decrease in the amount of glutamate removed from the media after 4 h incubation with 50 μM MeHg. Likewise, in this present study, we found a

significant increase in extracellular glutamate levels in cerebellar astrocytes at all MeHg concentrations. However, the increase in extracellular glutamate at 1 μM and 2 μM MeHg, when compared with 0 μM, may suggest a decrease in the amount of glutamate buffered or an increase in the amount of glutamate released from astrocytes. Because at 5 μM MeHg we obtained levels of glutamate that were higher than the normal levels present in media, we suggest that at this concentration there was a release of glutamate from astrocytes.

A study performed on cortical neurons and astrocytes found that glutamate concentrations were significantly decreased in neurons, but not in astrocyte cultures exposed to 10 μM MeHg for 6 h (Yin et al., 2009). However, another study found a significant reduction of L-glutamate and D-aspartate in neonatal cortical astrocytes in the presence of 10 μM MeHg (Aschner, Du, Gannon, & Kimelberg, 1993). In our study, we did not find a significant difference in the extracellular glutamate levels of cortical astrocytes after MeHg treatment, when compared with control. MeHg-induced increase in extracellular glutamate levels in cerebellar astrocytes, but not in cortical astrocytes, might contribute to the preferential sensitivity of the cerebellar granule cells to MeHg.

Then, we aimed to address if the effect of MeHg on the extracellular glutamate levels can be obtained immediately after MeHg exposure. There was a significant release of glutamate from cerebellar astrocytes immediately after 3 h of MeHg treatment. Since the treatment of MeHg was done in HBS instead of media, to avoid MeHg binding to serum protein, no buffering of glutamate was observed from astrocytes. No significant differences in the extracellular glutamate levels were found in cortical astrocytes immediately after the 3 h of MeHg treatment.

In Chapter 2, we demonstrated that the extracellular Ca^{2+} concentration that enters into the cell produces a more significant cytotoxicity effect on cerebellar astrocytes than on cortical

astrocytes. Because the changes in the extracellular levels of glutamate were observed in cerebellar astrocytes and not in cortical astrocytes, we aimed to determine where extracellular Ca^{2+} concentrations were related to the changes in extracellular glutamate after MeHg treatment. To determine the role of extracellular Ca^{2+}, we used EGTA in free Ca^{2+} buffer and observed a decrease in the extracellular levels of glutamate in cerebellar astrocytes at all MeHg concentrations. We found that changes in extracellular glutamate levels were extracellular Ca^{2+}-dependent.

In cortical astrocytes, when we compared MeHg group with MeHg + EGTA group, we obtained a significant difference at 0 μM MeHg. This means that EGTA in free Ca^{2+} buffer made an effect on cortical astrocytes. A previous study performed on cortical astrocytes found that the release of gliotransmitter D-serine can be inhibited by the removal of extracellular Ca^{2+} (Mothet et al., 2005). Other studies have found a decrease in glutamate release from cortical astrocytes after the use of EGTA in free Ca^{2+} buffer (Bal-Price, Moneer, & Brown, 2002; Mothet et al., 2005). This means that it is possible that cortical astrocytes in physiological conditions release a certain amount of glutamate that is extracellular Ca^{2+}-dependent. Another potential explanation for this significant difference at 0 μM MeHg is that the absence of extracellular Ca^{2+} caused an increase in glutamate buffering through the EAATs. However, this last explanation seems less likely since previous research has found that the glutamate uptake system of rat astroblasts is dependent on extracellular Ca^{2+} and that an increase in extracellular Ca^{2+}, not its absence, can significantly increase glutamate uptake (Flott & Seifert, 1991). This suggests that cortical astrocytes normally release glutamate into the extracellular environment; however, the levels of their glutamate release are not increased after MeHg treatment.

MeHg (5 μM) can induce an absolute release of glutamate in cerebellar astrocytes. A previous study has shown that 10 μM MeHg produced an efflux of glutamate and aspartate from astrocytes, and the authors examined whether blockage of conductive ion fluxes, which has been implicated in astrocytic swelling, could reverse the MeHg-induced efflux of this EAA. They concluded that the mechanisms associated with EAA efflux after MeHg treatment and the mechanisms associated with EAA after swelling differed (Aschner et al., 1993). Because we demonstrated that the extracellular levels of glutamate are Ca^{2+}-dependent, our next experiment was aimed to understand if MeHg can induce Ca^{2+}-dependent vesicular release of glutamate. Understanding the mechanisms of MeHg-induced release of glutamate from cerebellar astrocytes can help us understand if there is a release of glutamate at lower concentrations of MeHg (1 μM - 2 μM MeHg). By using Rose Bengal, we obtained a decrease in extracellular glutamate levels at all concentrations of MeHg. This demonstrated that there was a vesicular release of glutamate at 5 μM MeHg. The significant differences obtained at 1 μM and 2 μM MeHg + Rose Bengal when compared with 1 μM and 2 μM MeHg indicated that the increase in extracellular glutamate levels was not only because of a dysfunction on EAATs buffering, as suggested in previous studies (Mutkus, Aschner, Syversen, & Aschner, 2005; Qu et al., 2003) but also a release of glutamate from cerebellar astrocytes. This indicated that MeHg produced a vesicular release of glutamate from cerebellar astrocytes and that MeHg could induce an increase in extracellular glutamate levels since lower concentrations.

It has been demonstrated that the increase in extracellular glutamate levels can induce excitotoxicity not only in neurons, but also in astrocytes and that this excitotoxicity in astrocytes is region-dependent (Matute et al., 2002). After we found that Rose Bengal decreased the glutamate levels induced by MeHg, we verified if it could also increase the viability of

astrocytes. After the co-treatment with Rose Bengal, we found that astrocytic death was decreased, but not eliminated in both cerebellar and cortical astrocytes. This indicates that although excitotoxicity in astrocytes may play a role in MeHg induced toxicity, there are other factors that can also contribute to astrocyte death. However, by reducing the extracellular glutamate levels, we were able to eliminate the differences in susceptibility between cerebellar and cortical astrocytes. Although excitotoxicity of astrocytes is not the only factor in MeHg-induced decrease in viability, it plays an important factor in the susceptibility of cerebellar astrocytes.

Excess extracellular glutamate can be reduced by EAATs. Because the EAATs play a significant role in glutamate buffering in astrocytes, we evaluated the mean fluorescence intensity levels of EAAT1 and EAAT2 after an acute treatment of MeHg. In the present study, we found a significant increase in the mean fluorescence intensity levels of cerebellar EAAT2. We also found an increase in the mean fluorescence intensity levels of cortical EAAT1; however, the mean fluorescence intensity of cerebellar EAAT1 is higher at the same MeHg concentration. These studies suggest that despite the preferential susceptibility of the cerebellum to MeHg-induced excitotoxicity, the cerebellar astrocytes possess a higher EAATs levels than cortical astrocytes when treated with MeHg. Therefore, it is possible that MeHg causes a dysfunction in these cerebellar proteins that inhibits their normal buffering.

Our immunocytochemical results obtained in the cerebellar EAAT2 mean fluorescence intensity correlate with the northern blot results obtained in previous studies, in where CHO cells treated with mercury-chloride caused an increase in EAAT2 RNA levels. However, our study differs with their western blot analysis, in where they found a decrease in EAAT2 proteins levels after MeHg treatment. They also found an increase in EAAT1 proteins levels, which correlated

with our result in cortical astrocytes (Mutkus, Aschner, Syversen, & Aschner, 2005). Another western blot study performed on rat cortical astrocytes after MeHg treatment found a decrease in EAAT1 and EAAT2 proteins levels (Liu et al., 2016). The different results between studies could be due to differences in experimental models, technique, and MeHg concentrations used in the experiments. Despite the differences in results, the present study and the others studies agree that MeHg causes alterations in the EAATs that lead to glutamate dyshomeostasis.

In conclusion, MeHg significantly increases the levels of extracellular glutamate in cerebellar astrocytes, but not in cortical astrocytes. These increased levels of extracellular glutamate in cerebellar astrocytes can occur immediately after MeHg exposure and are extracellular Ca^{2+}-dependent. The changes in glutamate levels are due to a Ca^{2+}-dependent vesicular release of glutamate. The release of glutamate from cerebellar astrocytes contributes to the differences in susceptibility between cerebellar and cortical astrocytes and might play a role in the preferential susceptibility of cerebellar granule cells to MeHg toxicity.

In the current study, we did not examine whether extracellular glutamate changes produced by the effect of MeHg on extracellular Ca^{2+} were due to the interaction of MeHg with Ca^{2+} channels. Similar to neurons, astrocytes have L- and N-type Ca^{2+} channels. These channels have been affected by MeHg in rat granule cells (Sirois & Atchison, 2000). It is possible that the effect of MeHg on L- and N-type Ca^{2+} channels in cerebellar astrocytes produces the Ca^{2+}-depended vesicular release of glutamate. Another issue that needs to be addressed is whether alterations in intracellular Ca^{2+} concentrations can also induce changes in extracellular glutamate levels; hence, these questions should be investigated further.

CHAPTER FOUR:

CONTRIBUTION OF INTRACELLULAR STORAGES AND CALCIUM CHANNELS TO METHYLMERCURY-INDUCED RELEASE OF GLUTAMATE AND DECREASE IN VIABILITY IN CEREBELLAR ASTROCYTES

A. Abstract

The objective of the present study was to examine whether MeHg interaction with cell organelles such as the mitochondria and the SER, or interaction with membranes proteins such as bradykinin receptors and L-and N-type Ca^{+2} channels can induce a Ca^{+2}-dependent vesicular release of glutamate and a decrease in cerebellar astrocyte viability. Primary astrocyte cultures from the cerebellum were obtained from 7 to 8 day old C57BL/6 mice. At 13-15 DIV, cells were exposed for 3 h to 0 μM, 1 μM, 2 μM, or 5 μM MeHg. Extracellular glutamate levels and cytotoxicity was measured 24 h after exposure. To study the role of the mitochondria and the SER in MeHg-induced increase in extracellular glutamate levels and cell death, the drugs CCCP (5 μM) and thapsigargin (10 μM) were used respectively. To determine the role of L-type and N-type VGCCs, the inhibitors nimodipine (10 μM) and GVIA (1 μM) were used respectively. To evaluate if MeHg and bradykinin have a common pathway for astrocytic glutamate release and toxicity, a desensitization of bradykinin receptor was performed after a prolonged exposure of bradykinin (1 μM). All the cellular components studied, except the SER, played a role in MeHg-induced release of glutamate from astrocytes. The mitochondria and N-type VGCCs played a greater role in the increased levels of extracellular glutamate. There were no differences in the contribution of intracellular storage and Ca^{2+} channels in the reduction of viability after the exposure of MeHg. After the desensitization of bradykinin receptor, there was a decrease in extracellular glutamate levels, but not at high MeHg concentrations. Likewise, bradykinin was able to decrease, but not eliminate, astrocyte death at high MeHg concentrations. This suggests that both intracellular storages and membrane proteins can play a role in MeHg-induced glutamate release and a decrease in viability, and that bradykinin and lower MeHg concentrations seem to have a common pathway for astrocytic glutamate release and toxicity.

B. Introduction

MeHg still an environmental contaminant of worldwide concern. This pollutant can bioaccumulate and be biomagnified in the marine food web, which becomes a threat to populations with high consumptions of seafood (Li, Feng, & Qiu, 2010). MeHg can produce neurological disorders, such as ataxia, dysarthria, visual disturbance, sensory changes, weakness, hyperreflexia, involuntary movements, and muscle and joint pain (Amin-Zaki et al., 1979; Harada, 1978).

MeHg affects the nervous system, especially the granule cells in the cerebellum (Hunter & Russell, 1954). The acute exposure to MeHg can cause a severe loss of intracellular Ca^{2+} homeostasis, which contributes to the death of cerebellar granule cells (Atchison, 2005; Limke, Heidemann, & Atchison, 2004). Previous studies have demonstrated that MeHg can cause a decrease in cell viability by the release of Ca^{+2} from the mitochondria through the opening of the mPTP. MeHg can also decrease granule cell viability in rats by increasing the internal Ca^{+2} concentration ($[Ca^{+2}]_i$) from the SER through the activation of IP_3 receptors (Limke, Bearss, & Atchison, 2004). Additionally, this neurotoxicant can induce a dysregulation of Ca^{+2} through its interaction with membrane proteins. Pretreatment of NG108-15 cells with bradykinin reduced significantly the increase in $[Ca^{+2}]_i$ induced by MeHg, which suggests an interaction of MeHg with bradykinin receptors (Hare & Atchison, 1995). MeHg can also alter Ca^{+2} homeostasis in rat granule cells by nimodipine- and GVIA-sensitive pathways, which indicates that L-and N-type Ca^{+2} channels may play a role in the approach of action or entry of MeHg (Marty & Atchison, 1997; Sirois & Atchison, 2000).

The increase in $[Ca^{+2}]_i$ in neurons can produce an increase in glutamate release, which in high levels can become toxic to the cell (Mark et al., 2001; Olney, 1994). MeHg can also block

$GABA_A$ receptors, which can decrease the function of the channel to mediate inhibitory neurotransmission, causing an increase in the release of glutamate (Atchison, 2005; Herden, Pardo, Hajela, Yuan, & Atchison, 2008; Yuan & Atchison, 2003).

Astrocytes are the main cell type responsible for buffering the excess extracellular glutamate levels, preventing the excitotoxicity of neurons. However, astrocytes can also be affected by MeHg toxicity. It has been hypothesized that neurotoxicity by MeHg occurs secondary to effects on glial cell functions (Aschner, Yao, Allen, & Tan, 2000). In Chapter 2, we found that, like neurons, cerebellar astrocytes are more susceptible to MeHg toxicity than their cortical counterparts. Their susceptibility depends on extracellular and intracellular Ca^{2+} changes. In Chapter 3, we found that these changes in Ca^{+2} induced by MeHg produced a Ca^{+2}-dependent vesicular release of glutamate from cerebellar astrocytes that contributes to the decrease in cerebellar astrocyte viability and the differences in susceptibility between cerebellar and cortical astrocytes. This release of glutamate from cerebellar astrocytes might also play a role in the preferential susceptibility of cerebellar granule cells to MeHg toxicity.

In the current chapter, we examine whether the interaction of MeHg with cell organelles, such as the mitochondria and the SER, or its interaction with membranes proteins, such as bradykinin receptors and L-and N-type Ca^{+2} channels can induce a Ca^{+2}-dependent vesicular release of glutamate and a decrease in cerebellar astrocyte viability. Studying the effect of MeHg on cerebellar astrocytic organelles and membrane proteins will allow us to understand the mechanisms of MeHg toxicity in cerebellar astrocytes.

C. Materials and methods

C.1. Materials and experimental solutions

High glucose DMEM, FBS, heat inactivated horse serum, antibiotic-antimycotic, and Trypan Blue Stain (0.4%) were obtained from Gibco (Grand Island, NY). The following items were purchased from Sigma-Aldrich Co. (St. Louis, MO): trypsin, DNase I, HEPES, glutamine, poly-D-lysine, nimodipine, CCCP, GVIA, and thapsigargin. Methylmercuric chloride was obtained from ICN Biomedicals Inc. (Aurora, OH).

C.2. Preparation of primary cerebellar astrocyte cultures

Primary astrocyte cultures from the cerebellum were obtained from 7-8 days old C57BL/6 mice, using a modification of the method described by Inglefield et al (Inglefield, Mundy, & Shafer, 2001). Briefly, after the brain dissection and separation of the cerebellum, cells were digested for 4 min at 37°C with trypsin 0.025% (w/v) in a buffer that contained: 5.0 mM KCl, 0.20 mM KH_2PO_4, 137.0 mM NaCl, 0.17 mM Na_2HPO_4, 5.0 mM D-glucose, 59.0 mM sucrose, and 0.1 mg/ml antibiotics, pH 7.3. DNase I (0.016% (w/v)) was diluted in HBS, which contained (mM) 150 NaCl, 5.4 KCl, 1.8 $CaCl_2$, 0.8 MgSO4, 20 D-glucose, and 20 HEPES (free acid) (pH 7.3) and used for 4 min at 37°C to inactivate trypsin. Cell media containing warmed DMEM supplemented with 10% (w/v) heat-inactivated horse serum, 10 mM HEPES, 2 mM glutamine, and 0.1 mg/ml antibiotics was added to the cell culture. Cells were centrifuged at 500 X g for 5 min. The resulting pellet was resuspended in DMEM-containing DNase I and recentrifuged at 500 g X for 5 min. Finally, cells were resuspended in DMEM and recentrifuged at 500 X g for 5 min for the last time. Animal procedures were in adherence with NIH guidelines and accepted by MSU Institutional Animal Use and Care Committee.

C.3. Purification of astrocytes

Cerebellar cell cultures were purified separately by using Anti-GLAST (ACSA-1) MicroBead Kit (Miltenyi Biotec Inc., San Diego CA). Briefly, cells were incubated for 10 min with 20 μM of Anti-GLAST (ACSA-1)-Biotin and washed with ice-cold (PBS; containing 137 mM NaCl, 2.7 mM KCl, 1.4 mM NaH_2PO_4, and 4.3 mM Na_2HPO_4, pH 7.4) containing 0.5% FBS, and centrifuged for 10 min at 300 X g. The resulting pellet was dissociated and incubated for 15 min with 20 μL of Anti-Biotin MicroBeads. After the incubation, cells were washed with PBS containing 0.5% FBS and centrifuged at 300 X g for 10 min. The final pellet was dissociated with PBS and passed through a 70 μm nylon mesh (Miltenyi Biotec Inc., San Diego CA). Cerebellar cell cultures were loaded onto an MS column (Miltenyi Biotec Inc., San Diego CA), which was placed in a magnetic field of a MACS Separator (Miltenyi Biotec Inc., San Diego CA). The column was rinsed 3 times with PBS containing 0.5% FBS. The astrocytes were retained in the column and removed by using cell media.

C.4. Cell plating

Cerebellar astrocytes were plated at a density of 1×10^5 cells/dish onto 35-mm Petri dishes coated with poly-D-lysine and maintained in a 37°C incubator with 95% O_2 and 5% CO_2. To obtain an equal density of live astrocytes in all the cell dishes, we used the TC20 Automated Cell Counter (Bio-Rad Laboratories Inc., Hercules, CA). The astrocytes media was changed every other day. Non-antibiotic media was used after the third replacement of astrocytes media because it could affect the function of Ca^{2+} channels (Atchison, Adgate, & Beaman, 1988; Redman & Silinsky, 1994).

C.5. Methylmercury treatment

Methylmercuric chloride was dissolved in distilled water to a final concentration of 10 mM to serve as a stock solution. Experimental solutions were prepared on the same day by diluting stock solutions in HBS. At 13-15 DIV, cerebellar astrocytes were exposed for 3 h to 0 μM, 1 μM, 2 μM, and 5μM of MeHg. Due to MeHg affinity with serum proteins, cells were treated using HBS (Fang & Fallin, 1976). Nimodipine was dissolved in methanol at a final concentration of 10 μM, and pre-incubated for 15 min and co-incubated with MeHg. This concentration of nimodipine showed to reduce the current of the cells by more than 90% (Peng, Hajela & Atchison, 2002). GVIA was dissolved in water at 1 μM, and pre-incubated for 7 min and co-incubated with MeHg. At this concentration, GVIA was able to block granule cell current (Sirois & Atchison, 2000). Thapsigargin and CCCP were dissolved in DMSO at 10 μM and 5 μM, respectively. Thapsigargin was pre-incubated for 5 min and CCCP for 15 min. Both were co-incubated with MeHg. The concentration and pre-incubation time of thapsigargin were seen to cause a significant reduction in the amplitude of the first-phase increase of $[Ca^{2+}]_i$ in granule cells caused by MeHg. The concentration and pre-incubation time of CCCP were previously used to cause astrocytic and neuronal mitochondrial membrane depolarization (Limke, Otero-Montañez, & Atchison, 2003; Marty, Lundback, Autio, & Atchison, 2006). Bradykinin receptor desensitization was produced by using 1 μM of bradykinin for 15 min of pre-incubation and 3 h of co-treatment with MeHg. The desensitization of bradykinin receptor was confirmed by a reduction of glutamate release from astrocytes. There was no astrocyte death at this concentration and time of incubation (data not shown). All inhibitors were placed in the media for 21 h after the 3 h of co-treatments. The current experiments pretend to be parallel to previous experiments performed at our laboratory.

C.6. Assessment of extracellular glutamate levels

Extracellular glutamate levels in the media were determined by an enzymatic colorimetric assay, using a commercially available kit purchased from Sigma-Aldrich Co. (St. Louis, MO). Briefly, 50 µl of media was obtained from each well plate after the treatment of MeHg and mixed with the reaction mix. Glutamate levels in media were determined after 30 min of incubation in 37º C by an enzymatic activity, which resulted in a colorimetric (450 nm) product proportional to the glutamate present. The absorbance was obtained by using an Infinite m1000 Pro microplate reader (Tecan, San Jose, CA). To ensure equal amounts of glutamate in the media in all the experiments, the levels of glutamate in media were measured before each experiment. To avoid deterioration of cerebellar astrocytes, no additional glutamate was added into the media (Ye & Sontheimer, 1998).

C.7. Cytotoxicity

Viability/Cytotoxicity Assay Molecular Probes Inc., OR, USA) was used to identify the viability of cerebellar astrocytes after the treatments. Cells were incubated with 0.3 µM calcein-AM and 0.075 µM EthD-1 at room temperature for 20 min. Cells labeled with calcein-AM represented the healthy astrocytes and the ones labeled with EthD-1 represented the dead astrocytes.

C.8. Immunocytochemistry

Cerebellar astrocytes were fixed in cold 4.0% (v/v) p-formaldehyde in PBS for 15 min. Cells were treated for 30 min with 0.1% (v/v) Triton-X in PBS containing 5% (v/v) NGS after rinsed in PBS. To determine the percentage of cerebellar astrocytes in the cell cultures, an indicator for astrocytes called rabbit Anti-GFAP (Millipore Corporation, Temecula, CA) was

used at a concentration of 1:1000. After 24 h, cells were rinsed in PBS and labeled with secondary antibody Alexa Fluor 405 goat anti-rabbit (Invitrogen Corporation, Carlsbad, CA) at a concentration of 1:200. Cells were mounted on glass slides by using a mounting medium with DAPI (Vectashield Hard Set, Vector, Burlingame, CA). Cell cultures were ≥99% pure astrocytes.

C.9. Data acquisition and analysis

The total change in glutamate levels in the media was measured by subtracting the amount of glutamate obtained in the cell culture with the amount of glutamate obtained in a parallel dish that contained only media. Astrocytes were observed by using the Nikon Eclipse Ti with NIS-Elements BR software (Nikon Instruments Inc., Melville, NY, USA). All images were obtained with 20X oil immersion objectives by using the same acquisition configuration, including exposure time and neutral density filters. To determine the effect of MeHg, a one-way ANOVA was used. To compare between groups, a two-way ANOVA followed by Tukey's procedure for post-hoc comparisons were used. $P < 0.05$ was considered to be statistically significant.

D. Results

D.1. Effect of methylmercury on the mitochondria and the smooth endoplasmic reticulum: glutamate levels of cerebellar astrocytes

The 0 ng/mL, on the y-axis, represents the normal amount of glutamate in the media. Below 0 ng/mL, represents less amount of glutamate in the media than the normal amount of glutamate present in the media. Above 0 ng/mL, represents more amount of glutamate than the normal amount of glutamate present in the media. These experiments were designed to find if the effect of MeHg on the mitochondria and the SER can produce a release of glutamate from astrocytes. There was a significant increase in the concentration of glutamate in the media of cerebellar astrocytes to approximately 2.03, 3.11, and 3.7 ng/mL from control value (0 μM) at 1 μM, 2 μM, and 5 μM MeHg, respectively. In order to determine if there is glutamate release from astrocytes as a result of the effect of MeHg on the mitochondria, the inhibitor CCCP (5 μM) was used. There was a significant decrease in extracellular glutamate levels in cerebellar astrocytes co-treated with CCCP at (1.74 ng/ml) 1 μM, (3.14 ng/ml) 2 μM, and (3.93 ng/ml) 5 μM MeHg, when compared with the MeHg group. There were no significant differences in extracellular glutamate levels between concentrations of MeHg + CCCP and control. In order to determine if there is glutamate release from astrocytes as a result of the effect of MeHg on the SER, the inhibitor thapsigargin (10 μM) was used. There were no significant differences between MeHg and MeHg + thapsigargin groups. Also, there were no significant differences in extracellular glutamate levels between concentrations of MeHg + thapsigargin and control. However, there was a significant decrease in glutamate levels at (2.48 ng/ml) 5 μM MeHg, when compared MeHg + CCCP with MeHg + thapsigargin groups. Therefore, MeHg significantly increases the extracellular glutamate levels by interacting with the cerebellar astrocytic mitochondria, but not with the SER (Fig. 4.1).

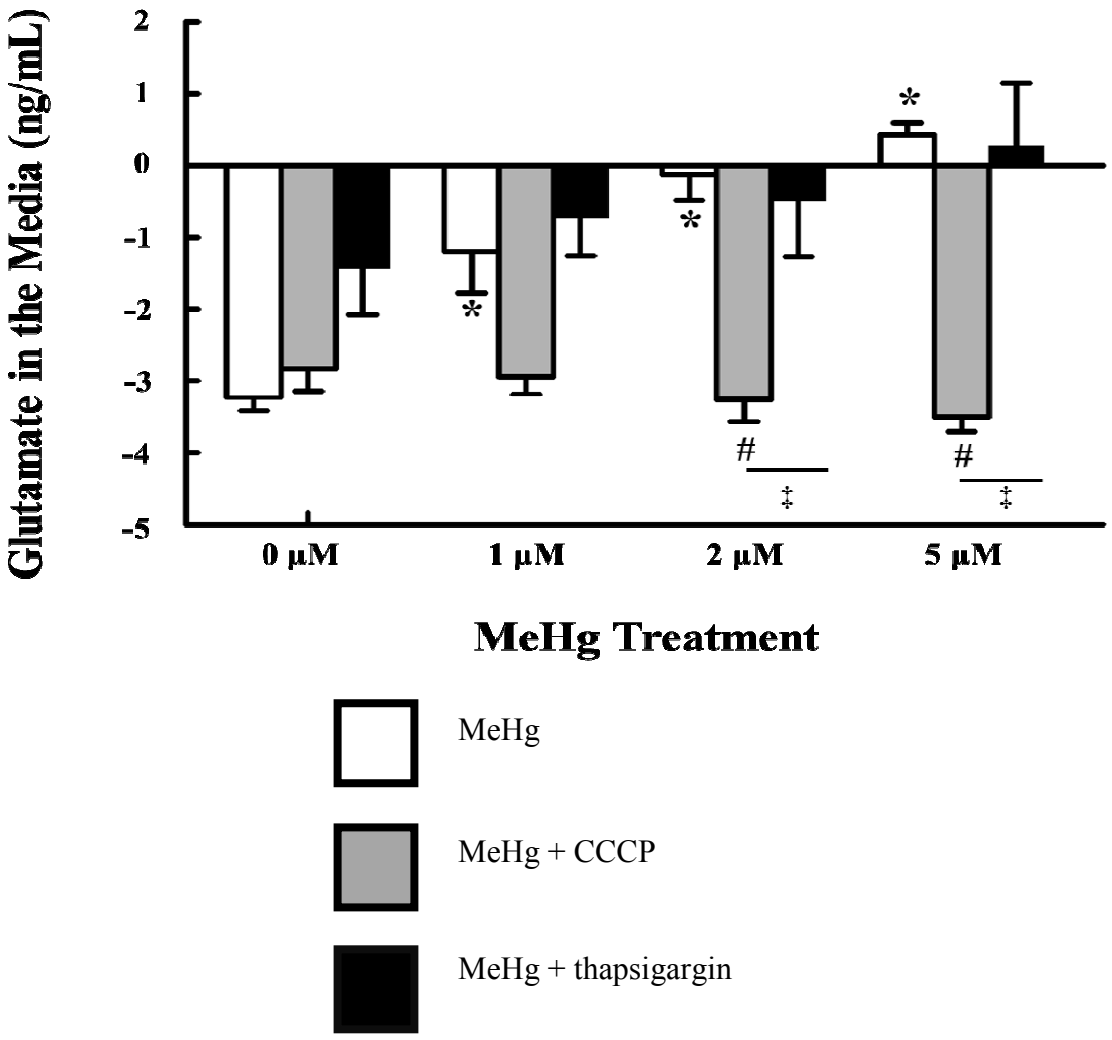

Figure 4.1. MeHg significantly increased the levels of extracellular glutamate by interacting with the cerebellar astrocytic mitochondria, but not with the SER. Glutamate in the media (ng/mL) at 0 µM, 1 µM, 2 µM, and 5 µM MeHg ($n \geq 5$). Values are mean ± SEM. * denotes $p < 0.05$ between MeHg group and 0 µM MeHg. # denotes $p < 0.05$ between MeHg and MeHg + CCCP groups. There were no significant differences between concentrations of MeHg + CCCP and 0 µM MeHg + CCCP. ‡ denotes $p < 0.05$ between MeHg + CCCP and MeHg + thapsigargin groups. There were no significant differences between concentrations of MeHg + thapsigargin and 0 µM MeHg + thapsigargin. There were no significant differences between MeHg and MeHg + thapsigargin groups. One-way ANOVA was used to compare within groups. Two-way ANOVA was used to compare between groups. Tukey's post-hoc comparison was used.

D.2. Effect of methylmercury on the mitochondria and the smooth endoplasmic reticulum: cytotoxicity

To determine if the effect of MeHg on the mitochondria and the SER can reduce cerebellar astrocyte viability, EthD-1 and calcein-AM were used. MeHg produced cytotoxicity in cerebellar astrocytes in a concentration-dependent manner with a significant reduction in viability to approximately 69% and 97% of control values at 2 μM and 5 μM MeHg, respectively. When MeHg and MeHg + CCCP groups were compared, there were significant increases in viability (70%) at 2 μM and (94%) at 5 μM MeHg with the use of CCCP. However, cerebellar astrocytes showed a significant reduction in viability (3%) at 5 μM MeHg + CCCP, when compared with 0 μM MeHg + CCCP. There were no decreases in viability at any MeHg + thapsigargin concentrations, when compared with 0 μM MeHg + thapsigargin. The viability of cerebellar astrocytes increased approximately 52% and 94% at 2 μM and 5 μM MeHg + thapsigargin respectively, when compared with MeHg group. There were no significant differences between MeHg + CCCP and MeHg + thapsigargin groups. Therefore, both the mitochondria and the SER play an equal role in MeHg-induced cytotoxicity in astrocytes (Fig. 4.2).

D.3. Effect of methylmercury on L-type and N-type voltage-gated calcium channels: glutamate levels of cerebellar astrocytes

These experiments were designed to find if the effect of MeHg on L-type and N-type VGCCs can produce a release of glutamate from astrocytes. In order to determine if there is glutamate release from astrocytes as a result of the effect of MeHg on L-type VGCCs, the inhibitor nimodipine (10 μM) was used. There was a significant decrease in extracellular

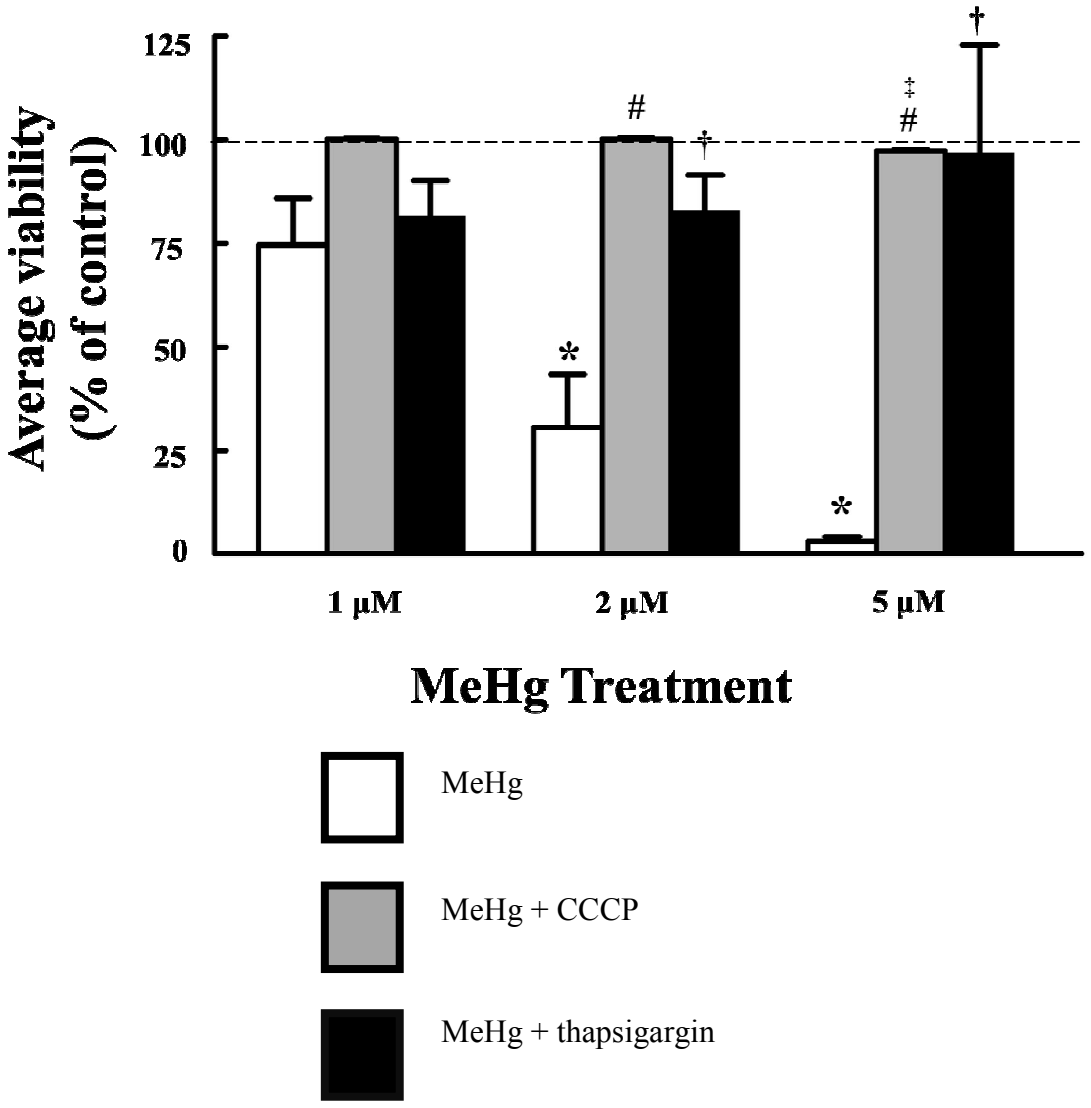

Figure 4.2. The effect of MeHg on the mitochondria and the SER reduced cerebellar astrocytic viability. Average viability (% of control) at 0 µM, 1 µM, 2 µM, and 5 µM MeHg ($n \geq 5$). Viability was measured 24 h after the exposure to MeHg using EthD-1 and calcein-AM. Results were normalized to 0µM MeHg, 0µM MeHg + CCCP or 0µM MeHg + thapsigargin. Values are mean ± SEM. * denotes $p < 0.05$ between MeHg group and 0 µM MeHg. # denotes $p < 0.05$ between MeHg and MeHg + CCCP groups. ‡ denotes significant differences with 0 µM MeHg + CCCP ($p < 0.05$). † denotes $p < 0.05$ between MeHg and MeHg + thapsigargin groups. There were no significant differences between concentrations of MeHg + thapsigargin and 0 µM MeHg + thapsigargin. There were no significant differences between MeHg + CCCP and MeHg + thapsigargin groups. One-way ANOVA was used to compare within groups. Two-way ANOVA was used to compare between groups. Tukey's post-hoc comparison was used.

glutamate levels in cerebellar astrocytes co-treated with nimodipine at (1.91 ng/ml) 1 μM, (2.46 ng/ml) 2 μM, and (1.91 ng/ml) 5 μM MeHg, when compared with the MeHg group. There were no significant differences in extracellular glutamate levels between concentrations of MeHg + nimodipine and control. In order to determine if there is glutamate release from astrocytes as a result of the effect of MeHg on N-type VGCCs, the inhibitor GVIA (1 μM) was used. There were significant decreases in extracellular glutamate levels in cerebellar astrocytes co-treated with GVIA at (2.42 ng/ml) 1 μM, (3.42 ng/ml) 2 μM, and (2.63 ng/ml) 5 μM MeHg, when compared with the MeHg group. There were no significant differences in extracellular glutamate levels between concentrations of MeHg + GVIA and control. Therefore, MeHg significantly increases the extracellular glutamate levels by interacting with both L-type and N-type VGCCs (Fig. 4.3).

D.4. Effect of methylmercury on L-type and N-type voltage-gated calcium channels: cytotoxicity

There were no significant differences in viability between concentrations of MeHg + nimodipine and 0 μM MeHg + nimodipine. When MeHg and MeHg + nimodipine groups were compared, there were significant differences in viability (57%) at 2 μM MeHg and (64%) at 5 μM MeHg. There were no decreases in viability at any MeHg + GVIA concentrations, when compared with 0 μM MeHg + GVIA. The viability of astrocytes increased approximately 69% and 58% at 2 μM and 5 μM MeHg + GVIA respectively, when compared with MeHg group. There were no significant differences between MeHg + nimodipine and MeHg + GVIA groups. Therefore, both L-type and N-type VGCCs play a role in MeHg-induced cytotoxicity in astrocytes (Fig. 4.4).

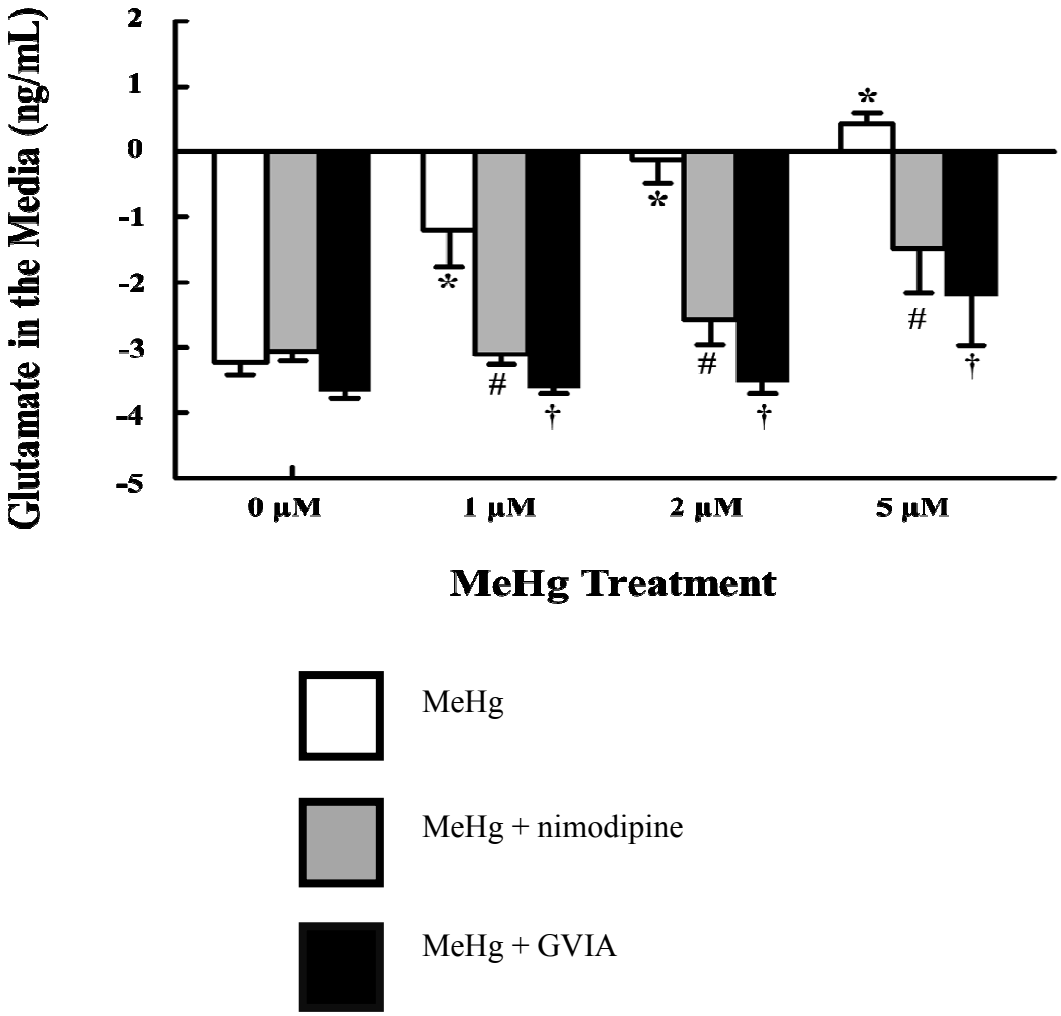

Figure 4.3. The effect of MeHg on L-type and N-type VGCCs significantly increased the extracellular glutamate levels. Glutamate in the media (ng/mL) at 0 µM, 1 µM, 2 µM, and 5 µM MeHg ($n \geq 5$). Values are mean ± SEM. * denotes $p < 0.05$ between MeHg group. # denotes $p < 0.05$ between MeHg and MeHg + nimodipine groups. There were no significant differences in extracellular glutamate levels between concentrations of MeHg + nimodipine and 0 µM MeHg + nimodipine. † denotes $p < 0.05$ between MeHg and MeHg + GVIA groups. There were no significant differences between concentrations of MeHg + GVIA and 0 µM MeHg + GVIA. There were no significant differences between MeHg + nimodipine and MeHg + GVIA groups. One-way ANOVA was used to compare within groups. Two-way ANOVA was used to compare between groups. Tukey's post-hoc comparison was used.

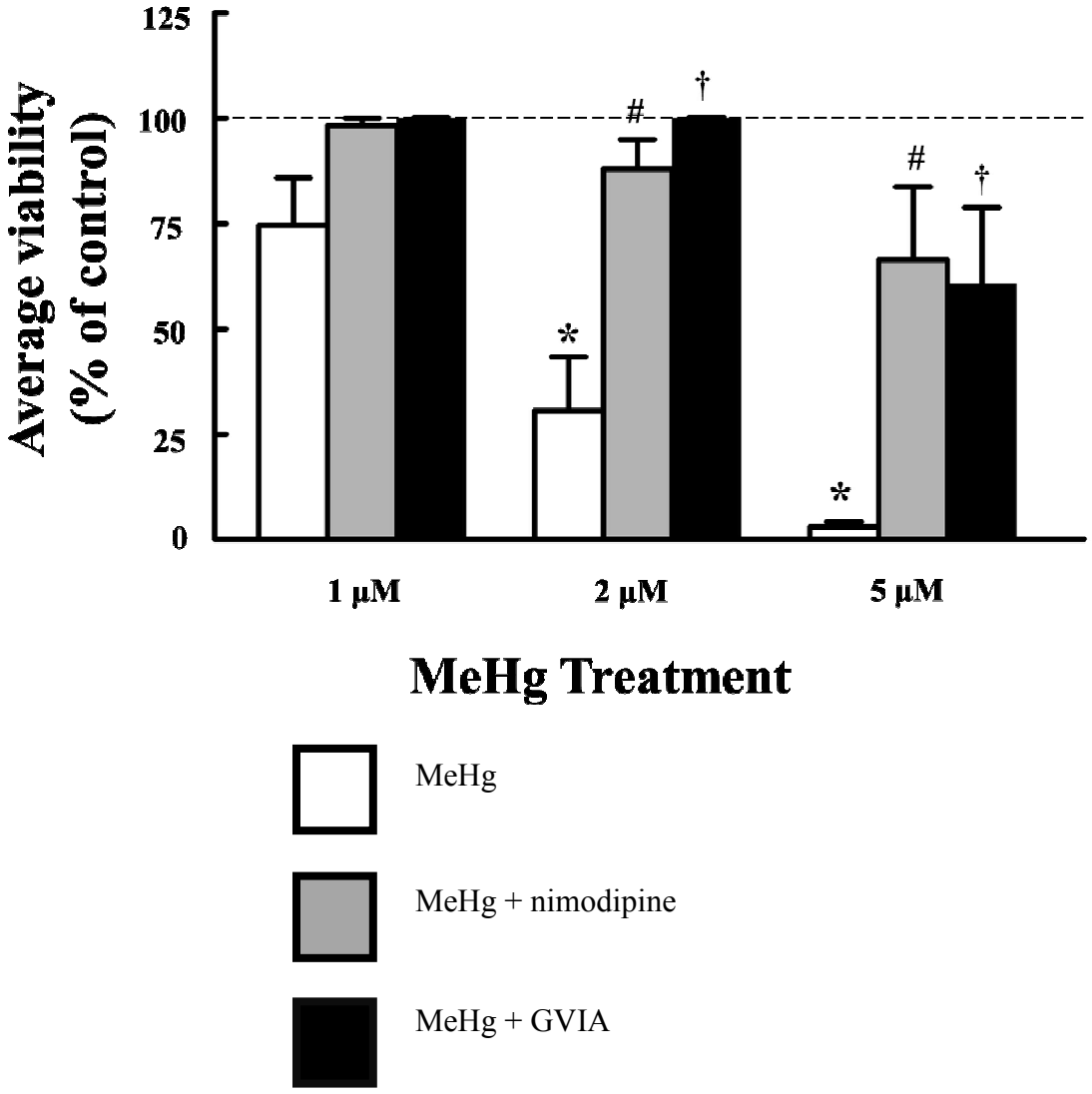

Figure 4.4 The effect of MeHg on L-type and N-type VGCCs reduced cerebellar astrocytic viability. Average viability (% of control) at 0 μM, 1 μM, 2 μM, and 5 μM MeHg ($n \geq 5$). Viability was measured 24 h after the exposure to MeHg using EthD-1 and calcein-AM. Results were normalized to 0μM MeHg, 0μM MeHg + nimodipine or 0μM MeHg + GVIA. Values are mean ± SEM. * denotes $p < 0.05$ between MeHg group and 0 μM MeHg. # denotes $p < 0.05$ between MeHg and MeHg + nimodipine groups. There were no significant differences between concentrations of MeHg + nimodipine and 0 μM. MeHg + nimodipine. † denotes $p < 0.05$ between MeHg and MeHg + GVIA groups. There were no significant differences between concentrations of MeHg + GVIA and 0 μM. MeHg + GVIA. There were no significant differences between MeHg + nimodipine and MeHg + GVIA groups. One-way ANOVA was used to compare within groups. Two-way ANOVA was used to compare between groups. Tukey's post-hoc comparison was used.

D.5. Comparing the role of intracellular storages with the role of calcium channels in methylmercury-induced glutamate release and toxicity

In order to discern the contribution of intracellular storages and Ca^{2+} channels to MeHg-induced glutamate release and cell death, all the studied drug treatments were compared. There were higher amounts of extracellular glutamate levels in MeHg + thapsigargin at (2.90 ng/ml) 1 μM, (3.05 ng/ml) 2 μM, and (2.48 ng/ml) 5 μM MeHg, when compared with the MeHg + GVIA group (Fig. 4.5). When comparing the contribution of intracellular storages and Ca^{2+} channels to the reduction of viability after the exposure to MeHg, no significant differences were observed (Fig. 4.6).

D.6. Effect of methylmercury on glutamate levels of cerebellar astrocytes after the *desensitization of bradykinin receptors*

In order to determine if there is glutamate release from astrocytes as a result of the desensitization of bradykinin receptors, a long-term exposure to the agonist bradykinin (1 μM) was used before and during MeHg treatment. There were significant decreases in extracellular glutamate levels in cerebellar astrocytes (1.88 ng/ml) co-treated with bradykinin at 1 μM, (3.16 ng/ml) 2 μM, and (2.06 ng/ml) 5 μM MeHg, when compared with the MeHg group. However, there was a significant increase in extracellular glutamate levels of approximately 1.54 ng/ml at 5 μM MeHg + bradykinin, when compared with its control. Therefore, the desensitization of bradykinin receptors can decrease glutamate levels in media, but not after high MeHg concentrations (Fig. 4.7).

D.7. Effect of methylmercury on cerebellar astrocyte viability after the *desensitization of bradykinin receptors*

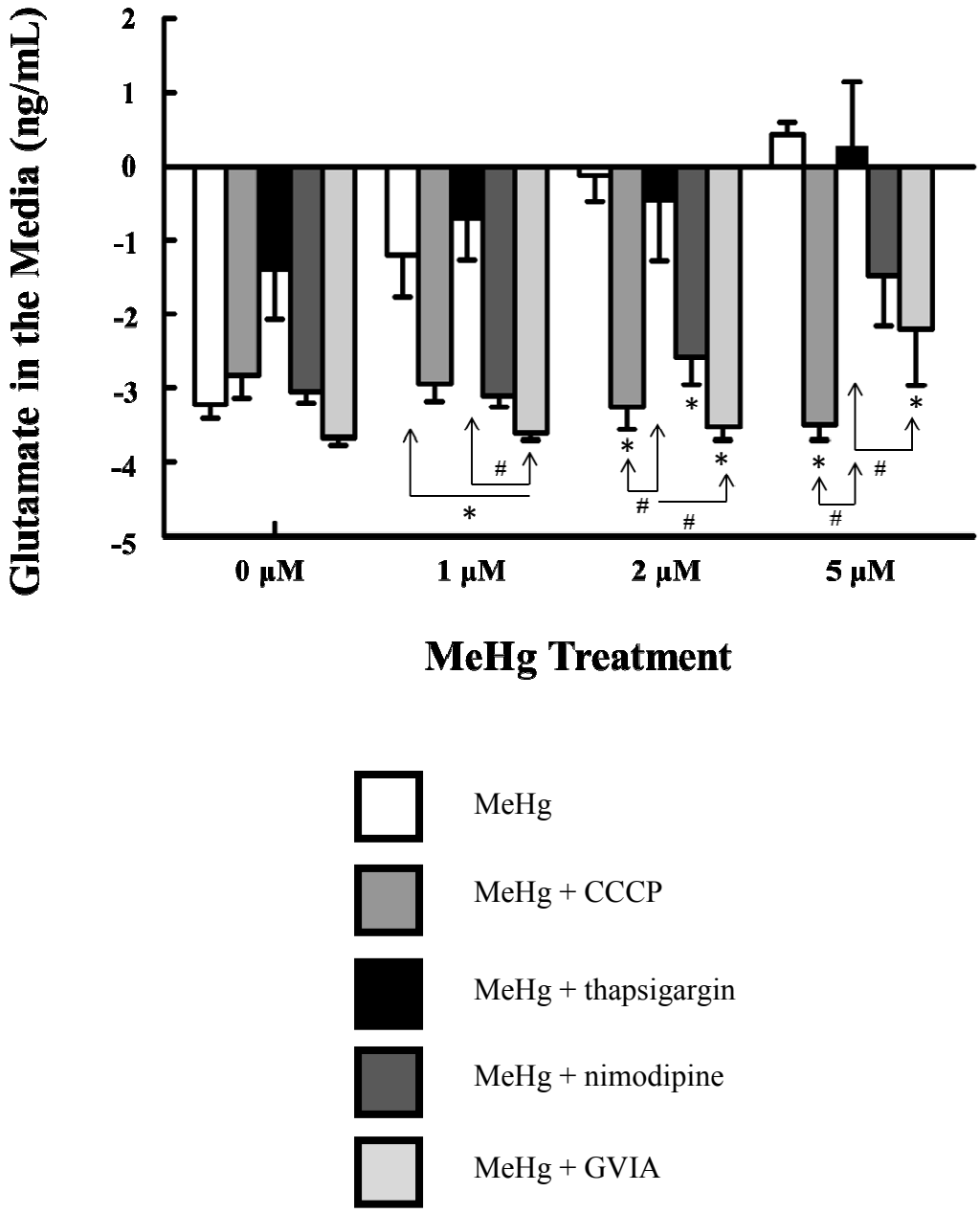

Figure 4.5. The effect of MeHg on N-type VGCCs produced a higher increase in extracellular glutamate at all MeHg concentrations, when compared with the effect of MeHg on the SER. Likewise, the effect of MeHg on the mitochondria produced a greater release of glutamate at higher MeHg concentrations (2-5 µM) in comparison with the effect of MeHg on the SER. Values are mean ± SEM. * denotes $p < 0.05$ compared to MeHg group. # denotes $p < 0.05$ compared to MeHg + thapsigargin. Two-way ANOVA followed by Tukey's post-hoc comparison were used.

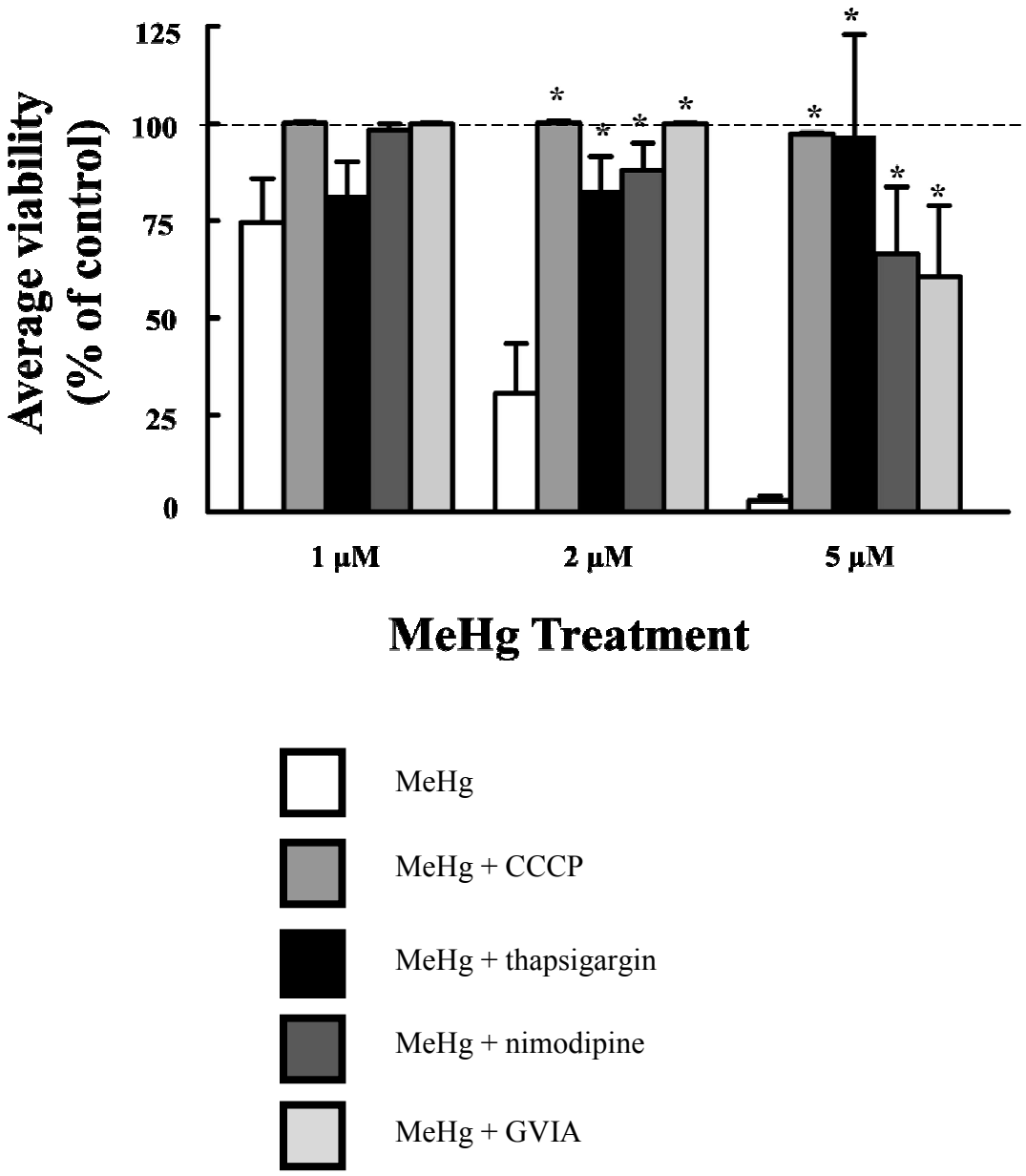

Figure 4.6. All the chemical treatments showed equal importance in the decrease in astrocyte death after MeHg exposure. Average viability (% of control) at 0 µM, 1 µM, 2 µM, and 5 µM MeHg ($n \geq 5$). Viability was measured 24 h after the exposure to MeHg using EthD-1 and calcein-AM. Results were normalized to 0 µM MeHg, 0 µM MeHg + CCCP, 0 µM MeHg + thapsigargin, 0 µM MeHg + nimodipine, or 0 µM MeHg + GVIA. Values are mean ± SEM. * denotes $p < 0.05$ compared to MeHg group. There were no significant differences between drug treatments. Two-way ANOVA followed by Tukey's post-hoc comparison were used.

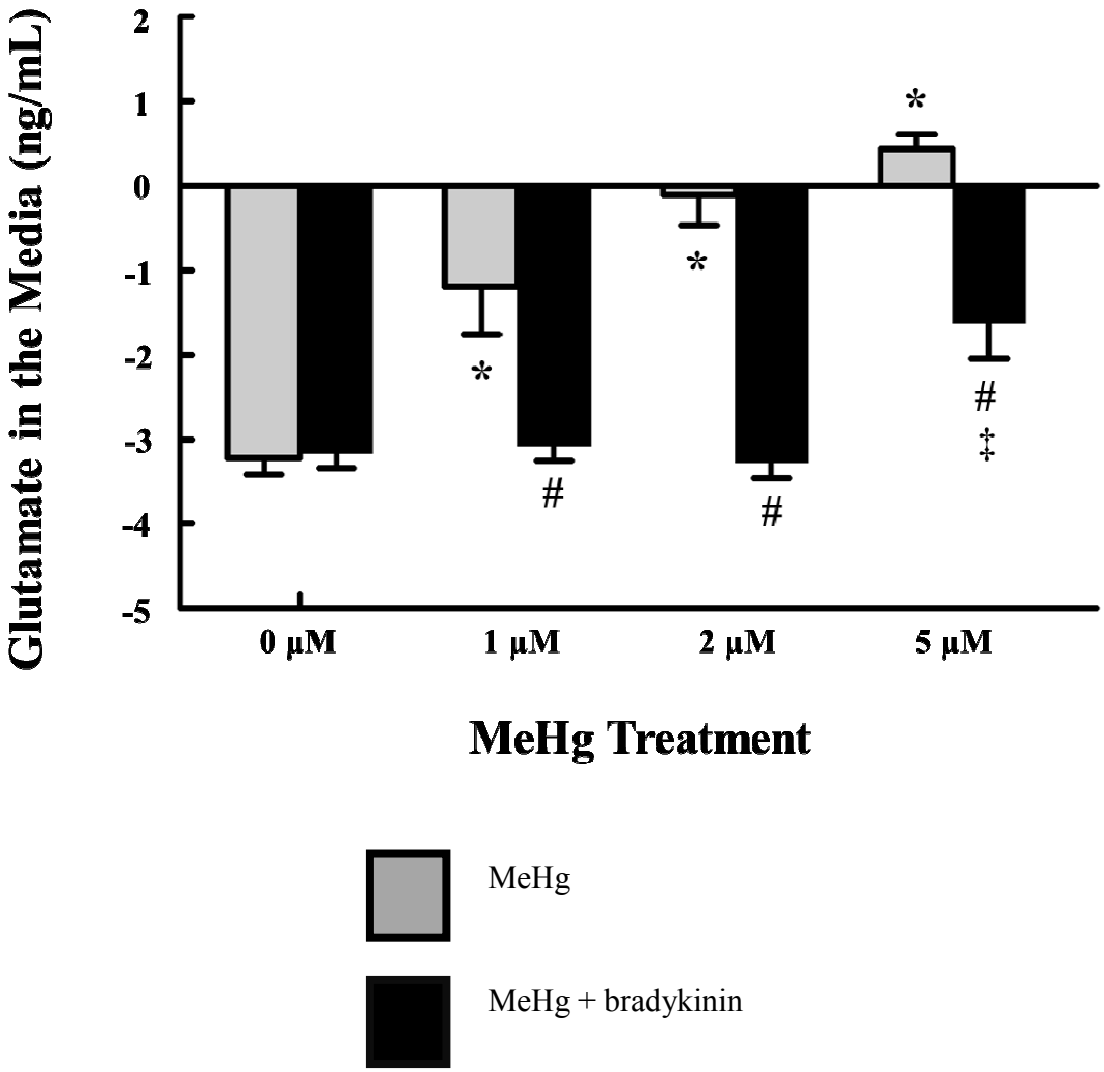

Figure 4.7. The desensitization of bradykinin receptors can decrease glutamate levels in media, but not after high MeHg concentrations. Glutamate in the media (ng/mL) at 0 µM, 1 µM, 2 µM, and 5 µM MeHg ($n \geq 5$). Values are mean ± SEM. * denotes $p < 0.05$ between MeHg group and 0 µM MeHg. # denotes $p < 0.05$ between MeHg and MeHg + bradykinin groups. ‡ denotes $p < 0.05$ betwen MeHg + bradykinin group and 0 µM MeHg + bradykinin. One-way ANOVA was used to compare within groups. Two-way ANOVA was used to compare between groups. Tukey's post-hoc comparison was used.

There were significant increases in astrocyte viability (65%) at 2 μM and (36%) at 5 μM MeHg with the co-treatment of bradykinin, when compared with MeHg group. However, cerebellar astrocytes showed a significant reduction in viability (61%) at 5 μM MeHg + bradykinin, when compared with 0 μM MeHg + bradykinin. Thus, the desensitization of bradykinin receptors can decrease, but not eliminate astrocyte death (Fig. 4.8).

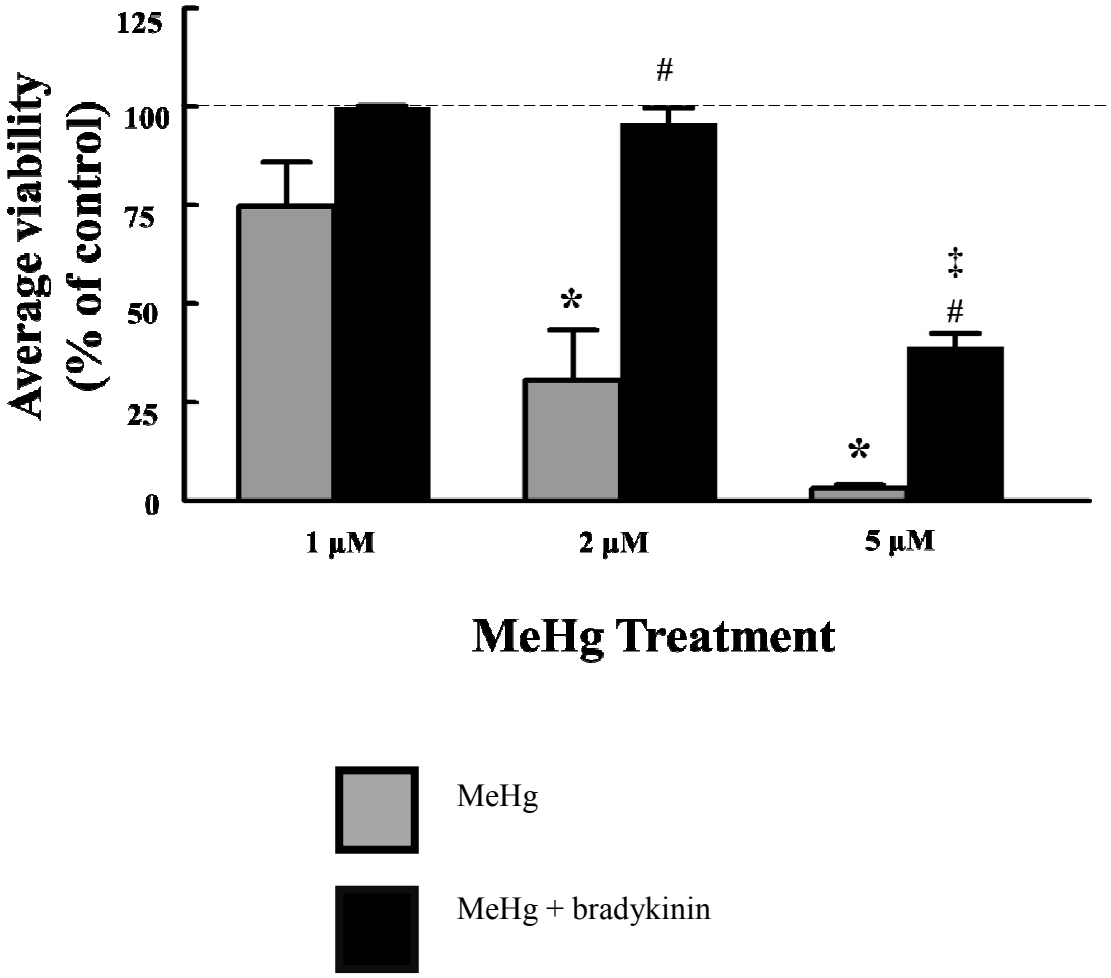

Figure 4.8. The desensitization of bradykinin receptors can decrease, but not eliminate astrocyte death. Average viability (% of control) at 0 µM, 1 µM, 2 µM, and 5 µM MeHg ($n \geq 5$). Viability was measured 24 h after the exposure to MeHg using EthD-1 and calcein-AM. Results are normalized to 0 µM MeHg or 0 µM MeHg + bradykinin. Values are mean ± SEM. * denotes $p < 0.05$ between MeHg group and 0 µM MeHg. # denotes $p < 0.05$ between MeHg and MeHg + bradykinin groups. ‡ denotes $p < 0.05$ between MeHg + bradykinin group and 0 µM MeHg + bradykinin. One-way ANOVA was used to compare within groups. Two-way ANOVA was used to compare between groups. Tukey's post-hoc comparison was used.

E. Discussion

In previous chapters, we showed that cerebellar astrocytes are more susceptible to MeHg-induced cytotoxicity than cortical astrocytes and that MeHg selectively increased the glutamate release from cerebellar astrocytes. The decrease in viability in cerebellar astrocytes after MeHg exposure is intracellular and extracellular Ca^{2+}-dependent, and the changes in glutamate levels are due to a Ca^{2+}-dependent vesicular release of glutamate. This vesicular release of glutamate contributes to the decrease in viability and susceptibility of cerebellar astrocytes to MeHg.

In the current chapter, we examine whether extracellular glutamate changes were due to interactions of MeHg with intracellular stores or membrane proteins, such as Ca^{2+} channels and bradykinin receptors. Studies of the effect of MeHg on intracellular stores and Ca^{2+} channels have been previously performed on non-astrocytes cells. To the best of our knowledge, this is the first study to analyze the release of glutamate after the effect of MeHg on astrocytic SER, mitochondria, and Ca^{2+} channels.

In the present study, we found a contribution of the mitochondria to astrocytic glutamate release. However, we did not see a contribution of the SER to glutamate release. This may be due to the small contribution of the SER to the increase of intracellular Ca^{2+} in primary cell cultures (Limke, Bearss, & Atchison, 2004; Marty, Lundback, Autio, & Atchison, 2006). In contrast to the SER, the mitochondria contribute to a large portion of the intracellular Ca^{2+} detected in cell cultures (Limke & Atchison, 2002; Marty, Lundback, Autio, & Atchison, 2006; Polunas et al., 2011), which may explain its high contribution to the increased levels of glutamate.

Regardless of the lack of contribution of the SER to the changes of extracellular glutamate levels, its inhibition plays an important factor in MeHg-induced cell death. Similarly,

previous experiments performed on granule cells demonstrated that despite the small amount of Ca^{2+} release from the SER, the inhibition of this release is an important factor in MeHg-induced granule cell death (Limke, Bearss, et al., 2004). The contribution of the SER to cell death, but not to astrocytic glutamate release suggests that the release of glutamate from astrocytes is not due a mere consequence of astrocyte death, but to an interaction of MeHg with certain cellular components.

By depleting Ca^{2+} levels in the mitochondria, we were able to significantly inhibit the vesicular release of glutamate at all MeHg concentrations. However, we were able to reduce, but not eliminate astrocyte death at higher MeHg concentrations (5 μM). These results suggest that the release of glutamate may not be the only factor associated with astrocyte death after high MeHg concentrations. This supports the results obtained in Chapter 2, in which Rose Bengal, a potent inhibitor of the vesicular release of glutamate, was able to decrease extracellular glutamate levels at all concentrations of MeHg, but unable to eliminate astrocytic death at higher MeHg concentrations.

Despite the significant decrease in cell death at 5 μM MeHg after the co-treatment with CCCP, we did not observe differences between MeHg + CCCP and MeHg + Thapsigargin groups. This suggests an equal contribution of the SER and the mitochondria to MeHg-induced toxicity.

Similar to neurons, astrocytes possess L-type and N-type Ca^{2+} channels. In this study, we found that both L-type and N-type VGCCs play a role in glutamate release and the decrease in viability in astrocytes after an acute treatment of MeHg. These findings are similar to those found in primary cultures of granule cells, in where MeHg induced entry of Ca^{2+} through L, N, and/or P/Q-type VGCCs and produced cell death (Marty & Atchison, 1997). There were no

differences between L-type and N-type VGCCs, suggesting an equal participation of these channels in MeHg-induced glutamate release and cytotoxicity.

When we compared the effect of MeHg on intracellular storages with Ca^{2+} channels, we could see how MeHg produced a higher release of glutamate through its effect on the N-type VGCCs than through its effect on the SER at all MeHg concentrations. The higher role of N-type VGCCs in the release of glutamate from astrocytes when compared with the SER, a significant difference that had not been seen when compared with L-type Ca^{2+} channels, might be due to the prominent role of N-type VGCCs in synaptic vesicle recycling and glutamate release (Iwasaki & Takahashi, 1998; Pravettoni et al., 2000; Scholz & Miller, 1995; Verderio, Coco, Fumagalli, & Matteoli, 1995).

When we studied the contribution of intracellular storages and Ca^{2+} channels to the reduction of viability after exposure to MeHg, we could see how there was no difference between these cellular components. In Chapter 2, we found that the extracellular Ca^{2+} played a more important role in the decrease in astrocyte viability than intracellular Ca^{2+} at a higher MeHg concentration. It is possible that the extracellular Ca^{2+} that enters into the astrocytic cytoplasm is pumped into the SER and the mitochondria. Therefore, the effect of MeHg on these intracellular organelles can liberate the buffered Ca^{2+}, explaining why the absence of extracellular Ca^{2+} has a predominant role in the decrease in viability. Another potential explanation for these results may be the disruption of the astrocytic membrane at higher MeHg concentrations, producing a high entry of Ca^{2+} and inducing cell death.

Another membrane protein studied in this chapter was bradykinin receptor. The activation of bradykinin receptors in astrocytes leads to an increase in Ca^{2+} concentration and glutamate release (Parpura et al., 1994). The continuous presence of a bradykinin receptor

agonist can rapidly desensitize this ligand-receptor-G protein (Blaukat, Micke, Kalatskaya, Faussner, & Müller-Esterl, 2003). In this study, we desensitized the bradykinin receptor by a pre-incubation and a prolonged exposure of bradykinin. Experiments with different exposure times were performed to assure a desensitization of the bradykinin receptor (experiment not showed). Results indicated a decrease in both glutamate release and cell death at lower (1 μM - 2 μM) MeHg + bradykinin concentrations. Similarly, previous experiments done on NG108-15 cells have shown that pretreatment with bradykinin significantly reduced the increase in $[Ca^{+2}]_i$ induced by 2 μM MeHg (Hare & Atchison, 1995a). However, at 5 μM MeHg, the desensitization of the bradykinin receptor was neither able to reduce the glutamate release nor the increase in viability.

This suggests that bradykinin and lower MeHg concentrations seem to have a common pathway for astrocytic glutamate release. It could also suggest an interaction between MeHg and bradykinin receptors.

This chapter demonstrates how both intracellular storages and membrane proteins can play a role in MeHg-induced glutamate release and cell death. Although we demonstrated different degrees of contribution of intracellular storages and membrane proteins to the changes of extracellular glutamate levels, we were unable to notice differences in the contribution of all these cell components to the decrease in viability. Future research should focus on the real-time effect of MeHg on these organelles and membrane proteins in order to obtain a better discernment of their contribution to MeHg-induced toxicity.

CHAPTER FIVE:

SUMMARY AND CONCLUSION

Summary and conclusion

A. Summary and Significance

MeHg can affect both the peripheral and central nervous system; however, granule cells in the cerebellum are preferential targets of MeHg neurotoxicity (Hunter & Russell, 1954). The loss of granule cell viability after MeHg exposure is believed to be the result of unregulated elevations in $[Ca^{2+}]_i$ that lead to glutamate excitotoxicity (Atchison, 2005; Limke et al., 2004). Astrocytes are the main cell type responsible for buffering the excess extracellular glutamate levels, preventing the excitotoxicity of neurons. It has been hypothesized that neurotoxicity by MeHg occurs secondary to effects on glial cell functions (Aschner et al., 2000). MeHg-induced cytotoxicity in astrocytes has been studied in the cortical layer (Aschner et al., 1998a; Aschner et al., 1996; Aschner et al., 1998b). However, little is known about the effect of MeHg on cerebellar astrocytes. Because regional differences can occur in astrocytes between the two areas (Morken et al., 2005), we compared MeHg toxicity on cerebellar and cortical astrocytes, and aimed to understand different toxicological effects of MeHg on these astrocytes, such as the increase in extracellular glutamate levels and cytotoxicity.

Several new findings presented in this dissertation are consistent with the following conclusions: (1) there is a regional, but not a typological difference in the effect of MeHg on astrocytes, in which cerebellar astrocytes are more susceptible to MeHg neurotoxicity; (2) the contribution of intracellular and extracellular Ca^{2+} to MeHg cytotoxicity differs in cortical and cerebellar astrocytes, in that intracellular Ca^{2+} plays a role in MeHg-induced cortical astrocyte death, and both intracellular and extracellular Ca^{2+} contribute to cerebellar astrocyte death; (3) MeHg causes a concentration-dependent, Ca^{2+}-dependent vesicular release of glutamate from cerebellar astrocytes; (4) MeHg-induced vesicular release of glutamate in cerebellar astrocytes contributes to the regional difference in astrocyte viability; (5) there are no differences in the

contribution of the SER, mitochondria or, L-type and N-type VGCCs to the reduction of viability, however their contribution to the Ca^{2+}-dependent vesicular release of glutamate differs.

In this chapter, we will discuss the implications of these findings, focusing on the role of intracellular and extracellular Ca^{2+} as contributors to the difference in susceptibility between cerebellar and cortical astrocytes; the relevance of the release of glutamate from cerebellar astrocytes; and the possible reasons for the similar contribution in viability, but differential contribution in vesicular release of glutamate of the SER, mitochondria, L-type and N-type VGCCs following MeHg treatment.

In Chapter 2, we studied whether there were typological or/and regional differences in the viability of cortical and cerebellar astrocytes after an acute exposure to MeHg, and tried to understand factors that can contribute to such differences. There were regional differences between cortical and cerebellar astrocytes. Cerebellar astrocytes were more susceptible to MeHg than cortical astrocytes in both immediate and delayed exposures. Although both groups had the same time of MeHg exposure (3 h), cerebellar astrocytes were more susceptible 24 h after MeHg treatment than cerebellar astrocytes studied immediately after MeHg treatment. The same delayed effects were seen in humans after acute and chronic MeHg exposures. In Iraq, for example, after an acute poisoning of MeHg caused by eating contaminated bread, victims started to show signs of poisoning weeks or months after the exposure ended (Bakir, 1973; Weiss et al., 2002). Likewise, in Minamata, low chronic doses of MeHg from contaminated fish did not produce visible behavioral effects for periods of time measured in years (Harada, 1995; Weiss et al., 2002). Because a delayed exposure to MeHg mimics a more realistic human exposure, we used this type of exposure for the rest of the experiments.

When we examined typological differences, we discovered that there were no differences between type 1 and type 2 astrocytes in either cortex and cerebellum. Therefore, there was a regional, but not a typological difference in astrocyte viability after an acute MeHg treatment. In other words, type 1 and type 2 astrocytes were equally affected at the given MeHg concentrations; nevertheless, cerebellar astrocytes are more susceptible to MeHg than cortical astrocytes.

Differences between cortical and cerebellar astrocytes after MeHg treatment have been studied (Adachi & Kunimoto, 2005; Gassó et al., 2001; Morken et al., 2005; Mundy & Freudenrich, 2000). Research demonstrates differences in the MTT activity and the ROS levels in cortical and cerebellar astrocytes (Kaur et al., 2007; Morken et al., 2005).

Morken and colleagues (2005) showed a difference between cortical and cerebellar astrocytes, in which, at low MeHg concentrations with prorogated exposure time of 24 h, there was a decrease in the MTT activity in cortical astrocytes. A decrease in MTT activity was not observed in cerebellar astrocytes. This suggests a susceptibility of the cortical astrocyte mitochondria to the toxic effects of MeHg (Morken et al., 2005). However, another study that used ^{13}C nuclear magnetic resonance spectroscopy found that the percentage of [U-^{13}C] glutamate used for energy production was decreased after 4 h of 25 μM and 50 μM MeHg exposures in cerebellar astrocytes (Qu et al., 2003). These results indicate a selective mitochondrial vulnerability due to the inhibitory effect of MeHg on these astrocytes. The mitochondria are shown to be affected in both cerebellar and cortical astrocytes after MeHg treatment; therefore, these studies do not provide enough evidence for the differential susceptibility between cortical and cerebellar astrocytes.

Another study that tried to understand differential susceptibility between cortical and cerebellar astrocytes found that 5 μM MeHg produces higher levels of ROS in cerebellar astrocytes than in cortical astrocytes (Kaur et al., 2007). One way for MeHg to induce ROS in astrocytes is by the reduction of the GSH levels in astrocytes through the inhibition of cysteine uptake. Cysteine is a precursor of GSH (Kranich et al., 1998); therefore, by inhibiting cysteine uptake, there is a reduction of the GSH levels in astrocytes. It was hypothesized that the higher amount of GSH in cortical astrocytes after MeHg exposure might be the reason why these astrocytes are less susceptible to MeHg toxicity. However, cerebellar neurons are more susceptible to MeHg toxicity than cortical neurons and there are no differences in their levels of GSH (Kaur et al., 2007). For this reason, differential levels of GSH do not provide an explanation for the differential susceptibility of cerebellar and cortical astrocytes after MeHg treatment. Thus, better explanations for the differences in susceptibility between astrocytes after MeHg treatment were needed.

This dissertation differs from previous research because it studies the contribution of Ca^{2+} to the differential susceptibility between cerebellar and cortical astrocytes. It expands the current knowledge on astrocyte heterogeneity in the brain by offering a possible reason for the regional susceptibility of cerebellar astrocytes to MeHg toxicity. Since it has been constantly proven that Ca^{2+} has an important role in the mechanisms of MeHg toxicity (Atchison, 2005; Hare & Atchison, 1995a; Levesque et al., 1992; Limke & Atchison, 2002; Limke et al., 2004; Limke et al., 2004; Marty & Atchison, 1997, 1998), we aimed to understand whether MeHg-induced changes in $[Ca^{2+}]_i$ were related to the regional differences that exist between cortical and cerebellar astrocytes.

Previous studies have demonstrated that MeHg can increase $[Ca^{2+}]_i$ in astrocytes (Marty et al., 2006). However, the contribution of the changes in $[Ca^{2+}]_i$ to astrocyte viability after MeHg exposure has never been studied. By determining the relative contribution of intracellular and extracellular Ca^{2+} to astrocyte viability, we found regional differences that exist between cortical and cerebellar astrocytes. In cortical astrocytes, only the intracellular Ca^{2+} played a role in MeHg-induced toxicity. In cerebellar astrocytes, both extracellular and intracellular Ca^{2+} played a role in the decrease in viability. However, the extracellular Ca^{2+} that entered the cell played a more important role in these astrocytes at a higher MeHg concentration. It is possible that the influx of Ca^{2+} into the cerebellar astrocytes causes an organelle Ca^{2+} overload and a failure of the electrochemical proton gradient, leading to their susceptibility and death.

In Chapter 3, we studied whether an acute exposure to MeHg can produce changes in extracellular glutamate levels in cortical and cerebellar astrocytes, and examined its role and mechanisms in astrocyte death. Previous studies have demonstrated changes in extracellular EAA levels in astrocytes after MeHg treatment and tried to understand the mechanism that underlies these changes. Because anion channel opening induced by astrocyte swelling produces glutamate release (Kimelberg et al., 1990) and MeHg produces swelling in astrocytes (Aschner et al., 1990), Aschner and colleagues (1993) hypothesized that MeHg-induced swelling in astrocytes produces glutamate release. They examined whether blockage of conductive ion fluxes, which has been implicated in astrocytic swelling, could reverse the MeHg-induced efflux of this EAA. They concluded that the mechanisms associated with glutamate efflux after MeHg treatment and the mechanisms associated with glutamate efflux after swelling differed. Therefore, other mechanism(s) of glutamate efflux from astrocytes must exist.

In this dissertation, we focused on the role of Ca^{2+} in MeHg-induced changes in extracellular glutamate levels. These studies expand the current knowledge on MeHg toxicity by offering a possible mechanism of glutamate efflux from astrocytes. We performed parallel experiments, using cerebellar and cortical astrocytes and aimed to understand the effect of MeHg on Ca^{2+}-induced vesicular release of glutamate from astrocytes.

We found a concentration-dependent increase in extracellular glutamate levels in cerebellar astrocytes. We also found that these increases in extracellular glutamate levels can be obtained immediately after MeHg exposure. However, no significant difference in extracellular glutamate levels of cortical astrocytes was found.

Because it was found that the extracellular Ca^{2+} affects the viability of cerebellar astrocytes but not that of cortical astrocytes, we determined whether extracellular Ca^{2+} concentrations were related to changes in extracellular glutamate levels after MeHg treatment. By using EGTA, an extracellular Ca^{2+} chelator, it was found that changes in glutamate levels were extracellular Ca^{2+}-dependent.

MeHg increased extracellular glutamate levels in cerebellar astrocytes at all MeHg concentrations. The increase in extracellular glutamate levels at 1 μM and 2 μM MeHg suggests a reduction in the amount of glutamate buffered or an increase in the amount of glutamate released from astrocytes. Because at 5 μM MeHg the levels of glutamate were higher than the normal levels present in media, we believed that there was a release of glutamate from astrocytes at this concentration. Since we demonstrated that extracellular levels of glutamate are Ca^{2+}-dependent, our next experiment was aimed to determine if MeHg can induce Ca^{2+}-dependent vesicular release of glutamate. By knowing the mechanisms of MeHg-induced release of glutamate from cerebellar astrocytes, we can understand if there is a release of glutamate at

lower MeHg concentrations (1 μM - 2 μM MeHg). For these experiments, we used Rose Bengal, a chemical that inhibits the uptake of glutamate into the vesicular lumen, which in turn, inhibits the glutamate release into the extracellular space (Montana et al., 2004). By using this chemical, we obtained a significant decrease in extracellular glutamate levels at all MeHg concentrations. This demonstrated that there was a vesicular release of glutamate at 5 μM MeHg. The significant differences obtained at 1 μM and 2 μM MeHg + Rose Bengal when compared with 1 μM and 2 μM MeHg suggest that the increase in extracellular glutamate levels was not just due to a dysfunction on EAAT buffering, as suggested in previous studies (Mutkus et al., 2005; Qu et al., 2003), but also due to a release of glutamate from cerebellar astrocytes. This indicates that MeHg causes a Ca^{2+}-dependent vesicular release of glutamate from cerebellar astrocytes and that this release of glutamate can occur from lower MeHg concentrations.

Like neurons, astrocytes can die as a result of glutamate excitotoxicity. However, the excitotoxicity in astrocytes could be region-dependent (Matute et al., 2002). After we found that Rose Bengal decreased the glutamate levels induced by MeHg, we verified if it could also increase the viability of astrocytes. After the co-treatment with Rose Bengal, it was found that astrocytic death was significantly reduced, but not eliminated. This indicates that even though excitotoxicity in astrocytes may play a role in MeHg induced toxicity, there are other factors that can also contribute to astrocyte death at higher MeHg concentrations. However, by reducing the extracellular glutamate levels, the differences in susceptibility between cerebellar and cortical astrocytes were eliminated, suggesting that excitotoxicity of astrocytes plays an important factor in the susceptibility of cerebellar astrocytes to MeHg.

In Chapters 1 and 2, we demonstrated that cerebellar astrocytes are more susceptible to MeHg-induced cytotoxicity than cortical astrocytes and that MeHg selectively increases

glutamate release from cerebellar astrocytes. In Chapter 3, we focused on cerebellar astrocytes and studied the role of organelles and membrane proteins, such as Ca^{2+} channels and bradykinin receptors in both the release of glutamate and the decrease in viability after an acute exposure to MeHg.

When we studied intracellular stores, we discovered that the mitochondria, but not the SER contributed to the astrocytic glutamate release. This may be due to the lack of contribution of the SER to the increase of intracellular Ca^{2+} in primary astrocyte cultures. Unlike the SER, the mitochondria contributes to a large portion of the intracellular Ca^{2+} detected in astrocytes (Marty et al., 2006), which may explain its extensive contribution to the increased levels of glutamate.

Regardless of the poor contribution of the SER to the increase in extracellular glutamate levels, its inhibition plays an important factor in MeHg-induced astrocyte death. Similarly, previous studies done on granule cells discovered that the SER only has a small contribution to $[Ca^{2+}]_i$, but it plays an important factor in MeHg-induced granule cell death (Limke et al., 2004). The contribution of the SER to cell death, but not to astrocytic glutamate release suggests that the released glutamate from astrocytes is not due to a mere result of astrocyte death, but to the interaction of MeHg with certain cellular components.

By depleting Ca^{2+} levels in the mitochondria, we were able to significantly inhibit the vesicular release of glutamate at all MeHg concentrations. However, we were able to reduce, but not eliminate astrocyte death at a high MeHg concentration (5 μM). These results suggest that the release of glutamate may not be the only factor associated with astrocyte death after high MeHg concentrations. This supports the results obtained in Chapter 2, in which Rose Bengal, a potent inhibitor of the vesicular release of glutamate, was able to decrease the extracellular

glutamate levels at all MeHg concentrations, but not to eliminate astrocytic death at higher MeHg concentrations.

When we studied the contribution of VGCCs to astrocytes toxicity induced by MeHg, we found that both L-type and N-type Ca^{2+} channels played a role in glutamate release and decrease in viability in astrocytes after MeHg exposure. These results were similar to those found in primary cultures of granule cells, in which MeHg induced entry of Ca^{2+} through L-type and N-type VGCCs and produced cell death (Marty & Atchison, 1997).

When we compared the effect of MeHg on intracellular storages with its effect on Ca^{2+} channels, we could see how MeHg induced a higher release of glutamate through its effect on the N-type VGCCs than through its effect on the SER at all MeHg concentrations. The higher role of N-type VGCCs in the release of glutamate from astrocytes when compared with the SER, a significant difference that has not been seen when compared with L-type Ca^{2+} channels, might be due to the prominent role of N-type VGCCs in synaptic vesicle recycling and glutamate release (Iwasaki & Takahashi, 1998; Pravettoni et al., 2000; Scholz & Miller, 1995; Verderio et al., 1995).

When we studied the contribution of intracellular storages and Ca^{2+} channels to the reduction of viability, we found that there was no significant difference between any of the cellular components. In Chapter 2, we discovered that the decrease in viability of cerebellar astrocytes after MeHg exposure was dependent on both intracellular and extracellular Ca^{2+} and that extracellular Ca^{2+} played a more important role in this decrease than intracellular Ca^{2+} at higher MeHg concentrations. It is possible that at high MeHg concentrations there was an increased amount of Ca^{2+} influx into the cytoplasm that was pumped into the SER and the mitochondria. Therefore, the effect of MeHg on these intracellular organelles can liberate the

buffered Ca^{2+}, explaining why the absence of extracellular Ca^{2+} has a predominant role in the decrease in viability at high MeHg concentrations. Another potential explanation for these results might be the disruption of the astrocytic membrane at higher MeHg concentrations that could produce an enhanced entry of Ca^{2+} and induce cell death.

Another membrane protein studied was bradykinin receptor. It is well known that the activation of bradykinin receptors in astrocytes leads to an increase in Ca^{2+} concentration and glutamate release (Parpura et al., 1994); therefore, we wanted to know if MeHg and bradykinin have a common pathway for toxicity and astrocytic glutamate release. After the desensitization of bradykinin receptors, there was a decrease in extracellular glutamate levels, but not at high MeHg concentrations. Likewise, bradykinin was able to decrease, but not eliminate astrocyte death at high MeHg concentrations. This suggests that bradykinin receptors at lower MeHg concentrations seem to have a common pathway for astrocytic glutamate release. It could also suggest an interaction between MeHg and bradykinin receptors.

Since the EAATs, especially EAAT1 and EAAT2, can buffer most of the glutamate released and prevent glutamate excitotoxicity (Danbolt, 2001; Rothstein et al., 1996), we performed immunocytochemistry and studied the effect of MeHg on the mean fluorescence intensity levels of these proteins. We found a significant increase of mean fluorescence intensity in cerebellar EAAT2. We also found an increase of mean fluorescence intensity in cortical EAAT1. However, the mean fluorescence intensity in cerebellar EAAT1 was higher than the mean fluorescence intensity in cortical EAAT1 at the same MeHg concentrations. These studies suggest that despite the preferential susceptibility of the cerebellum to MeHg-induced excitotoxicity, cerebellar astrocytes possess higher EAATs levels than cortical astrocytes when

treated with MeHg. Therefore, it is possible that MeHg causes a dysfunction in these cerebellar proteins that inhibits their normal buffering, causing glutamate dyshomeostasis.

B. Conclusion

There is a regional, but not a typological difference in astrocyte viability after an acute MeHg treatment, in where cerebellar astrocytes are more susceptible to MeHg than cortical astrocytes. One factor that might contribute to the differences in susceptibility between these two astrocytes is the changes in $[Ca^{2+}]_i$ induced by MeHg. MeHg induces an increase of $[Ca^{2+}]_i$ in astrocytes. MeHg causes a release of Ca^{2+} from the mitochondria and an influx of extracellular Ca^{2+} into the astrocytic cytosol (Marty et al., 2006). We discovered that intracellular Ca^{2+} played a role in MeHg-induced cortical astrocyte death. However, both intracellular and extracellular Ca^{2+} contribute to cerebellar astrocyte death.

Another factor that contributes to the regional susceptibility of cerebellar astrocytes to MeHg was the Ca^{2+}-dependent vesicular release of glutamate. This effect occurred in cerebellar but not in cortical astrocytes, and was not due to the effects on the SER, but rather to the interaction of MeHg with the mitochondria, L-type and N-type VGCCs. However, there were no differences in the contribution of these intracellular storages and Ca^{2+} channels to the reduction of viability. MeHg can also produce dysfunction of the EAATs. The vesicular release of glutamate from cerebellar astrocytes and the dysfunction of the EAATs contribute to cerebellar astrocyte susceptibility to MeHg, and might contribute to the susceptibility of granule cells by further increasing neuronal excitotoxicity. This is demonstrated in Figure 5.1.

We recognize that this dissertation possesses several limitations. The effect of MeHg was measured 24 h after the 3 h of exposure. Although we demonstrated different degrees of contribution of the intracellular storages and membrane proteins to the changes in extracellular glutamate levels, we were unable to detect differences in viability between these cell components. It is possible that, like granule cells, all the cellular components studied contribute

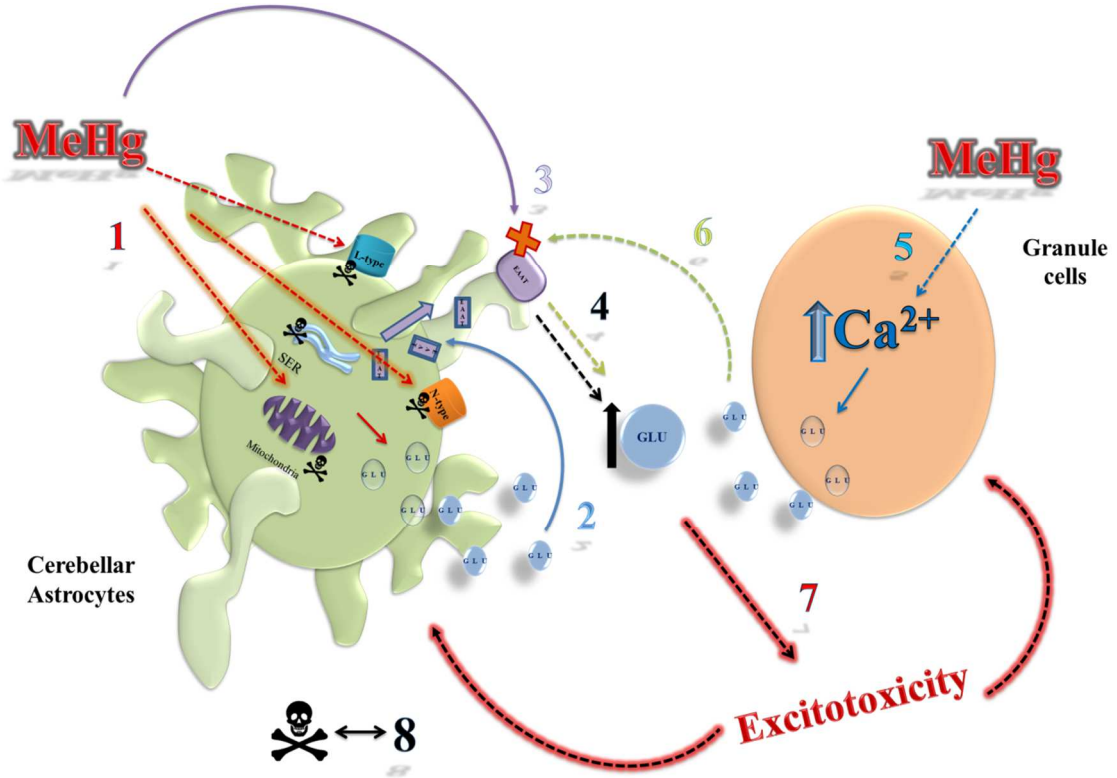

Figure 5.1. Mechanisms of MeHg-induced toxicity in astrocytes and granule cells. 1. (In red) MeHg induces a Ca^{2+}-dependent release of vesicular glutamate from the mitochondria and Ca^{2+} channels. The mitochondria and the N-type VGCCs have a higher contribution to the release of glutamate. 2. (In blue) It is possible that higher levels of extracellular glutamate produce an upregulation of the EAAT2. 3. (In purple) MeHg-induces dysfunction on the EAAT2. 4. (In black) Due to the dysfunction of the EAAT2, these proteins are unable to buffer the increased levels of extracellular glutamate released by astrocytes. 5. (In blue) MeHg induces an increase in $[Ca^{2+}]_i$ in granule cells, which produces a release of glutamate. 6. (In green) Due to the dysfunction of the astrocytic EAATs, the glutamate released by cerebellar granule cells are not buffered by astrocytes. 7. (In red) The release of glutamate by astrocytes and neurons, and the dysfunction of the EAATs produce glutamate excitotoxicity in granule cells and cerebellar astrocytes.

to MeHg-induced toxicity in an additive or synergistic manner. Nevertheless, to obtain a better discernment of the contribution of these cell components, future studies should focus on the real-time effect of MeHg on astrocytes. Another improvement to determine if there is an additive contribution of these cell components to MeHg-induced astrocyte toxicity might be to increase the amount of exposure time and the range of MeHg concentrations. In the EAAT experiments, we observed an increase of mean fluorescence intensity in the EAATs that suggests an increase in proteins levels, but because there was also an increase in glutamate levels, we suggest that there was a dysfunction in these transporters. Future studies should examine the effect of MeHg on the EAATs function in order to better understand the dyshomeostasis of glutamate.

BIBLIOGRAPHY

BIBLIOGRAPHY

Aberg, B., Ekman, L., Falk, R., Greitz, U., Persson, G., & Snihs, J. O. (1969). Metabolism of methyl mercury (203Hg) compounds in man: Excretion and distribution. *Archives of Environmental Health: An International Journal, 19*(4), 478-484.

Abudara, V., Roux, L., Dallérac, G., Matias, I., Dulong, J., Mothet, J. P., ... & Giaume, C. (2015). Activated microglia impairs neuroglial interaction by opening Cx43 hemichannels in hippocampal astrocytes. *Glia*, 63(5), 795-811.

Adachi, T., & Kunimoto, M. (2005). Acute cytotoxic effects of mercuric compounds in cultured astrocytes prepared from cerebral hemisphere and cerebellum of newborn rats. *Biological and Pharmaceutical Bulletin, 28*(12), 2308-2311.

Albrecht, J., Talbot, M., Kimelberg, H. K., & Aschner, M. (1993). The role of sulfhydryl groups and calcium in the mercuric chloride-induced inhibition of glutamate uptake in rat primary astrocyte cultures. *Brain research, 607*(1-2), 249-254.

Ali, S., LeBel, C., & Bondy, S. (1991). Reactive oxygen species formation as a biomarker of methylmercury and trimethyltin neurotoxicity. *Neurotoxicology, 13*(3), 637-648.

Ahlijanian, M. K., Westenbroek, R. E., & Catterall, W. A. (1990). Subunit structure and localization of dihydropyridine-sensitive calcium channels in mammalian brain, spinal cord, and retina. *Neuron, 4*(6), 819-832.

Amin-Zaki, L., Majeed, M. A., Elhassani, S. B., Clarkson, T. W., Greenwood, M. R., & Doherty, R. A. (1979). Prenatal methylmercury poisoning: clinical observations over five years. *American Journal of Diseases of Children, 133*(2), 172-177.

Anderson, C. M., & Swanson, R. A. (2000). Astrocyte glutamate transport: review of properties, regulation, and physiological functions. *Glia, 32*(1), 1-14.

Aosaki, T., & Kasai, H. (1989). Characterization of two kinds of high-voltage-activated Ca-channel currents in chick sensory neurons. *Pflügers Archiv European Journal of Physiology, 414*(2), 150-156.

Arakawa, O., Nakahiro, M., & Narahashi, T. (1991). Mercury modulation of GABA-activated chloride channels and non-specific cation channels in rat dorsal root ganglion neurons. *Brain research, 551*(1), 58-63.

Araque, A., Carmignoto, G., Haydon, P. G., Oliet, S. H., Robitaille, R., & Volterra, A. (2014). Gliotransmitters travel in time and space. *Neuron, 81*(4), 728-739.

Araque, A., Li, N., Doyle, R. T., & Haydon, P. G. (2000). SNARE protein-dependent glutamate release from astrocytes. *Journal of Neuroscience, 20*(2), 666-673.

Araque, A., Sanzgiri, R. P., Parpura, V., & Haydon, P. G. (1998). Calcium elevation in astrocytes causes an NMDA receptor-dependent increase in the frequency of miniature synaptic currents in cultured hippocampal neurons. *Journal of Neuroscience, 18*(17), 6822-6829.

Arriza, J. L., Eliasof, S., Kavanaugh, M. P., & Amara, S. G. (1997). Excitatory amino acid transporter 5, a retinal glutamate transporter coupled to a chloride conductance. *Proceedings of the National Academy of Sciences, 94*(8), 4155-4160.

Arriza, J. L., Fairman, W. A., Wadiche, J. I., Murdoch, G. H., Kavanaugh, M. P., & Amara, S. G. (1994). Functional comparisons of three glutamate transporter subtypes cloned from human motor cortex. *Journal of Neuroscience, 14*(9), 5559-5569.

Aschner, M., Du, Y.-L., Gannon, M., & Kimelberg, H. (1993). Methylmercury-induced alterations in excitatory amino acid transport in rat primary astrocyte cultures. *Brain research, 602*(2), 181-186.

Aschner, M., Conklin, D. R., Yao, C. P., Allen, J. W., & Tan, K. H. (1998a). Induction of astrocyte metallothioneins (MTs) by zinc confers resistance against the acute cytotoxic effects of methylmercury on cell swelling, Na^+ uptake, and K^+ release. *Brain research, 813*(2), 254-261.

Aschner, M., Eberle, N., Goderie, S., & Kimelberg, H. (1990). Methylmercury uptake in rat primary astrocyte cultures: the role of the neutral amino acid transport system. *Brain research, 521*(1), 221-228.

Aschner, M., Eberle, N., & Kimelberg, H. (1991). Interactions of methylmercury with rat primary astrocyte cultures: methylmercury efflux. *Brain research, 554*(1), 10-14.

Aschner, M., Eberle, N. B., Miller, K., & Kimelberg, H. K. (1990). Interactions of methylmercury with rat primary astrocyte cultures: inhibition of rubidium and glutamate uptake and induction of swelling. *Brain research*, *530*(2), 245-250.

Aschner, M., Mullaney, K., Wagoner, D., Lash, L., & Kimelberg, H. (1994). Intracellular glutathione (GSH) levels modulate mercuric chloride (MC)-and methylmercuric chloride (MeHgCl)-induced amino acid release from neonatal rat primary astrocytes cultures. *Brain research, 664*(1), 133-140.

Aschner, M., Rising, L., & Mullaney, K. J. (1996). Differential sensitivity of neonatal rat astrocyte cultures to mercuric chloride (MC) and methylmercury (MeHg): studies on K^+ and amino acid transport and metallothionein (MT) induction. *Neurotoxicology, 17*(1), 107.

Aschner, M., Vitarella, D., Allen, J. W., Conklin, D. R., & Cowan, K. S. (1998b). Methylmercury-induced astrocytic swelling is associated with activation of the Na^+/H^+ antiporter, and is fully reversed by amiloride. *Brain research, 799*(2), 207-214.

Aschner, M., Yao, C. P., Allen, J. W., & Tan, K. H. (2000). Methylmercury alters glutamate transport in astrocytes. *Neurochemistry international, 37*(2), 199-206.

Atchison, W. D. (1986). Extracellular calcium-dependent and-independent effects of methylmercury on spontaneous and potassium-evoked release of acetylcholine at the neuromuscular junction. *Journal of Pharmacology and Experimental Therapeutics, 237*(2), 672-680.

Atchison, W. D. (1987). Effects of activation of sodium and calcium entry on spontaneous release of acetylcholine induced by methylmercury. *Journal of Pharmacology and Experimental Therapeutics, 241*(1), 131-139.

Atchison, W. D. (2005). Is chemical neurotransmission altered specifically during methylmercury-induced cerebellar dysfunction? *Trends in pharmacological sciences, 26*(11), 549-557.

Atchison, W.D., Adgate, L., & Beaman, C. (1988). Effects of antibiotics on uptake of calcium into isolated nerve terminals. *Journal of Pharmacology and Experimental Therapeutics, 245*(2), 394-401

Atchison, W. D., & Hare, M. F. (1994). Mechanisms of methylmercury-induced neurotoxicity. *The FASEB Journal, 8*(9), 622-629.

Atchison, W., Joshi, U., & Thornburg, J. (1986). Irreversible suppression of calcium entry into nerve terminals by methylmercury. *Journal of Pharmacology and Experimental Therapeutics, 238*(2), 618-624.

Atwell, L., Hobson, K. A., & Welch, H. E. (1998). Biomagnification and bioaccumulation of mercury in an arctic marine food web: insights from stable nitrogen isotope analysis. *Canadian Journal of Fisheries and Aquatic Sciences, 55*(5), 1114-1121.

Balakrishnan, S., & Bellamy, T. C. (2009). Depression of parallel and climbing fiber transmission to Bergmann glia is input specific and correlates with increased precision of synaptic transmission. *Glia, 57*(4), 393-401.

Balakrishnan, S., Dobson, K. L., Jackson, C., & Bellamy, T. C. (2014). Ectopic release of glutamate contributes to spillover at parallel fibre synapses in the cerebellum. *The Journal of physiology, 592*(7), 1493-1503.

Bak, L. K., Schousboe, A., & Waagepetersen, H. S. (2006). The glutamate/GABA□glutamine cycle: aspects of transport, neurotransmitter homeostasis and ammonia transfer. *Journal of neurochemistry, 98*(3), 641-653.

Bakir, F. (1973). Methylmercnry poisoning in Iraq. An interuniversity report. *Science (Washington), 181*, 230-241.

Bal□Price, A., Moneer, Z., & Brown, G. C. (2002). Nitric oxide induces rapid, calcium□ dependent release of vesicular glutamate and ATP from cultured rat astrocytes. *Glia, 40*(3), 312-323.

Barres, B., Chun, L., & Corey, D. (1989). Calcium current in cortical astrocytes: induction by cAMP and neurotransmitters and permissive effect of serum factors. *Journal of Neuroscience, 9*(9), 3169-3175.

Bayraktar, O. A., Fuentealba, L. C., Alvarez-Buylla, A., & Rowitch, D. H. (2015). Astrocyte development and heterogeneity. *Cold Spring Harbor perspectives in biology*, *7*(1), a020362.

Bearrs, J., Limke, T., & Atchison, W. (2001). Methylmercury (MeHg) causes calcium release from smooth endoplasmic reticulum (SER) inositol-1, 4, 5-triphosphate receptors in rat cerebellar granule neurons. *The Toxicologist, 60*, 184.

Bender, M., Lymberidi-Settimo, E., & Groth III, E. (2014). New mercury treaty exposes health risks. *Journal of public health policy, 35*(1), 1-13.

Benoit, J. M., Gilmour, C. C., Mason, R. P., & Heyes, A. (1999). Sulfide controls on mercury speciation and bioavailability to methylating bacteria in sediment pore waters. *Environmental Science & Technology, 33*(6), 951-957.

Bernardi, P. (2013). The mitochondrial permeability transition pore: a mystery solved? *Frontiers in physiology, 4*, 95.

Bernardi, P., & von Stockum, S. (2012). The permeability transition pore as a Ca^{2+} release channel: new answers to an old question. *Cell calcium, 52*(1), 22-27.

Berridge, M. J., & Taylor, C. (1988). *Inositol trisphosphate and calcium signaling.* Paper presented at the Cold Spring Harbor symposia on quantitative biology.

Bezprozvanny, I., Scheller, R., & Tsien, R. (1995). Functional impact of syntaxin on gating of N-type and Q-type calcium channels. *Nature, 378*(6557), 623.

Bezzi, P., Carmignoto, G., Pasti, L., Vesce, S., Rossi, D., Rizzini, B. L., . . . Volterra, A. (1998). Prostaglandins stimulate calcium-dependent glutamate release in astrocytes. *Nature, 391*(6664), 281-285.

Bi, G.-q., & Poo, M.-m. (1998). Synaptic modifications in cultured hippocampal neurons: dependence on spike timing, synaptic strength, and postsynaptic cell type. *Journal of Neuroscience, 18*(24), 10464-10472.

Blaukat, A., Micke, P., Kalatskaya, I., Faussner, A., & Müller-Esterl, W. (2003). Downregulation of bradykinin B2 receptor in human fibroblasts during prolonged agonist exposure. *American Journal of Physiology-Heart and Circulatory Physiology, 284*(6), H1909-H1916.

Blomstrand, F., Åberg, N. D., Eriksson, P. S., Hansson, E., & Rönnbäck, L. (1999). Extent of intercellular calcium wave propagation is related to gap junction permeability and level of connexin-43 expression in astrocytes in primary cultures from four brain regions. *Neuroscience, 92*(1), 255-265.

Bollmann, J. H., Sakmann, B., & Borst, J. G. G. (2000). Calcium sensitivity of glutamate release in a calyx-type terminal. *Science, 289*(5481), 953-957.

Booth, S., & Zeller, D. (2005). Mercury, food webs, and marine mammals: implications of diet and climate change for human health. *Environmental health perspectives, 113*(5), 521.

Bradford, A. B., Mancini, J. D., & Atchison, W. D. (2016). Methylmercury-dependent increases in Fluo4 fluorescence in neonatal rat cerebellar slices depend on granule cell migrational stage and GABAA receptor modulation. *Journal of Pharmacology and Experimental Therapeutics, 356*(1), 2-12.

Brickley, S. G., Cull-Candy, S. G., & Farrant, M. (1996). Development of a tonic form of synaptic inhibition in rat cerebellar granule cells resulting from persistent activation of GABAA receptors. *The Journal of physiology, 497*(3), 753-759.

Brookes, N. (1992). In vitro evidence for the hole of glutamate in the CNS toxicity of mercury. *Toxicology, 76*(3), 245-256.

Brookes, N., & Kristt, D. (1989). Inhibition of amino acid transport and protein synthesis by $HgCl_2$ and methylmercury in astrocytes: selectivity and reversibility. *Journal of neurochemistry, 53*(4), 1228-1237.

Burnashev, N., Khodorova, A., Jonas, P., Helm, P. J., Wisden, W., Monyer, H., . . . Sakmann, B. (1992). Calcium-permeable AMPA-kainate receptors in fusiform cerebellar glial cells. *Science, 256*(5063), 1566-1571.

Catterall, W. A., Perez-Reyes, E., Snutch, T. P., & Striessnig, J. (2005). International Union of Pharmacology. XLVIII. Nomenclature and structure-function relationships of voltage-gated calcium channels. *Pharmacological Reviews, 57*(4), 411-425.

Cavalcante, L. A., Garcia-Abreu, J., Moura, N. V., Silva, L., & Barradas, P. C. (1996). Heterogeneity of median and lateral midbrain radial glia and astrocytes. *Revista brasileira de biologia, 56*, 33-52.

Chang, L. W., & Hartmann, H. A. (1972). Ultrastructural studies of the nervous system after mercury intoxication. *Acta Neuropathologica, 20*(2), 122-138.

Charbonneau, S., Munro, I., Nera, E., Willes, R., Kuiper-Goodman, T., Iverson, F., . . . Uthe, J. (1974). Subacute toxicity of methylmercury in the adult cat. *Toxicology and applied pharmacology, 27*(3), 569-581.

Charles, A. C., Merrill, J. E., Dirksen, E. R., & Sandersont, M. J. (1991). Intercellular signaling in glial cells: calcium waves and oscillations in response to mechanical stimulation and glutamate. *Neuron, 6*(6), 983-992.

Chen, C. J., Liao, S. L., & Kuo, J. S. (2000). Gliotoxic action of glutamate on cultured astrocytes. *Journal of neurochemistry, 75*(4), 1557-1565.

Choi, B. H., Lapham, L. W., Amin-Zaki, L., & Saleem, T. (1978). Abnormal neuronal migration, deranged cerebral cortical organization, and diffuse white matter astrocytosis of human fetal brain: a major effect of methylmercury poisoning in utero. *Journal of Neuropathology & Experimental Neurology, 37*(6), 719-733.

Cholewinski, A., Hanley, M., & Wilkin, G. (1988). A phosphoinositide-linked peptide response in astrocytes: evidence for regional heterogeneity. *Neurochemical research, 13*(4), 389-394.

Cholewinski, A., & Wilkin, G. (1988). Bradykinin and vasopressin both stimulate phosphoinositide turnover in astrocytes in high serum-and low serum-containing media but have no effect on [^{3}H] thymidine incorporation. *Neurochemistry international, 13*(3), 393-396.

Clapham, D. E. (1995). Calcium signaling. *Cell, 80*(2), 259-268.

Clarkson, T. W. (1995). Environmental contaminants in the food chain. *The American journal of clinical nutrition, 61*(3), 682S-686S.

Clarkson, T. W., Friberg, L., Nordberg, G. F., & Sager, P. R. (2012). *Biological monitoring of toxic metals*: Springer Science & Business Media.

Cornell-Bell, A. H., Finkbeiner, S. M., Cooper, M. S., & Smith, S. J. (1990). Glutamate induces calcium waves in cultured astrocytes: long-range glial signaling. *Science, 247*(4941), 470.

Corvalan, V., Cole, R., de Vellis, J., & Hagiwara, S. (1990). Neuronal modulation of calcium channel activity in cultured rat astrocytes. *Proceedings of the National Academy of Sciences, 87*(11), 4345-4348.

Council, N. r. (2000). *Toxicological effects of methylmercury*: National Academies Press.

Crippa, D., Schenk, U., Francolini, M., Rosa, P., Verderio, C., Zonta, M., . . . Carmignoto, G. (2006). Synaptobrevin2□expressing vesicles in rat astrocytes: insights into molecular characterization, dynamics and exocytosis. *The Journal of physiology, 570*(3), 567-582.

D'Ascenzo, M., Vairano, M., Andreassi, C., Navarra, P., Azzena, G. B., & Grassi, C. (2004). Electrophysiological and molecular evidence of L□(Cav1), N□(Cav2. 2), and R□(Cav2. 3) type Ca^{2+} channels in rat cortical astrocytes. *Glia, 45*(4), 354-363.

Danbolt, N. C. (2001). Glutamate uptake. *Progress in neurobiology, 65*(1), 1-105.

David, J. C., Yamada, K. A., Bagwe, M. R., & Goldberg, M. P. (1996). AMPA receptor activation is rapidly toxic to cortical astrocytes when desensitization is blocked. *Journal of Neuroscience, 16*(1), 200-209.

Davidson, P. W., Cory-Slechta, D. A., Thurston, S. W., Huang, L.-S., Shamlaye, C. F., Gunzler, D., . . . Klein, J. D. (2011). Fish consumption and prenatal methylmercury exposure: cognitive and behavioral outcomes in the main cohort at 17 years from the Seychelles child development study. *Neurotoxicology, 32*(6), 711-717.

Davidson, P. W., Myers, G. J., Cox, C., Shamlaye, C. F., Marsh, D. O., Tanner, M. A., . . . Choisy, O. (1994). Longitudinal neurodevelopmental study of Seychellois children following in utero exposure to methylmercury from maternal fish ingestion: outcomes at 19 and 29 months. *Neurotoxicology, 16*(4), 677-688.

de Matos, L. L., Trufelli, D. C., de Matos, M. G. L., & da Silva Pinhal, M. A. (2010). Immunohistochemistry as an important tool in biomarkers detection and clinical practice. *Biomarker insights*, *5*, 9.

Denny, M. F., & Atchison, W. D. (1994). Methylmercury□induced elevations in intrasynaptosomal zinc concentrations: An 19F□NMR study. *Journal of neurochemistry, 63*(1), 383-386.

Denny, M. F., Hare, M. F., & Atchison, W. D. (1993). Methylmercury alters intrasynaptosomal concentrations of endogenous polyvalent cations. *Toxicology and applied pharmacology, 122*(2), 222-232.

De Pina-Benabou, M. H., Srinivas, M., Spray, D. C., & Scemes, E. (2001). Calmodulin kinase pathway mediates the K^+-induced increase in Gap junctional communication between mouse spinal cord astrocytes. *Journal of Neuroscience, 21*(17), 6635-6643.

De Zeeuw, C. I., & Hoogland, T. M. (2015). Reappraisal of Bergmann glial cells as modulators of cerebellar circuit function. *Frontiers in cellular neuroscience, 9*.

Doi, R. (1991). Individual difference of methylmercury metabolism in animals and its significance in methylmercury toxicity *Advances in mercury toxicology* (pp. 77-98): Springer.

Dringen, R., Pfeiffer, B., & Hamprecht, B. (1999). Synthesis of the antioxidant glutathione in neurons: supply by astrocytes of CysGly as precursor for neuronal glutathione. *Journal of Neuroscience, 19*(2), 562-569.

Duan, S., Anderson, C. M., Keung, E. C., Chen, Y., Chen, Y., & Swanson, R. A. (2003). P2X7 receptor-mediated release of excitatory amino acids from astrocytes. *Journal of Neuroscience, 23*(4), 1320-1328.

Duffy, S., & MacVicar, B. A. (1996). In vitro ischemia promotes calcium influx and intracellular calcium release in hippocampal astrocytes. *Journal of Neuroscience, 16*(1), 71-81.

Dunlap, K., Luebke, J. I., & Turner, T. J. (1995). Exocytotic Ca^{2+} channels in mammalian central neurons. *Trends in neurosciences, 18*(2), 89-98.

Dunn, J., & Clarkson, T. (1980). Does mercury exhalation signal demethylation of methyl mercury. *Health physics, 38*(3), 411-414.

Edwards, J. R., Marty, M. S., & Atchison, W. D. (2005). Comparative sensitivity of rat cerebellar neurons to dysregulation of divalent cation homeostasis and cytotoxicity caused by methylmercury. *Toxicology and applied pharmacology, 208*(3), 222-232.

Elinder, C.-G., Gerhardsson, L., & Oberdoerster, G. (1988). Biological monitoring of toxic metals-overview *Biological monitoring of toxic metals* (pp. 1-71): Springer.

Emsley, J. G., & Macklis, J. D. (2006). Astroglial heterogeneity closely reflects the neuronal-defined anatomy of the adult murine CNS. *Neuron glia biology, 2*(03), 175-186.

Eto, K., & Takeuchi, T. (1978). A pathological study of prolonged cases of Minamata disease—with Particular Reference to 83 Autopsy Cases—. *Pathology International, 28*(4), 565-584.

Fairman, W., Vandenberg, R., Arriza, J., Kavanaugh, M., & Amara, S. (1995). An excitatory amino-acid transporter with properties of a ligand-gated chloride channel. *Nature, 375*(6532), 599.

Fang, S., & Fallin, E. (1976). The binding of various mercurial compounds to serum proteins. *Bulletin of environmental contamination and toxicology, 15*(1), 110-117.

FDA (U.S Food and Drug Administration). 2012. Mercury Levels in Commercial Fish and Shellfish (1990-2012). Available: https://www.fda.gov/food/foodborneillnesscontaminants/metals/ucm115644.htm [accessed July 02, 2017].

Finkbeiner, S. M. (1993). Glial calcium. *Glia, 9*(2), 83-104.

Fox, A., Nowycky, M., & Tsien, R. (1987). Kinetic and pharmacological properties distinguishing three types of calcium currents in chick sensory neurones. *The Journal of physiology, 394*, 149.

Fritzsche, M., & Mandenius, C. F. (2010). Fluorescent cell-based sensing approaches for toxicity testing. *Analytical and bioanalytical chemistry*, *398*(1), 181-191

Fujiyama, J., Hirayama, K., & Yasutake, A. (1994). Mechanism of methylmercury efflux from cultured astrocytes. *Biochemical pharmacology, 47*(9), 1525-1530.

Furuta, A., Rothstein, J. D., & Martin, L. J. (1997). Glutamate transporter protein subtypes are expressed differentially during rat CNS development. *Journal of Neuroscience, 17*(21), 8363-8375.

Gabryel, B., Adamek, M., Pudełko, A., Małecki, A., & Trzeciak, H. I. (2002). Piracetam and vinpocetine exert cytoprotective activity and prevent apoptosis of astrocytes in vitro in hypoxia and reoxygenation. *Neurotoxicology*, *23*(1), 19-31.

Ganther, H., Goudie, C., Sunde, M., Kopecky, M., Wanger, P., Hoh, S., & Hoekstra, W. (1972). Selenium: relation to decreased toxicity of methylmercury added to diets containing tuna. *Science,(Wash.). 175*(4026), 1122-1124.

Gassó, S., Cristofol, R. M., Selema, G., Rosa, R., Rodríguez-Farré, E., & Sanfeliu, C. (2001). Antioxidant compounds and Ca^{2+} pathway blockers differentially protect against methylmercury and mercuric chloride neurotoxicity. *Journal of neuroscience research, 66*(1), 135-145.

Giaume, C., Leybaert, L., Naus, C. C., & Sáez, J. C. (2013). Connexin and pannexin hemichannels in brain glial cells: properties, pharmacology, and roles. *Frontiers in pharmacology*, *4*.

Gimpl, G., Walz, W., Ohlemeyer, C., & Kettenmann, H. (1992). Bradykinin receptors in cultured astrocytes from neonatal rat brain are linked to physiological responses. *Neuroscience letters, 144*(1), 139-142.

Grandjean, P., Weihe, P., Debes, F., Choi, A. L., & Budtz-Jørgensen, E. (2014). Neurotoxicity from prenatal and postnatal exposure to methylmercury. *Neurotoxicology and teratology, 43*, 39-44.

Gunson, A., & Veiga, M. M. (2004). Mercury and artisanal mining in China. *Environmental Practice, 6*(02), 109-120.

Gunter, K. K., & Gunter, T. E. (1994). Transport of calcium by mitochondria. *Journal of bioenergetics and biomembranes, 26*(5), 471-485.

Hall, J. M. (1992). Bradykinin receptors: pharmacological properties and biological roles. *Pharmacology & therapeutics, 56*(2), 131-190.

Hall, J. M. (1997). Bradykinin receptors. *General Pharmacology: The Vascular System, 28*(1), 1-6.

Hamdy, M., & Noyes, O. (1975). Formation of methyl mercury by bacteria. *Applied microbiology, 30*(3), 424-432.

Han, B. C., Koh, S. B., Lee, E. Y., & Seong, Y. H. (2004). Regional difference of glutamate-induced swelling in cultured rat brain astrocytes. *Life sciences, 76*(5), 573-583.

Hansson, E. (1988). Astroglia from defined brain regions as studied with primary cultures. *Progress in neurobiology, 30*(5), 369-397.

Harada, M. (1978). Congenital Minamata disease: intrauterine methylmercury poisoning. *Teratology, 18*(2), 285-288.

Harada, M. (1995). Minamata disease: methylmercury poisoning in Japan caused by environmental pollution. *Critical reviews in toxicology, 25*(1), 1-24.

Hare, M., McGinnis, K., & Atchison, W. (1993). Methylmercury increases intracellular concentrations of Ca^{2+} and heavy metals in NG108-15 cells. *Journal of Pharmacology and Experimental Therapeutics, 266*(3), 1626-1635.

Hare, M. F., & Atchison, W. D. (1995a). Methylmercury mobilizes Ca^{2+} from intracellular stores sensitive to inositol 1, 4, 5-trisphosphate in NG108-15 cells. *Journal of Pharmacology and Experimental Therapeutics, 272*(3), 1016-1023.

Hare, M. F., & Atchison, W. D. (1995b). Nifedipine and tetrodotoxin delay the onset of methylmercury-induced increase in $[Ca^{2+}]_i$ in NG108-15 cells. *Toxicology and applied pharmacology, 135*(2), 299-307.

Hashimoto, M., & Hibi, M. (2012). Development and evolution of cerebellar neural circuits. *Development, growth & differentiation, 54*(3), 373-389.

Hepp, R., Perraut, M., Chasserot□Golaz, S., Galli, T., Aunis, D., Langley, K., & Grant, N. J. (1999). Cultured glial cells express the SNAP□25 analogue SNAP□23. *Glia, 27*(2), 181-187.

Herden, C. J., Pardo, N. E., Hajela, R. K., Yuan, Y., & Atchison, W. D. (2008). Differential effects of methylmercury on γ-aminobutyric acid type A receptor currents in rat cerebellar granule and cerebral cortical neurons in culture. *Journal of Pharmacology and Experimental Therapeutics, 324*(2), 517-528.

Hewett, J. A. (2009). Determinants of regional and local diversity within the astroglial lineage of the normal central nervous system. *Journal of neurochemistry*, *110*(6), 1717-1736.

Hunter, D., Bomford, R. R., & Russell, D. S. (1940). Poisoning by methyl mercury compounds. *Qj Med, 9*(3), 193-226.

Hunter, D., & Russell, D. S. (1954). Focal cerebral and cerebellar atrophy in a human subject due to organic mercury compounds. *Journal of Neurology, Neurosurgery & Psychiatry, 17*(4), 235-241.

Iino, M., Goto, K., Kakegawa, W., Okado, H., Sudo, M., Ishiuchi, S., . . . Tsuzuki, K. (2001). Glia-synapse interaction through Ca2+-permeable AMPA receptors in Bergmann glia. *Science, 292*(5518), 926-929.

Inglefield, J. R., Mundy, W. R., & Shafer, T. J. (2001). Inositol 1, 4, 5-triphosphate receptor-sensitive Ca^{2+} release, store-operated Ca^{2+} entry, and cAMP responsive element binding protein phosphorylation in developing cortical cells following exposure to polychlorinated biphenyls. *Journal of Pharmacology and Experimental Therapeutics, 297*(2), 762-773.

Iwasaki, S., & Takahashi, T. (1998). Developmental changes in calcium channel types mediating synaptic transmission in rat auditory brainstem. *The Journal of physiology, 509*(2), 419-423.

Jain, A., Mårtensson, J., Stole, E., Auld, P., & Meister, A. (1991). Glutathione deficiency leads to mitochondrial damage in brain. *Proceedings of the National Academy of Sciences, 88*(5), 1913-1917.

Jakoby, P., Schmidt, E., Ruminot, I., Gutiérrez, R., Barros, L. F., & Deitmer, J. W. (2012). Higher transport and metabolism of glucose in astrocytes compared with neurons: a multiphoton study of hippocampal and cerebellar tissue slices. *Cerebral cortex, 24*(1), 222-231.

Jeftinija, S. D., Jeftinija, K. V., & Stefanovic, G. (1997). Cultured astrocytes express proteins involved in vesicular glutamate release. *Brain research, 750*(1), 41-47.

Jensen, S., & Jernelöv, A. (1969). Biological methylation of mercury in aquatic organisms. *Nature, 223*(5207), 753-754.

Jernelov, A. (1969). Conversion of mercury compounds, Chapt. 4. *Chemical Fallout, Springfield, Illinois: Chas. C Thomas*.

Johansson, C. B., Momma, S., Clarke, D. L., Risling, M., Lendahl, U., & Frisén, J. (1999). Identification of a neural stem cell in the adult mammalian central nervous system. *Cell*, *96*(1), 25-34.

Johnson, F. O., Yuan, Y., Hajela, R. K., Chitrakar, A., Parsell, D. M., & Atchison, W. D. (2011). Exposure to an environmental neurotoxicant hastens the onset of amyotrophic lateral sclerosis-like phenotype in human Cu^{2+}/Zn^{2+} superoxide dismutase 1 G93A mice: glutamate-mediated excitotoxicity. *Journal of Pharmacology and Experimental Therapeutics*, *338*(2), 518-527.

Jourdain, P., Bergersen, L. H., Bhaukaurally, K., Bezzi, P., Santello, M., Domercq, M., . . . Volterra, A. (2007). Glutamate exocytosis from astrocytes controls synaptic strength. *Nature neuroscience, 10*(3), 331-339.

Kajiwara, Y., Yasutake, A., Adachi, T., & Hirayama, K. (1996). Methylmercury transport across the placenta via neutral amino acid carrier. *Archives of toxicology, 70*(5), 310-314.

Kalyani, A., Hobson, K., & Rao, M. S. (1997). Neuroepithelial stem cells from the embryonic spinal cord: isolation, characterization, and clonal analysis. *Developmental biology*, *186*(2), 202-223.

Kasai, H., Aosaki, T., & Fukuda, J. (1987). Presynaptic Ca^{2+}-antagonist ω-conotoxin irreversibly blocks N-type Ca^{2+}-channels in chick sensory neurons. *Neuroscience research, 4*(3), 228-235.

Kaur, P., Aschner, M., & Syversen, T. (2006). Glutathione modulation influences methyl mercury induced neurotoxicity in primary cell cultures of neurons and astrocytes. *Neurotoxicology, 27*(4), 492-500.

Kaur, P., Aschner, M., & Syversen, T. (2007). Role of glutathione in determining the differential sensitivity between the cortical and cerebellar regions towards mercury-induced oxidative stress. *Toxicology, 230*(2), 164-177.

Kerper, L. E., Ballatori, N., & Clarkson, T. W. (1992). Methylmercury transport across the blood-brain barrier by an amino acid carrier. *American Journal of Physiology-Regulatory, Integrative and Comparative Physiology, 262*(5), R761-R765.

Kerper, L. E., Mokrzan, E. M., Clarkson, T. W., & Ballatori, N. (1996). Methylmercury efflux from brain capillary endothelial cells is modulated by intracellular glutathione but not ATP. *Toxicology and applied pharmacology, 141*(2), 526-531.

Kerr, L. M., & Yoshikami, D. (1984). A venom peptide with a novel presynaptic blocking action. *Nature, 308*(5956), 282-284.

Kershaw, T. G., Dhahir, P. H., & Clarkson, T. W. (1980). The relationship between blood levels and dose of methylmercury in man. *Archives of Environmental Health: An International Journal, 35*(1), 28-36.

Kimelberg, H., Goderie, S., Higman, S., Pang, S., & Waniewski, R. (1990). Swelling-induced release of glutamate, aspartate, and taurine from astrocyte cultures. *Journal of Neuroscience, 10*(5), 1583-1591.

Kochegarov, A. A. (2003). Pharmacological modulators of voltage-gated calcium channels and their therapeutical application. *Cell calcium, 33*(3), 145-162.

Komulainen, H., & Bondy, S. C. (1987). Increased free intrasynaptosomal Ca^{2+} by neurotoxic organometals: distinctive mechanisms. *Toxicology and applied pharmacology, 88*(1), 77-86.

Komuro, H., & Kumada, T. (2005). Ca 2+ transients control CNS neuronal migration. *Cell calcium, 37*(5), 387-393.

Kunimoto, M., & Suzuki, T. (1997). Migration of granule neurons in cerebellar organotypic cultures is impaired by methylmercury. *Neuroscience letters, 226*(3), 183-186.

Koos, B. J., & Longo, L. D. (1976). Mercury toxicity in the pregnant woman, fetus, and newborn infant: a review. *American journal of obstetrics and gynecology, 126*(3), 390-409.

Kranich, O., Dringen, R., Sandberg, M., & Hamprecht, B. (1998). Utilization of cysteine and cysteine precursors for the synthesis of glutathione in astroglial cultures: preference for cystine. *Glia, 22*(1), 11-18.

Kromidas, L., Trombetta, L. D., & Jamall, I. S. (1990). The protective effects of glutathione against methylmercury cytotoxicity. *Toxicology letters, 51*(1), 67-80.

Kunimoto, M. (1994). Methylmercury induces apoptosis of rat cerebellar neurons in primary culture. *Biochemical and biophysical research communications, 204*(1), 310-317.

Latour, I., Gee, C. E., Robitaille, R., & Lacaille, J. C. (2001). Differential mechanisms of Ca^{2+} responses in glial cells evoked by exogenous and endogenous glutamate in rat hippocampus. *Hippocampus, 11*(2), 132-145.

Latour, I., Hamid, J., Beedle, A. M., Zamponi, G. W., & Macvicar, B. A. (2003). Expression of voltage□gated Ca^{2+} channel subtypes in cultured astrocytes. *Glia, 41*(4), 347-353.

Lehre, K. P., & Danbolt, N. C. (1998). The number of glutamate transporter subtype molecules at glutamatergic synapses: chemical and stereological quantification in young adult rat brain. *Journal of Neuroscience, 18*(21), 8751-8757.

Leonhardt, R., Pekel, M., Platt, B., Haas, H., & Büsselberg, D. (1995). Voltage-activated calcium channel currents of rat DRG neurons are reduced by mercuric chloride ($HgCl^2$) and methylmercury (CH^3HgCl). *Neurotoxicology, 17*(1), 85-92.

Letts, V. A., Felix, R., Biddlecome, G. H., Arikkath, J., Mahaffey, C. L., Valenzuela, A., . . . Frankel, W. N. (1998). The mouse stargazer gene encodes a neuronal Ca^{2+}-channel γ subunit. *Nature genetics, 19*(4), 340-347.

Levesque, P. C., Hare, M. F., & Atchison, W. D. (1992). Inhibition of mitochondrial Ca^{2+} release diminishes the effectiveness of methyl mercury to release acetylcholine from synaptosomes. *Toxicology and applied pharmacology, 115*(1), 11-20.

Leyshon-Sørland, K., Jasani, B., & Morgan, A. (1994). The localization of mercury and metallothionein in the cerebellum of rats experimentally exposed to methylmercury. *The Histochemical Journal, 26*(2), 161-169.

Li, P., Feng, X., & Qiu, G. (2010). Methylmercury exposure and health effects from rice and fish consumption: a review. *International Journal of Environmental Research and Public Health, 7*(6), 2666-2691.

Limke, T. L., & Atchison, W. D. (2002). Acute exposure to methylmercury opens the mitochondrial permeability transition pore in rat cerebellar granule cells. *Toxicology and applied pharmacology, 178*(1), 52-61.

Limke, T. L., Bearss, J. J., & Atchison, W. D. (2004). Acute exposure to methylmercury causes Ca^{2+} dysregulation and neuronal death in rat cerebellar granule cells through an M_3 muscarinic receptor-linked pathway. *Toxicological Sciences, 80*(1), 60-68.

Limke, T. L., Heidemann, S. R., & Atchison, W. D. (2004). Disruption of intraneuronal divalent cation regulation by methylmercury: are specific targets involved in altered neuronal development and cytotoxicity in methylmercury poisoning? *Neurotoxicology, 25*(5), 741-760.

Limke, T. L., Otero-Montañez, J. K., & Atchison, W. D. (2003). Evidence for interactions between intracellular calcium stores during methylmercury-induced intracellular calcium dysregulation in rat cerebellar granule neurons. *Journal of Pharmacology and Experimental Therapeutics, 304*(3), 949-958.

Liu, W., Xu, Z., Yang, T., Deng, Y., Xu, B., & Feng, S. (2016). Tea polyphenols protect against methylmercury-induced cell injury in rat primary cultured astrocytes, involvement of oxidative stress and glutamate uptake/metabolism disorders. *Molecular neurobiology, 53*(5), 2995-3009.

Luddens, H., Pritchett, D. B., Kohler, M., Killisch, I., & Keinanen, K. (1990). Cerebellar GABA (A) Receptor Selective for a Behavioural Alcohol Antagonist. *Nature, 346*(6285), 648.

MacVicar, B. (1984). Voltage-dependent calcium channels in glial cells. *Science, 226*, 1345-1348.

MacVicar, B., & Tse, F. (1988). Norepinephrine and cyclic adenosine 3′: 5′□cyclic monophosphate enhance a nifedipine□sensitive calcium current in cultured rat astrocytes. *Glia, 1*(6), 359-365.

Macvicar, B. A., Hochman, D., Delay, M. J., & Weiss, S. (1991). Modulation of intracellular Ca^{2+} in cultured astrocytes by influx through voltage□activated Ca^{2+} channels. *Glia, 4*(5), 448-455.

Magee, J. C., & Johnston, D. (1997). A synaptically controlled, associative signal for Hebbian plasticity in hippocampal neurons. *Science, 275*(5297), 209-213.

Magos, L., Brown, A., Sparrow, S., Bailey, E., Snowden, R., & Skipp, W. (1985). The comparative toxicology of ethyl-and methylmercury. *Archives of toxicology, 57*(4), 260-267.

Mahaffey, K. R., Clickner, R. P., & Jeffries, R. A. (2009). Adult women's blood mercury concentrations vary regionally in the United States: association with patterns of fish consumption (NHANES 1999–2004). *Environmental health perspectives, 117*(1), 47.

Maienschein, V., Marxen, M., Volknandt, W., & Zimmermann, H. (1999). A plethora of presynaptic proteins associated with ATP storing organelles in cultured astrocytes. *Glia, 26*(3), 233-244.

Malarkey, E. B., & Parpura, V. (2008). Mechanisms of glutamate release from astrocytes. *Neurochemistry international, 52*(1), 142-154.

Mancini, J. D., Autio, D. M., & Atchison, W. D. (2009). Continuous exposure to low concentrations of methylmercury impairs cerebellar granule cell migration in organotypic slice culture. *Neurotoxicology, 30*(2), 203-208.

Mapelli, L., Solinas, S., & D'Angelo, E. (2014). Integration and regulation of glomerular inhibition in the cerebellar granular layer circuit. *Frontiers in cellular neuroscience, 8*.

Mark, L. P., Prost, R. W., Ulmer, J. L., Smith, M. M., Daniels, D. L., Strottmann, J. M., . . . Hacein-Bey, L. (2001). Pictorial review of glutamate excitotoxicity: fundamental concepts for neuroimaging. *American journal of neuroradiology, 22*(10), 1813-1824.

Martinez-Hernandez, A., Bell, K. P., & Norenberg, M. D. (1977). Glutamine synthetase: glial localization in brain. *Science, 195*(4284), 1356-1358.

Marty, M. S., & Atchison, W. D. (1997). Pathways Mediating Ca^{2+} Entry in Rat Cerebellar Granule Cells Followingin VitroExposure to Methyl Mercury. *Toxicology and applied pharmacology, 147*(2), 319-330.

Marty, M. S., & Atchison, W. D. (1998). Elevations of intracellular Ca^{2+} as a probable contributor to decreased viability in cerebellar granule cells following acute exposure to methylmercury. *Toxicology and applied pharmacology, 150*(1), 98-105.

Marty, M.S., Lundback, S.S., Autio, D., & Atchison, W. D. (2006). Methylmercury-induced alterations in Ca^{2+} homeostasis in rat cerebellar type II astrocytes. Unpublished manuscript.

Mattson, M. P., & Kater, S. B. (1987). Calcium regulation of neurite elongation and growth cone motility. *Journal of Neuroscience, 7*(12), 4034-4043.

Matute, C., Alberdi, E., Ibarretxe, G., & Sánchez-Gómez, M. V. (2002). Excitotoxicity in glial cells. *European journal of pharmacology, 447*(2), 239-246.

Matyash, V., & Kettenmann, H. (2010). Heterogeneity in astrocyte morphology and physiology. *Brain research reviews, 63*(1), 2-10.

Mayer-Proschel, M., Kalyani, A. J., Mujtaba, T., & Rao, M. S. (1997). Isolation of lineage-restricted neuronal precursors from multipotent neuroepithelial stem cells. *Neuron*, *19*(4), 773-785.

McDowell, M. A., Dillon, C. F., Osterloh, J., Bolger, P. M., Pellizzari, E., Fernando, R., . . . Jones, R. L. (2004). Hair mercury levels in US children and women of childbearing age: reference range data from NHANES 1999–2000. *Environmental health perspectives, 112*(11), 1165.

Mi, H., & Barres, B. A. (1999). Purification and characterization of astrocyte precursor cells in the developing rat optic nerve. *Journal of Neuroscience*, *19*(3), 1049-1061.

Miettinen, J. (1973). Absorption and elimination of dietary (Hg^{2+}) and methylmercury in man. *Mercury, Mercurials, and Mercaptans (Miller MW, Clarkson TW, eds). Springfield, IL: Charles C Thomas*, 233-246.

Miller, R. H., & Raff, M. C. (1984). Fibrous and protoplasmic astrocytes are biochemically and developmentally distinct. *Journal of Neuroscience, 4*(2), 585-592.

Miller, R. J. (1990). Receptor-mediated regulation of calcium channels and neurotransmitter release. *The FASEB Journal, 4*(15), 3291-3299.

Miura, K., Imura, N., & Clarkson, T. W. (1987). Mechanism of methylmercury cytotoxicity. *CRC Critical Reviews in Toxicology, 18*(3), 161-188.

Montana, V., Ni, Y., Hua, X., & Parpura, V. (2004). Vesicular glutamate transporter-dependent glutamate release from astrocytes. *Journal of Neuroscience, 24*(11), 2633-2642.

Montgomery, D. (1994). Astrocytes: form, functions, and roles in disease. *Veterinary Pathology Online, 31*(2), 145-167.

Morken, T. S., Sonnewald, U., Aschner, M., & Syversen, T. (2005). Effects of methylmercury on primary brain cells in mono-and co-culture. *Toxicological Sciences, 87*(1), 169-175.

Mothet, J.-P., Pollegioni, L., Ouanounou, G., Martineau, M., Fossier, P., & Baux, G. (2005). Glutamate receptor activation triggers a calcium-dependent and SNARE protein-dependent release of the gliotransmitter D-serine. *Proceedings of the National Academy of Sciences of the United States of America, 102*(15), 5606-5611.

Mullaney, K., Fehm, M., Vitarella, D., Wagoner, D., & Aschner, M. (1994). The role of-SH groups in methylmercuric chloride-induced D-aspartate and rubidium release from rat primary astrocyte cultures. *Brain research, 641*(1), 1-9.

Mundy, W. R., & Freudenrich, T. M. (2000). Sensitivity of immature neurons in culture to metal-induced changes in reactive oxygen species and intracellular free calcium. *Neurotoxicology, 21*(6), 1135-1144.

Mutkus, L., Aschner, J. L., Syversen, T., & Aschner, M. (2005). Methylmercury alters the in vitro uptake of glutamate in GLAST-and GLT-1-transfected mutant CHO-K1 cells. *Biological trace element research, 107*(3), 231-245.

Myers, G. J., & Davidson, P. W. (1998). Prenatal methylmercury exposure and children: neurologic, developmental, and behavioral research. *Environmental health perspectives, 106*(Suppl 3), 841.

Nagashima, K., Fujii, Y., Tsukamoto, T., Nukuzuma, S., Satoh, M., Fujita, M., . . . Akagi, H. (1995). Apoptotic process of cerebellar degeneration in experimental methylmercury intoxication of rats. *Acta neuropathologica, 91*(1), 72-77.

Nakada, S., & Imura, N. (1983). Susceptibility of lipids to mercurials. *Journal of Applied Toxicology, 3*(3), 131-134.

Nakazawa, K., Nagafuchi, O., Kawakami, T., Inoue, T., Yokota, K., Serikawa, Y., . . . Elvince, R. (2016). Human health risk assessment of mercury vapor around artisanal small-scale gold mining area, Palu city, Central Sulawesi, Indonesia. *Ecotoxicology and environmental safety, 124*, 155-162.

Nielsen, J. B. (1992). Toxicokinetics of mercuric chloride and methylmercuric chloride in mice. *Journal of Toxicology and Environmental Health, Part A Current Issues, 37*(1), 85-122.

Norenberg, M. D., & Martinez-Hernandez, A. (1979). Fine structural localization of glutamine synthetase in astrocytes of rat brain. *Brain research, 161*(2), 303-310.

Ogita, K., Hirata, K., Bole, D. G., Yoshida, S., Tamura, Y., Leckenby, A. M., & Ueda, T. (2001). Inhibition of vesicular glutamate storage and exocytotic release by Rose Bengal. *Journal of neurochemistry, 77*(1), 34-42.

Ogura, H., Yasuda, M., Nakamura, S., Yamashita, H., Mikoshiba, K., & Ohmori, H. (2002). Neurotoxic damage of granule cells in the dentate gyrus and the cerebellum and cognitive deficit following neonatal administration of phenytoin in mice. *Journal of Neuropathology & Experimental Neurology, 61*(11), 956-967.

Ohgoh, M., Yamazaki, K., Ogura, H., Nishizawa, Y., & Tanaka, I. (2000). Apoptotic cell death of cerebellar granule neurons in genetically ataxia (ax) mice. *Neuroscience letters, 288*(3), 167-170.

Olivera, B. M., McIntosh, J. M., Curz, L. J., Luque, F., & Gray, W. R. (1984). Purification and sequence of a presynaptic peptide toxin from Conus geographus venom. *Biochemistry, 23*(22), 5087-5090.

Olney, J. W. (1994). Excitatory transmitter neurotoxicity. *Neurobiology of aging, 15*(2), 259-260.

Olney, J. W. (1978). Neurotoxicity of excitatory amino acids *Kainic acid as a tool in neurobiology* (pp. 95-121): Raven Press New York.

Olney, J. W., Price, M. T., Samson, L., & Labruyere, J. (1986). The role of specific ions in glutamate neurotoxicity. *Neuroscience letters, 65*(1), 65-71.

Oyake, Y., Tanaka, M., Kubo, H., & Chichibu, M. (1966). Neuropathological studies on organic mercury poisoning with special reference to the staining and distribution of mercury granules. *Shinkei kenkyu no shimpo. Advances in neurological sciences, 10*(4), 744-750.

Oyama, Y., Carpenter, D. O., Ueno, S., Hayashi, H., & Tomiyoshi, F. (1995). Methylmercury induces Ca^{2+}-dependent hyperpolarization of mouse thymocytes: a flow cytometric study using fluorescent dyes. *European Journal of Pharmacology: Environmental Toxicology and Pharmacology, 293*(2), 101-107.

Park, S., Lim, K., Chung, Y., & Kim, S. (1995). Methylmercury-induced neurotoxicity in cerebral neuron culture is blocked by antioxidants and NMDA receptor antagonists. *Neurotoxicology, 17*(1), 37-45.

Parpura, V., Basarsky, T. A., Liu, F., Jeftinija, K., Jeftinija, S., & Haydon, P. G. (1994). Glutamate-mediated astrocyte–neuron signalling.

Parpura, V., Fang, Y., Basarsky, T., Jahn, R., & Haydon, P. G. (1995). Expression of synaptobrevin II, cellubrevin and syntaxin but not SNAP-25 in cultured astrocytes. *FEBS letters, 377*(3), 489-492.

Pasti, L., Zonta, M., Pozzan, T., Vicini, S., & Carmignoto, G. (2001). Cytosolic calcium oscillations in astrocytes may regulate exocytotic release of glutamate. *Journal of Neuroscience, 21*(2), 477-484.

Patel, M. (1974). The effect of ketone bodies on pyruvate carboxylation by rat brain mitochondria. *Journal of neurochemistry, 23*(4), 865-867.

Peng, S., Hajela, R. K., & Atchison, W. D. (2002). Effects of methylmercury on human neuronal L-type calcium channels transiently expressed in human embryonic kidney cells (HEK-293). *Journal of Pharmacology and Experimental Therapeutics*, *302*(2), 424-432.

Petroni, D., Tsai, J., Mondal, D., & George, W. (2013). Attenuation of low dose methylmercury and glutamate induced□cytotoxicity and tau phosphorylation by an N□methyl□D□

aspartate antagonist in human neuroblastoma (SHSY5Y) cells. *Environmental toxicology, 28*(12), 700-706.

Pierozan, P., Biasibetti, H., Schmitz, F., Ávila, H., Fernandes, C. G., Pessoa-Pureur, R., & Wyse, A. T. (2016). Neurotoxicity of Methylmercury in Isolated Astrocytes and Neurons: the Cytoskeleton as a Main Target. *Molecular Neurobiology*, 1-16.

Pines, G., Danbolt, N. C., Bjørås, M., Zhang, Y., Bendahan, A., Eide, L., . . . Kanner, B. I. (1992). Cloning and expression of a rat brain L-glutamate transporter. *Nature, 360*(6403), 464-467.

Plummer, M. R., Logothetis, D. E., & Hess, P. (1989). Elementary properties and pharmacological sensitivities of calcium channels in mammalian peripheral neurons. *Neuron, 2*(5), 1453-1463.

Poblete-Naredo, I., Guillem, A. M., Juárez, C., Zepeda, R. C., Ramírez, L., Caba, M., . . . Ortega, A. (2011). Brain-derived neurotrophic factor and its receptors in Bergmann glia cells. *Neurochemistry international, 59*(8), 1133-1144.

Polunas, M., Halladay, A., Tjalkens, R. B., Philbert, M. A., Lowndes, H., & Reuhl, K. (2011). Role of oxidative stress and the mitochondrial permeability transition in methylmercury cytotoxicity. *Neurotoxicology, 32*(5), 526-534.

Pravettoni, E., Bacci, A., Coco, S., Forbicini, P., Matteoli, M., & Verderio, C. (2000). Different localizations and functions of L-type and N-type calcium channels during development of hippocampal neurons. *Developmental biology, 227*(2), 581-594.

Prieto, M., & Alonso, G. (1999). Differential sensitivity of cultured tanycytes and astrocytes to hydrogen peroxide toxicity. *Experimental neurology, 155*(1), 118-127.

Purves, D., Augustine, G., Fitzpatrick, D., Katz, L., LaMantia, A., McNamara, J., & Williams, S. (2001). Circuits within the Cerebellum*.). Neuroscience, 2nd edition edn. Sunderland (MA): Sinauer Associates. p^ pp*.

Qu, M., Nan, X., Gao, Z., Guo, B., Liu, B., & Chen, Z. (2013). Protective effects of lycopene against methylmercury-induced neurotoxicity in cultured rat cerebellar granule neurons. *Brain research, 1540*, 92-102.

Qu, H., Syversen, T., Aschner, M., & Sonnewald, U. (2003). Effect of methylmercury on glutamate metabolism in cerebellar astrocytes in culture. *Neurochemistry international, 43*(4), 411-416.

Raff, M., Abney, E., Cohen, J., Lindsay, R., & Noble, M. (1983). Two types of astrocytes in cultures of developing rat white matter: differences in morphology, surface gangliosides, and growth characteristics. *The Journal of Neuroscience, 3*(6), 1289-1300.

Raff, M. C. (1986). The oligodendrocyte-type-2 astrocyte cell lineage is specialized for myelination. *Nature, 323*(6086), 335-338.

Raff, M. C., Abney, E. R., & Miller, R. H. (1984). Two glial cell lineages diverge prenatally in rat optic nerve. *Developmental biology, 106*(1), 53-60.

Raff, M. C., Miller, R. H., & Noble, M. (1983). A glial progenitor cell that develops in vitro into an astrocyte or an oligodendrocyte depending on culture medium.

Raff, M. C., Williams, B. P., & Miller, R. H. (1984). The in vitro differentiation of a bipotential glial progenitor cell. *The EMBO journal, 3*(8), 1857.

Ramachandran, S., Xie, L. H., John, S. A., Subramaniam, S., & Lal, R. (2007). A novel role for connexin hemichannel in oxidative stress and smoking-induced cell injury. PLoS one, 2(8), e712.

Ramos-Vara, J. A. (2011). Principles and methods of immunohistochemistry. *Drug Safety Evaluation: Methods and Protocols*, 83-96.

Rao, M. S. (1999). Multipotent and restricted precursors in the central nervous system. *The Anatomical Record*, *257*(4), 137-148.

Rao M, Noble M, Mayer-Pröschel M: A tripotential glial precursor cell is present in the developing spinal cord. Proc Natl Acad Sci USA. 1998, 95: 3996-4001. 10.1073/pnas.95.7.3996.

Ray, J., Peterson, D. A., Schinstine, M., & Gage, F. H. (1993). Proliferation, differentiation, and long-term culture of primary hippocampal neurons. *Proceedings of the National Academy of Sciences*, *90*(8), 3602-3606.

Redman, R., & Silinsky, E. (1994). Decrease in calcium currents induced by aminoglycoside antibiotics in frog motor nerve endings. *British journal of pharmacology, 113*(2), 375-378.

Reichenbach, A., & Wolburg, H. (2005). Astrocytes and ependymal glia. *Neuroglia, 2*, 19-35.

Retamal, M. A., Froger, N., Palacios-Prado, N., Ezan, P., Sáez, P. J., Sáez, J. C., & Giaume, C. (2007). Cx43 hemichannels and gap junction channels in astrocytes are regulated oppositely by proinflammatory cytokines released from activated microglia. *Journal of Neuroscience*, *27*(50), 13781-13792.

Rice, D. C., & Gilbert, S. G. (1982). Early chronic low-level methylmercury poisoning in monkeys impairs spatial vision. *Science, 216*(4547), 759-761.

Rizzuto, R. (2003). Calcium mobilization from mitochondria in synaptic transmitter release. *J Cell Biol, 163*(3), 441-443.

Rizzuto, R., Brini, M., Murgia, M., & Pozzan, T. (1993). Microdomains with high Ca^{2+} close to IP_3-sensitive channels that are sensed by neighboring mitochondria. *Science, 262*(5134), 744-748.

Rizzuto, R., De Stefani, D., Raffaello, A., & Mammucari, C. (2012). Mitochondria as sensors and regulators of calcium signalling. *Nature reviews Molecular cell biology, 13*(9), 566-578.

Roda, E., Coccini, T., Acerbi, D., Castoldi, A., Bernocchi, G., & Manzo, L. (2008). Cerebellum cholinergic muscarinic receptor (subtype-2 and-3) and cytoarchitecture after developmental exposure to methylmercury: an immunohistochemical study in rat. *Journal of chemical neuroanatomy, 35*(3), 285-294.

Roos, D., Seeger, R., Puntel, R., & Vargas Barbosa, N. (2012). Role of calcium and mitochondria in MeHg-mediated cytotoxicity. *BioMed Research International, 2012*.

Rothstein, J. D., Dykes-Hoberg, M., Pardo, C. A., Bristol, L. A., Jin, L., Kuncl, R. W., . . . Schielke, J. P. (1996). Knockout of glutamate transporters reveals a major role for astroglial transport in excitotoxicity and clearance of glutamate. *Neuron, 16*(3), 675-686.

Rubin, R. (1970). The role of calcium in the release of neurotransmitter substances and hormones. *Pharmacological Reviews, 22*(3), 389-428.

Rustam, H., & Hamdi, T. (1974). Methyl mercury poisoning in Iraq a neurological study. *Brain, 97*(1), 499-510.

Saab, A. S., Neumeyer, A., Jahn, H. M., Cupido, A., Šimek, A. A., Boele, H.-J., . . . Monyer, H. (2012). Bergmann glial AMPA receptors are required for fine motor coordination. *Science, 337*(6095), 749-753.

Sass, J., Haselow, D., & Silbergeld, E. (2001). Methylmercury-induced decrement in neuronal migration may involve cytokine-dependent mechanisms: a novel method to assess neuronal movement in vitro. *Toxicological Sciences, 63*(1), 74-81.

Sáez, J. C., Schalper, K. A., Retamal, M. A., Orellana, J. A., Shoji, K. F., & Bennett, M. V. (2010). Cell membrane permeabilization via connexin hemichannels in living and dying cells. *Experimental cell research*, *316*(15), 2377-2389.

Salm, A., & McCarthy, K. D. (1990). Norepinephrine□evoked calcium transients in cultured cerebral type 1 astroglia. *Glia, 3*(6), 529-538.

Schipke, C. G., Ohlemeyer, C., Matyash, M., Nolte, C., Kettenmann, H., & Kirchhoff, F. (2001). Astrocytes of the mouse neocortex express functional N-methyl-D-aspartate receptors. *The FASEB Journal, 15*(7), 1270-1272.

Schmahmann, J. D., & Sherman, J. C. (1997). Cerebellar cognitive affective syndrome. *International review of neurobiology, 41*, 433-440.

Schober, S. E., Sinks, T. H., Jones, R. L., Bolger, P. M., McDowell, M., Osterloh, J., . . . Sun, Y. (2003). Blood mercury levels in US children and women of childbearing age, 1999-2000. *Jama, 289*(13), 1667-1674.

Scholz, K. P., & Miller, R. J. (1995). Developmental changes in presynaptic calcium channels coupled to glutamate release in cultured rat hippocampal neurons. *Journal of Neuroscience, 15*(6), 4612-4617.

Schousboe, A., & Waagepetersen, H. S. (2005). Role of astrocytes in glutamate homeostasis: implications for excitotoxicity. *Neurotoxicity research, 8*(3), 221-225.

Shafer, T. J., & Atchison, W. D. (1991). Methylmercury blocks N-and L-type Ca^{2+} channels in nerve growth factor-differentiated pheochromocytoma (PC12) cells. *Journal of Pharmacology and Experimental Therapeutics, 258*(1), 149-157.

Shank, R. P., Bennett, G. S., Freytag, S. O., & Campbell, G. L. (1985). Pyruvate carboxylase: an astrocyte-specific enzyme implicated in the replenishment of amino acid neurotransmitter pools. *Brain research, 329*(1), 364-367.

Shanker, G., Syversen, T., & Aschner, M. (2003). Astrocyte-mediated methylmercury neurotoxicity. *Biological trace element research, 95*(1), 1-10.

Shapiro, A. M., & Chan, H. M. (2008). Characterization of demethylation of methylmercury in cultured astrocytes. *Chemosphere, 74*(1), 112-118.

Sharp, A., Black, J., 3rd, Dubel, S., Sundarraj, S., Shen, J.-P., Yunker, A., . . . McEnery, M. (2001). Biochemical and anatomical evidence for specialized voltage-dependent calcium channel γ isoform expression in the epileptic and ataxic mouse, stargazer. *Neuroscience, 105*(3), 599-617.

Simpson, P. B., & Russell, J. T. (1998). Role of mitochondrial Ca 2+ regulation in neuronal and glial cell signalling. *Brain research reviews, 26*(1), 72-81.

Sirois, J. E., & Atchison, W. D. (2000). Methylmercury affects multiple subtypes of calcium channels in rat cerebellar granule cells. *Toxicology and applied pharmacology, 167*(1), 1-11.

Shenker, B., Berthold, P., Decker, S., Mayro, J., Rooney, C., Vitale, L., & Shapiro, I. (1992). Immunotoxic effects of mercuric compounds on human lymphocytes and monocytes. II. Alterations in cell viability. *Immunopharmacology and immunotoxicology, 14*(3), 555-577.

Shenker, B., Berthold, P., Rooney, C., Vitale, L., DeBolt, K., & Shapiro, I. (1993). Immunotoxic effects of mercuric compounds on human lymphocytes and monocytes. III. Alterations in B-cell function and viability. *Immunopharmacology and immunotoxicology, 15*(1), 87-112.

Skerfving, S. (1988). Mercury in women exposed to methylmercury through fish consumption, and in their newborn babies and breast milk. *Bulletin of environmental contamination and toxicology, 41*(4), 475-482.

Sotelo, C. (1975). Anatomical, physiological and biochemical studies of the cerebellum from mutant mice. II. Morphological study of cerebellar cortical neurons and circuits in the weaver mouse. *Brain research, 94*(1), 19-44.

Stanley, E. F. (1997). The calcium channel and the organization of the presynaptic transmitter release face. *Trends in neurosciences, 20*(9), 404-409.

Sugiura, Y., Tamai, Y., & Tanaka, H. (1978). Selenium protection against mercury toxicity: high binding affinity of methylmercury by selenium-containing ligands in comparison with sulfur-containing ligands. *Bioinorganic chemistry, 9*(2), 167-180.

Szatkowski, M., Barbour, B., & Attwell, D. (1990). Non-vesicular release of glutamate from glial cells by reversed electrogenic glutamate uptake. *Nature, 348*(6300), 443.

Takata, N., & Hirase, H. (2008). Cortical layer 1 and layer 2/3 astrocytes exhibit distinct calcium dynamics in vivo. *PLoS One, 3*(6), e2525.

Takeuchi, T., Morikawa, N., Matsumoto, H., & Shiraishi, Y. (1962). A pathological study of Minamata disease in Japan. *Acta Neuropathologica, 2*(1), 40-57.

Tan, X., Tang, C., Castoldi, A. F., Manzo, L., & Costa, L. G. (1993). Effects of inorganic and organic mercury on intracellular calcium levels in rat T lymphocytes. *Journal of Toxicology and Environmental Health, Part A Current Issues, 38*(2), 159-170.

Thayer, S. A., Perney, T. M., & Miller, R. J. (1988). Regulation of calcium homeostasis in sensory neurons by bradykinin. *Journal of Neuroscience, 8*(11), 4089-4097.

Tower, D. B. (1988). Development of knowledge about astrocytes since Virchow *The biochemical pathology of astrocytes* (pp. 3-18): Alan R. Liss New York.

Tsacopoulos, M., & Magistretti, P. J. (1996). Metabolic coupling between glia and neurons. *Journal of Neuroscience, 16*(3), 877-885.

UNEP (United Nations Environment Programme). 2013. Global Mercury Assessment 2013—Sources, Emissions, Releases and Environmental Transport. Available:http://www.unep.org/chemicalsandwaste/what-we-do/technology-and-metals/mercury/global-mercury-assessment [accessed 23 June 2017].

Vahter, M., Mottet, N. K., Friberg, L., Lind, B., Shen, D. D., & Burbacher, T. (1994). Speciation of mercury in the primate blood and brain following long-term exposure to methyl mercury. *Toxicology and applied pharmacology, 124*(2), 221-229.

Varecka, L., Wu, C. H., Rotter, A., & Frostholm, A. (1994). GABAA/benzodiazepine receptor α6 subunit mRNA in granule cells of the cerebellar cortex and cochlear nuclei: expression in developing and mutant mice. *Journal of Comparative Neurology, 339*(3), 341-352.

Vaughan, P. J., Pike, C. J., Cotman, C. W., & Cunningham, D. D. (1995). Thrombin receptor activation protects neurons and astrocytes from cell death produced by environmental insults. *Journal of Neuroscience*, *15*(7), 5389-5401.

Veiga, M. M., Baker, R. F., Fried, M. B., & Withers, D. (2004). *Protocols for environmental and health assessment of mercury released by artisanal and small-scale gold miners*: United Nations Publications.

Verderio, C., Coco, S., Fumagalli, G., & Matteoli, M. (1995). Calcium-dependent glutamate release during neuronal development and synaptogenesis: different involvement of omega-agatoxin IVA-and omega-conotoxin GVIA-sensitive channels. *Proceedings of the National Academy of Sciences, 92*(14), 6449-6453.

Verity, M., Brown, W. J., & Cheung, M. (1975). Organic mercurial encephalopathy: in vivo and in vitro effects of methyl mercury on synaptosomal respiration. *Journal of neurochemistry, 25*(6), 759-766.

Verkhratsky, A., & Kirchhoff, F. (2007). NMDA receptors in glia. *The Neuroscientist, 13*(1), 28-37.

Von Lenhossék, M. (1891). *Zur Kenntnis der Neuroglia des menschlichen Rückenmarkes*.

Waagepetersen, H. S., Qu, H., Schousboe, A., & Sonnewald, U. (2001). Elucidation of the quantitative significance of pyruvate carboxylation in cultured cerebellar neurons and astrocytes. *Journal of neuroscience research, 66*(5), 763-770.

Walz, W. (2000). Role of astrocytes in the clearance of excess extracellular potassium. *Neurochemistry international, 36*(4), 291-300.

Wang, L., Jiang, H., Yin, Z., Aschner, M., & Cai, J. (2009). Methylmercury toxicity and Nrf2-dependent detoxification in astrocytes. *Toxicological Sciences, 107*(1), 135-143.

Warr, O., Takahashi, M., & Attwell, D. (1999). Modulation of extracellular glutamate concentration in rat brain slices by cystine□glutamate exchange. *The Journal of physiology, 514*(3), 783-793.

Weiss, B., Clarkson, T. W., & Simon, W. (2002). Silent latency periods in methylmercury poisoning and in neurodegenerative disease. *Environmental health perspectives, 110*(Suppl 5), 851.

Weiss, B., & Simon, W. (1975). Quantitative perspectives on the long-term toxicity of methylmercury and similar poisons *Behavioral toxicology* (pp. 429-437): Springer.

West, A. E., Chen, W. G., Dalva, M. B., Dolmetsch, R. E., Kornhauser, J. M., Shaywitz, A. J., . . . Greenberg, M. E. (2001). Calcium regulation of neuronal gene expression. *Proceedings of the National Academy of Sciences, 98*(20), 11024-11031.

Westenbroek, R. E., Ahlijanian, M. K., & Catterall, W. A. (1990). Clustering of L-Type Ca^{2+} Channels at the Base of Major Dendrites in Hippocampal Pyramidal Neurons. *Nature, 347*(6290), 281.

Wojda, U., Salinska, E., & Kuznicki, J. (2008). Calcium ions in neuronal degeneration. *IUBMB life, 60*(9), 575-590.

Wu, L.-G., Westenbroek, R. E., Borst, J. G. G., Catterall, W. A., & Sakmann, B. (1999). Calcium channel types with distinct presynaptic localization couple differentially to transmitter release in single calyx-type synapses. *Journal of Neuroscience, 19*(2), 726-736.

Xu, J., Peng, H., Kang, N., Zhao, Z., Lin, J. H., Stanton, P. K., & Kang, J. (2007). Glutamate-induced exocytosis of glutamate from astrocytes. *Journal of Biological Chemistry, 282*(33), 24185-24197.

Yamakage, M., & Namiki, A. (2002). Calcium channels—basic aspects of their structure, function and gene encoding; anesthetic action on the channels—a review. *Canadian Journal of Anesthesia, 49*(2), 151-164.

Yang, F., He, X.-p., Russell, J., & Lu, B. (2003). Ca^{2+} influx–independent synaptic potentiation mediated by mitochondrial Na^{+}- Ca^{2+} exchanger and protein kinase C. *J Cell Biol, 163*(3), 511-523.

Ye, Z.-C., & Sontheimer, H. (1998). Astrocytes protect neurons from neurotoxic injury by serum glutamate. *Glia, 22*(3), 237-248.

Ye, Z.-C., Wyeth, M. S., Baltan-Tekkok, S., & Ransom, B. R. (2003). Functional hemichannels in astrocytes: a novel mechanism of glutamate release. *Journal of Neuroscience, 23*(9), 3588-3596.

Yu, A. C. H., Lau, A. M. F., Fu, A. W. Y., Lau, L. T., Lam, P. Y., Chen, X. Q., & Xu, Z. Y. (2002). Changes of ATP and ADP in cultured astrocytes under and after in vitro ischemia. *Neurochemical research*, *27*(12), 1663-1668.

Yuan, Y., & Atchison, W. D. (1997). Action of methylmercury on $GABA_A$ receptor-mediated inhibitory synaptic transmission is primarily responsible for its early stimulatory effects on hippocampal CA1 excitatory synaptic transmission. *Journal of Pharmacology and Experimental Therapeutics, 282*(1), 64-73.

Yuan, Y., & Atchison, W. D. (2003). Methylmercury Differentially Affects $GABA_A$ Receptor□ Mediated Spontaneous IPSCs in Purkinje and Granule Cells of Rat Cerebellar Slices. *The Journal of physiology, 550*(1), 191-204.

Yuste, R., & Denk, W. (1995). Dendritic spines as basic functional units of neuronal integration. *Nature, 375*(6533), 682.

Zhang, Q., Pangršič, T., Kreft, M., Kržan, M., Li, N., Sul, J.-Y., . . . Haydon, P. G. (2004). Fusion-related release of glutamate from astrocytes. *Journal of Biological Chemistry, 279*(13), 12724-12733.

Zhong, J., Deng, J., Phan, J., Dlouhy, S., Wu, H., Yao, W., . . . Lee, W. H. (2005). Insulin□like growth factor□I protects granule neurons from apoptosis and improves ataxia in weaver mice. *Journal of neuroscience research, 80*(4), 481-490.

Zündorf, G., & Reiser, G. (2011). Calcium dysregulation and homeostasis of neural calcium in the molecular mechanisms of neurodegenerative diseases provide multiple targets for neuroprotection. *Antioxidants & redox signaling, 14*(7), 1275-1288.